Endothelial injury in atherosclerosis: identification of mediators and attenuation of inflammation by adenoviral augmentation of elafin and SLPI

Peter Andrew Henriksen

DECLARATION

I hereby declare that this thesis has been composed entirely by myself and that no part of this work has been submitted for any other degree or professional qualification. All work presented was executed by myself except where otherwise acknowledged.

Dr Peter A. Henriksen

ABSTRACT

Atherosclerosis is a chronic inflammatory process occurring within arterial blood vessels. Clinical sequelae of atherosclerotic plaque build up include angina, myocardial infarction and ischaemic stroke, imposing a massive burden on healthcare provision. The retention and subsequent oxidative modification of low-density lipoprotein within the subintimal space provides a persistent stimulus for inflammation throughout atherosclerotic plaque development. Understanding the inflammatory mechanisms of oxidised LDL-induced endothelial cell injury will be necessary before devising therapies that intercept, reverse and prevent atherosclerotic plaque development. The work in this thesis is based on a conviction that strategies aimed at augmenting endogenous anti-inflammatory and repair mediators through local gene delivery have the potential to provide lasting effectiveness with low toxicity.

An *in vitro* model of atherosclerotic endothelial cells was established using cultured human umbilical vein endothelial cells and oxidised LDL. Gene expression profiling identified angiopoietin-2 as a target gene up regulated by oxidised LDL incubation in endothelial cells. High levels of this angiogenic factor were also found in endothelial cell culture supernatants following oxidised LDL incubation and within zones of neointimal angiogenesis in atherosclerotic human coronary arteries.

Gene expression profiling failed to identify candidate 'endothelial protective' mediators and attention focused on elafin and secretory leucocyte protease inhibitor (SLPI), two low molecular weight elastase inhibitors. Elafin has been demonstrated within human coronary arteries although its function as a locally active antiprotease,

antagonising the inflammatory effects of human neutrophil elastase (HNE) and bacterial injury has been characterised best within the lung.

Here we have used adenovirus as a vector to deliver elafin and SLPI genes to human endothelial cells and macrophages. We have devised a protocol involving precomplexing of adenovirus with lipofectamine to enhance gene delivery and subsequent gene expression in human endothelial cells and to facilitate gene delivery to human macrophages.

Elafin and SLPI overexpression were associated with reduced inflammatory cytokine production in endothelial cells and macrophages in response to a range of atherogenic stimuli including oxidised LDL. This anti-inflammatory activity was associated with reduced activation of the transcription factor NF-κB and preservation of its inhibitory sub-unit IκBα. Furthermore, elafin overexpression protected endothelial cells from HNE mediated injury and attenuated HNE mediated impairment of macrophage apoptotic cell recognition.

In summary, angiopoietin-2 was identified as a novel mediator produced by endothelial cells in response to oxidised LDL and may contribute to plaque development through facilitation of neointimal angiogenesis. Adenoviral overexpression of elafin and SLPI exhibited therapeutic potential through reducing inflammatory responses and protecting the structure and function of endothelial cells and macrophages in the presence of atherogenic stimuli.

ACKNOWLEDGEMENTS

ABBREVIATIONS

aa	Amino acid
Ad	Adenovirus
Ad-elafin	Adenovirus encoding human elafin cDNA
Ad-dl703	Empty adenoviral vector
Ad-GFP	Adenovirus encoding green fluorescent protein cDNA
Ad-IκBα	Adenovirus encoding super-repressor IκBα cDNA
Ad-βGal	Adenovirus encoding β-galactosidase cDNA
Ad-meotaxin	Adenovirus encoding murine eotaxin cDNA
Ad-mSLPI	Adenovirus encoding murine SLPI cDNA
Ang-2	Angiopoietin-2
AP-1	Activator protein-1
ApoB-100	Apolipoprotein B100
ApoE	Apolipoprotein E
CaCl$_2$	Calcium Chloride
CaPi	Calcium Phosphate precipitates
CAR	Coxsackie adenovirus receptor
CD	Cluster of Differentiation
cDNA	Complementary deoxyribonucleic acid
CMV	Cytomegalovirus
CMF-PBS	Calcium and magnesium free PBS
DMEM	Dulbecco's Modified Eagle's Medium
EBM-2	Endothelial Basal Medium-2
E. Coli	*Escherichia coli*

ECL	Enhanced Chemiluminescence
EDTA	Ethylene diamine tetraacetic acid
ELISA	Enzyme-linked immunoabsorbent assay
EMSA	Electromobility shift assay
FACS	Fluorescent activated cell sorting
FGF	Fibroblast growth factor
FCS	Foetal calf serum
GAPDH	Glyceraldehyde phosphate dehydrogenase
GRE	Glucocorticoid response element
h	hour(s)
HDL	High density lipoprotein
HNE	Human neutrophil elastase
HNF	Hepatocyte nuclear factor
HPRT	Hypoxanthine ribosyl transferase
HRP	Horseradish peroxidase
HUVECs	Human umbilical vein endothelial cells
ICAM	Intracellular adhesion molecule
IκB	Inhibitor of κB
IKK	Inhibitor of κB kinase
IL	Interleukin
IRAK	Interleukin-1 receptor associated kinase
IRF	Interferon regulatory factor
JNK	c-Jun N-terminal kinase
kDa	Kilodaltons
LAL	Limulus amebocyte lysate

LDH	Lactate dehydrogenase
LDL	low density lipoprotein
LOX-1	Lectin like oxidised LDL receptor type 1
LPS	Lipopolysaccharide
mAb	Monoclonal antibody
MAPK	Mitogen activated protein kinase
mCMV	Murine cytomegalovirus
MCP	Monocyte chemoattractant protein
MEEM	Minimum Essential Eagle's Medium
min	minute(s)
Moi	Multiplicity of infection
MM-LDL	Minimally modified LDL
MMP	Matrix metalloprotease
MTT	3-(4,5-Dimethylthiazol-2-yl)-2,5-diphenyltetrazolium-bromide
MyD88	Myeloid differentiation factor 88
NF	Nuclear factor
NF-IL6	Nuclear factor interleukin-6
NO	Nitric oxide
PAGE	Polyacrylamide gel electrophoresis
PAMP	Pathogen-associated molecular pattern
PBS	Phosphate buffered saline
PCR	Polymerase chain reaction
PI	Propidium iodide
PIGF	Placental growth factor

PRR	Pattern recognition receptor
RPA	Ribonuclease protection assay
RT	Reverse transcription
s	seconds
SEC	Serpin enzyme complex
SD	Standard deviation
SDS	Sodium dodecyl sulphate
SLPI	Secretory leukocyte protease inhibitor
SMA	Smooth muscle actin
SRA	Scavenger receptor A
SRB	Scavenger receptor B
TH_1	T helper lymphocyte, involved in cell mediated immunity
TH_2	T helper lymphocyte, involved in humoral response
TEMED	N,N,N'N'-tetramethylethylenediamine
TGF	Transforming growth factor
TIMP	Tissue inhibitor of metalloprotease
TLR	Toll-like receptor
TMB	3,3',5'5-tetramethylbenzidine
TNF	Tumour necrosis factor
VCAM	Vascular-cell adhesion molecule
VEGF	Vascular endothelial growth factor
VLDL	Very low-density lipoprotein
X-gal	5-bromo-4-chloro-3-indolyl-β-D-galactopyranoside

TABLE OF CONTENTS

CHAPTER 2: MATERIALS AND METHODS

CHAPTER 3: AN EXPERIMENTAL SYSTEM TO STUDY HUMAN ENDOTHELIAL CELL INFLAMMATORY RESPONSES TO OXIDISED LDL

CHAPTER 4: GENE EXPRESSION PROFILING OF OXIDISED LDL STIMULATED ENDOTHELIAL CELLS

CHAPTER 5: ADENOVIRAL GENE DELIVERY OF ELAFIN AND SLPI ATTENUATES THE INFLAMMATORY RESPONSES OF ENDOTHELIAL CELLS AND MACROPHAGES TO ATHEROGENIC STIMULI

CHAPTER 6: GENE DELIVERY OF ELAFIN REDUCES HNE MEDIATED ENDOTHELIAL CELL INJURY AND PROTECTS MACROPHAGES FROM HNE MEDIATED IMPAIRMENT OF APOPTOTIC CELL RECOGNITION

LIST OF FIGURES

CHAPTER 1

CHAPTER 3

CHAPTER 4

CHAPTER 5

CHAPTER 6

LIST OF TABLES

CHAPTER 1

INTRODUCTION

1.1 Overview

Atherosclerosis is a chronic inflammatory disease of arterial blood vessels that can begin in fetal life. The rate of atherosclerotic plaque development determines the time of onset of plaque erosion or rupture, the events responsible for morbid and fatal clinical sequelae including myocardial infarction and ischaemic stroke. The work described in this thesis has two principle aims. The first is to identify and if possible characterise key mediators responsible for driving plaque development and protecting the endothelium from inflammatory insult. The second is to investigate a strategy for slowing or halting endothelial inflammation through gene transfer of the antiproteases elafin and secretory leucocyte protease inhibitor.

Against this background, the importance of low-density lipoprotein, its retention and oxidative modification in the subendothelial space as initiating and driving forces in atherosclerotic plaque development, is outlined in the following sections. Methods to characterise diseased cells and tissues using gene expression profiling will be examined and strategies to augment endothelial defence against inflammatory insult using gene transfer techniques, in particular, the use of recombinant adenoviral vectors, will be discussed.

1.2 Chronic Inflammation

Inflammation is described by the sequence of events involving leukocytes leaving the vascular space and entering tissues in response to a perceived pathogen or

1

other noxious stimuli. Inflammatory responses have evolved to counter microbial infection, cellular damage and necrosis. It is useful to recall these principles when trying to understand processes within the arterial wall that lead to inflammation. Although inflammatory cells were first recognised within the endothelium of rabbits with experimental atheroma almost half a century ago (Poole et al 1958), focus on atherosclerosis as an inflammatory process has only intensified in the last 15 years (Ross 1986; Ross 1999). Atheroma is characterised by persistent inflammation, beginning insidiously with later concomitant cellular injury, necrosis and repair in the form of connective tissue replacement and angiogenesis within the arterial wall. Macrophages and lymphocytes predominate within the cellular infiltrate and persistent exposure to a noxious stimulus in the form of oxidised low-density lipoprotein (oxidised LDL) occurs along with evidence of an adaptive immune response and autoimmune mechanisms together evoking a self-perpetuating immune reaction. These features illustrate why atherosclerosis may be considered a paradigm of chronic inflammatory disease (Cotran et al 1999).

Atherosclerosis is a maladaptive process serving no benefit to the host. This is in contrast to chronic inflammatory responses to microbial pathogens such as tuberculosis. Clinical manifestations usually occur after the procreational period and genetic predisposition to early plaque development and complications do not exert strong selection pressures. Important factors responsible for the inexorable climb in atheroma related disease across the world include the decline in other (infectious) diseases, allowing sufficient lifespan to develop atheroma related complications and the adoption of a diet and lifestyle conducive to unfavourable lipid profiles with particular emphasis on circulating levels of the cholesterol transport particle, low density lipoprotein.

1.3. LIPOPROTEINS AND ATHEROGENESIS

1.3.1 Low-density lipoprotein: retention and oxidative modification within the subendothelial space

Serum cholesterol is carried by several lipoprotein particles that perform the complex physiological tasks of transporting dietary and endogenously produced lipids (Tall et al 1999). Chylomicrons provide the primary means of transport of dietary lipids, while very low-density lipoproteins (VLDL), low-density lipoproteins (LDL), and high-density lipoproteins (HDL) function to transport endogenous lipids. Triglyceride-rich VLDL particles containing apolipoprotein B-100 (apo B-100) and apolipoprotein E (apo E) are synthesized by the liver and transport fatty acids to adipose tissue and muscle. After triglyceride removal in peripheral tissues, a fraction of the remaining VLDL remnants is metabolised to LDL particles by further removal of core triglycerides and dissociation of apolipoproteins other than apo B-100. In humans, most of the serum cholesterol is carried by LDL particles.

LDL is taken up by cells via LDL receptors that recognise an N-terminal domain of apo B-100. The circulating level of LDL is determined in large part by its rate of uptake through the hepatic LDL receptor pathway, as evidenced by the fact that lack of functional LDL receptors is responsible for the massive accumulation of LDL in patients with homozygous familial hypercholesterolemia (Anderson et al 1977). Targeted disruption of the apolipoprotein E or LDL receptor genes in mice, results in marked increases in VLDL and/or LDL cholesterol levels. When such animals are fed high cholesterol diets, plasma cholesterol levels are greatly increased (Breslow 1996; Smithies et al 1995). Although mice are resistant to the development of atherosclerosis, the combination of these genetic and dietary manipulations results in massive hypercholesterolemia leading to extensive atherosclerotic disease that occurs throughout the aorta and recapitulates many of the features of human lesions.
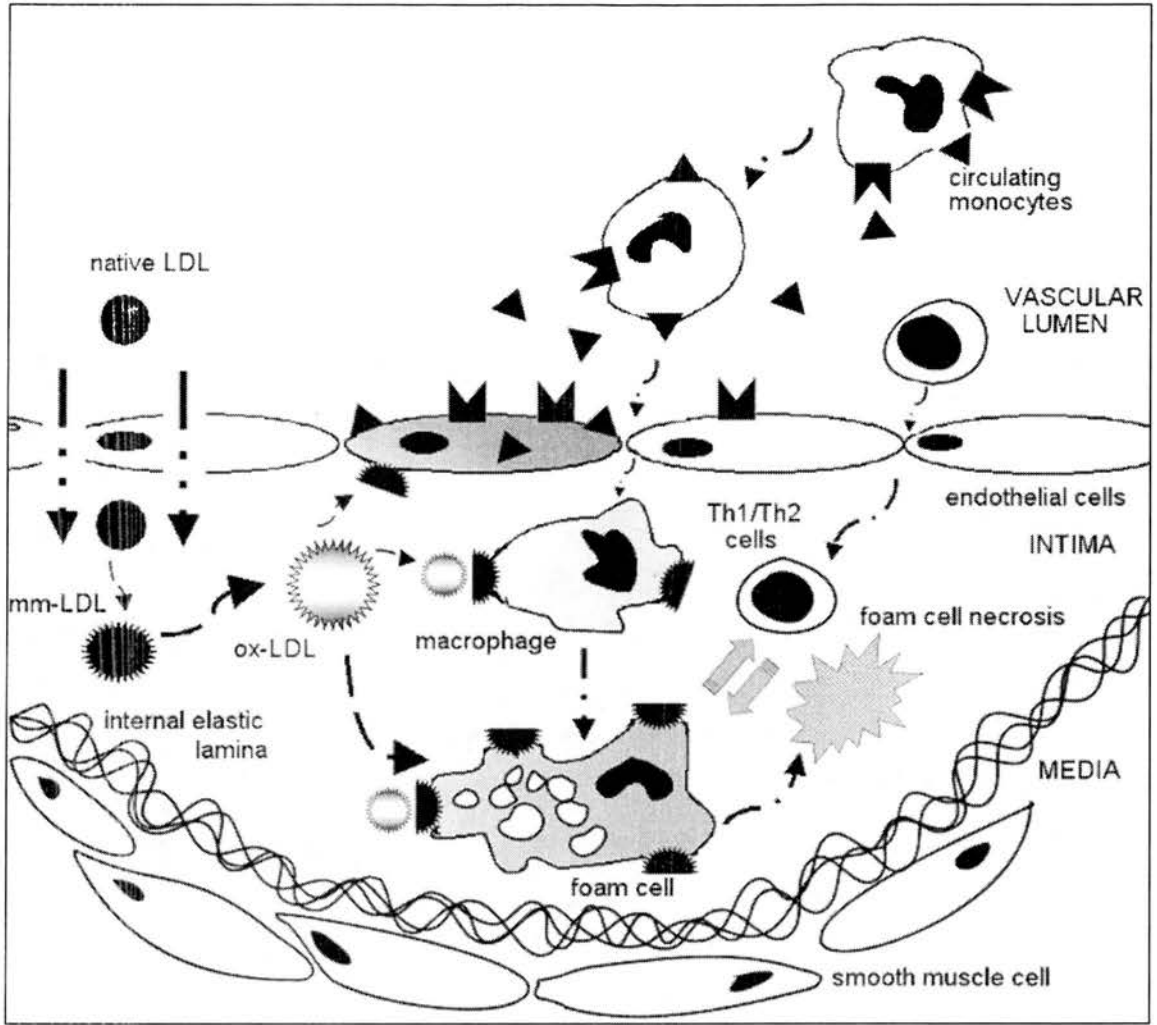
Figure 1.1 Initiating events in the development of an atherosclerotic fatty streak lesion

Key to figure 1.1

Adhesion molecules: VCAM-1, ICAM-1, P-Selectin, E-selectin

Chemokines: MCP-1, IL-8

Chemokine receptors: CXCR-2, CCR-2

Scavenger receptors: CD36 and SR-A on macrophages, LOX-1 on endothelial cells

4

Figure 1.1 Initiating events in the development of an atherosclerotic fatty streak lesion (continued)

This diagram illustrates the central role of entrapment of circulating LDL within the intimal space with subsequent oxidative modification to minimally modified (mm-LDL) and fully oxidised LDL (ox-LDL). Candidate oxidant generating systems within the intimal space include 15-lipoxygenase, myeloperoxidase and inducible NO synthase. Both mm-LDL and oxidised LDL are recognised by scavenger receptors resulting in adhesion molecule expression and chemokine release by endothelial cells. Monocytes are recruited into the intimal space in regions with high chemokine and adhesion molecule expression. Uptake of oxidised LDL results in macrophage foam cell formation. There exists the potential for cholesterol efflux and reverse cholesterol transport through membrane transporters (not shown). Oxidised LDL epitopes are immunogens and contribute to the cellular and humoral immune responses that help perpetuate the chronic inflammatory state. There is evidence of T cell activation within the plaque with the production of Th1 cytokines such as interferon γ and Th2 cytokines such as IL-4. Continued oxidised LDL uptake by macrophages and vascular smooth muscle cells (stimulated to proliferate and migrate into the intima), combined with the local cytokine environment result in apoptotic and necrotic cell death. The subsequent release of insoluble lipid material leads to the formation of a necrotic lipid 'gruel' characteristic of advanced lesions.

Chapter 1

The development of murine models of atherosclerosis has facilitated evaluation of specific genes and the proteins they encode in lesion development. The crossing of these animals with mice that have been engineered to overexpress or lack genes of interest has led to a growing list of mediators that accelerate or retard the rate at which lesions develop, and/or alter lesion composition.

Atherosclerotic lesions begin as fatty streaks underlying the endothelium of large arteries. Figure 1.1 summarises initiating events in the development of atheroma. Factors responsible for retention of LDL in the matrix within the subendothelial space are important. Early accumulation of atherogenic lipoproteins within the arterial wall is concentrated in areas such as bifurcations, known to be prone to later development of atheroma, although the rates of LDL entry into susceptible and resistant sites are the same (Schwenke et al 1989a; Schwenke et al 1989b). Recently the matrix proteoglycan binding site in apo B-100 was identified (Boren et al 1998) and atherosclerotic mice expressing proteoglycan binding defective LDL have reduced plaque burden (Skalen et al 2002).

Many lines of evidence suggest that oxidative modifications in the lipid and apo B-100 components of LDL drive the initial formation of fatty streaks (Navab et al 1996; Steinberg et al 1989a). Indeed, immunological evidence of LDL oxidation is observed even in human fetal arteries prior to the presence of macrophages (Napoli et al 1997). The specific properties of oxidised LDL, usually studied following oxidation of native LDL in vitro, depend on the extent of modification. This can range from "minimal" modification, (mm-LDL) in which the LDL particle can still be recognized by LDL receptors (Navab et al 1996), to extensive oxidation, in which the apo B-100 component is fragmented and lysine residues are covalently modified with reactive breakdown products of oxidised lipids (Steinberg et al 1989a). Endothelial cells, smooth muscle cells or macrophages may oxidise LDL and a number of

6

Chapter 1

potential oxidant-generating systems within the subendothelial space have been investigated that could directly or indirectly target LDL lipids, including myeloperoxidase, nitric oxide synthase and 15-lipoxygenase (15-LO) (Daugherty et al 1994; Steinberg et al 1989b)

1.3.2. Proatherogenic properties of oxidised LDL

Both mm-LDL and oxidised LDL elicit inflammatory responses from endothelial cells, vascular smooth muscle cells and macrophages. The oxidation-specific neo-epitopes within oxidised LDL are recognised by pattern-recognition receptors (PRRs) that have evolved within the host innate immune defences to identify conserved motifs on pathogens. Such PRRs typically recognise a restricted pattern of ligands called pathogen-associated molecular patterns (PAMPs) (Janeway, Jr. et al 2002). In addition to being ligands on microbes PAMPs come from a diverse array of compounds including bacterial lipopolysaccharide, aldehyde derived proteins and necrotic cell debris (Janeway, Jr. et al 2002; Medzhitov et al 2002). Many of the proatherogenic properties of oxidised LDL previously identified *in vitro* probably reflect interaction with PRRs (Binder et al 2002). The defining property of oxidised LDL is its ability to bind and be taken up by scavenger receptors A (SR-A) and CD 36 on macrophages and smooth muscle cells (Navab et al 1996). The lectin-like oxidised LDL receptor (LOX-1) receptor, a further PRR on endothelial cells, mediates inflammatory activation in response to oxidised LDL (Cominacini et al 2000b; Li et al 2003b; Moriwaki et al 1998). Table 1.1 provides a summary of the inflammatory actions of oxidised LDL on various intimal cells. The recruitment of monocytes to lesion-prone sites depends upon endothelial cell up regulation of adhesion molecules and chemokines. This occurs in part through activation of the transcription factor NF-κB.

7

Chapter 1

Cell type	Effect of oxidised LDL
Endothelial cell	Increased expression of adhesion molecule ICAM-1 (Poston et al 1992). Increased chemokines IL-8, MCP-1 and increased macrophage colony stimulating factor facilitating leucocyte (monocyte) recruitment (Claise et al 1996; Li et al 2000; Rajavashisth et al 1990). Increased PAI-1 and tissue factor expression favouring thrombus formation (Allison et al 1999). Increased MMP-1 expression facilitating matrix remodelling within the intima (Huang et al 1999). Apoptotic and necrotic cell death possibly leading to endothelial denudation as a prelude to acute thrombus formation (Harada-Shiba et al 1998).
Macrophage	Oxidised LDL exhibits direct chemotactic activity towards monocytes and enhanced uptake by macrophages leading to cholesteryl ester enrichment and foam cell formation (Quinn et al 1987). Up-regulation of scavenger CD36 receptor further enhances oxidised LDL uptake (Han et al 1997). Induction of apoptotic and necrotic cell death leading to formation of central necrotic, lipid rich plaque core (Kinscherf et al 1998). Presentation of oxidised LDL antigen in association with MHC class II molecules and CD40 stimulation (Binder et al 2002).
Vascular smooth muscle cell	Smooth muscle cell migration and proliferation (Heery et al 1995). Production of platelet derived growth factor, a smooth muscle cell mitogen (Stiko-Rahm et al 1992). Oxidised LDL uptake and foam cell formation (Pitas 1990). Vascular smooth muscle cell apoptotic death (Okura et al 2000).
Lymphocyte	T cells are present in early and late lesions. Presentation of oxidised LDL antigen by macrophages leads to activation of cytokine producing CD4+ T-helper cells (Binder et al 2002). TH$_1$ cells predominate producing interferon γ which has multiple proatherogenic properties including activation of macrophages. B cells are less numerous and present in the adventitia. There is strong evidence for a B cell-plasma cell mediated humoral response to oxidised LDL epitopes (Shaw et al 2000; Yla-Herttuala et al 1994).

Table 1.1. The pro-atherogenic effects of oxidised LDL on different cell types within the neointima

This table indicates the scope of pro-atherogenic actions across several cell types and is not an exhaustive summary of all published data.

1.3.2.1. Activation of the inflammatory transcription factor NF-κB

Activated NF-κB has been identified *in situ* in human atherosclerotic plaques but is virtually absent in vessels devoid of atherosclerosis (Brand et al 1996). NF-κB activates a variety of genes relevant to pathophysiology of the vessel wall including cytokines, chemokines and leucocyte adhesion molecules, as well as genes that regulate cell proliferation and mediate cell survival. NF-κB is composed of members of the Rel family that share a 300 amino acid domain, known as the Rel homology domain. This mediates dimerisation, nuclear translocation, DNA binding and interaction with NF-κB inhibitors (Karin 1999). NF-κB activation is controlled by a family of inhibitors or IκBs that bind NF-κB dimers masking the nuclear localisation sequence, thus retaining the entire complex in the cytoplasm. Diverse stimuli activate NF-κB, through phosphorylation and activation of the IκB kinase (IKK) complex. This complex consists of IKK-α and IKK-β heterodimers, and a number of IKK-γ subunits. The activated IKK complex specifically phosphorylates the IκBs, which are rapidly polyubiquinated, targeting them for degradation by the proteosome. Following release from the IκB inhibitor, NF-κB dimers translocate from the cytoplasm to the nucleus, where they bind target genes and stimulate transcription (Karin 1999). NF-κB also activates the IκB-α gene thus replenishing the cytoplasmic pool of its own inhibitor and facilitating an autoregulatory system that tends to push the activated cell back to the quiescent state.

Multiple genes involved in the atherosclerotic process are regulated by NF-κB. Leucocyte adhesion molecules such as VCAM-1, ICAM-1 and E-selectin as well as chemoattractant cytokines, monocyte chemoattractant protein-1 (MCP-1) and interleukin-8 (IL-8), regulate leucocyte recruitment. The induction of tissue factor could tip the endothelial pro/anticoagulant balance towards coagulation. Further target gene products such as cyclin D1 may induce cell proliferation or stimulate cell survival. NF-κB-dependent genes exert a substantial atherogenic effect on the vessel wall and are heavily involved both with initial responses to the atherogenic signal

9

Chapter 1

and to subsequent amplification steps during expansion and progression of lesions. Activation of NF-κB by oxidised LDL is discussed in detail in chapter 3. Other candidates for induction of NF-κB activity within the atherosclerotic plaque include cytokines such as TNF-α, advanced glycation end products, angiotensin-2, haemodynamic forces and heat shock proteins (Collins et al 2001)

1.3.2.2. Adhesion molecule and chemokine expression

Several cell adhesion molecules have been shown to have roles in leucocyte recruitment. VCAM-1 was implicated because of its increased expression on endothelial cells over lesion-prone areas, its preferential recruitment of monocytes, and its pattern of regulation by proinflammatory stimuli (Cybulsky et al 1991). Studies to confirm a role of VCAM-1 in atherosclerosis in the mouse have been complicated by the fact that systemic deletion of the VCAM-1 gene results in early embyronic death. E selectin and P selectin appear to play quantitative roles in monocyte entry based on a 40% to 60% decrease in atherosclerosis in apo E–deficient mice lacking both genes (Dong et al 1998). Similarly, gene deletion of ICAM-1 resulted in small but significant reductions in monocyte recruitment to atherosclerotic lesions in apo E–deficient mice (Collins et al 2000). Together, these findings suggest the involvement of several adhesion molecules in the recruitment of monocytes and T cells to the atherosclerotic lesion.

Monocyte entry into the artery wall is stimulated in part by oxidised LDL, which can directly attract monocytes (Quinn et al 1988) and can also induce the expression of chemotactic molecules by endothelial cells, such as monocyte chemotactic protein 1 (MCP-1) and interleukin-8 (IL-8) (Claise et al 1996; Li et al 2000a). Monocyte expression of CCR2, the receptor for MCP-1, is stimulated by hypercholesterolaemia and monocytes derived from hypercholesterolaemic patients exhibit increased chemotactic responses to MCP-1 (Han et al 1999). Disruption of the MCP-1 or CCR2 genes markedly reduces the development of atherosclerosis in

apoE knockout mice (Gosling et al 1999; Gu et al 1998). IL-8 is present in large quantities within atherosclerotic tissue and has predominantly been characterised as a neutrophil chemoattractant. This is surprising given that paucity of neutrophils is a characteristic of atherosclerotic lesions. These seemingly disparate observations may be reconciled by evidence for an active role for neutrophil derived proteins within atheroma and this is discussed in detail in Chapter 6. IL-8 can promote firm adherence of rolling monocytes to endothelial cell monolayers expressing E-selectin (Gerszten et al 1999) and may be involved in stimulating endothelial cell migration and angiogenesis within the atherosclerotic plaque. Although a clear homologue of IL-8 has not been established in the mouse, reconstitution of the hematopoietic system of LDL R knockout mice with bone marrow cells lacking CXCR2, one of two high-affinity receptors for IL-8, resulted in significantly less atherosclerosis than mice reconstituted with wild-type bone marrow cells (Boisvert et al 1998). In concert, these findings suggest that inhibition of macrophage chemotaxis mediated by MCP-1, IL-8 and their respective receptors may be of therapeutic potential.

1.3.2.3. Oxidised LDL uptake by macrophages and foam cell formation

Interaction of oxidised LDL with scavenger receptors on macrophages (SR-A and CD36) results in internalisation, massive accumulation of cholesterol and foam cell formation (de Villiers et al 1999), a hallmark of both early and late atherosclerotic lesions. Apo E knockout mice lacking the SR-A or CD36 scavenger receptors developed significantly less atherosclerosis than control apo E knockout mice, with quantitatively greater reductions in lesion area observed in CD36/ApoE double knockout mice (Febbraio et al 2000; Suzuki et al 1997). Foam cells are a source of inflammatory mediators including cytokines, proteases and growth factors that modulate plaque development. The factors controlling progression from fatty streak to complicated atherosclerotic plaque with fibroproliferative stenosis or development of a central necrotic core with a propensity to intraluminal rupture have not been determined although it seems likely that central to this is the fate of the macrophage foam cell.

11

Firstly, the ability of macrophages to function as antigen presenting cells is related to the generation of a variety of autoantibodies to oxidatively modified lipids and an adaptive immune response. There is abundant evidence for immune activation within atherosclerotic lesions with activation of T cells and a florid Th1 response associated with interferon γ expression (Binder et al 2002). There have been several antigens proposed including bacterial components and heat shock proteins although the data support oxidised LDL itself as the most important antigen. Intriguingly, the cloning of autoantibodies from Apo E knockout mice led to identification of the EO6 clone that binds both oxidised LDL and apoptotic cells (Shaw et al 2000). It was later discovered to be identical to T15 natural antibodies to phosphorylcholine that provide protection against *S. pneumoniae* in mice (Briles et al 1982). These findings lend further support to the theory that oxidised LDL is subject to a concerted innate immune response through recognition by PRRs.

Secondly, necrotic death of lipid-laden macrophages and vascular smooth muscle cells contributes to the formation of 'gruel' characterising advanced lesions. Oxidised LDL can induce apoptosis in all intimal cell types and whereas apoptosis may be a pathway to the resolution of inflammation, clearance of apoptotic cells is likely to be impaired, their build up contributing to the necrotic core (Bennett 1999). Finally, cholesterol accumulation is not irreversible. Mechanisms for cholesterol efflux from lipid laden macrophages have been identified involving ABC A1, a member of the ATP binding cassette family of membrane transporters (Bodzioch et al 1999) and HDL as the extracellular receptor.

The next two sections will review evidence indicating involvement of proteases and bacterial components and signalling pathways in lesion development.

Chapter 1

1.4. Atherosclerotic lesion progression: the role of inflammatory proteases

A variety of proteases have been identified within atherosclerotic tissue. Their activity is responsible for structural and functional changes that facilitate plaque development including breaching of the basement membrane of the neointima and internal elastic lamina, migration and proliferation of vascular smooth muscle cells, influx of macrophages and weakening of vulnerable shoulder regions of complicated plaques prior to rupture.

1.4.1. Matrix metalloproteases

Matrix metalloproteinases (MMPs) are a family of zinc dependent endopeptidases capable of cleaving all components of the extracellular matrix. Interstitial collagenases MMP-1, MMP-13 and MMP-8 are produced at sites of interstitial collagen cleavage and MMPs 2, 3, 7, 9, 12 and 14 also localise in human atherosclerotic plaques (Jones et al 2003). MMPs are produced by intimal cells (macrophages, endothelial cells and vascular smooth muscle cells) and transcriptional regulation is in response to a range of inflammatory stimuli including inflammatory cytokines TNF-α and interleukin-1β (IL-1β), hypoxia, heat shock protein 60 (HSP 60) and oxidised LDL. MMPs are produced as proenzymes requiring proteolytic cleavage, most commonly after release into the extracellular space, for activation and this is performed by other proteases such as plasmin or by active MMPs. The effects of metalloproteases on plaque development are complex and relate to their action on matrix degradation and the tensile strength of the vessel wall. The accumulation of macrophage foam cells in atherosclerotic lesions correlates on immunohistochemical examination with increased local release of MMPs and a thin fibrous cap (Galis et al 1995a; Moreau et al 1999). MMPs may reduce plaque volume. Concentration of MMP activity at the shoulder regions of plaques where they are most prone to rupture has implicated them in this process (Herman et al 2001b).

13

Chapter 1

It may be of clinical benefit to alter the expression or activities of metalloproteinases. To date, there are no animal models of atherosclerosis in which plaque rupture and acute thrombotic events contribute to plaque growth. This has prevented testing the hypothesis that MMP inhibition may prevent plaque rupture and has led to a focus on whether MMPs contribute to plaque growth. Atherosclerotic mice deficient in an endogenous inhibitor of matrix metalloproteases (Tissue inhibitor of metalloprotease-1; TIMP-1) had reduced plaque burden (Silence et al 2002). In contrast, MMP-1 knockout mice backcrossed onto the same atherosclerotic apoE knockout background had increased plaque burden with a greater fibrillar collagen content. Although vessel ectasia and aneurysm formation were reduced compared to control ApoE knockout mice. This suggests an important effect of MMP-1 on the structural integrity of the vessel wall (Silence et al 2001).

1.4.2. The plasminogen-plasmin system

The blood fibrinolytic system comprises an inactive proenzyme (plasminogen) that can be converted to the active enzyme plasmin (a serine protease) that degrades fibrin. Two plasminogen activating enzymes have been characterised: tissue plasminogen activator (t-PA) and urokinase plasminogen activator (u-PA). u-PA binds a cell surface receptor, resulting in cleavage of cell-bound plasminogen. This in turn facilitates pericellular proteolysis, including degradation of matrix and the activation of latent growth factors and proteases. Expression of u-PA is increased in human atherosclerotic coronary arteries (Kienast et al 1998). Overexpression of u-PA cDNA in the carotid arteries of cholesterol fed rabbits (a further experimental model of atherosclerosis) led to increased intimal growth and degradation of elastic laminae (Falkenberg et al 2002). Similarly, Apo E:u-PA double knockout mice had less elastin fibre degradation and media destruction than Apo E knockout mice although total plaque burden was no different (Carmeliet et al 1997). Plasmin has no capacity to degrade elastin or collagen and these observations are probably a result of its activation of MMPs.

14

1.4.3. Cathepsins

Cathepsins are cysteine proteases with potent collagenolytic and elastolytic activity. Professor Libby's group has identified cathepsin S and cathepsin K production with human atherosclerotic tissue (Sukhova et al 1998). *In vitro* experiments demonstrated production of cathepsin S by macrophages, vascular smooth muscle cells and endothelial cells, following exposure to inflammatory cytokines found within atheroma. Cathepsin S knockout mice backcrossed on the atherogenic LDL receptor knockout background had reduced plaque burden and reduced intimal content of macrophages, smooth muscle cells, CD4 T lymphocytes and interferon γ expression (Sukhova et al 2003). The latter finding possibly reflected the role of cathepsin S in antigen presentation (Shi et al 1999) and the striking quantitative and qualitative changes in plaque composition illustrate the influence of proteolytic activity in plaque growth.

1.4.4. Other sources of elastolytic activity within atherosclerotic tissue

Elastin is one of the most proteolytically resistant matrix components and proteases with elastase activity may generally exhibit a broad range of substrates including extracellular matrix components, cell surface receptors and cytokines. Cathepsins and metalloproteases contribute to the elastolytic activity within human atheroma. Elastolytic activity increases in human aortas with age and degree of atheromatous involvement (Hornebeck et al 1975). In diseased vessels, the appearance of elastin degradation fragments correlates with an increase in collagen to elastin ratio and also with loss of elastance and windkessel effect responsible for smoothing and hydraulic filtering of pulsatile blood flow from the heart. In addition to changes in the physical properties of the vessel wall, recognition of elastin-derived fragments by the elastin receptor (Hinek et al 1988; Mochizuki et al 2002) leads to a range of proatherogenic effects including monocyte and vascular smooth muscle cell chemotaxis (Robert et al 1998). Identification and regulation of the proteases predominantly responsible for elastolytic activity within atherosclerotic tissue are therefore important goals. Hornebeck et al (1975) were the first to demonstrate serine

elastase activity from atherosclerotic tissue and cultured vascular smooth muscle cells. Professor Rabinovitch's group in Toronto isolated a 20-kDa molecule with serine elastase activity from cultured rat pulmonary artery smooth muscle cells which they designated endovascular elastase (EVE) (Rabinovitch 1999; Thompson et al 1996; Zhu et al 1994). This protein is immunoreactive with adipsin, a serine protease previously characterised from adipose tissue. The protein and gene sequences of EVE have yet to be published.

More recently, another serine elastase, human neutrophil elastase (HNE), has been demonstrated within human atherosclerotic tissue (Dollery et al 2003). The enzyme was strongly expressed and co-localised with plaque macrophages. In-situ hybridisation also identified expression in cultured human saphenous vein endothelial cells and peripheral blood derived macrophages. HNE had hitherto been considered solely as a neutrophil derived enzyme and the presence of such a potent inflammatory protease within atherosclerotic tissue is surprising. HNE has a broad range of substrates including elastin and collagen. It also activates metalloproteases and regulates inflammatory cytokines, activating pro-IL-1-β and IL-8 and inactivating TNF-α by proteolytic cleavage (Owen et al 1997; Padrines et al 1994). In addition to direct cellular toxicity, HNE can degrade inter-endothelial junctional proteins (Carden et al 1998) and surface receptors (Le Barillec et al 1999). HNE degradation of elastin produces peptide fragments that are chemotactic for monocytes (Senior et al 1984) and disruption of the endothelial basement membrane may facilitate invasion of inflammatory cells into the vessel wall (Watanabe et al 1990b; Watanabe et al 1990c).

Finally, HNE induces proliferation of vascular smooth muscle cells in a mechanism involving release of matrix bound fibroblast growth factor (Thompson et al 1996). HNE's wide spectrum of activity makes it an interesting therapeutic target and its inflammatory actions on endothelial cells and macrophages are considered in greater detail in chapter 6.

1.5. Antiproteases and atherosclerosis

All endogenous proteases have their activities checked in varying degrees by antiprotease molecules. Excessive or unbalanced protease activity is a prominent feature of both acute inflammatory pathologies such as acute pancreatitis and chronic disease such as emphysema and liver cirrhosis in patients deficient in the circulating antiprotease, $\alpha1$-antitrypsin. The host response to inflammatory insult includes up regulation of antiproteases. This response assists resolution of inflammation by containing and neutralising injurious proteases. Some antiproteases are released into the circulation from the liver (systemically) and production of others is heightened locally at sites of inflammation and tissue injury. This mechanism has best been elicited in the lung, an organ prone to acute infection and inflammation and exhibiting a spectrum of locally produced antiproteases that form a protective shield against unchecked protease activity (Sallenave et al 1999; Sallenave 2000).

The preceding sections outlined the growing evidence implicating various protease families in atherosclerosis. By contrast, less is known about the role and identity of inhibitory antiproteases within the vessel wall and the following sections will introduce this topic which forms a central investigative theme in the following work.

1.5.1. Metalloprotease inhibitors

Tissue inhibitors of metalloproteases (TIMPs) are specific inhibitors that bind MMPs in a 1:1 stoichiometry. Four TIMPs (TIMP-1, TIMP-2, TIMP-3, and TIMP-4) have been identified in vertebrates (Bode et al 1999; Bode et al 2003; Visse et al 2003). Their expression is regulated during development and tissue remodelling. In pathological conditions associated with unbalanced MMP activity, changes of TIMP levels are considered to be important through directly affecting the level of MMP activity. TIMPs inhibit all MMPs tested to date, except that TIMP-1 fails to inhibit membrane type MT1-MMP. The inhibitory spectrum of TIMP-3 is broader

17

Chapter 1

encompassing members of the disintegrin and metalloproteinase (ADAM) family. TIMPs 1-3 have been characterised in vascular tissue (Brophy et al 1991; Galis et al 1994b). Production of TIMP-1 and TIMP-2 from vascular smooth muscle cells is constitutive (Galis et al 1994a) and their secretion is increased twofold in the aortic explants of cholesterol fed rabbits (Zaltsman et al 1999). An excess of MMPs over TIMPs is believed to promote extracellular matrix turnover and has been demonstrated directly in tissue sections from human atherosclerotic plaques (Galis et al 1994b) and plaques from balloon injured arteries from cholesterol fed rabbits (Galis et al 1995b) using *in situ* zymography.

The regulation of TIMP production and MMP/TIMP balance are important determinants of plaque development and stability. In this regard, it is relevant that both oxidised LDL and IL-8 are associated with attenuated macrophage TIMP-1 production (Moreau et al 1999; Xu et al 1999). TIMPS 1-3 exhibit *in vitro* properties that protect against plaque development, including inhibition of vascular smooth muscle cell migration and proliferation. Adenoviral overexpression of TIMP-1 in Apo E knockout mice reduced lesion development (Rouis et al 1999). In conflict with this result, ApoE:TIMP-1 double knockout mice also exhibited decreased plaque development (Silence et al 2002). The role of TIMPs in atheroma development is complex in part because of their broad ranging interference with all MMPs. The opposing results observed in the latter two studies may reflect changing actions for MMPs during plaque development, serving both facilitatory and inhibitory roles at different stages of plaque growth.

TIMPs are the best characterised inhibitors of MMPs. Recently, tissue factor pathway inhibitor-2 (TFPI-2) was identified as an inhibitor of several MMPs within human arterial vessels (Herman et al 2001a). That a serine protease inhibitor should have activity against MMPs is novel and breaks the dogma that protease inhibitors exhibit inhibitory activity within certain structural classes of proteases. TFPI-2 expression fits the potential profile of a biologically important MMP inhibitor, being

18

Chapter 1

heavily expressed in non-diseased vessels and exhibiting reduced expression in diseased vessels (Herman et al 2001a). Circulating α-macroglobulin exhibits strong binding and inhibition of MMP-1 (Cawston et al 1986) and the role of circulating proteinase inhibitors in atherosclerosis is largely unknown with published work remaining scant.

1.5.2. Elafin and secretory leucocyte protease inhibitor

Elafin and secretory leucocyte protease inhibitor (SLPI) are two serine protease inhibitor members of the antileukoprotease family. Elafin expression has been identified within the intima of human atherosclerotic arteries (Sumi et al 2002a) and Professor Rabinovitch's group in Toronto has been singularly successful in characterising the impressive therapeutic potential of elafin augmentation in various models of vascular disease including transplant arteriosclerosis, myocarditis, vein graft degeneration and myocardial infarction. By contrast, SLPI has yet to be studied directly in the context of vascular disease but in terms of structure and function, it is closely related to elafin.

Elafin and SLPI are relatively low molecular mass molecules (10 kDa and 11.7 kDa respectively) sharing 40% sequence homology. They contain similar reactive sites (Ala-Met and Leu-Met respectively) and have a high content of cysteine residues arranged as disulfide bonds in their C-terminal protease inhibiting regions making them compact, proteolytically resistant molecules. The NH_2-terminal domain of elafin contains VKGQ motifs (Sallenave et al 1993). This sequence acts as a substrate for transglutaminase with the resultant formation of covalent isopeptide bonds between glutamine and lysine. Transglutaminase has been shown to effect polymerization of elafin and the covalent binding of elafin to laminin *in vitro* (Nara et al 1994), raising the possibility that tissue transglutaminase may anchor elafin to extracellular matrix *in vivo*. In this context it is important that elafin was described as

19

Chapter 1

colocalising with tissue transglutaminase within human coronary arteries (Sumi et al 2002a).

Elafin and SLPI were originally characterised in the search for molecules responsible for the anti-elastase activity from human bronchial secretions (Hochstrasser et al 1972; Sallenave et al 1991). Elafin and SLPI are produced widely by epithelial tissues including bronchial, cervical and seminal secretions (SLPI) and lung and skin (elafin) (Sallenave et al 1999). Both elafin and SLPI are produced by neutrophils and macrophages. SLPI is induced by LPS and phagocytosis of apoptotic cells in murine macrophages (Jin et al 1997; Odaka et al 2003) and is the main elastase inhibitor present within the cytosol of human neutrophils (Sallenave et al 1997b). Low levels of elafin expression have also been identified in neutrophils (Sallenave et al 1997), macrophages (Sallenave 2000) and vascular smooth muscle cells (Nara et al 1994).

The cytokines IL-1 and TNF-α effect up regulation of SLPI and elafin production from epithelial cells (Sallenave et al 1994; Sallenave et al 1997b). HNE is also capable of increasing their gene expression implying a central role for both antiproteases in protection of the airway epithelium during the earliest phase of the inflammatory response. SLPI inhibits HNE, cathepsin G, trypsin, chymotrypsin and mast cell chymase. HNE and elafin or SLPI form fully reversible 1:1 stoichiometric complex (Ying et al 1993) but the bond is tight with a slow rate of dissociation and they may therefore be regarded as a "pseudo-reversible inhibitors". Elafin's spectrum of activity is less broad, inhibiting HNE, porcine pancreatic elastase and proteinase 3.

Inhibition of HNE is believed to be the major physiological function of both SLPI and elafin. Their importance in the clinical setting has been examined largely in patients with pulmonary disease including cystic fibrosis, chronic obstructive airways disease, asthma and acute respiratory distress syndrome. No human

20

Chapter 1

deficiency state resulting in disease has been described for either antiprotease. SLPI knockout mice exhibit impaired cutaneous wound healing with increased inflammation and elastase activity (Ashcroft et al 2000). No murine orthologue of elafin has been identified.

Elafin and SLPI have additional anti-inflammatory actions. Direct antimicrobial activity has been demonstrated for both molecules (Simpson et al 1999; Wiedow et al 1998). SLPI also reduces activation of the transcription factor NF-κB and macrophage cytokine production (Jin et al 1997; Lentsch et al 1999a). These properties are discussed in chapter 5.

In order to characterise the roles of elafin and SLPI, several groups have applied these molecules in animal models of inflammatory injury. SLPI and elafin have beneficial effects in models of pulmonary inflammation. Topical instillation of SLPI reduced extra-vascular leakage of albumin, up regulation of ICAM-1 and lung homogenate NF-κB activity in a rat model of acute lung injury induced by IgG immune complexes (Lentsch et al 1999a). Similar protective, anti-inflammatory effects for elafin have been demonstrated. Adenoviral overexpression in murine lungs reduced markers of pulmonary injury following intratracheal instillation with *Pseudomonas aeruginosa* (Simpson et al 2001b). Transgenic mice overexpressing human elafin under the control of the murine CMV promoter exhibit altered responsiveness to LPS challenge (Sallenave et al 2003). Serum TNF-α levels were lower in elafin compared to wild type mice following intraperitoneal administration of LPS. Similarly, TNF-α production by peritoneal macrophages to LPS challenge *ex-vivo* was reduced in elafin expressing mice.

Elafin has also shown great potential as a therapeutic target in models of vascular inflammation. Post-cardiac transplant arteriopathy is particularly associated with increased elastolytic activity, smooth muscle cell migration and proliferation

21

(Billingham 1994). Continuous intravenous infusion of recombinant elafin leads to an impressive decline in the intimal thickening and involvement of coronary arteries in rabbits post-cardiac transplant. This effect was associated with reduced vascular wall elastolytic activity as judged by fewer breaks in the internal elastic lamina (Cowan et al 1996). In a related study examining jugular vein grafts interposed into rabbit carotid arteries, elafin gene transfer (using haemagglutinating virus of Japan liposomes) reduced vein graft degeneration, neointimal formation and leucocyte infiltration (O'Blenes et al 2000).

Elafin transgenic mice expressing elafin under the control of the pre-proendothelin promoter were protected from viral myocarditis (Zaidi et al 1999) and hypoxia induced pulmonary hypertension (Zaidi et al 2002). They also exhibit less intimal and medial thickening following wire-induced endothelial denudation of the carotid artery (Zaidi et al 2000) and preserved myocardial chamber size and function following experimentally induced myocardial infarction (Ohta et al 2004).

The models of vascular disease listed above share the common mechanism of heightened elastase activity within the diseased tissue following acute injury, whether it is immune rejection of transplanted tissue, wire induced endothelial denudation or acute myocardial infarction. Infiltrating leucocytes are one source of elastase activity including HNE from neutrophils. Smooth muscle cells may also release endogenous elastase (Zhu et al 1994). The pro-inflammatory actions of HNE within the vessel wall have been outlined in the preceding section and it seems likely that elafin's protective effect in these models of acute vascular injury is mediated through neutralisation of HNE. It is particularly noteworthy that in the vein graft degeneration model, gene transfer of elafin conferred protection out to 3 months with lipid and macrophage accumulation being less in the elafin treated animals on a high fat diet (O'Blenes et al 2000). This finding is an indication that elafin's protective role may extend to chronic inflammatory processes occurring during atherosclerosis.

1.5.3. Inhibitors of fibrinolysis

Variation in levels of several coagulation factors, including fibrinogen and factor VII, are associated with increased risk of cardiovascular disease. Extensive fibrin deposition is observed in most complex human atherosclerotic lesions and decreased fibrinolytic activity has been proposed to accelerate atherogenesis by facilitating thrombosis and fibrin deposition within developing atherosclerotic lesions (Lee et al 1997). However, Apo E–deficient mice lacking fibrinogen develop lesions that are similar in size and complexity to control apo E knockout mice (Xiao et al 1998).

Inhibition of the fibrinolytic system may occur either at the level of plasminogen activators by specific plasminogen activator inhibitors (PAIs; PAI-1 and PAI-2) or at the level of plasmin through α_2-antiplasmin. LDL receptor knockout mice lacking plasminogen activator inhibitor-1 (PAI-1), should have the balance shifted toward greater fibrin hydrolysis, but they also develop typical atherosclerotic lesions (Sjoland et al 2000). Overexpression of PAI-1 reduced aneurysm formation in a guinea pig to rat aortic xenograft model. In this model, PAI-1 overexpression was associated with reduced activation of MMPs and consequently reduced degradation of matrix components including fibronectin and laminin (Allaire et al 1998). Oxidised LDL increases expression of PAI-1 in human endothelial cells and vascular smooth muscle cells (Allison et al 1999; Dichtl et al 1999). PAI-1 expression is increased in human atherosclerotic arteries compared to healthy arteries (Schneiderman et al 1992). This would be expected to confer a prothrombotic effect on the endothelium.

In summary, despite evidence of increased expression of inhibitors of the fibrinolytic pathway in atherosclerosis, the few studies performed to date (on animal models of atherosclerosis) have failed to demonstrate substantial effects on plaque development. Fibrin deposition is a common finding in complex human plaques but

Chapter 1

not a prominent feature of murine plaques and this important difference between human atheroma and experimental, murine atheroma may have explained the negative findings following overexpression of PAI-1 (Sjoland et al 2000).

1.5.4. Circulating antiproteases; α_1-antitrypsin

The liver releases a series of molecules termed 'acute phase reactants' in response to signals emanating from distant sites of inflammatory injury. This acute phase response is regulated by inflammatory cytokines including IL-1 and TNF-α that induce IL-6 production, an important initiator of hepatic acute phase reactant production. Associations between atherosclerotic disease and the acute phase reactants C-reactive protein and serum amyloid protein A are well established (Johnson et al 2004; Ridker et al 2003). α_1-antitrypsin is an acute phase reactant synthesised in the liver with serine protease inhibitory activity and high circulating levels are associated with progression of human carotid artery atheroma (Zureik et al 2002). A major physiological function is to inhibit HNE, although it has inhibitory action against a wide range of serine proteases and the human deficiency state is associated with emphysema. Mutations resulting in reduction of circulating α_1-antitrypsin activity are also associated with more angiographically advanced coronary artery disease (Talmud et al 2003). Monocytes also produce α_1-antitrypsin and studies *in vitro* support direct inflammatory actions of the carboxyl terminal, having an activating effect on monocytes through the LDL and CD36 receptors (Janciauskiene et al 2001). α_1-antitrypsin is responsible for a large proportion of the HNE inhibitory capacity of serum and it would be expected to impact on HNE activity within atherosclerotic lesions assuming it could access the vascular space. To date, there is no published information from human or animal studies on the presence and activity of α_1-antitrypsin within atherosclerotic tissue.

24

1.6. The application of gene expression profiling to atherosclerosis

The precise combination of environmental and genetic factors driving atheroma may vary between patients, producing phenotypically similar manifestations but potentially requiring different interventions to correct them. More detailed characterisation of pathological processes at the molecular and cellular levels will enhance understanding of underlying mechanisms. Cellular phenotype is determined by the set of proteins translated from the small fraction of the genomic information that is expressed. Proteins form the cellular machinery, regulating responses to stimuli and generally there is a good correlation between the amount of messenger RNA (mRNA) and the production of corresponding protein by the cell. Profiling of gene expression may therefore provide insights into the functional state of the cell in health and disease. Sequence databases, generated by genome sequencing programs, have provided the opportunity to characterise cells and tissues in terms of the pattern and relative quantity of messenger RNA they produce. This analysis has been termed gene expression profiling (Duggan et al 1999).

1.6.1 Gene expression profiling methodology

Differential display, subtraction suppression hybridisation and DNA microarrays are three methods used for expression profiling. Microarrays facilitate parallel quantification of thousands of specific mRNAs in a sample through hybridisation to a complementary sequences placed at specified positions on glass or silicon supports (Gerhold et al 1999). In contrast to differential display and subtractive hybridisation the sequence of the target gene or expressed sequence tag (EST) is known, obviating the need for further cloning steps for identification. Two techniques for high density spotting of DNA molecules on glass or silicone surfaces have become available. One format involves robotic deposition of PCR fragments amplified from cDNA clones and was developed at Stanford University (Schena et al 1995). 10,000 genes may be arrayed on a compact area of 3.6cm^2. Affymetrix adopt an alternative approach based on photolithographic synthesis of oligonucleotides *in situ.* Ultraviolet light is used to direct base by base synthesis, in parallel, for up to

Chapter 1

400,000 oligos on one silicone chip (Gerhold et al 1999). Specific oligo design allows the user to avoid regions of repetitive or homologous sequence between different genes.

Microarrays work on a principle that is the reverse to that of Northern blot analysis. Instead of labelling a specific cDNA probe and hybridising to a pool of mRNAs immobilised on a membrane, a pool of labelled mRNAs is hybridised to numerous cDNA probes immobilised on a solid support in specific positions. The cDNA populations from two experimental samples are labelled with different fluorescent dyes and hybridised to the same microarray allowing direct comparison of signal intensity. Smaller amounts of RNA are required for the analysis of a greater number of genes than is possible with Northern blotting without a big loss of sensitivity. In one study comparing the two methods, a microarray was able to detect 90% of the expression changes demonstrated in one sample by Northern blotting (Taniguchi et al 2001).

The array fabrication technique is critical for producing high resolution and minimising background 'noise' and cross hybridisation signals. For cDNA arrays, signals vary depending on the slide surface, the spotting buffer and the temperature and humidity during array printing (Hegde et al 2000). Following hybridisation and image processing the data must be normalised to adjust for labelling and detection efficiencies for different fluorescent labels and differences in the quantity of starting RNA between samples.

Normalisation strategies (reviewed in (Hegde et al 2000) include correcting for total intensity by assuming that although fluorescence varies between individual transcripts, this should even out over many thousands and be identical for the same quantity of RNA labelled with two different fluorescent markers. A second approach utilises the signal ratio of the gene of interest to that of housekeeping genes, the

26

expression levels of which are assumed not to vary between samples. A third uses the fact that the predicted slope of a scatterplot of housekeeping and added equimolar controls for the two probes should be unity. The data can be rescaled using this slope with regression analysis.

1.6.2. Expression profiling and models of atherosclerosis

The above techniques have wide application in the study of developmental and pathophysiological processes in the cardiovascular system. Difficulties may arise in the interpretation of gene profiles from tissues containing multiple cell types. This can be circumvented in part by the use of *in vitro* single cell models of disease.

Professor Gimbrone's group used differential display to isolate genes which are up regulated in cultured endothelial cells in response to laminar or turbulent flow shear stress (Topper et al 1996). The genes for manganese superoxide dismutase and cyclooxygenase-2 (COX-2) were up regulated in cells exposed to laminar shear stress and these findings were confirmed by reverse northern blotting. Importantly, the investigators confirmed that enhanced gene expression was translated into increased protein synthesis by immunoblotting. The contribution of turbulent flow to endothelial dysfunction and atheromatous plaque development at 'lesion prone areas', such as arterial bifurcations and curvatures, is well established. The putative protective effects of an antioxidant enzyme and prostacyclin (the major product of endothelial COX-2) induced by laminar shear stress are particularly interesting in this regard. The failure of differential display to detect enhanced expression of endothelial cell nitric oxide synthase (eNOS) in endothelial cells exposed to laminar flow illustrated the limited sensitivity of this technique. The influence of mechanical stimuli has also been studied on vascular smooth muscle cells grown on fibronectin coated supports using cDNA microarrays (Feng et al 1999). Only a handful of the 5000 genes monitored at two time points after the onset of mechanical stretch varied by more than the 2.5-fold threshold change in expression set by the investigators. Applying this threshold may facilitate more reproducible results although the

27

majority of genes varied by less than 2-fold in their expression and quantitatively small but functionally important changes in expression may have been overlooked.

PAI-1 and Tenascin-C were induced following stretch. These findings were confirmed with Northern blotting, ELISA and Western blotting for corresponding changes in RNA and protein production. Tenascin-C is prominent in remodelling tissues and has anti-adhesive properties. Whether a stretch stimulus applied to endothelial cells growing in a monolayer reproduces the mechanical environment of a vessel wall is questionable and studies on *ex-vivo* vessel preparations to follow up the array findings form *in vitro* experiments would have been instructive.

Foam cell formation within the atherosclerotic plaque has been modelled by incubating the monocytic THP-1 cell line with oxidised LDL and comparing expression profiles to untreated cells using microarrays (Shiffman et al 2000). Of the 6805 genes arrayed, 268 (4%) altered their expression, a minimum of 2 fold, at one of the time points ranging up to 4 days. Data was presented in clusters according to temporal expression patterns and results were confirmed using quantitative real time PCR. Genes previously demonstrated to be responsive to oxidised LDL loading of macrophages such as thrombomodulin, were induced in the THP-1 cells offering some validation of the model. The scavenger receptors A and CD36 involved in oxidised LDL uptake were up-regulated along with nuclear receptors that control lipid metabolism reflecting a lipid storage phenotype similar to maturing adipocytes.

Vascular smooth muscle cell (VSMC) behaviour in an atheromatous plaque has been modelled by treating cultured VSMCs with the cytokine, tumour necrosis factor α (Haley et al 2000). Eotaxin, a chemokine characterised by its chemotactic properties for eosinophils was induced greater than 20-fold on a cDNA microarray. Eosinophils are not present within atherosclerotic plaques and the finding prompted immunohistochemical studies to localise eotaxin, which was expressed in plaque

28

smooth muscle cells and its receptor, present on plaque macrophages and mast cells. The latter study demonstrated how transcriptional profiling can complement traditional hypothesis driven research through producing unexpected findings, in this case the presence of a signalling pathway in atherosclerotic plaques.

1.6.3. Conclusions: scope and limitations of gene expression profiling

Complex interactions between multiple cell types and matrix are lost with *in vitro* systems. Further information may be gained by summative expression profiles obtained directly from animal model tissues or clinical specimens. Gene expression changes associated with unstable plaques were identified using total RNA extracted from coronary atherosclerotic plaques by directional atherectomy (Randi et al 2003). A central difficulty with interpreting gene expression changes in two different diseased tissues is understanding to what degree expression changes merely represent different cellular content rather than changes in gene expression within the same cell type. This is particularly pertinent when comparing an unstable or ruptured coronary plaque with associated influx of inflammatory cells to a stable plaque.

The interpretation of data from any expression profiling technique requires caution. The risk of false positive signals or bands is high. In microarray studies this may arise through cross hybridisation of homologous or conserved repeat sequences. One study demonstrated that for a specified cDNA sample the ability of a DNA chip to distinguish correctly, the presence of any sequence, was 90% per run (Lee et al 2000b). Costly repeat analysis of the same sample is therefore required and ideally all findings should be confirmed in a separate system such as Northern blotting and quantitative PCR. Secondly, attaching functional significance to changes in gene expression level alone is difficult. No information is provided on alternative splice variants, post translational modifications or the rate of protein degradation. Studies in yeast indicate that expression of important growth regulatory genes may not vary between quiescent and proliferative conditions (Winzeler et al 1999). If this finding

29

Chapter 1

can be extrapolated to eukaryotes then expression profiling may only be capable of detecting subpopulations of functionally important genes whose transcription level is subject to regulation.

Setting these caveats aside, the potential uses for systematic expression profiling on a genome wide scale in atherosclerosis research are clear. The enormous amounts of data produced by profiling studies pose challenges for publication and journals frequently use supplemental web pages to release data fully. The development of expression databanks akin to the sequence databanks already available will facilitate more rapid comparisons between cells and tissues in health and disease.

1.7. Principles of Gene Therapy

1.7.1. Overview and comparison with recombinant protein

Gene therapy may be defined as a strategy of delivering beneficial genes either systemically or directly into tissue. The initial concept of delivering replacements for defective genes in monogenetic disorders has been expanded to include delivery or augmentation of therapeutic genes in both inherited and acquired diseases. In spite of effective drug treatments, poor patient compliance affects our ability to control chronic disorders such as atherosclerosis and hypertension. The side effect profile from systemic actions of many drugs is a further limitation. From the few studies that have been performed in conditions such as Type 2 Diabetes Mellitus it seems that regular drug compliance may be practised in fewer that 50% of patients (Morris 2002). In addition to having adverse effects on disease control, this problem has important implications for cost in terms of unused prescriptions.

30

A central question in considering a gene therapy strategy for atherosclerosis is whether it offers advantages over more direct delivery of drug or therapeutic protein. Firstly, recombinant protein and drug treatments have limited half-lives with attendant problems of peak and trough levels as a result of repeat administrations. Recombinant proteins in particular have short half-lives usually measured in hours and techniques for preparation are often expensive.

Secondly, it is hard to target specific cells or to control levels of drug or recombinant protein in tissues. In contrast gene therapy offers the possibility of using promoters which may be inducible (Gossen et al 1992; No et al 1996) or tissue and cell specific (Strayer et al 1998). The targeting of gene vectors in the case of adenovirus through modifying viral capsid proteins or using bispecific antibodies (Nicklin et al 2000; Wickham et al 1996; Wickham 2003) allows cell specific expression.

Vascular catheterisation is a routine diagnostic and therapeutic procedure in patients with cardiovascular disease offering direct access to much of the venous and arterial vasculature. During cardiac surgery further access is obtained to the myocardium, epicardial surface of coronary arteries and vein grafts during harvesting for bypass surgery. Gene therapy protocols require a period of contact between the target cell and gene vector and this is not easily afforded in the coronary artery bed where blood flow across the endothelium is rapid and under high pressure. In order to circumvent this problem investigators have employed arterial occlusion with balloons to temporarily interrupt flow, delivery of vectors through the balloon while it is opposed to the vessel wall during angioplasty and impregnation of gene vectors onto stents allowing more prolonged juxtaposition and release into the vessel wall (Sharif et al 2004a; Walter et al 2004; Yuan et al 2001). Of necessity these approaches are invasive, involving heavy instrumentation of the target blood vessel. Improved targeting methodologies may avoid this problem in the future.

31

Chapter 1

By offering the potential of targeted and time controlled delivery, gene therapy is attractive in chronic disease processes such as atherosclerosis. Gene therapy strategies may be classed as viral or non-viral according to the vector system.

1.7.2. Non-viral gene therapy

Naked plasmid DNA can be added to cultured cells or injected directly into tissues. Cardiac myocytes are one of the few cell types receptive to this form of gene delivery although low transfection efficiency is an important drawback (Lin et al 1990). Naked DNA has also been used to transduce cells in the arterial wall of rabbits after introduction on a hydrophilic gel-coated catheter albeit with very low efficiency (Riessen et al 1993). Plasmid DNA has a number of attractions being inexpensive and easy to construct in large quantities. The injection of pure plasmid DNA is not generally associated with immune responses either to the DNA or transgene product making it possible to readminister (Tripathy et al 1996). Clinical trials with naked DNA have had limited success. However, for ischaemic leg ulcers where the target tissue is both receptive and accessible, intramuscular injection of plasmid DNA encoding the VEGF gene led to significant improvement (Baumgartner et al 1998). Low transduction efficiency limits the use of naked DNA alone but complexing with cationic or neutral lipids reduces this problem. DNA-lipid liposomes increase the stability of DNA and facilitate cellular entry by promoting fusion with the plasma membrane. Liposomes are relatively easy to prepare and facilitate gene transfer to a range of cell types. Alteration of the lipid structure (Felgner 1996) and incorporation of adenoviral or fusogenic viral proteins into the complexes (Dzau et al 1996) can improve transfection efficiency and even allow targeting of the vectors. Although transfection efficiency is improved compared to naked DNA, particularly for proliferating cells in culture, it is still low when compared to viral vectors for primary non-proliferating cells *in vivo*.

1.7.3. Viral gene therapy

Mammalian viruses have evolved efficient mechanisms for infecting and transducing a wide variety of cell types. Vectors derived from viruses are effective in delivering therapeutic transgenes to human tissues. The host immune system has evolved to respond to and destroy viruses. Circumventing the immune response to allow persistent transgene expression within the host, without a damaging inflammatory response, remains the most important obstacle to viral gene therapy. The vast majority of clinical trials and animal studies in cardiovascular disease have used recombinant adenovirus as a viral vector. This is discussed in a separate section. The remainder of this section will consider briefly other viruses important to gene therapy protocols.

Retroviruses are single stranded, enveloped RNA-viruses whose viral genes can be removed and replaced with transgene sequences and transcriptional regulatory elements (Miller 1992). Retroviruses enter mammalian cells through specific surface receptors. Once inside the cytosol, the RNA genome is reverse transcribed into double-stranded DNA which typically requires a break in the nuclear membrane during mitosis before it can translocate to the nucleus and integrate into the host cell genome. This is problematic for cells with low proliferation rates such as vascular smooth muscle cells and endothelial cells. Within the retrovirus family, lentiviruses are exceptional in that their double stranded DNAs can pass through the pores of intact nuclear membranes in non-dividing cells. Retroviruses are difficult to produce in the large quantities needed for gene therapy. Although they integrate producing long term gene expression *in vitro* the transcription may be shut off *in vivo* after a short time. Random integration of wild type lentiviral vectors also poses the threat of insertional mutagenesis and in particular of neoplastic transformation (Vanin et al 1994). Gene therapy of children with X-linked severe combined immune deficiency resulted in impressive levels of immune reconstitution although two patients developed leukaemia (Kohn et al 2003). Multiple factors could have contributed to the development of leukaemia in the patients involved in this trial. These include the high level of engraftment and expansion of the genetically modified cells, unique

properties of the haematopoietic stem and progenitor cells in bone marrow of X-linked SCID patients, the immune deficiency of the X-linked SCID patients and/or the transferred gene itself.

The adeno-associated virus (AAV) is an integrational vector that infects a broad range of cell types and can be produced at high titres (Muzyczka 1992). It displays the useful property of becoming integrated in a site-specific manner into a single, seven-kilobase region on human chromosome 19 (Kotin et al 1992). Recombinant AAV is stable and has low immunogeneicity although its carrying capacity is also relatively low (around 4.7 kb). Production of AAVs is dependent on the use of a helper virus (usually adenovirus) and producing sufficient quantities of AAV free of contamination from helper virus is technically challenging. However, AAV vectors have been used successfully to provide long term gene expression. Infusion of an AAV containing cDNA for factor IX into the portal vein of factor IX deficient dogs led to 5% of normal factor IX levels within the plasma (Wang et al 2000).

1.7.4. Adenovirus as a vector for gene delivery to the endothelium

Adenoviruses are double-stranded DNA viruses. Serotypes 2 and 5 are most commonly modified for use in gene therapy protocols. The adenoviral genome comprises early regions (E1A, E1B, E2A, E2B, E3 and E4, which are transcribed prior to viral replication) and the late regions (L1-5, which are transcribed after viral replication). Late regions generally encode structural proteins whereas the gene products of the early regions are concerned with viral transcription and evading the host immune response (Kremer et al 1995; Russell 2000). The E1 region initiates viral transcription and is the only region not controlled by *trans* activators encoded by the adenovirus. Deletion of the E1 segment renders the virus replication-deficient whilst freeing space for insertion of a therapeutic transgene.

Chapter 1

Wild-type adenovirus capsid takes the form of an icosahedron, approximately 80 nm in diameter. Adherent to the capsid are penton subunits, from which project fibre protein. Studies have demonstrated the role of the knob protein engaging a specific coxsackie adenovirus receptor (CAR) on the cell surface (Bergelson et al 1997). Internalisation of the virus also depends on recognition of an RGD motif exposed on the penton base that interacts with cellular αV integrins (Wickham et al 1993). Interaction of the virus with the plasma membrane induces a number of signalling pathways including the Rho family of GTPases and the polymerisation and re-organistation of actin filaments to facilitate endocytosis (Li et al 1998; Rauma et al 1999). Once inside the cell, the adenoviral DNA is transported to an epichromosomal location within the nucleus (reviewed by Russell, 2000).

An efficient method for generating recombinant adenovirus deleted in E1 has been described by Professor Frank Graham's group at McMaster University, Hamilton, Ontario (Bett et al 1994; Graham et al 1991). The method was used to generate most of the adenovirus vectors used in this work (Sallenave et al 1998). Briefly, two plasmids were used to co-transfect the 293 cell line, an embryonal kidney cell line which produces E1 in *trans* (Graham et al 1977). One plasmid contains all adenoviral sequences required to produce infectious virus when transfected into the 293 cells with the important exception of the packaging sequence required for encapsidation of adenoviral DNA (Bett et al 1994). A second plasmid contains left-ended sequences less the E1 domain and part of the E3 domain which are not essential for viral replication (Haj-Ahmad et al 1986). The second plasmid contains a packaging signal, a promoter, a polylinker sequence and further short adenoviral sequences sharing homology with DNA in the first plasmid. Transgenes of interest of up to 8.3 kb in size can be cloned into the polylinker site. Homologous recombination occurs within the common segment shared by both plasmids when they are cotransfected into 293 cells resulting in an E1 deleted construct with transgene and packaging sequences. E1 products are provided in *trans* by the 293 cells facilitating production of a replication-deficient adenovirus.

Chapter 1

Following recombination, lytic plaques develop within the 293 cell culture as high yields of replication deficient adenovirus are produced. The process of homologous recombination is inefficient and can be improved through Cre-mediated site-specific recombination between two plasmids, each bearing a loxP site. Adenovirus vectors are generated as a result of Cre-mediated site-specific recombination between the two plasmids after their cotransfection into 293 cells expressing Cre recombinase. The frequency of adenovirus vector rescue by Cre-mediated site-specific recombination is significantly higher (approximately 30-fold) than by homologous recombination (Ng et al 1999). This approach was used to generate the murine SLPI vector used in this work.

Recombinant adenoviruses can infect efficiently both dividing and non-dividing cells including endothelial cells and smooth muscle cells both *in vitro* and after catheter-mediated delivery (Guzman et al 1993; Lee et al 1993). Adenoviral vectors do not integrate into the host genome, can be produced in high yield in the laboratory and are relatively stable (Hitt et al 1995). Wild type adenovirus has no association with malignancy and provides a favourable safety profile in humans, having been used to vaccinate military recruits (Gurwith et al 1989).

The biggest hurdle to successful adenoviral gene therapy is the host immune response preventing any form of prolonged transgene expression. The innate immune system recognises and responds to adenoviral infection. Adenoviral infection may lead to release of multiple chemokines that in turn recruit neutrophils invoking an inflammatory response in the liver or heart (Muruve et al 1999). Cytotoxic lymphocytes recognise neoproteins in complex with class I proteins of the MHC on the surface of infected cells (Yang et al 1994; Yang et al 1996a). This leads to perforin release and host cell lysis. Macrophages internalise adenovirus and present viral antigen in association with class II MHC, activating CD4 helper T cells and the adaptive wing of the immune response (van Ginkel et al 1997). Helper T cells can also facilitate proliferation of B cells and generation of both local and systemic

neutralising antibodies. Antibodies are directed against epitopes on the fibre and penton base and the efficacy of the humoral response depends on the nature of pre-existing immunity as well as the route and target of infection (Harvey et al 1999). The immune response may also be directed towards the transgene. The bulk of evidence for anti-adenoviral immunity has been generated from experiments in rodents and it is possible that different mechanisms may take precedence in human hosts.

1.8. An overview of gene therapy for atherosclerosis

1.8.1. Targets for gene therapy in atherosclerosis

Development of atherosclerotic vascular disease is slow, (usually) occurring over many decades and the clinical manifestations of obstructive arterial disease producing symptoms of angina and intermittent claudication or atherosclerotic plaque rupture leading to arterial occlusion and myocardial infarction occur late in the natural history of the disease. A preventive strategy could reduce disease progression by targeting risk factors such as hypercholesterolaemia and hypertension. This would require long-term gene expression either through stable transfection or repeated gene delivery.

Repair of the diseased vessel wall represents an alternative direction, inducing plaque regression or changing plaque properties making it is less 'vulnerable' or less prone to rupture (Naghavi et al 2003b; Naghavi et al 2003a). The processes occurring immediately following balloon angioplasty or stent deployment when arterial wall remodelling produces a proliferative vascular smooth muscle cell response with subsequent restenosis may also be considered targets for repair strategies.

37

Finally, in patients with advanced obstructive atherosclerotic disease the focus of treatment could move away from prevention or repair to creating new vessels. This approach is arguably the most ambitious of the directions outlined above. To date, gene therapy for angiogenesis in patients with coronary artery disease and peripheral limb ischaemia makes up the vast majority of human gene therapy trials in patients with atherosclerotic disease. In relation to the findings in this thesis, the following sections will examine the potential of gene therapy as a strategy to prevent and modulate atherosclerotic plaque development, drawing on animal studies and early clinical trials.

1.8.2. Lipid metabolism and risk factor modification

Inherited defects in lipid metabolism such as LDL receptor deficiency in familial hypercholesterolaemia culminate in premature ischaemic heart disease. Gene therapy approaches have focused on replacing normal LDL receptors in the liver. Adenoviral delivery of both the low density lipoprotein and very low density lipoprotein receptors led to correction of serum LDL cholesterol and slowed development of atheromatous changes in LDL receptor deficient mice (Ishibashi et al 1993; Kozarsky et al 1996). In both studies, therapeutic transgene effect was transient lasting less than 40 days as a result of immune responses against both adenovirus and transgene proteins. The first clinical trial used transplantation of autologous hepatocytes that had been genetically corrected with a recombinant retrovirus carrying the LDL receptor. Reductions of between 6% and 23% in plasma LDL levels were observed in 3 of the 5 patients (Grossman et al 1995). Susceptibility to atherosclerosis in humans is correlated inversely with plasma HDL and adenoviral overexpression of apolipoprotein A-1 led to increased HDL levels and a strong antiatherogenic effect for up to 10 weeks in atherosclerotic mice (Benoit et al 1999). Murine models have illustrated the feasibility of correcting genetic defects in lipid metabolism or augmenting factors to produce a more favourable lipid profile to slow progression of atherosclerosis.

Hypertension is a major risk factor for atherosclerosis and a significant cause of morbidity and mortality in its own right. A complex and multifactorial aetiology led some investigators to question the feasibility of gene therapy for this disorder. Overexpression of vasodilator genes including atrial natriuretic peptide and endothelial nitric oxide synthase (eNOS) reduced blood pressure over a 12 week period in hypertensive rats (Lin et al 1997; Lin et al 1998). In order to have an impact on atherosclerosis prevention in humans, gene expression would have to persist.

Hypertension and hyperlipidaemia are continuous variables and in most patients they equate to only a fraction of the total risk of future atherosclerotic related events. Correction of rare genetic deficiencies like familial hypercholesterolaemia aside, preventive gene therapy approaches for these disorders would entail treatment of large numbers of patients. Mechanisms would need to be devised to switch therapeutic gene expression off when the patient develops an intercurrent illness: for example. With improvements in vector design and increasing clinical experience with gene therapy this approach may become feasible in the future.

1.8.3. Protection and repair of the arterial wall.

Treatment and stabilisation of atherosclerotic lesions would entail either direct gene delivery to the arterial wall or, possibly, distant expression of a therapeutic transgene in skeletal muscle or the liver, the product of which could reach diseased vessels through the circulation. The hurdles for direct gene transfer to cells lining arterial vessels carrying blood under high pressure were outlined earlier. Modifications of vascular catheters will be required to facilitate juxtaposition of vectors against the endothelium for more prolonged periods and progress has been made in this area (Laitinen et al 2000; Sharif et al 2004).

39

Chapter 1

Cell proliferation is a prominent feature of atherosclerotic lesions. Gene therapy strategies directed at inhibiting vascular smooth muscle cell proliferation and migration, by interfering with intracellular transduction pathways, has been shown to be effective in retarding the development of intimal disease, particularly with respect to restenosis following angioplasty. Adenoviral overexpression of the cell cycle inhibitor p21 limited vascular smooth muscle cell proliferation and neointimal formation following arterial balloon injury in rats and pigs (Chang et al 1995; Yang et al 1996b). An alternative is to augment local production of endothelial factors that prevent VSMC proliferation and neointimal formation. Gene transfer of eNOS and PGI synthase inhibited luminal narrowing following balloon angioplasty (Numaguchi et al 1999; Varenne et al 1998).

Acceleration of re-endothelialisation following balloon injury was proposed by Isner's group as an approach to limit VSMC migration and proliferation (Losordo et al 2003). Periadventitial gene transfer of VEGF has been demonstrated to reduce neointima formation via a NO-mediated mechanism (Laitinen et al 1997). There is a close relationship between endothelial integrity and neointimal thickening in human coronary arteries (Davies et al 1988) and poor re-endothelialisation is associated with adverse outcomes following angioplasty (Gravanis et al 1989). This array of information has led to clinical trials of VEGF gene therapy with adenoviral vectors to prevent restenosis after coronary stenting. The phase II results have been reported indicating good safety and tolerability (Hedman et al 2003).

To date, all clinical studies and the majority of animal studies have examined gene delivery in the context of acute vessel injury during angioplasty and stent deployment. Genetic augmentation of protective factors to modulate atherosclerotic plaque development is an alternative preventive strategy, facilitating plaque regression and stabilisation. Augmentation of the anti-inflammatory cytokine IL-10 in LDL receptor knockout mice with adenovirus led to reduced atherosclerotic lesion formation following placement of perivascular Silastic collars (Der Thusen et al

40

2001). This effect was associated with reduced activation of monocytes and the unexpected finding of reduced serum cholesterol levels. Similarly, adenovirus mediated overexpression of platelet-activating factor-acetylhydrolase led to significant reductions in aortic arch atheroma in apoE mice (Quarck et al 2001). Systemic gene delivery of adiponectin an adipocyte derived anti-inflammatory cytokine, and TIMP-1 have both been demonstrated to reduce atherosclerotic development in murine models (Okamoto et al 2002; Rouis et al 1999).

All the preceding studies were based on adenoviral gene delivery to the liver with subsequent release of therapeutic transgene products into the circulation. Local production of gene products within the atherosclerotic lesion may be preferable and was achieved in part by adenovirus mediated heme-oxygenase-1 gene transfer to the arterial wall in apoE knockout mice through injection of adenovirus into the left ventricle of anaesthetised animals (Juan et al 2001).

Murine models of atherosclerosis have repeatedly been shown to be amenable to gene delivery or knockout strategies, often resulting in dramatic reductions in the rate of disease development and atherosclerotic burden. Earlier sections have alluded to the multiple growth factors, cytokines and proteases implicated in atherosclerosis and aetiological factors in humans may be more complex compared to the primarily lipid driven disease in murine models. There may be greater redundancy where multiple factors are involved giving rise to concern that genetic augmentation of a single factor would be less successful in humans.

The majority of large myocardial infarctions arise from thrombus development within the proximal third of one of the three main coronary arteries (Wang et al 2004) and these regions can readily be accessed by cardiac catheterisation. Improved methods for assessing the composition of atherosclerotic plaques will be required to assess when reparative treatments are required and to monitor treatment response.

41

Chapter 1

Quantitative coronary angiography effectively identifies fixed obstructive stenoses but development in additional imaging modalities such as intravascular ultrasound (Newby et al 2002) will be required to identify vulnerable plaques, the target of therapy.

1.9. Summary

This introduction highlights the importance of oxidised low density lipoprotein as a central cause at all stages of atherosclerotic plaque development. Inflammatory chemokines and proteases produced within the artery wall are instrumental in the inflammatory changes that occur. The hypothesis that elafin augmentation may reduce endothelial cell and macrophage inflammatory responses to atherogenic stimuli was introduced. Finally, the rationale for gene delivery as a treatment for coronary artery disease was outlined.

2.0. Aims

The principal aim of the experiments cited in succeeding chapters is the identification of mediators of damage and repair in atherosclerosis The initial aim, after establishing an *in vitro* model of endothelial cell injury, is to identify novel candidates exhibiting altered expression through gene expression profiling of endothelial cells incubated with oxidised LDL. A further aim is to establish whether overexpression of the protease inhibitors elafin and SLPI could attenuate the inflammatory responses to atherogenic stimuli of human endothelial cells and macrophages.

The experiments described in chapter 3 and 4 seek to characterise the *in vitro* model of atherosclerosis. The work in chapters 5 and 6 is directed towards developing protocols for adenoviral gene delivery to endothelial cells and

42

macrophages and establishing the anti-inflammatory actions of elafin (and SLPI) overexpression.

43

Chapter 1

CHAPTER 2

MATERIAL AND METHODS

2.1. Materials

2.1.1. Source of chemicals and reagents

Unless stated otherwise, chemicals and reagents were obtained from Sigma, Poole, UK

2.1.2. Native and oxidised LDL

Human plasma was obtained from the Department of Transfusion Medicine, Royal Infirmary of Edinburgh. LDL isolation and oxidation was performed by Professor Rudolph Riemersema (Cardiovascular Research Unit, University of Edinburgh). LDL was isolated by sequential ultracentrifugation, followed by dialysis against PBS and 0.2 g/L chelex (pH 7.4). The LDL was oxidised against $CuCl_2$ and the degree of oxidation was monitored by the formation of conjugated dienes at 234 nm (Lewin et al 2002). At maximum absorbance (usually 60-90 min after initiation) oxidation was terminated by the addition of 10% excess EDTA. Both native and oxidised LDL were concentrated in an ultrafiltration unit (Amicon 52, Millipore (UK) Limited, Watford, UK) using polyethersulfone membranes (Dia:44.5 mm-NMWL: 30 000, Millipore) to yield 5 ml of concentrated material. Traces of Cu^{2+} were then removed by gel filtration chromatography over a Sephadex G25 column (PD-10, Amersham Pharmacia, Uppsala, Sweden). Protein concentrations were measured by the Lowry method (Fryer et al 1986).

44

2.1.3. Adenoviral Constructs

Production and purification of adenoviral vectors was not part of the experimental work in this thesis. All adenovirus vectors described below were available in-house or were obtained or produced in collaboration with other workers during the course of this work.

2.1.3.1. Ad-elafin

The Ad-elafin vector was produced as described by Sallenave et al (1998). Briefly, full length elafin cDNA (538 bp) was obtained by RT-PCR from total RNA extracted from bronchial epithelial cell line NCI-H322. Elafin cDNA was cloned into a shuttle plasmid (pDK6) containing adenovirus type 5 sequences from 0-1 mu and 9.8-15.8 mu, a polyadenylation signal and a 1.4 kb fragment from the murine cytomegalovirus (mCMV) promoter. The resulting plasmid was cotransfected with pBHG10 in 293 cells. PBHG10 lacks a packaging sequence and is partially E3-deleted (i.e. it contains the entire Ad5 gene sequence apart from 0.5-3.7 mu and 78-85.6 mu). Homologous recombination resulted in E1, partially E3-deleted adenovirus encoding elafin cDNA downstream of the mCMV promoter. Plaque forming unit and particle concentrations from the batch of virus used were as follows; 4.8×10^{10} pfu/ml, 5.3×10^{12} particles/ml.

2.1.3.2. Ad-murine SLPI (Ad-mSLPI)

Cloning of mSLPI cDNA was performed in the lab by other investigators. Briefly, fresh lung from a murine C57Bl6/CBA hybrid was obtained, snap-frozen in liquid nitrogen and total RNA was prepared using Trizol reagent as a template for mSLPI RT-PCR. Amplified products were then analysed on 0.8 % agarose gels, cut from the gel and purified and ligated by conventional methods into pGEM T-easy (Promega, Southampton, UK). An EcoR1 mSLPI cDNA digest was then subcloned into pDK6. The correct orientation was assessed and sequencing performed to rule

out any unwanted mutagenesis. Further directional cloning was performed by subcloning the XbaI-EcoRV mSLPI cDNA fragment into NheI-EcoRV digested pIRESGFP2 (gift from Drs F. Graham and R.Marr, McMaster University, Ontario, Canada) to generate pIRESmSLPI-GFP2. Ad-mSLPI was prepared by Mrs Alyson Harris in collaboration with Dr Mary Hitt, McMaster University. pIRES-mSLPI-GFP2 and pBHGloxΔE1,3Cre were used to cotransfect 293 cells. Cre mediated site specific recombination resulted in the generation of E1, E3-deleted adenovirus encoding mSLPI and green fluorescent protein (Ng et al 1999a). Plaque forming unit and particle concentrations from the batch of virus used were as follows; 6.1×10^{10} pfu/ml, 7.8×10^{12} particles/ml.

2.1.3.3. Ad-murine eotaxin (Ad-meotaxin)

The Ad-meotaxin vector was prepared by Professor Zhou Xing's team, McMaster University. m-eotaxin cDNA was amplified by RT-PCR from total RNA extracted from female Balb/c murine lung that had been subjected to induced allergic airway eosinophilia (Xing et al 1996). An 800-bp EcoRI/BamHI fragment of full-length m-eotaxin was ligated into the multicloning site of the shuttle vector pDK6 to generate pDK6-meotaxin. The pDK6m-eotaxin plasmid was co-transfected into 293 cells along with the rescuing vector pBHG10. Homologous recombination resulted in the generation of E1, E3-deleted adenovirus encoding m-eotaxin under the control of the mCMV promoter. Plaque forming unit and particle concentrations from the batch of virus used were as follows; 1.7×10^{10} pfu/ml, 5.6×10^{12} particles/ml.

2.1.3.4. Ad-IκBα, Ad-dl703 and Ad-GFP

The construction of the vector expressing a mutant form of IκBα protein (the super repressor where serines 32 and 36 are replaced by alanine residues, therefore preventing inducible IκBα phosphorylation) has been described before (Jobin et al 1997). The Ad-IκBα vector differs from the other vectors used in that it contains the

46

Chapter 2

human CMV promoter. Ad-IκBα was a kind gift from Dr R. Balfour Sartor, University of North Carolina, NC, USA. The generation by homologous recombination of an empty viral vector containing deletions in the E1 and E3 regions, using the same protocol as for Ad-elafin has been described previously (Bett et al 1994). Ad-GFP was also an E1, E3 deleted serotype 5 adenovirus encoding the green fluorescent marker protein. Ad-dl703 and Ad-GFP were kindly provided by Professor Jack Gauldie and Dr Mary Hitt, McMaster University. Plaque forming unit and particle concentrations from the batches of viruses used were as follows; Ad-IκBα-3.5× 10^{10} pfu/ml, 5.6× 10^{11} particles/ml; Ad-dl703-2.7× 10^{11} pfu/ml, 2.1× 10^{12} particles/ml; Ad-GFP-1.1× 10^{10} pfu/ml, 7.3× 10^{11} particles/ml.

2.1.4. Recombinant human elafin

A truncated recombinant human elafin (57 amino acids in length, H_2N-$^{39}AQE...^{95}Q$-OH, approximately 6kDa, representing the COOH-terminus of pro-elafin) was available in-house and was originally a kind gift from Dr J Fitton, ICI Pharmaceuticals, Macclesfield, UK.

2.1.5. Primers

The primers chosen for sense (3'-5') and antisense (5'-3') respectively were for human angiopoietin-2 (GenBank™ accession number AF004227) ggatctggggagagaggaac and ctctgcaccgagtcatcgta (535 base pair product); for human IL-8 (GenBank™ accession number Y00787) aatgagagtggaccacactgcgcc and cactgattcttggataccacagag (181 base pair product); for human midkine (GenBank™ accession number M69148) caaggattgcggcgtgggtttccg and tgtgacaccaggggctccttggca (323 base pair product); for human matrix metalloprotease-1 (MMP-1) (GenBank™ accession number X05231) ttgccaagagcagatgtggac and gctgaacatcaccactgaagg (369 base pair product); for human GAPDH (GenBank™ accession number M33197) ccacccatggcaaattccatggca and tctagacggcaggtcaggtcaacc (599 base pair product); for

47

Chapter 2

human HPRT (GenBank™ accession number V00530) acattgtagccctctgtgtgctca and gcgaccttgaccatctttggatta (300 base pair product). IL-8 and GAPDH primers were kind gifts from Dr Nik Hirani Rayne Laboratory, University of Edinburgh. All other primers were ordered from MWG Biotech, Ebersberg, Germany.

2.1.6. IL-8 promoter constructs

The IL-8 promoter constructs were based on the pXP2 vector and were a kind gift from Professor Naofumi Mukaida, Cancer Research Institute, Kanazawa University, Japan. XL-1 Blue bacteria were transformed with the plasmids using a heat shock protocol as follows. Plasmid DNA (500 ng) was added to a 50 μl suspension of XL-1 Blue bacteria and incubated on ice for 20 min. The mix was then heated at 42 °C for 45 s and returned to ice for a further 2 min. SOC medium (900 μl) was added to the mix and incubated at 42 °C for 5 min. The mix was then incubated at 37 °C in a shaker for 30 min. The mix (100 μl) was plated out on an LB plate containing ampicillin as a selection antibiotic. The LB plate was incubated at 37 °C over night and colonies were picked for maxi-prep (see section 2.2.4.6.) the following day.

2.1.7. Source of other reagents used

Oxidised LDL and native LDL obtained commercially were from Intracel Corporation, Rockville, MD, USA.

Panorama Cytokine Gene Arrays and specific Human Cytokine Labelling Primers were form Sigma Genosys, Haverhill, UK.

Penicillin-streptomycin, trypsin-EDTA, Trizol, and Iscove's medium were from Gibco BRL, Paisley, Scotland, UK.

Endothelial cell growth medium-2 and growth factor bulletkit were from Clonetics, Biowhittaker, Wokingham, UK.

48

Chapter 2

X-Vivo 10 serum-free medium was from Cambrex, Nottingham, UK

Dextran and Percoll were from Pharmacia, Uppsala, Sweden.

HNE was from Elastin Products, Owensville, MO, USA.

LPS (from *E. coli* 0127:B8 in all experiments) was from Difco laboratories, Detroit, MI, USA.

The Celltiter 96 One Solution cell Proliferation Assay and Cytotox 96 non-radioactive cytotoxicity assay were obtained form Promega, Southampton, UK.

Iononmycin was obtained from Calbiochem, Nottingham, UK.

Nitrocellulose membrane was from Millipore, Watford, UK.

Dried skimmed milk was from Marvel, Premier Brands UK, Moreton, UK.

Western Lightning Chemiluminescence Reagent Plus (ECL) was from Perkin-Elmer Life Sciences, Cambridge, UK.

ELISAs for human IL-8, TNF-α and MCP-1 were from R&D Systems, Abingdon, UK.

The assay for protein concentration was NHS-LC-Biotin kit from Pierce, Rockford, IL, USA.

Diff-quik was from Dade Diagnostika, Germany.

Normal Goat serum was from the Scottish Antibody Production Unit, Edinburgh, UK.

The Limulus amebocyte lysate assay for detecting LPS was from Chromogenix, Charleston, SC, US.

49

Chapter 2

2.1.8. Plastic Ware

All tissue culture plates were from Corning Costar, Cambridge, MA, USA. Polyurethane intravenous venflon cannulas were obtained form Becton Dickinson Ltd, Oxford, UK. Falcon tissue culture material was from A. & J. Beveridge Edinburgh, UK.

2.2. Methods

2.2.1. Cell Culture

2.2.1.1. Preparation and culture of human umbilical vein endothelial cells (HUVECs).

Ethical approval was obtained from Lothian Research and Ethics Committee (LREC No. 2001/R/UO/01) for the procurement of human umbilical veins from healthy term pregnancies during elective caesarean sections (Appendix I). The preparation of HUVECs has been described previously (Gimbrone, Jr. et al 1974). Human umbilical cord was collected in a container in PBS and transferred on ice to the laboratory. The cord was clamped at one end and the vein was cannulated at the other using an 18 gauge intravenous cannula (Venflon, Becton Dickinson Ltd, Oxford, UK). A solution containing collagenase type IV (0.1%) in PBS was infused (approximate volume 5ml) into the vein and the cord was clamped, with cannula in situ, at both ends. Following a 20 min incubation at 37 °C, the cord was gently massaged and the distal clamp was released. The vein was flushed through with sterile PBS and the effluent containing HUVECs was collected. The effluent was centrifuged at $700 \times g$ for 6 min at room temperature and the cell pellet was resuspended in 10 ml of EBM-2 culture medium. The cells were allowed to adhere for 6 hours to a T75 culture flask before replenishment with 15 ml of fresh medium. On average cells from a cord preparation would take around 5-6 days to grow to confluence in a T75 flask with this protocol. Cells were grown in EBM2 culture medium containing growth supplements at 37 °C, 5 % CO_2. Medium was changed every other day and cells were not grown beyond 5 passages.

2.2.1.2. Preparation of peripheral blood-mononuclear cells

Mononuclear cells were isolated from peripheral blood as described (McCutcheon et al 1998). Freshly citrated blood was centrifuged at $400 \times g$ for 20 min and the platelet-rich plasma supernatant was used to prepare autologous serum by addition of $CaCl_2$ (10 mM final concentration). Leukocytes were isolated after removal of erythrocytes by sedimentation using 6 % (w/v) dextran T500 in saline by fractionation on a discontinuous gradient of isotonic Percoll solutions made in Ca^{2+}/Mg^{2+}- free PBS (CMF-PBS). Percoll concentrations of 55 %, 68 % and 79 % were used and the leukocytes were centrifuged at $700 \times g$ for 20 min. Mononuclear cells were aspirated from the 55 %/68 % interface and washed three times in CMF-PBS prior to culture. Monocytes were enriched from the mononuclear fraction by selectively attaching them to 48 or 12-well plates for 40 min at 37 °C. Non-adherent lymphocytes were removed and adherent monocytes were washed twice in PBS. Monocytes were then cultured in Iscove's modified DMEM containing 10 % autologous serum, penicillin G (final concentration 100 U/ml) and streptomycin sulphate (final concentration 100 µg/ml). For serum-free experiments, cells were cultured in X-vivo 10 serum-free medium with antibiotic. Incubator conditions were the same as for HUVECs. Maturation into macrophages with this culture protocol has previously been demonstrated using myeloid specific markers including CD16 and CD51/CD61 (McCutcheon et al 1998).

2.2.1.3. Preparation of A549 cells

A549 cells (Lieber et al 1976) were available in-house. Cells were suspended in DMEM containing 10% FCS, penicillin G (final concentration 100 U/ml), streptomycin sulphate (final concentration 100 µg/ml) and L-glutamine (2 µM) before seeding onto multi-well plates or culture flasks. Incubator conditions were the same as for HUVECs.

Chapter 2

2.2.1.4. Preparation of apoptotic Mutu I cells

The group I Burkitt lymphoma cell line Mutu I, is an established target cell for macrophage interaction assays (Devitt et al 1998) and was available in house. The Mutu I cells were induced into apoptosis by 16h incubation with 1 μg/ml of the calcium ionophore ionomycin.

2.2.2. Gene transfer protocols

2.2.2.1. Transfection of HUVECs with plasmid DNA: calcium precipitate method

HUVECs were grown in 6-well Costar plates to 60% confluence in usual growth medium. The dsRed2 plasmid (kindly provided by Dr J King, from our group) encoding red fluorescent protein was used to establish the efficiency of transfection. DNA (3 μg) was mixed with 4.3 μl 3 M $CaCl_2$ to a final volume of 64 μl. The mixture was diluted with 2 × Hank's Balanced Salt Solution, vortexed for 15 s and allowed to stand for 1 min before being vortexed again and added to 1 ml DMEM containing 10 % FCS. The precipitates could be visualised under light microscopy over the surface of the HUVEC culture. DMEM containing the precipitates was incubated with the HUVECs for 5 h, removed and replenished with usual growth medium. The cell culture was examined for red fluorescence at 14 and 24 h.

2.2.2.2. Transfection of HUVECs with plasmid DNA: lipofectin method

HUVECs were grown in 6-well Costar plates to 60% confluence in usual growth medium. 1 μg of DNA was diluted in 100 μl OptiMEM I reduced serum medium (Invitrogen, Paisley, UK). 6 μl of Lipofectin reagent (Invitrogen) was mixed in 100 μl of OPTI-MEM medium and the 2 solutions were combined and mixed gently with a Gilson pipette at room temperature for 15 min. A further 800 μl OptiMEM I was added directly to the mix, the cell culture was washed once with OptiMEM I and the mix was applied for 2 h before removing and replenishing with

usual medium. The cultures were examined for red fluorescence according to the protocol above.

2.2.2.3. Adenoviral infection of HUVECs, macrophages and A549 cells.

All adenoviral work was performed in the Adenoviral Facility Class II Ventilation Hood. Adenoviral infections were initially performed without precomplexing. Adenovirus was incubated with the cells for 2 h in the usual culture medium for each cell type before removing and replenishing with fresh medium.

2.2.2.3.1. Adenovirus infection in association with calcium precipitates

Calcium precipitates were generated in Eagle's MEM (Sigma). This contains Ca^{2+} (1.8 mM) and PO_4^{2-} (0.86 mM). Calcium chloride (stock solution 2.5 M) was added to Eagle's MEM (serum-free) to increase the Ca^{2+} concentration to form calcium phosphate precipitates. Unless indicated otherwise the final total concentration of Ca^{2+} ion used for precipitate formation was 8.3 mM. Adenovirus was precomplexed in the Eagle's MEM precipitate suspension for 15 min with gentle mixing at room temperature before adding to the cell culture. Adenoviral infections were performed (200 μl volume) on HUVECs and A549 cells grown to confluence in 48-well Costar plates. Macrophages were also matured on 48-well Costar plates and infected on culture day 6 (following initial plating of 4×10^6 mononuclear cells on day 1). Adenoviral incubations were for 2 h unless stated otherwise.

2.2.2.3.2. Adenovirus infection in association with lipofectamine

HUVECs and A549 cells were grown to confluence and one well was used for cell count determination. Adenovirus vectors were pre-incubated for 15 min at room temperature in OptiMEM I reduced serum medium (Invitrogen) with lipofectamine (Invitrogen) at a ratio of 5×10^4 lipofectamine molecules to each adenovirus particle. Particle concentration was determined from absorbance at 260 nm for each

Chapter 2

adenovirus construct according to published protocols (Maizel, Jr. et al 1968). HUVECs and A549s were incubated in the virus-containing medium for 2 h before replenishment with their respective usual growth media. Peripheral blood derived macrophages were infected using the same protocol on culture day 4 before replenishment with normal growth medium

2.2.3 Cell based assays

2.2.3.1. Flow cytometric analysis of CD31 and annexin V in HUVECs.

HUVECs were cultured in 12-well Costar plates. Culture medium was removed and the cells were washed with PBS before being detached with trypsin. For CD31 staining, the cells were pelleted ($1000 \times g$ for 5 min) and resuspended in PBS (100 μl) in polystyrene round bottom test tubes (BD Falcon). This step was repeated and 1 μl of phycoerythrin conjugated murine anti-human CD31 IgG (BD PharMingen, Oxford, UK) or FITC conjugated murine anti-human polyclonal IgG (BD Pharmingen), as control, was added to the cell suspension. The antibody cell suspension mix was incubated at room temperature for 30 min prior to analysis with FACS analysis (FACSCalibur, BD Biosciences, San Jose, US).

Phosphatidylserine translocation, a process ocurring early in apoptotic cell death and later in both apoptotic and necrotic cell death was analysed by annexin V staining after incubation with stimulus (Vermes et al 1995). Cells were washed with PBS and trypsinised as above. Following a further wash, they were pelleted again and resuspended in Hanks' Balanced Salt Solution (HBSS: 200 μl) containing $CaCl_2$ (5 mM) and FITC conjugated Annexin-V-FLUOS (Boehringer-Mannheim Biochemicals, Mannheim, Germany: diluted 1 μl in 3 ml HBSS). Control cells were incubated in HBSS alone. Incubations were performed on ice for 5 min before FACS analysis (FACSCalibur).

Chapter 2

2.2.3.2. Measurement of cell lysate luciferase activity

HUVECs were cultured to 60% confluence in 12-well Costar plates. Transfections with the IL-8 promoter-luciferase plasmids were performed with lipofectin according to the protocols described except that a transfection volume of 500 µl was used. The pGL3 plasmid encoding luciferase under the control of the SV40 promoter (Promega, kind gift from Dr Karen Chapman, Molecular Medicine Centre, University of Edinburgh) was also transfected as a positive control. Cells were cultured for 48 h following transfection and stimuli (TNF-α, PMA, oxidised LDL and LPS) were added for a period of 8 h. Cells were then lysed in ice cold cell lysate buffer (Tris base adjusted to pH 7.8 with phosphoric acid, 8 mM $MgCl_2$, 1 mM DTT, 1% Triton $\times$ 100, 15% Glycerol). Lysates were centrifuged at 12 000 $\times$ g for 5 min and supernatants removed for analysis of luciferase activity. The assay was performed on a Luminometer (Lumac, Biocounter M2500, MWG). The Luminometer injected luciferin reagent (1 mM ATP, 0.25 mM Luciferin, 1% bovine serum albumin in lysis buffer) into a 50 µl assay volume and the mean of 3 recordings was calculated from each sample.

2.2.3.3. Lactate dehydrogenase assay

The CytoTox Non-radioactive Cytotoxicity Assay (Promega) quantitates lactate dehydrogenase (LDH) released into culture supernatants upon cell lysis. LDH activity is measured through formation of a coloured product following hydrolysis of o-nitrophenyl-β-D-galactopy-ranoside. The colour intensity measured at 420 nm is proportional to the number of lysed cells. This technique is sensitive for LDH release and has been used previously to quantify cell death after treatment with cytotoxic agents and can indicate low levels of cell membrane damage missed using other approaches (Decker et al 1988). Assays were performed according to manufacturer's protocol with a spectrophotometer (MR5000 Plate Reader, Dynatech, Dynex, Billinghurst, UK). Supernatant LDH activity was expressed (after correction for background within the culture medium) as a percentage of the activity resulting from total cell lysis produced using 1% Triton X-100.

2.2.3.4. Cell Titer Aqueous One Solution Cell Proliferation Assay

This assay uses a tetrazolium compound and electron coupling agent (phenazine ethosulfate; PES). The MTS tetrazolium compound is reduced by cells into a coloured formazan product that is soluble in tissue culture medium. Production of the coloured agent can be measured directly by recording absorbance at 490 nm. This reduction is mediated by NADPH and NADH produced by dehydrogenase enzymes in metabolically active cells. The assay can reliably discriminate changes in viable cell number caused by proliferation *or* necrotic and apoptotic cell death (Cory et al 1991). The reduction of the tetrazolium compound is also affected by interference with cell mitochondrial activity (Berridge et al 1993). In experiments examining the effects of HNE incubation on viable cell number, cells were exposed to HNE for 24 h. HNE-containing culture medium was then replenished with fresh culture medium and 20 μl of Cell Titer Aqueous One Solution reagent was added and incubated at 37 °C for a further 4 h. Absorbance was then measured directly at 490 nm. Results are presented after correction for absorbance from medium alone.

2.2.3.5. Elafin ELISA

The ELISA was performed on 96-well plastic plates. Wells were coated overnight at 4 °C with anti-elafin IgG in carbonate buffer, pH 9.6 (final concentration IgG 7.7 μg/ml), with the exception that blank wells received buffer alone. The plate was washed with wash buffer (0.1% Tween-20 in PBS, pH 7.4). Gelatin (final concentration 1% in PBS, pH 7.4) was added to all wells (as a blocking agent) for 2 h at 37 °C and the plate washed with wash buffer, prior to addition of samples and standard. Standards comprised recombinant human elafin diluted in 1% gelatin and were applied in duplicate at a dose range from 0.5 to 30 ng/ml (blanks received 1% gelatin alone). Samples were serially diluted in 1% gelatin and for each sample 2 different dilutions were applied in duplicate. The volume of each standard and sample was 100 μl, and incubation proceeded for 2 h at 37 °C, after which all wells were washed with wash buffer. Anti-elafin IgG, biotinylated using an NHS-LC-Biotin kit was diluted in 1% gelatin and added to each well (except blanks which

56

received 1% gelatin alone) for 2 h at 37 °C. The plate was then washed with wash buffer. Streptavidin-biotin-horeseradish peroxidase complex (final concentration 10 ng/ml in 1% gelatin) was added to each well (except blanks which received 1% gelatin alone) for 2 h at 37 °C. The plate was washed with wash buffer. Substrate (comprising 0.006% H_2O_2 and 1mg/ml 2,2'azino bis 3-ethyl benzthiazolidine sulfonic acid, in 0.1M citric acid, pH 4.0) was added to all wells and absorbance against elafin concentration in samples determined by extrapolation from the curve.

2.2.3.6. Staining of macrophages and HUVECs for β-galactosidase

Macrophages and HUVECs infected with Ad-βGal were fixed for 10 min at room temperature in a solution comprising 0.2% glutaraldehyde, 0.8% formaldehyde and 2 mM $MgCl_2$ in PBS. Fixative was discarded and 200 µl of staining solution was added for 5 h at 37 °C (staining solution comprised 5 mM $K_4Fe(CN)_6$, 2 mM $MgCl_2$, 0.05% Triton X-100, 0.5 mg/ml X-gal, in PBS). Cells were washed with PBS to remove residual stain, air dried and photographed.

2.2.3.7. IL-8, MCP-1 and TNF-α ELISAs

Culture supernatants were collected and either used in an assay directly or frozen at - 20 °C. The human IL-8, MCP-1 and TNF-α ELISAs were commercial kits (R&D Systems, Abingdon, UK) containing optimised capture and biotinylated detection antibody pairs along with recombinant protein standard and manufacturer's protocols were followed.

2.2.3.8. Limulus Amebocyte Lysate Assay for LPS contamination

The COAMATIC Chromo-LAL kit was purchased (Chromogenix, Milan, Italy). This contained extract from the blood cells of the horseshoe crab, *L. polyphemus*. This extract contains enzymes that are activated in a series of reactions in the

presence of LPS. The last enzyme activated in the cascade splits the chromophore, para-nitro aniline (pNA) producing a yellow colour. Samples were diluted in endotoxin free water (Chromogeneix), transferred to a microplate (100 µl) at 37 °C and the Chromo-LAL reagent (containing lysate and chromogen) was added to each well (100 µl). The microplate was then placed in a plate reader and LPS content was calculated from the change in absorbance at 405 nm plotted against time. Endotoxin standard (*Escherichia coli* 0113:H10, Chromogeneix) was used to produce a standard curve to estimate LPS contamination in endotoxin units.

2.2.4. RNA based assays and plasmid preparation

2.2.4.1. Preparation of total RNA from HUVECs

RNA for semi quantitative RT-PCR and the miniarray experiments was prepared using TRIzol reagent (Gibco BRL). TRIzol reagent is a monophasic solution of phenol and guanidine isothiocyanate and works through disrupting cell membrane while maintaining the integrity of RNA (Chomczynski 1993). TRIzol was added directly to HUVECs cultured in multi-well plates following removal of culture medium (600 µl for 48-well plates, 800 µl for 24-well plates and 1 ml for 6-well plates). The samples were transferred to Eppindorf tubes and chloroform was added to produce phase separation (0.2 ml of chloroform was added per 1 ml of TRIzol) and the mix was centrifuged at 12000 × *g* at 4 °C for 10 min. The colourless upper aqueous phase was transferred to a fresh eppindorf with care taken to avoid disturbing the interphase. RNA precipitation was performed with isopropyl alcohol (IPA, 0.5 ml of IPA per ml of TRIzol) for 30 min at –20 °C. A further centrifugation (12000 × *g* at 4 °C for 10 min) was performed. The aqueous phase was removed from the eppindorf leaving a visible pellet against the side of the eppindorf tube. This was washed with a 75% ethanol/DEPC water solution, gently agitated and centrifuged again at 7500× *g* for 5 min. The 75% ethanol/DEPC water was removed and the eppindorf was inverted and allowed to dry for 5 min. The pellet was then dissolved in between 50 and 100 µl of DEPC water. RNA integrity was checked by

58

assessing the ratio of 28s to 16s subunits on a 1% agarose gel. A ratio of greater than or equal to 2 was taken to indicate absence of significant degradation. RNA was quantified by measuring the absorbance at 260 nm in a spectrophotometer and concentration was calculated from the formula (OD_{units} × dilution factor × 40 µg/ml). Protein contamination was considered to be absent if the 260nm/280nm absorbance ratios were between 1.6 and 1.9.

2.2.4.2. Miniarray protocols

2.2.4.2.1. Prepartion of labelled cDNA

Total RNA form untreated native LDL and oxidised LDL treated cells (2 µg) was mixed with Human Cytokine cDNA Labelling Primers (4 µl) and diluted to 15 µl with DEPC water. The primers were annealed by incubating at 90 °C for 2 min and then programming a temperature ramp to 42 °C over 20 min. Once the thermal cycler (MJ Research, DNA Engine, MJ Research, Ma, US), had reached 42 °C the components for cDNA synthesis and labelling were added as follows; RT buffer (6 µl of 5× buffer), dATP, dGTP, dTTP (all 333 µM) and dCTP (1.67 µM) along with 20 µCi [α-^{32}P] dCTP (3000 Ci/mmol), 20 U ribonuclease inhibitor and 50 U AMV reverse transcriptase to a final volume of 30 µl with DEPC water. The mix was pippetted carefully and incubated for 3 h. Unincorporated label was removed by purification over a Sephadex G-25 gel filtration column centrifuged at × 1100g for 4 min. A 0.5 µl sample was taken before and after purification for determination of percent incorporation on a scintillation counter. Labelled nucleotide incorporation was between 20 and 30 %.

2.2.4.2.2. Hybridisation and array analysis

The arrays were rinsed in 50 ml of 2 × SSPE (0.18 M NaCl, 10 mM sodium phosphate pH7.7, 1 mM EDTA) at room temperature for 5 min. Incubations with 5

Chapter 2

ml hybridisation solution (5 × SSPE, 2% SDS, 5 × Denhardt's reagent, 100 μg/ml sonicated denatured salmon testes DNA) were performed at 65 °C in a hybridisation oven for 60 min rotating at 6 r.p.m. Labelled sample (cDNA) was denatured with a 10 min incubation at 95 °C, suspended in 5 ml hybridisation solution and incubated with the array in the hybrisdisation oven for 14 hr. The hybridisation mix was then decanted and the array washed for 2-3 min by gently agitating in 20 ml of wash solution I (0.5 × SSPE, 1% SDS). This step was repeated 3 times and then a further 3 times with a more stringent wash solution II (0.1 × SSPE, 1% SDS). The final wash with wash solution II was for 20 min. The wash solution was discarded and the array removed form the hybridisation bottle and placed onto blotting paper. After 2 min exposure to air it was wrapped in plastic food wrap and exposed to a phosphor screen (Molecular Dynamics, Sunnyvale, Ca, US) for 14 hr. The phosphorimaging was performed with a Storm 860 phosphorimager and ImageQuant software (Molecular Dynamics). Scanning resolution was set at 50 μM and a quantitation template was set up to analyse pixel intensity for each spot of the array. Background signal was selected from a clear area of the array and subtracted from each spot. Signal values were exported to a spreadsheet (Microsoft Excel) and average signal intensity was determined for each duplicate spot pair representing a gene. A simple normalisation approach of comparing housekeeping gene expression between arrays was employed to account for differences in hybridisation efficiency and sample loading. Normalised signals were then compared between different array hybridisations to determine fold change in gene expression between the different samples.

2.2.4.2.3. Washing and repeat hybridisation with the miniarray

The nylon miniarrays were stripped and used again once only. The arrays were placed together in a boiling stripping solution (10 mM Tris-HCL, pH 8.0, 1 mM EDTA, 1% SDS) in an autoclaved pyrex flask on a hot plate for 20 min. The stripping solution was drained off and the arrays were covered with plastic food wrap and re-exposed against the phosphor screen to check that signal had been removed. The arrays were stored at -20°C between hybridisations.

Chapter 2

2.2.4.3. Semi-quantitative reverse transcription polymerase chain reaction

Total RNA was isolated from HUVECs as described in section 2.2.4.1. For IL-8 semiquantitative RT-PCR, 0.35μg of total RNA was reverse transcribed. For other RT reactions 1μg of total RNA was used. RNA was heated to 93°C for 5 min and added to the mix containing 3.0 mM $MgCl_2$, 0.5 μg oligodT, 16 U RNasin, 1 mM of each dNTP and 200 U of Moloney murine leukaemia virus (MMLV) reverse transcriptase (all Promega) to a total volume of 20 μl. The mix was incubated at 42 °C for 45 min and then heated at 95 °C for a further 5 min. For PCR a 30 μl reaction containing 3 μl cDNA, 0.2 mM of each dNTP, 2 mM $MgCl_2$, 1.5 U Taq polymerase (all Promega) and 1 μM each oligonucleotide primer was subjected to the following temperature cycles; denaturing at 95 °C for 30 s, annealing at 55 °C for 1 min and extension at 72 °C for 1 min for 35 cycles with a final 5 min extension period. For IL-8 semiquantitative RT-PCR, GAPDH was used as a reference with GAPDH primers (0.5 μM) added in a multimix with IL-8 primers (1 μM). Temperature cycles of 95°C for 30s, 60°C for 1 minute and 72°C for 1 minute for 31 cycles were performed.

Semi-quantitative RT-PCR for Ang2 was performed using the housekeeping gene, HPRT as reference. Briefly, 1 μg of total RNA was used in the RT reaction (37 ^{0}C for 45 min) with 0.5 μg oligo dT, 0.1 mM of dNTPs, 10 U/μl of reverse-transcriptase (MMLV) and 1 U/μl of RNAsin in PCR buffer containing 3 mM of $MgCl_2$. After a 5 min incubation at 95 ^{0}C, 2 μl of RT-mixture was added for PCR (final volume 28 μl of PCR buffer: 1 ng/μl of reverse and forward primers, 0.03 U/μl Taq polymerase, 0.5 mM $MgCl_2$).

Amplifications of HPRT and Ang2 were carried out for 26 and 30 cycles respectively in a thermal cycler (MJ Research, DNA Engine), using the following conditions for each cycle; 94 ^{0}C for 30s, 55 ^{0}C for 60 s, 72 ^{0}C for 60 s. These cycle

61

numbers had previously been determined to allow quantification within the curvilinear phase of PCR amplification. PCR products were analysed on a 1.2% agarose gel with ethidium bromide staining and densitometry was performed using a gel documentation system (Ultra Violet Products, Cambridge, UK).

2.2.4.4. Northern blotting for angiopoietin-2, midkine, MMP-1 and HPRT

Angiopoietin-2, midkine, MMP-1 and HPRT cDNA generated by PCR were used to amplify cDNA for use as template to produce radiolabelled cDNA probe for Northern blotting. cDNA bands were cut out of agarose gels with a scalpel and purified using the QIAquick Gel extraction kit (Qiagen, Crawley, UK). Excess agarose was trimmed away and the gel slice containing the cDNA was weighed. 3 volumes of Buffer QG (Qiagen) were added to 1 volume gel and incubated (50 °C for 10 min) until the gel slice was solubilised. Isopropanol (1 gel volume) was added and the mixture was applied onto a spin column containing a DNA binding resin (QIAquick spin-column) and centrifuged (17000 × g for 1 min). The flow through was discarded and a further centrifugation was performed with Buffer QG (0.5 ml) to remove all trace of agarose. The centrifugation was repeated with wash Buffer PE (0.75 ml, Qiagen), the flow through discarded and a further centrifugation performed to remove all trace of alcohol. The QIAquick spin-column was placed into a fresh centrifuge tube and DNA was eluted from the column by centrifugation (17000 × g for 1 min) with Buffer EB (10 mM Tris-CL, pH 8.5). Radiolabelled cDNA probe was synthesised using a Ready-to-Go kit (Amersham, Little Chalfont, UK). cDNA template (50 ng) was denatured at 94 °C for 4 min and added to a reaction mix containing Klenow Fragment (7-12 Units), dATP, dGTP, dTTP and random oligodeoxyribonucleotides. 5 μl of $[\alpha\text{-}^{32}P]$ dCTP (3000 Ci/mmol) was added to a final 50 μl reaction volume. The mix was incubated at 37 °C for 30 min and then allowed to cool to room temperature for 2 h. Unincorporated nucleotides were separated from the radiolabelled probe in TE buffer using Sephadex G50 Nick Spin Columns (Amersham).

62

Chapter 2

The Northern blotting protocol was based on a method previously described to improve sensitivity (Fourney et al 1988). Total RNA was dissolved in 25 mM EDTA, 0.1% SDS. The RNA sample was adjusted to a volume of 5 µl and added to 25 µl Electrophoresis Sample Buffer (0.75 ml deionised formamide, 0.15 ml 10× MOPS/EDTA buffer, 0.24 ml formaldehyde, 0.1 ml DEPC water, 0.1 ml glycerol, 0.08 ml 10% (w/v) bromophenol blue). The mix was heated at 65 °C for 15 min and placed on ice. 1 µl ethidium bromide solution (1.0 mg/ml) was added to the sample and mixed thoroughly prior to loading onto the gel. The gel was prepared as follows; 1 g agarose, 10 ml 10× MOPS/EDTA and 87 ml DEPC water were added to an autoclaved flask. The mixture was heated to dissolve the agarose and cooled to 50 °C to allow addition of 5.1 ml 37% formaldehyde. The solution was gently mixed and poured into a gel tray and allowed to set for 1 h. Prior to loading, sample wells were flushed and the gel was run in 1× MOPS/EDTA buffer. The gel was run at 30V at room temperature overnight (14 h). The gel was prepared for transfer by soaking it in 10 × SSC with gentle shaking. The nylon membranes (Genescreen Plus, DuPont, Wilmington, USA) were pre-soaked in DEPC water and then 10 × SSC for 5 min. RNA was transferred in 10 × SSC using a sponge to enhance capillary attraction. The sponge had been washed thoroughly, was made from polyurethane foam and had been obtained from a camping bed mattress. The gel was sandwiched between 3MM Whatmann paper on top of the sponge sitting in a tank of 10 × SSC with paper towels and a weight on top.

RNA transfer was performed overnight (14 h) and the gel was examined under UV light for residual RNA. RNA was fixed to the membrane by baking at 80 °C for 2 h. Hybridisation was performed using ULTRAhyb buffer (Ambion, Huntingdon, UK). ULTRAhyb was preheated to 68 °C to dissolve all precipitated material. The blot was soaked in buffer for 30 min at 68 °C with enough volume to keep it uniformly wet in the hybridisation bottle. Radiolabelled probe was added (10^6 cpm/ml buffer) and hybridised overnight (14 h) at 68 °C. Hybridisation buffer and probe were then discarded and the blot was washed twice with 2 × 5 min washes (2 ×

SSC, 0.1% SDS) at 68 °C. a further 2 × 15 min washes were performed (0.1 × SSC, 0.1% SDS) at 68 °C. The blot was then wrapped in sandwich wrap and exposed to a phosphor screen. The phosphor screen was analysed with a Storm 860 Phosphorimager and ImageQuant software.

2.2.4.5. Preparation of plasmids for angiopoietin-2, midkine, HPRT and MMP-1.

The PGEM-T Easy Vector System (Promega) was used to clone PCR inserts for generation of cDNA and riboprobes. This vector contains T7 and SP6 RNA polymerase promoters flanking a multiple cloning region. The multiple cloning region is also flanked by recognition sites for restriction enzymes *EcoR* 1, *BsfZ* 1 and *Not* 1 facilitating single enzyme digest release of insert. Angiopoietin-2, MMP-1, HPRT and MMP-1 cDNA were extracted form PCR mixes using the following protocol. PCR mix was added (1:1 vol ratio) to a phenol/chloroform mix (25:1 vol ratio), vortexed and centrifuged for 5 min at 12000 × g. A further volume of chloroform (0.9 vol of original PCR mix) was added and centrifuged at 12000 × g for 5 min. The upper aqueous phase was transferred to a clean tube and cDNA was precipitated for 40 min at –20 °C with 3 M sodium acetate pH 4.3 (0.1 vol original PCR mix) and 100 % ethanol (2.5 vol original PCR mix). A further centrifugation (12000 × g for 5 min) was performed, the supernatant removed and the pellet washed with 70% ethanol. A final spin centrifugation (12000 × g for 5 min) was performed, the ethanol was removed, the pellet air dried and resuspended in 20 μl of DEPC water. cDNA concentrations were measured from absorbance at 240 nm in a spectrophotometer.

Ligations were performed overnight at 4 °C using pGEM-T easy vector (50 ng) and cDNA products in a 3:1 molar ratio with ligation buffer and T4 DNA ligase (3 Weiss units). A negative ligation with no PCR product and a positive control ligation with a control insert DNA provided with the pGEM-T Easy vector were also set up. DH5α competent cells (Life Technologies, Invitrogen, Paisley, UK) were

64

transformed with vector. Electroporation was performed with 2 µl of vector mix (approx 25 ng) added to 50 µl DH5α *E. Coli* stock (25 µF, 200 Ohms, 2.5 kV: Equibo 'EasyJect Plus' electroporator Eurogentec, Liège, Belgium). Following the shock, 300 µl of SOC medium was added immediately and the mix was further incubated for 40 min at 37 °C. The mix (100 µl) was then plated onto Luria-Bertani (LB) agar plates containing ampicillin (100 µg/ml).

2.2.4.6. Isolation of plasmid DNA from DH5α *E. Coli*

Single, well isolated colonies from LB agar plates containing ampicillin were picked and inoculated into 10 ml of LB culture medium containing ampicillin (0.5 mg/ml). The tip from a colony was also placed in a sterile microfuge tube with 30 µl of LB agar. The tube was vortexed vigorously and 10 µl was transferred to a PCR tube and boiled at 100 °C for 5 min to liberate plasmid. This suspension was used as template for PCR to screen colonies for angiopoietin-2, midkine, MMP-1 and HPRT inserts. Colonies containing inserts were incubated overnight (10 ml) on a shaker at 37 °C. The Wizard *Plus* SV Miniprep DNA purification System (Promega) was used to isolate plasmid DNA from transformed bacteria. 5 ml of bacterial culture was harvested and centrifuged (10,000 × g for 5 min at 21 °C). Supernatant was poured off and the tube was inverted onto blotting paper to remove excess media. Cell Resuspension Solution (250 µl, Promega) was added and the cells were resuspended by vortexing and transferred to a 1.5 ml microfuge tube. Cell Lysis Solution (250 µl, Promega) was added and the tube inverted gently 4 times and incubated at room temperature for 4 min. The pitfall in the lysis step to be avoided was that the SDS within the lysis solution might not be fully dissolved. The solution clarified during this period and Alkaline Protease Solution (10 µl, Promega) was added, the tube inverted 4 times and incubated for 4 min. The Wizard *Plus* Neutraliastion Solution (350 µl, Promega) was then added and mixed immediately by inverting 4 times.

65

The bacterial lysate was then centrifuged ($14000 \times g$ for 10 min at room temperature). Cleared lysate was transferred to a Spin Column by pipette without disturbing or transferring any of the white precipitate. Supernatant was then centrifuged ($14000 \times g$ for 1 min) at room temperature and the flow-through was discarded. Column Wash Solution (750 µl, Promega) was then added and a further centrifugation performed. The wash was repeated with 250 µl of Column Wash Solution ($14000 \times g$ for 2 min). The spin column containing bound plasmid DNA was then transferred to a fresh microfuge tube with care taken to avoid transferring any wash solution. Plasmid DNA was eluted with 100 µl of Nuclease Free Water (Promega) by centrifugation ($14000 \times g$ for 1 min at room temperature).

2.2.4.7. Generation of riboprobes for ribonuclease protection assays

The vectors containing HPRT and angiopoietin-2 PCR fragment inserts were sequenced to ascertain orientation and verify sequence of the insert. Riboprobes were generated using the Maxiscript In Vitro Transcription Kit (Ambion). The angiopoietin-2 and HPRT inserts could be linearised with *Sph* I following incubation at 37 °C for 2 h. The linearised plasmid was then digested with proteinase K (200 µg/ml, 0.5% SDS at 50 °C) for 30 min. Linearised plasmid was then phenol chloroform extracted and resuspended in DEPC water. Transcription reactions were set up with 1 µg of DNA template, transcription buffer, ATP, CTP, GTP (all 0.5 mM), UTP and α^{32}P-[UTP] (2 µM and 1 µM respectively) to a final limiting concentration of 3 µM. In riboprobe synthesis a balance exists between probes generated with high specific activity, where the ratio of radiolabelled to cold nucleotide is high but overall concentration is lower, limiting full chain synthesis. SP6 RNA polymerase was added to the transcription mix and diluted to a final volume of 20 µl. The mix was incubated at 37 °C for 15 min and template DNA was digested with DNase I (2U) for 15 min at 37 °C. Free nucleotides were removed by elution of probe through a Nick spin column using TE buffer (10 mM Tris-Cl pH 8.0, 1 mM EDTA).

66

Chapter 2

2.2.4.8. Ribonuclease protection assays

The ribonuclease protection assay is a sensitive method for detecting RNA transcripts (Lee and Costlow, 1987). Radiolabelled antisense RNA transcripts (riboprobes) were generated from the vectors containing PCR fragment inserts according to the method in section 2.2.4.7. The assay works on the principle that hybridisation of riboprobe to complementary sequences in the RNA sample will protect it from digestion by ribonuclease. The greater the amount of complementary RNA the more probe is protected and the higher the signal.

Sample RNA and labelled riboprobe were mixed together (approximately 5×10^4 cpm per 10 µg RNA sample) and co-precipitated by adding ammonium acetate (0.5 M) and 2.5 vol of ethanol and incubating at -20 °C for 15 min. For each probe, 2 additional control reactions were set up using yeast RNA (1 µg). RNA was pelleted by centrifugation (12000 × g for 15 min at 4 °C) and pellets were washed with 70% ethanol. Eluants were monitored for radioactivity to ensure that probe was not being removed from the mix. The pellets were then resuspended in 10 µl of hybridisation buffer, vortexed and centrifuged briefly to mix and collect the reaction at the bottom of the tube. RNA was denatured (94 °C for 4 min) and hybridised overnight (42 °C for 14 h). A mix of RNase A and RNase T1 (250 U/ml and 10,000 U/ml respectively) was diluted 100-fold in RNase digestion III buffer (Ambion) and then added (150 µl) to each hybridisation reaction and to one of the yeast control reactions. RNase digestion III buffer was added alone to the other control yeast reaction. The tubes were briefly vortexed and centrifuged to collect the reaction mix and incubated at 37 °C for 30 min. RNase Inactivation/Precipitation III Solution (Ambion) was added (225 µl) and the reaction was incubated at -20 °C for 20 min. The precipitated RNA was then centrifuged (12,000 × g for 15 min at 4 °C) and supernatants were carefully removed from each tube and monitored for radioactivity. The pellets were washed with 70% ethanol and resuspended in 5 µl of Gel loading Buffer II (Ambion). The samples were run on 6% acrylamide gels (Sequagel-6, National Diagnostics, Georgia, US) 15 cm wide and 25 cm long with wells 5 mm in

width. The acrylamide was polymerised with ammonium persulphate and run between two siliconised glass plates separated by plastic spacers and sealed with autoclave tape. Around 35 ml of acrylamide was required to fill the sequencing gel.

The gel was placed in a sequencing gel tank (Base Runner, GENEQ inc. Montreal, Canada) consisting of two tanks each containing 500 ml TBE buffer connected to the gel plates and sealed with gel grease. The gel was run at 600 V for 20 min and urea was flushed out of the wells prior to sample loading. Prior to loading, the samples were heated at 94 °C for 3 min to solubilise and denature the RNA. The gel was run at 250V for 2.5 h until the leading dye band had reached the bottom of the gel. The gel was then blotted onto Whatmann paper and dried on a gel drier before exposure overnight to a phosphor screen. The phosphor screen was analysed with a Storm 860 Phosphorimager and ImageQuant software.

2.2.5. Protein based assays

2.2.5.1. Immunoprecipitation and SDS-PAGE to detect angiopoietin-2 from HUVEC culture supernatants

The immunoprecipitation protocol was developed by Mr Charlie Mayor, Department of Cardiovascular Sciences, University of Edinburgh. Mr Mayor also performed the majority of immunoprecipitation experiments. HUVECs were cultured with oxidised LDL (100 μg/ml), native LDL (100 μg/ml) and TNF-α (R&D Systems, Abingdon, UK - 10ng/ml) for 8 h. Conditioned HUVEC supernatant (1 ml) was incubated at room temperature for 30 min with goat polyclonal anti-Ang2 (N-18) antibody (Santa Cruz Biotechnology, Santa Cruz, Ca, US) at a concentration of 200 ng/ml. 50 μl of ProteinG sepharose (Amersham) that had been washed three times in lysis buffer (1% Triton-X100, 150 mM NaCl, 50 mM Tris.HCl pH 7.4, 0.2 mM PMSF, 1 mM EDTA, 0.2 mM sodium orthovanadate, 0.1 μg/ml pepstatin) was added

overnight at 4°C under rotation. The pellet was washed three times with lysis buffer and immmunoprecipitates eluted by boiling for 5 min in 40 µl sample buffer.

Equal volumes of sample were diluted with 30 µl distilled water and separated by SDS-PAGE. Proteins were resolved by electrophoresis on 10 % polyacrylamide gels (100 V/50-100 mA for 2h) and transferred to a polyvinylidene difluoride membrane in 25 mM Tris, 190 mM glycine, 0.05 % SDS, 20 % methanol (100 V/400 mA for 2h). Membranes were blocked in Tris-buffered saline (TBS pH 7.6) with 0.1 % Tween, 5 % non-fat dry milk overnight at 4° C prior to a 2 h incubation at room temperature with anti-Ang2 antibody (1:1000). After washing, membranes were incubated (1 h at room temperature) with anti-goat-IgG conjugated to horseradish peroxidase (Dako, Ely, UK; 1:2500). After washing, immunoreactive bands were visualised by enhanced chemiluminescence (ECL). Recombinant Ang2 (rAng2-R&D Systems) was run as a positive control.

2.2.5.2. Immunostaining of human coronary arteries

All immunostaining was performed by Mrs Frances Rae, Department of Pathology, University of Edinburgh. The work was conducted in collaboration with Dr Lee Jordan, Specialist Registrar and Lecturer in Histopathology, University of Edinburgh. A series of human tissues including four coronary arteries were obtained (following clearance from the relevant ethics committee) from the University of Edinburgh Department of Pathology living (non-post mortem) archive of patients with atherosclerosis undergoing coronary artery bypass surgery. Non-diseased vascular tissues including temporal and splenic arteries, renal and umbilical/placental tissues were also obtained for comparison. Full local Lothian Research and Ethics Committee (LREC) approval was received. The tissue was in formalin fixed (10% aqueous solution of formaldehyde), paraffin embedded blocks. Traditional haematoxylin and eosin stained sections were viewed by the histopathologist for morphological description. A series of 5-7 micron thick sections were exposed to a

69

panel of immunohistochemical agents to establish the cell type within vessel walls. These included: CD3 (rabbit polyclonal anti-human CD3, clone A452 – Dako, UK); CD31 (mouse monoclonal anti-human endothelial cell CD31, clone JC/70A – Dako, UK); CD68 (mouse monoclonal anti-human macrophage CD68, clone PG-M1 – Dako, UK); Smooth Muscle Actin (mouse monoclonal anti-human SMA, clone 1A4 – Dako, UK). Ang2 immunohistochemistry was performed using goat polyclonal antihuman Ang2, (Santa Cruz). Manufacturers' protocols were used. Recommended positive and negative controls were used where possible (Lymph node – CD3, CD68; Small Intestine – SMA, Vascularised tissue – CD31). The control tissue for Ang2 was placenta, previously recognised as a site of Ang2 expression (Wulff et al 2002).

2.2.5.3. Extraction of nuclear fractions from HUVECs and macrophages

Nuclear protein analysis was performed according to published protocols (Staal et al 1990) with some modifications as follows. Cells were grown in 12-well Costar plates and following treatments, culture medium was removed and 400 μl of ice cold buffer A (10 mM HEPES-KOH; pH 7.9, 10 mM KCl, 2 mM $MgCl_2$, 1 mM DTT, 0.1 mM EDTA, 0.2 mM NaF, 0.2 mM Na_3VO_4 and proteinase inhibitors; 0.5 mM PMST, and 1 μg/ml of leupeptin and aprotinin added immediately prior to use) was added. The cells were scraped off and suspended in an eppindorf. Buffer B (25 μl, 10% NP-40) was added and the suspension was vortexed vigorously for 15 s. The suspension was then centrifuged (12000 × g for 45 s) and cytoplasmic fractions were removed with care taken not to disturb the pellet. Pelleted nuclei were then resuspended in 50 μl of Buffer C and incubated on ice on a shaker for 20 min vortexing for 15 s every 5 min. The suspensions were then centrifuged (13000 × g for 5 min) and the supernatants collected for analysis. Protein concentrations were measured using the Bio-Rad Protein Assay (Bio-Rad, Hemel Hempstead, UK) which had been shown to be compatible with the extraction buffers used in this protocol.

Chapter 2

2.2.5.4. Electromobility shift assay

This assay is based on the principle that complexes of protein and DNA migrate more slowly on polyacrylamide gel than free DNA or double stranded oligonucleotides. Consensus NF-κB oligonucleotide, antisense (5'-3') AGT-TGA-GGG-GAC-TTT-CCC-AGG-C (2.5 pmol; Promega) or a mutant consensus oligo containing a single base pair substitution antisense AGT-TGA-GGC-GAC-TTT-CCC-AGC-C (Santa Cruz) were mixed with T4 polynucleotide kinase, $[\gamma^{-32}P]ATP$ (1 µl, 3000 Ci/mmol at 10 mCi/ml) and reaction buffer to a final volume of 10 µl. The reaction was incubated at 37 °C for 30 min and then terminated with 1 µl EDTA (0.5 M). The mix was then diluted to 100 µl with TE buffer. Nuclear protein (7 µg) was added to a 10 µl binding reaction containing radiolabelled consensus or mutant oligo (1 µl) 10 mM Tris-CL, 10 mM KCL, 1 mM EDTA, 0.5 mM $MgCl_2$ 8% glycerol, 1mM DTT and 0.5 µl of stock poly(dI-dC)poly(dI-dC) (1 mg/ml).

The binding reaction was incubated at room temperature for 20 min. An additional control binding reaction was set up with 2.5 pmol of excess unlabelled consensus oligo as a further control for specific binding to compete with the radiolabelled probe. The protein-oligo binding mix was then added to a 6% polyacrylamide gel. Dye was added to a separate well to visualise migration without interfering with nuclear protein binding. The gel was run at 100 volts until the dye had migrated to the bottom end. The gel was dried on Whatman paper, wrapped in sandwich wrap and exposed to a phosphor screen.

2.2.5.5. SDS PAGE and Western blotting for IκBα (and angiopoietin-2)

For angiopoietin-2, cell culture supernatants were collected and cell lysates taken in RIPA buffer (10 mM sodium phosphate buffer pH 7.5, 150 mM NaCl, 1 mM DTT, 1% Nonidet P-40, 1% sodium deoxycholate, 0.1% SDS, 10 µg/ml aprotinin, 10 mg/ml PMSF). Lysates were collected in an eppindorf and centrifuged

(12000 × g at 4 °C for 5 min). The soluble component of the lysate was removed and loaded (50 μg) onto a 12% SDS polyacrylamide gel. SDS-PAGE was performed using a vertical electrophoresis tank Mini-Protean II system. Samples were electrophoresed at 100 V using SDS-Tris-Glycine electrode buffer for 2 hours beside prestained molecular weight markers (Life Technologies) and using 20 ng of angiopoietin-2 (R&D Systems) protein as a positive control. Following separation, proteins were transferred onto Hybond ECL nitrocellulose membrane (Amersham), at 100 V for 1 h. Non-specific protein binding sites were blocked overnight at 4 °C with PBS/0.1% Tween 20 containing 5% skimmed milk. The membrane was then incubated with 1:1000 dilution of goat anti-angiopoietin-2 IgG (Santa Cruz) in blocking solution for 2 h at room temperature and washed thoroughly with PBS/0.1% Tween. HRP conjugated rabbit anti-goat immunoglobulin diluted 1:5000 (Dako) in blocking solution was added for 30 min at room temperature, and then the membrane was washed as above. Finally, immunoreactive bands were detected by ECL and membrane developed on X-omat film.

For IκBα, HUVECs and macrophage extracts were prepared as above with cell lysate buffer (10% glycerol, 2% SDS, 62.5 mM Tris-Cl, 2 μg/ml leupeptin, 2 μg/ml aprotinin, and 1 mM PMSF) after 10 min of LPS (100 ng/ml) or TNF-α (100 pg/ml) stimulation. Pilot studies were performed to determine the optimum time point for observing IκBα degradation in response to stimulus. Cell extracts were analysed for IκBα protein content by SDS-PAGE. The majority of these gels were performed by Miss Tara Sheldrake (from our group). Briefly, equal volumes were loaded onto a prefabricated 12% Bis-Tris/MES polyacrylamide gel (Nu-PAGE, Invitrogen) and electrophoresis was performed as above. Electroblotting was then conducted on nitrocellulose and membranes were treated with rabbit anti-IκBα antibody, 1/1000 dilution (Cell Signaling Technology, New England Biolabs, Hitchin, UK), for either 16 h at 4°C or 2 h at room temperature and subsequently with goat anti-rabbit, 1/2000 dilution (Dako) for 1.5 h at room temperature. The Western blots were then developed by ECL and exposed to film as above.

72

Chapter 2

Formulations: 4 × SDS-PAGE sample buffer: 0.5 M Tris-HCl, 40% (v/v) glycerol, 8% (w/v) SDS, 0.2 M EDTA, 0.5% (v/v) bromphenol blue and 4% (v/v) mercaptoethanol. Separating gel (angiopoietin-2): ph 8.8, 0.375 M Tris-HCL, 2 mM EDTA, 0.1% (w/v) SDS, 12% acrylamide, 0.1% (v/v) APS and 0.05% (v/v) TEMED. Electrode buffer: 0.6% (w/v) Tris base, 2.9% (w/v) glycine, 0.7% (w/v) EDTA, 0.1% (w/v) SDS. Transfer buffer: 24.7 mM Tris base, 210 mM glycine and 20% (v/v) methanol.

2.2.6. Techniques related to human neutrophil elastase (HNE) assays

2.2.6.1. Treatment of HUVECs with HNE

For HNE mediated injury experiments HUVECs were washed with PBS to remove serum (because of the presence of HNE inhibitors in serum) and incubated in serum-free EBM2 containing HNE for 8 h (at the concentration indicated), after which photomicrographs were taken. For HNE pretreatment studies, HUVECs were washed in PBS and pre-incubated with HNE for 1 h before replenishment with serum-containing EBM2 containing the second LPS (100 ng/ml) or oxidised LDL stimulus (100 µg/ml). All incubations with LPS, TNF-α (1 ng/ml) and oxidised LDL were for 8 h.

2.2.6.2. Treatment of macrophages with HNE and flow cytometric analysis

On culture day-4 macrophages were removed with cold CMF-PBS and plated at 70000 cells/ well on 48-well plates in X-Vivo 10 serum-free culture medium (Cambrex Bio Science). Where indicated, HNE (1 µM) was added directly the following day and incubated for 1 hour prior to removal. Following HNE treatments, cells were washed with ice cold CMF-PBS and suspended in 2 % goat serum (Serotec Ltd, Oxford, UK). Cells were incubated with 61D3, a CD14 blocking monoclonal antibody (Devitt et al 1998), for 30 min, washed twice and then incubated with phycoerythrin-conjugated goat anti-mouse IgG secondary antibody

73

Chapter 2

(Dako) for 15 minutes. Washed macrophages were then analysed on a FACScan cytometer (BD Biosciences).

2.2.6.3. HNE inhibition assay

The HNE activity of macrophage supernatants, following incubation with HNE, was examined to determine any inhibitory effect conferred by infection with Ad-elafin or incubation with r-elafin. Briefly, all dilutions were performed in assay buffer (50 mM Tris, 0.5M NaCl, 0.1% Triton X-100, pH 8.0). Cell culture supernatant (90 µl) was incubated in a 96-well microtitre plate for 30 min at 37 °C before addition of the chromogeneic substrate N-methoxysuccinyl-Ala-Ala-Pro-Val-p-nitroanilide. The change in absorbance measured spectrophotometrically at 405 nm (MR5000 Plate Reader), was expressed as a function of time.

In a separate experiment to measure HNE activity within apoptotic Mutu cells, two independent batches of apoptotic Mutu cells (3 million cells) were pelleted and washed with PBS and lysed in 0.4 ml of HNE buffer assay. Cell lysate (50 µl) was added to a microtitre plate and HNE activity recorded according to the protocol above.

2.2.6.4. Apoptotic cell recognition assay

Macrophages were cultured in 48-well plates. Adenovirus infections were performed in X-vivo 10 serum-free using the precomplexing protocol with lipofectamine, described in section 2.2.2.3.2. Macrophages were treated 24 h after adenoviral infection. Where indicated, HNE (1 µM) and r-elafin (15 µg/ml) were added directly for 1 hour prior to the interaction assay with apoptotic cells. The group I Burkitt lymphoma cell line Mutu I, induced into apoptosis by 16 h incubation with 1 µg/ml of the calcium ionophore ionomycin was used as a source of apoptotic

74

Chapter 2

cells. Typically, around 70% of cells were apoptotic following this treatment as determined by FACS analysis of annexin V staining. For some experiments the 61D3 CD14-blocking monoclonal antibody was mixed with the apoptotic Mutu cells. The culture medium was removed and 750000 apoptotic Mutu cells were added to each 48-well for 1 h at 37 °C before being washed extensively with ice cold CMF-PBS to remove unbound apoptotic cells. Cells were then fixed in 1% paraformaldehyde and stained with Diff-quick for counting. Cultures were scored by light microscopy according to the proportion of macrophages that had internalised or bound apoptotic Mutu cells by established criteria (Devitt et al 1998). At least 300 macrophages were assessed per sample.

2.2.7. Statistical analysis

Results are reported either as pooled data from a series of n separate experiments and presented as mean ± SD or as individual experiments, carried out in triplicate and presented as mean ± SD. Statistical significance was analysed using the Student t-test except for data except for data in Figure 5.12 which were analysed using oneway ANOVA with post-hoc Boneferrpni correction. Statistical significance was assigned to data returning a P value of less than 0.05.

75

Chapter 3

An experimental system to study human endothelial cell inflammatory responses to oxidised LDL

3.1. Aims

The central aim is to create and characterise an *in-vitro* culture system to model endothelial injury occurring during the development of atherosclerosis.

Firstly, primary endothelial cell cultures were established from human umbilical cord veins. The purity of these cultures was demonstrated.

The purity of LDL preparations and in particular, the presence of contaminating LPS was then investigated.

The effects of oxidised LDL on endothelial cell survival and inflammatory cytokine production were established.

Finally, the signalling events associated with oxidised LDL stimulation of endothelial cells were investigated.

3.2. Results

3.2.1. Preparation of a pure culture of human endothelial cells from umbilical veins.

The Lothian Research and Ethics Committee (LREC/R/UO/01) gave approval to obtaining consent from pregnant mothers for donation of the umbilical cord following healthy term pregnancies delivered by Caesarean section. The information sheet for this study, given to expectant mothers prior to obtaining consent, is shown in Appendix I at the end of this chapter. Cells were extracted according to techniques outlined in the methods section. Human endothelial cells, obtained by collagenase

76

treatment of term umbilical cord veins were cultured in EBM-2 medium with 4.5% fetal calf serum and growth factor supplements (see Materials and Methods, section 2.2.1.1). Small clusters of cells, initially spread out in the 75 cl culture flask, coalesced and grew to form confluent monolayers of polygonal cells within 5 to 7 days. Endothelial cells were recognised morphologically by their cobblestone appearance in culture and staining for the CD31 antigen was performed (Figure 3.1).

CD31 expression is limited to endothelial cells and leucocytes (Newman 1997) and is absent from the major possible contaminating cell types, vascular smooth muscle cells and fibroblasts. After 2 passages, cells were dislodged from culture plastic and suspended following trypsin treatment. FACS analysis demonstrated a homogeneous population of cells with greater than 99% positivity for CD31 antigen (Figure 3.1). The homogeneous appearance of the cultures was in keeping with results of FACS analysis, indicating an essentially pure culture.

3.2.2. Characterisation of native (non-oxidised) and oxidised LDL preparations and their effects on endothelial cell cultures.

Human plasma was obtained from the Department of Transfusion Medicine, Royal Infirmary of Edinburgh. LDL was isolated by sequential ultracentrifugation and oxidised against $CuCl_2$. The degree of oxidation was monitored by the formation of conjugated dienes at 234 nm (Lewin et al 2002). The effect of incubation with native and oxidised LDL on endothelial cell inflammatory cytokine production was examined (Figure 3.2). Both preparations of LDL stimulated interleukin-8 (IL-8) and monocyte chemoattractant protein-1 (MCP-1) production in endothelial cell culture supernatants. Oxidised LDL was the more potent stimulus for these chemoattractant cytokines (Figure 3.2A, B).

77

Chapter 3
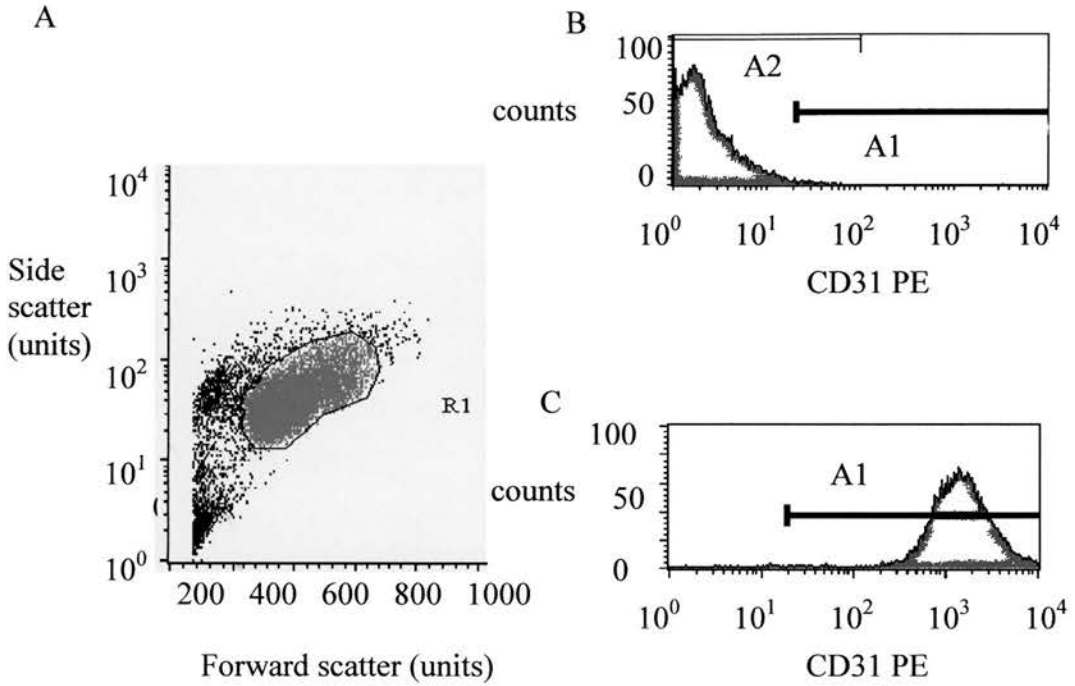
Figure 3.1. Collagenase digestion of human umbilical cords produced a pure yield of CD31+ endothelial cells on FACS analysis.

A. Cells were suspended in a single cell suspension and sorted by charge and granularity using fluorescent activated cells sorting analysis (FACS). A population of intact cells uncontaminated by debris was identified within the scatter plot. This population was termed region 1 (R1) and selected for further interrogation. B. Histogram analysis of region 1 following incubation of cells with an isotype matched PE labelled antibody. There was little if any staining in the R1 population of cells with 100% of cells lying in area 2 (A2). C. Incubation with an anti-CD31 PE conjugated antibody produced a shift in the fluorescence of the R1 population with 99.77% of cells lying in area 2 (A2).

Similar results were seen form different umbilical vein preparations.

78

Chapter 3

This result indicates the importance of oxidative modification of LDL for its inflammatory properties. A central theme of this chapter is the characterisation of signalling events responsible for induction of inflammatory cytokine production by oxidised LDL. Firstly, the possibility of LPS contamination of LDL during preparation was investigated. LPS would be expected to produce a similar cytokine response from endothelial cells (von Asmuth et al 1991). The sensitive limulus amebocyte lysate (LAL) assay was used to detect LPS. LDL preparations produced by Professor Riemersma (Cardiovascular Research Unit, University of Edinburgh) and obtained commercially from Intracel were analysed (Table 3.1). Both commercial and locally produced native and oxidised LDL contained LPS. There was considerable variation in the LPS content between different preparations. It is important to note that the LPS content of the locally produced native LDL (batch 1) was higher or similar to the corresponding oxidised LDL batch (batch 2) despite the more involved processing associated with oxidised LDL preparation. The LPS content of sterile PBS was also measured to provide a negative control for the LAL assay and as an indication of a minimum level of endotoxin contamination for tissue culture grade material.

This magnitude of endotoxin contamination in the LDL preparations was surprising and experiments were devised to find where LPS was being introduced in the LDL preparation process and to what degree LPS was contributing to the observed stimulatory effect of LDL on endothelial cell cytokine production (Figure 3.1). In order to identify the source of contamination, LPS levels were measured in aliquots from different stages of the LDL preparation (Figure 3.3). LPS levels were undetectable in donor human plasma. Following ultracentrifugation (and oxidation) to produce native (and oxidised) LDL, low levels of LPS were found. Passage through the Amicon ultrafiltration unit produced the biggest step up in LPS concentration for the native LDL component of the analysed batch (Figure 3.3). The Amicon ultrafiltration unit was the only component of the LDL preparation apparatus that could not be autoclaved and had been identified as a likely source for LPS contamination prior to the experiment.

Chapter 3

A

IL-8 pg/ml

3000

2000

1000

0

100 µg/ml

B

untreated
nLDL
oxLDL

MCP-1 pg/ml

6000
5000
4000
3000
2000
1000

100 µg/ml
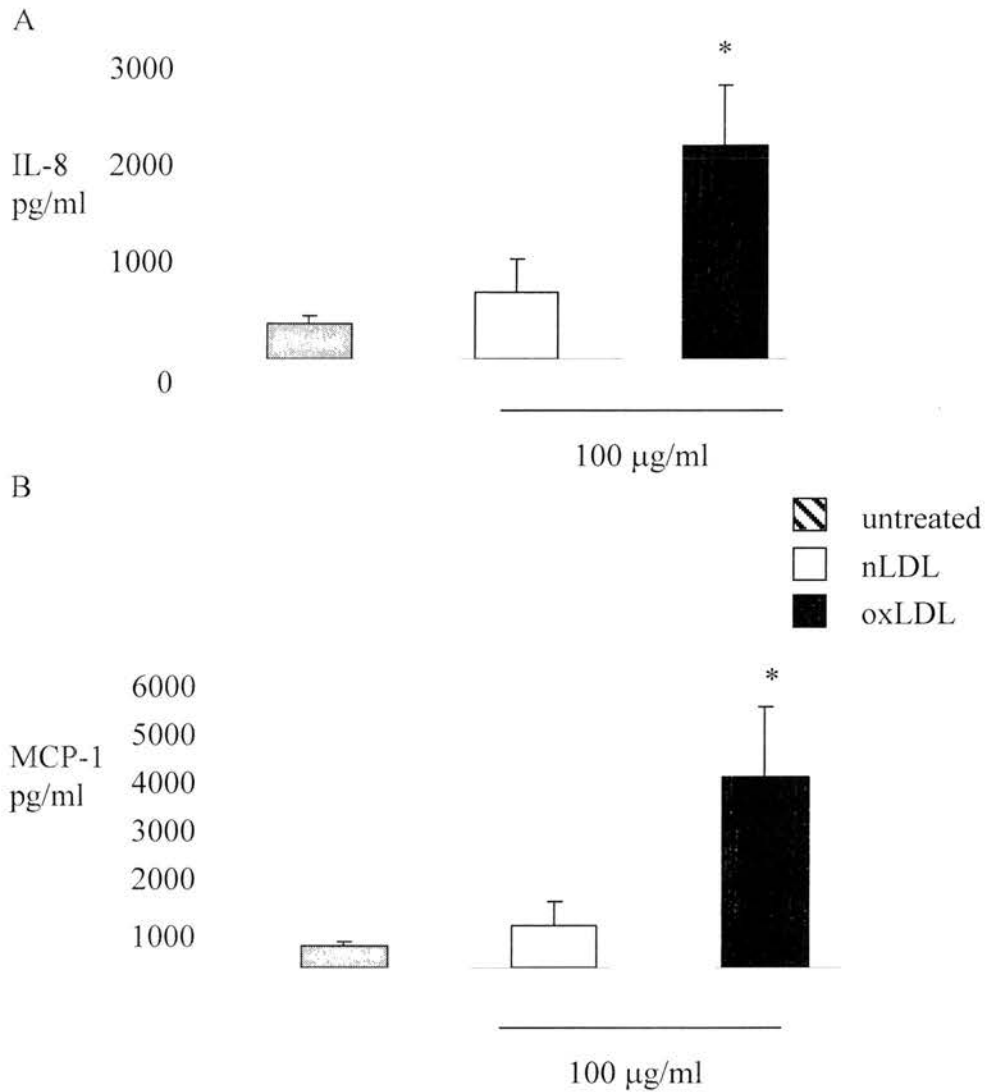
Figure 3.2. Both oxidised LDL and native LDL induced HUVEC production of IL-8 and MCP-1.

Confluent HUVECs in 48-well format at passage 4 were incubated in EBM-2 (2.5% fetal calf serum) alone or with locally produced preparations of native LDL or oxidised LDL for 16 hours. Supernatants were removed and IL-8 (Panel A) and MCP-1 (Panel B) levels were quantified by ELISA. Results for IL-8 and MCP-1 are mean ± SD from 3 experiments performed in triplicate representing 2 different HUVEC donors and LDL preparations (batches 2 and 3). * Significantly greater than native LDL, $p < 0.05$.

80

Chapter 3

Lipid batch (#)	LPS EU/ml (approx. pg/ml)
Local nLDL # 1	1340 (111667)
Local oxLDL # 1	4.97 (414)
Local nLDL # 2	46.8 (3900)
Local oxLDL # 2	44.7 (3725)
Intracel oxLDL # 351	1.38 (115)
Intracel oxLDL # 353	189.2 (15767)
Intracel oxLDL # 354	187.2 (15600)
Intracel oxLDL # 356	13.5 (1125)
Sterile PBS	0.009 (0.75)

Table 3.1. LPS concentration within different preparations of locally produced and commercial LDL.

The LPS content of LDL was measured against a standard LPS (United States standard endotoxin EC-6). Results are in endotoxin units/ml (EU/ml) where 12 EU approximates 1000 pg LPS.

81

Chapter 3

The contribution of contaminating LPS to LDL's stimulatory effect on inflammatory cytokine production was assessed by incubating LDL with polymyxin-B (Figure 3.4). Polymyxin-B is a naturally occurring antibiotic known to bind and inhibit various biological activities induced by LPS (Pier et al 1981). Pre-incubation of a batch of locally produced native and oxidised LDL with polymyxin B significantly reduced subsequent MCP-1 production by endothelial cells (Figure 3.4). This is consistent with a significant contribution from LPS to MCP-1 production. In a further experiment the effect on MCP-1 production of spiking a sample of locally produced oxidised LDL with LPS was examined. MCP-1 production was heightened considerably and the effect was attenuated by pre-incubating the spiked sample with polymyxin-B (Figure 3.5).

A saturating dose of polymyxin-B reduced but did not annul completely the stimulatory effect of LPS alone (Figure 3.5). The negative control limb of this experiment produced an unexpected result. Polymyxin-B had an inhibitory effect on TNF-α induced MCP-1 production by endothelial cells suggesting an inhibitory action that extends beyond neutralisation of LPS (Figure 3.5).

Together, these results indicated the potential for LPS contamination of LDL preparations produced locally or obtained commercially. With locally produced LDL the Amicon ultrafiltration unit appeared to be a particularly important source of contamination. The studies with polymyxin-B suggested that contaminating LPS may be contributing to LDL stimulated cytokine production although this conclusion was weakened by an apparent LPS independent inhibitory effect of polymyxin-B on endothelial MCP-1 production. Because doubt remained it was clear that the amount of contaminating LPS in LDL had to be reduced for further experiments.

.

82

Chapter 3
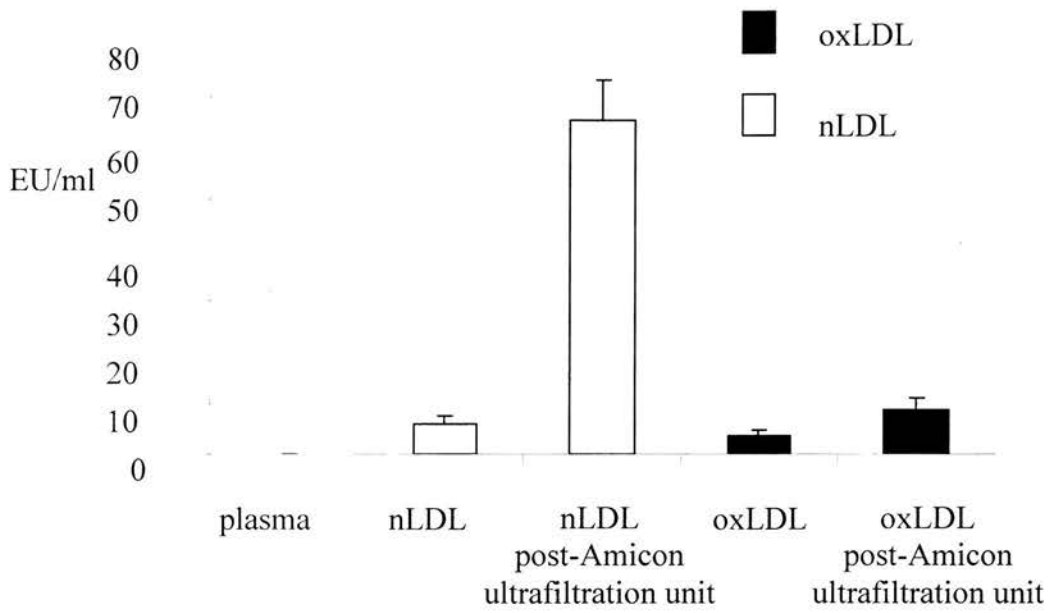
Figure 3.3. LPS levels at different stages from an LDL preparation.

Results are in endotoxin units/ml (EU/ml) from the mean ± SD of 3 measurements from one LDL preparation. LPS levels are shown in plasma, following ultracentrifugation (native: nLDL), oxidation with copper sulphate (oxidised LDL: oxLDL) and following passage through the concentrator.

83

Chapter 3
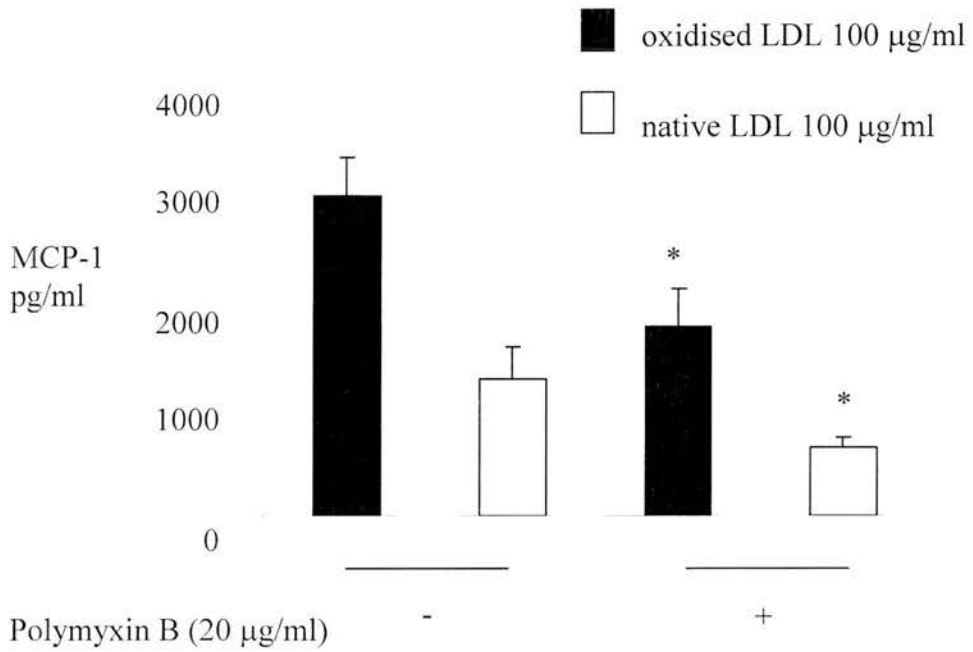
Figure 3.4. Polymyxin B reduces both oxidised LDL and native LDL induced HUVEC MCP-1 production.

LDL was pre-incubated with 20 μg/ml polymyxin B for 30 minutes at room temperature. MCP-1 levels were measured in the supernatants following 8 h incubations with the different treatments. The results from one locally produced batch of lipid are shown. Results are presented as mean ± SD from one experiment performed in triplicate. * significantly less following incubation with polymyxin B, $p < 0.05$)

84

Chapter 3
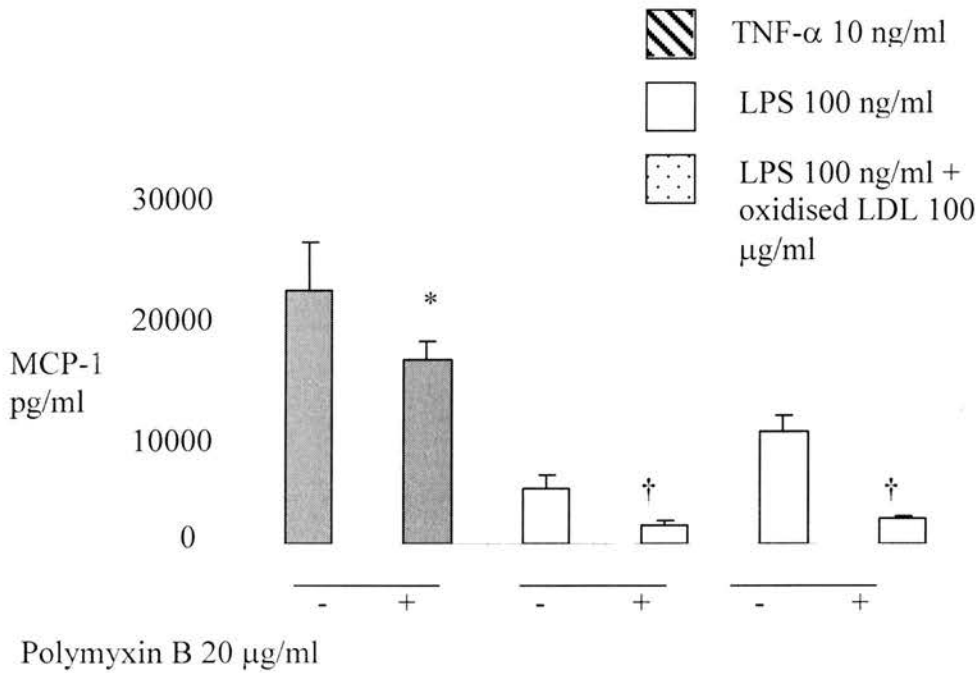
Figure 3.5. Polymyxin B attenuates LPS and TNF-α signalling in HUVECs.

Polymyxin B was pre-incubated with TNF-α, LPS or oxidised LDL that had been spiked with LPS to a final concentration of 100 ng/ml. MCP-1 levels were measured in the supernatants following 8 h incubations with the different treatments. Results are presented as the mean ± SD from one experiment performed in triplicate. *, † significantly less following incubation with polymyxin B, $p < 0.05$, $p < 0.01$.

85

The effort to reduce levels of contaminating LPS focused on the Amicon ultrafiltration unit, the only component of the LDL preparation process that had to be reused between preparations. Although the Amicon ultrafiltration unit was rigorously cleaned between preps it could not withstand autoclaving. The protocol to remove LPS by soaking the concentrator in potassium hydroxide was employed for all further LDL preparations. Where possible, a switch to disposable equipment was made and LPS levels were measured in fresh LDL preparations (Table 3.2). The changes to the preparation protocol reduced LPS contamination from the Amicon ultrafiltration unit in LDL preparations. LPS levels were measured for all subsequent batches of locally produced LDL. LDL was diluted in culture medium prior to use and working concentrations of LPS became less than 25 pg/ml. This level of contamination for native and oxidised LDL was accepted for the remaining experiments described in this thesis

3.2.3. The inflammatory effects of oxidised LDL on cultured endothelial cells

Following detection of significant LPS contamination within early LDL preparations, with the possibility that this may have contributed to the impressive stimulation of endothelial cell chemokine production (Figure 3.2), it was important to assess the inflammatory effects of LDL produced after introduction of measures to reduce LPS contamination. Oxidised LDL induced up-regulation of IL-8 message was demonstrated using semi-quantitative RT-PCR (Figure 3.6). Endothelial cells incubated with oxidised LDL had increased amount of IL-8 mRNA within 4 hours. Incubation with native LDL for this period also produced a faint but discernible signal indicating an increase in IL-8 transcription over basal levels of activity (Figure 3.6).

The amount of IL-8 released into culture supernatants following 16 h incubations with oxidised and native LDL was quantified by ELISA. A dose relationship was seen with oxidised LDL (Figure 3.7A). For the same concentration,

86

Batch no. (#)	EU/ml (approx pg/ml)
Local nLDL # 7-9	0.75 +/- 0.14 (62.5 +/- 12.5)
Local oxLDL # 7-9	0.98 +/- 0.18 (81.6 +/- 15.0)

Table 3.2. LPS contamination levels in LDL following cleaning of Amicon ultrafiltration unit.

Results are mean and standard deviation of three separate LDL preparations.

87

Chapter 3

native LDL was a much less potent stimulus for IL-8 production (after preparation using the method to reduce LPS contamination) and there was a trend towards increased IL-8 over untreated cells only at the highest concentration (100 μg/ml, Figure 3.7A). Similar results were seen with different preparations of LDL using different endothelial cell donors. The variation in IL-8 production from 4 LDL batches incubated with 2 different endothelial cell donors is shown (Figure 3.7B).

Oxidised LDL also stimulated MCP-1 production by human endothelial cells. Native LDL had a weaker stimulatory effect. These results closely paralleled their effects upon IL-8 production (Figure 3.8). The experiments with LDL produced with the modified protocol designed to reduce LPS contamination demonstrated that oxidised LDL retained its ability to stimulate endothelial cell production of the chemokines IL-8 and MCP-1. The quantity of cytokine production appeared to be less with oxidised LDL prepared using the modified protocol (compare Figure 3.2A with Figure 3.7A) and although LPS content data for one of the lipid batches used in Figure 3.2A are not available, the higher potency of earlier LDL preparations was probably related in part to LPS contamination (Table 3.1).

Oxidised LDL exerted its effect on IL-8 release in part through up regulating IL-8 transcription and indeed, IL-8 production is regulated primarily at the level of gene transcription (Roebuck 1999). The work described in the rest of this chapter was directed towards the inflammatory signalling mechanisms of oxidised LDL. Because native LDL had at most, a very weak effect on inflammatory cytokine production, the remaining work compared oxidised LDL with untreated cells only. Functional studies indicate that IL-8 transcriptional responses to proinflammatory mediators are rapid and require only 100 nucleotides of 5' flanking DNA upstream of the TATA box. Binding sites for the inducible transcription factors AP-1, NF-IL-6 and NF-κB are contained within the promoter. Deletion constructs of the IL-8

88
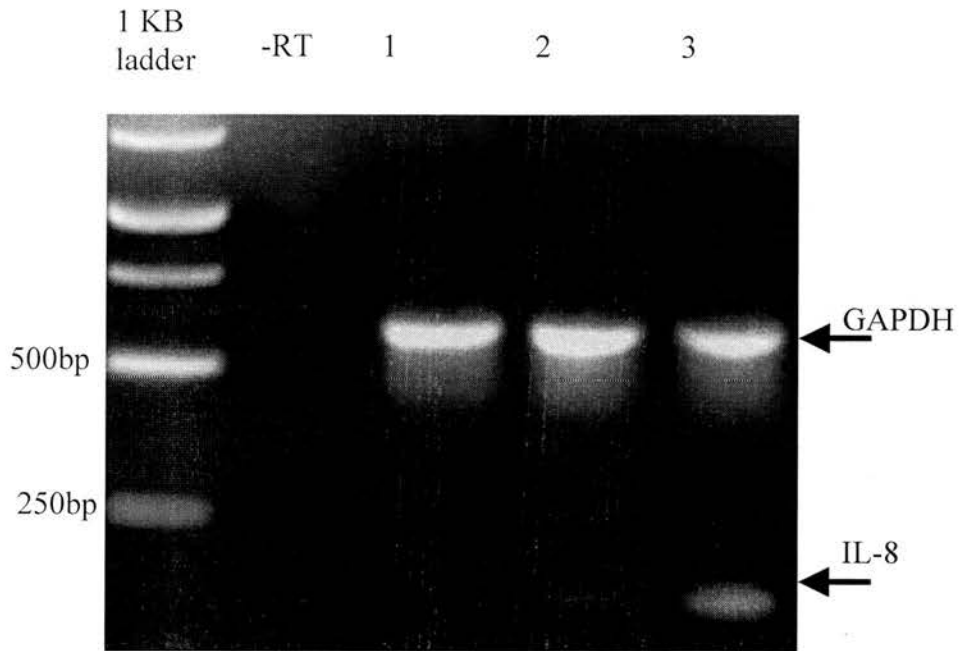
Figure 3.6. Semi-quantitative RT-PCR for IL-8 gene expression in HUVECs treated with oxidised LDL.

HUVECs were incubated at confluence in medium alone (lane 1) or in the presence of nLDL 100 µg/ml (lane 2) or oxLDL 100 µg/ml (lane 3) for 4 hours. Total RNA was extracted using TRIZOL reagent and 0.5 µg was used in a reverse transcription reaction. 2 µl of resulting cDNA was then used from each reaction condition to perform semi-quantitative PCR in a multiplex reaction with primers for the housekeeping gene GAPDH (product 545bp) and IL-8 (product 180bp). A reaction was also performed in the absence of reverse transcriptase (-RT) to check for the presence of contaminating genomic DNA. The gel is representative of an experiment performed in triplicate.

89

Chapter 3

A

B
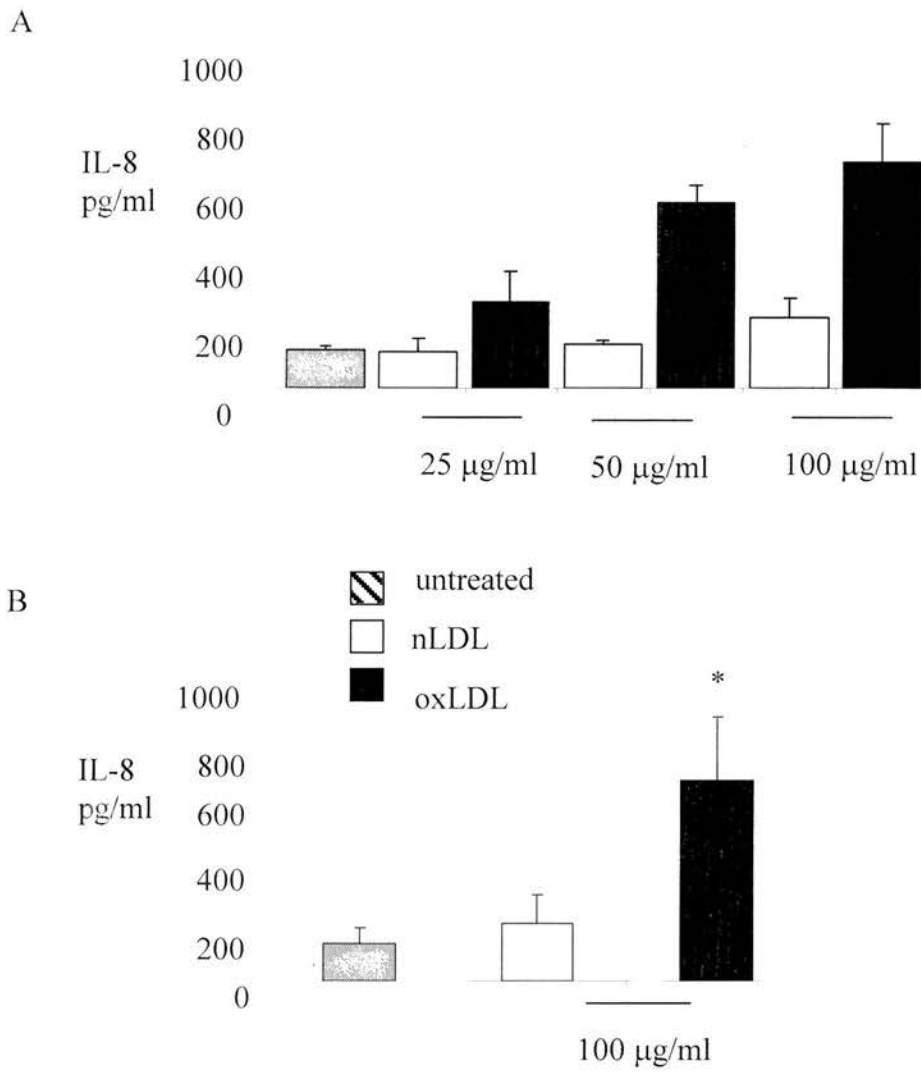
Figure 3.7. Oxidised LDL stimulated release of IL-8 from HUVECs exhibited dose dependence.

A. HUVECS were stimulated with clean preparations of oxidised LDL or native LDL at the concentrations indicated for 16 hours. Supernatants were retrieved and IL-8 concentration measured by ELISA. Results shown are from a single LDL preparation and HUVEC donor (n=3). B. The pooled results (mean ± SD) from 4 separate lipid preparations and HUVEC donors (performed in triplicate) are shown. * significantly greater than native LDL, $p < 0.05$.

90

Chapter 3
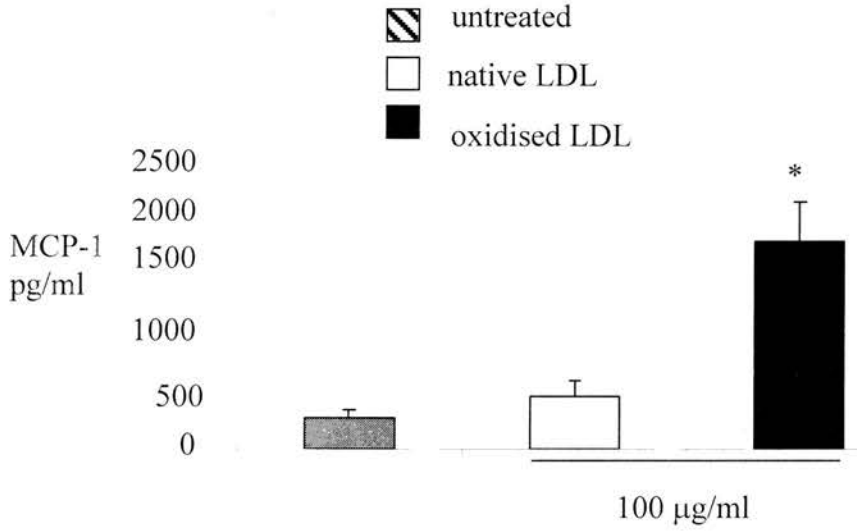
Figure 3.8. MCP-1 production is increased in HUVECs incubated with oxidised LDL

HUVECS were incubated with native LDL and oxidised LDL for 16 hours. Supernatants were retrieved and MCP-1 levels were measured by ELISA. Results are mean and standard deviation from one donor performed in triplicate. * significantly greater than native LDL, $p < 0.01$.

91

Chapter 3

promoter tagged to a luciferase reporter gene were generously donated by Professor N Mukaida (Kanazawa University, Japan) in order to dissect out transcriptional mechanisms responsible for oxLDL induced IL-8 production. A schematic of the different plasmids is shown (Figure 3.9).

XL-1 Blue bacteria were transformed with the IL-8 promoter constructs in a pXP2 backbone. In comparison to many cell lines, HUVECs are relatively refractory to transfection. They are susceptible to toxicity from lipids used in lipofection and are readily damaged during electroporation (Segura et al 2001). The efficiency of different transfection methods was established using pDsRed2-C1 (Clontech), containing the red fluorescent protein (RFP) reporter gene DsRed2 under the simian virus promoter (SV40). High transfection efficiency of HUVECs has been reported using both calcium phosphate precipitates (Segura et al 2001) and liposomes (Kaiser et al 2001). Both methods were compared using the DsRed2 reporter plasmid (Figure 3.10).

Lipofectin provided a transfection efficiency of around 20-25%, estimated by inspection, compared to calcium phosphate (5-10%). The calcium phosphate protocol was also directly cytotoxic, producing rounding and detachment of cells following incubation with the precipitates. No toxicity was seen with calcium phosphate precipitates alone and this effect may have been caused by the larger quantity of DNA used in this protocol.

Lipofectin provided the highest transfection efficiency without toxicity and was therefore chosen as method of delivery for the IL-8 promoter constructs. In a preliminary experiment, HUVEC luciferase activity was compared following transfection with pGL3 vector, expressing luciferase under the control of the SV40 promoter and the full length IL-8 promoter construct 1 (-1481 bp) following treatment with PMA, TNF-α and oxidised LDL (Figure 3.11). This was a pilot experiment and no corrections were made for transfection efficiency or cell lysate

92

Chapter 3

Figure 3.9. A schematic of the IL-8 promoter constructs.

Transcription factor binding sites and the luciferase promoter are shown. Construct 1 is the full length IL-8 promoter (-1481 to + 44) constructs 2 and 3 are deletion constructs that contain nucleotides (-546 to + 44) and (-133 to +44) respectively. Construct 3 was also used with site directed mutations in the AP-1, NF-IL-6 and NF-κB binding sites (indicated by arrows; ΔAP-1, ΔNF-IL6, ΔNF-κB). IRF: Interferon regulatory factor; AP: Activator protein, HNF-1: Hepatocyte nuclear factor; GRE: glucocorticoid response element; NF-IL-6: Nuclear factor interleukin-6.

93

Chapter 3
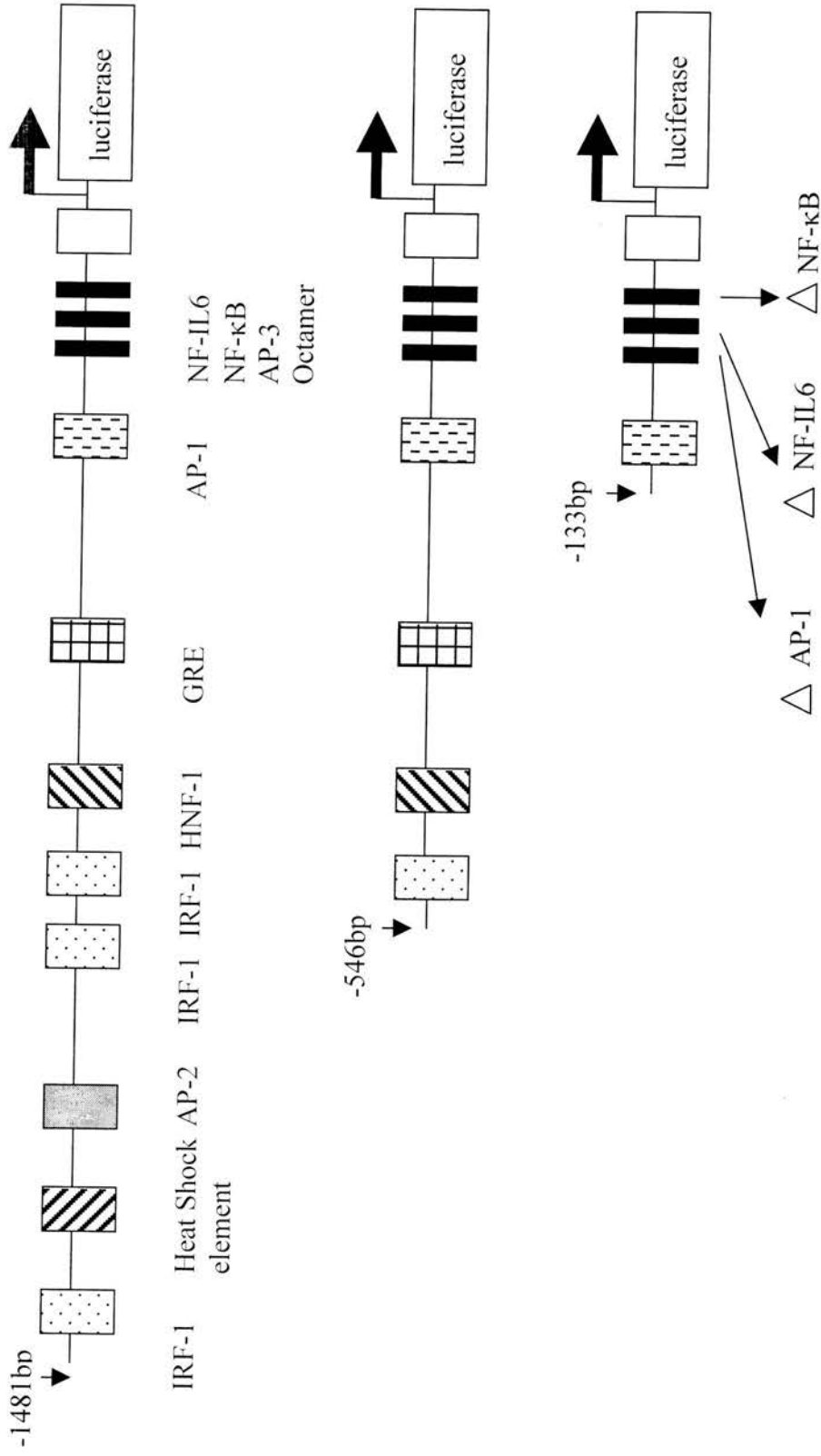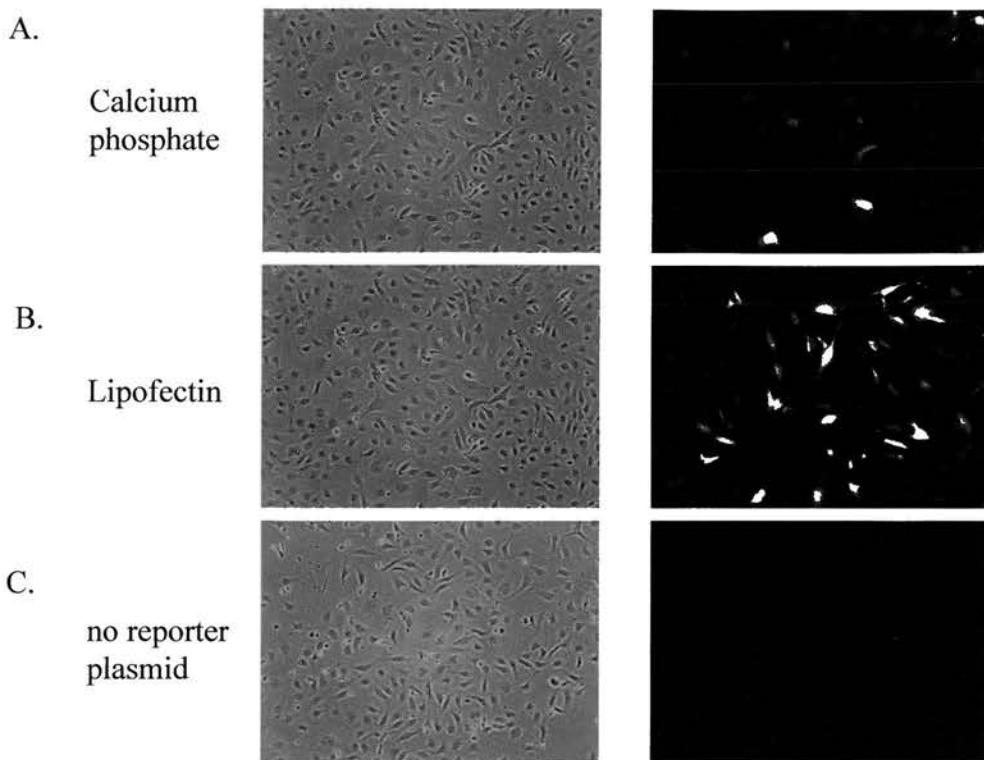
Figure 3.10. Comparison of liposome and calcium phosphate mediated transfection of HUVECS.

HUVECs were grown to 60% confluence in 12-well plate format. Pictures were taken 24 hours after transfection at low power in light microscopy and fluorescent views (left and right slides respectively). A. Transfections of DsRed2 (3 µg plasmid DNA) with calcium phosphate were as described in Materials and Methods. B. Liposome transfections using Lipofectin (Invitrogen). Cells were washed in serum-free medium (OptiMEM I, Gibco Brl) and DsRed2 (0.4µg plasmid DNA) was pre-incubated with Lipofectin in OptiMEM I prior to incubation with the HUVECs. C. Neither liposome nor calcium phosphate (not shown) treatment induced red fluorescent activity in the absence of DsRed2. Slides shown are representative from one experiment performed in triplicate wells.

95

Chapter 3
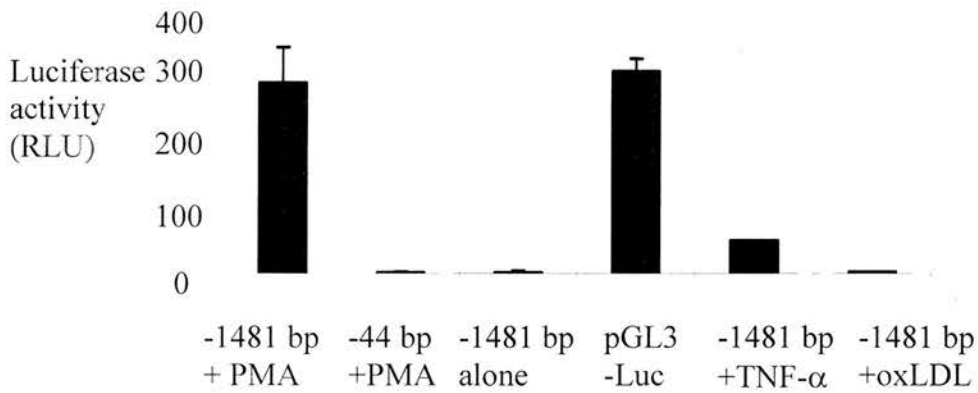
Figure 3.11. Comparison of induction of luciferase activity by PMA, TNF-α and oxidised LDL in HUVECs transfected with the –1481 IL-8 promoter –Luc construct.

HUVECs were grown to 60% confluence in 12-well plates and transfected with plasmid DNA in complex with lipofectin. The cells were allowed to grow to confluence and treated with the stimuli for 14 hours. Following stimulation with PMA (1×10^{-7}M), TNF-α (100 ng/ml) and oxidised LDL (100 μg/ml) cell lysates were harvested for luciferase activity. Results are mean and standard deviation, expressed in luciferase relative light units (RLU) from one experiment performed in triplicate.

Chapter 3

concentration. A construct containing only the luciferase gene (-44bp) was included as a negative control. PMA treatment of cells transfected with the −1481bp plasmid and transfection with the pGL3-Luc plasmid produced strong luciferase activity in the cell lysates. Activity in the lysates from cells transfected with the mock plasmid (-44 bp) was negligible. Stimulation of cells transfected with the full length plasmid (-1481 bp) with high concentrations of TNFα (100 ng/ml) produced considerably less luciferase activity than the potent PMA stimulus and incubation with oxidised LDL did not increase luciferase activity above baseline levels in unstimulated transfected cells. Similarly, no increase in luciferase activity could be detected following incubation of oxidised LDL with cells transfected with the −546bp and − 133bp plasmids (not shown). TNF-α and PMA are established as powerful stimuli for inflammatory cytokine production (data on TNF-α induced IL-8 production from endothelial cells is presented later in chapter 5). The observation that a high concentration of TNF-α was required to produce detectable luciferase levels suggested that absence of a detectable increase in luciferase activity in response to oxidised LDL was probably a combined result of low plasmid transfection efficiency and relatively low potency as a stimulus for IL-8 production.

The potential of this approach for dissecting out the DNA binding sites modulating IL-8 transcription was demonstrated for TNF-α stimulation (Figure 3.12). TNF-α induced luciferase activity was less in the full length promoter construct than in the −546 and −133 bp constructs. This is consistent with the possibility of an upstream negative regulatory element. Mutation of the NF-IL6, NF-κB and AP-1 binding sites reduced luciferase activity compared to the intact −133 promoter construct. Activity was least in the promoter constructs with AP-1 and NF-κB binding site mutations. This is consistent with the cooperative role of these transcription factors in IL-8 message production (Roebuck 1999).

Chapter 3

Despite optimising a protocol for plasmid delivery to HUVECs, the experiments using reporter constructs to elucidate oxidised LDL transcriptional mechanisms were limited by failure to detect luciferase reporter gene activity from any of the constructs following oxidised LDL stimulation. The importance of NF-κB for IL-8 transcription following TNF-α was indicated by the absence of luciferase activity in cells transfected with the luciferase reporter containing a mutated NF-κB binding site (Δ NF-kB, Figure 3.12). For this reason, nuclear fractions from HUVECs stimulated with oxidised LDL were examined directly for active NF-κB using electromobility shift assays (EMSA).

Incubation of oxidised LDL with endothelial cells for 1 hour resulted in increased binding activity within nuclear extracts for a consensus NF-κB oligonucleotide. The specificity of binding was demonstrated by competing out radiolabelled probe in the presence of excess unlabelled (cold) oligonucleotide and by the failure of a radiolabelled consensus oligonucleotide with a single base substitution to bind nuclear extracts. The intensity of the NF-κB band varied among the 3 different preparations of oxidised LDL. NF-κB activity was not detected in untreated cells and a discernible NF-κB band could only be seen in one (Figure 3.13, lane 7) of the three batches of native LDL, indicating at most, slight activation of NF-κB above baseline levels.

There are several NF-κB proteins and most can dimerise with themselves (homodimers) or other family members (heterodimers) to form active NF-κB (Tak et al 2001). NF-κB complexes can be incubated with antibodies against specific NF-κB proteins and further retardation of the complex on a gel (supershift) indicates the presence of the specific protein within the active NF-κB complex. Supershift analysis on NF-κB complexes induced by oxidised LDL, TNF-α and LPS was performed using antibody against the p50 protein (Figure 3.14). The p50 antibody

98

Chapter 3
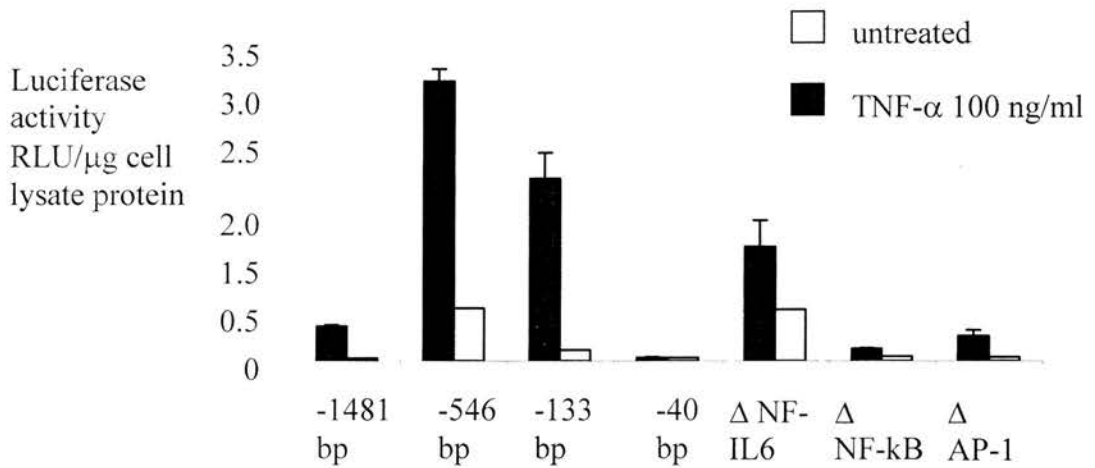
Figure 3.12. Luciferase activity following TNF-α stimulation of HUVECs transfected with IL-8 promoter-luciferase plasmids 1-7.

Cells were transfected and treated as for figure 3.11. Luciferase activity was expressed after correction for the quantity of cell lysate placed in the luminometer (RLU/µg of cell lysate). Results for the different promoter constructs including the – 133 promoter constructs containing mutations in the NF-IL6, NF-κB and AP-1 (Δ NF-IL6, ΔNF-κB and ΔAP-1 respectively) are shown. Results are mean and standard deviation from one experiment performed in triplicate.

Chapter 3
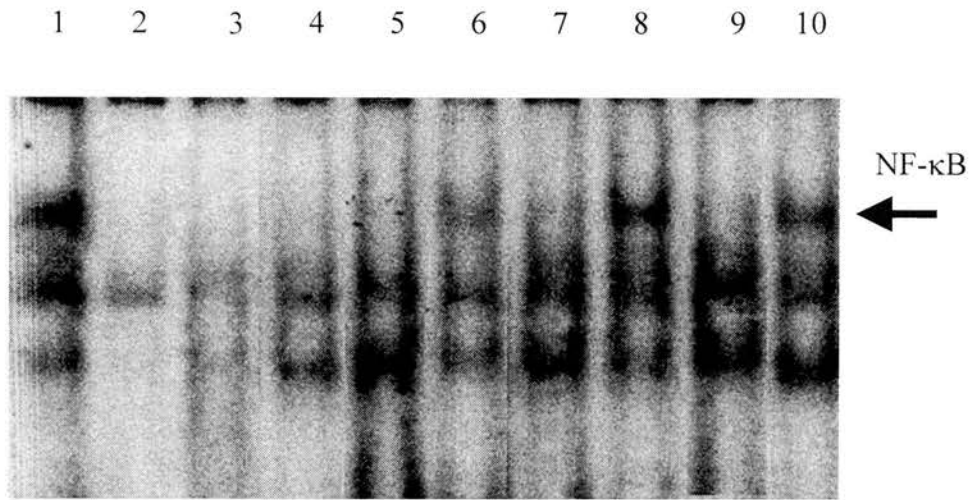
Figure 3.13. EMSA demonstrating oxidised LDL induced activation of the transcription factor NF-κB in HUVECs.

HUVECs were incubated for 1 h with TNF-α (1 ng/ml) as a positive control of NF-κB activation (lanes 1-3), medium alone (lane 4), 3 different preparations of native LDL (100 μg/ml, lanes 5, 7, 9) and oxidised LDL (100 μg/ml, lanes 6, 8, 10). NF-κB was assayed in nuclear extracts (7 μg) from HUVECs by electromobility shift assays (EMSA) with ^{32}P-labelled, double stranded consensus NF-κB oligonucleotides. The specificity of binding was demonstrated by incubating with both 100-fold excess cold oligo (lane 2) and a scrambled oligo containing a single base pair substitution (lane 3). The results are from 3 separate batches of LDL on the same HUVEC donor.

100

Chapter 3
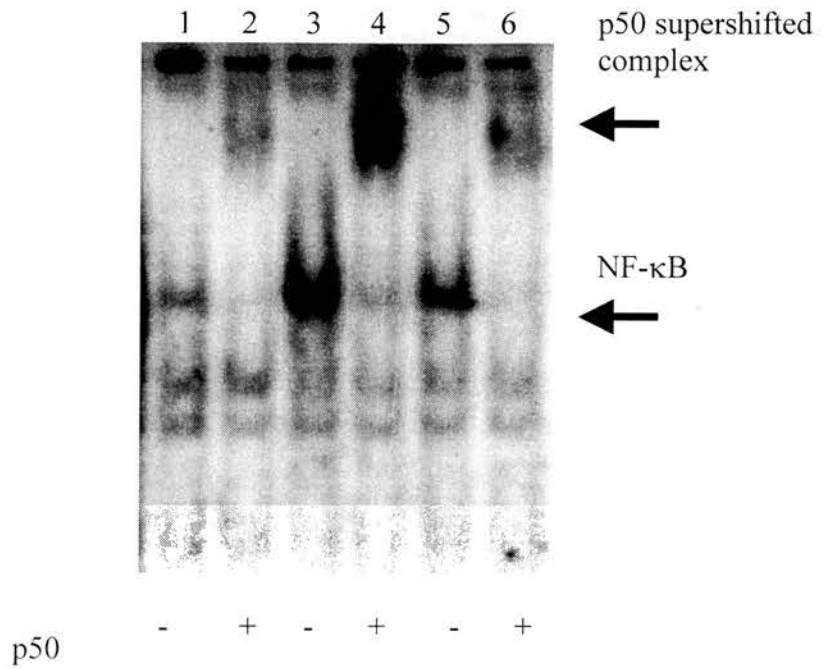
Figure 3.14. Supershift analysis of active NF-κB

Supershift analysis of oxidised LDL (100 μg/ml lanes 1, 2), TNF-α (1 ng/ml lanes 3, 4) and LPS (5 μg/ml lanes 5, 6) induced complexes using a specific antibody against p50 (Santa Cruz). Antibody was pre-incubated with the nuclear binding mix for 50 min before being run on the polyacrylamide gel.

101

Chapter 3

was effective at supershifting complexes induced by all 3 stimuli, indicating a prominent role for p50 either in the form of a homodimer or possibly as a heterodimer with other NF-κB family members. It is important to note the low concentration of TNF-α used to demonstrate NF-κB activation (1 ng/ml, Figure 3.14) compared to the concentrations required to observe a strong luciferase signal from the IL-8 promoter constructs (100 ng/ml, Figure 3.12). Preliminary experiments indicated that NF-κB activation could be observed in HUVECs with TNF-α concentrations as low as 100 pg/ml (Figure 5.16). This discrepancy probably reflected the relatively poor transfection efficiency of the IL-8 promoter plasmids and is discussed further on.

After establishing temporal and quantitative aspects of oxidised LDL regulated transcription and release of the chemokine IL-8 from endothelial cells, experiments were planned to assess the impact of prolonged LDL incubations on cell viability. A working LDL concentration of 100 μg/ml provided a clear differential in response with respect to IL-8 transcription, release and NF-κB activation. Although the experiments examining IL-8 message up-regulation and NF-κB activation involved incubations lasting 4 hours, it was important to account for any impact on cell necrosis or apoptosis following the more prolonged 16 h experiments examining IL-8 release.

3.2.4. Oxidised LDL induced endothelial cell death

Cellular necrosis and apoptosis within the atherosclerotic plaque contribute to lesion instability and rupture. Oxidised LDL is cytotoxic and has been shown to induce both apoptosis and necrosis in vascular cells. Oxidised LDL causes the release of lactic dehydrogenase (LDH) from cultured vascular smooth muscle cells, endothelial cells and fibroblasts (Morel et al 1984). Oxidised LDL has been shown to induce apoptosis in smooth muscle cells, endothelial cells (Harada-Shiba et al 1998)

102

(Dimmeler et al 1997) and macrophages. The effects of LDL preparations on HUVEC LDH release and annexin V positivity were therefore examined.

LDH activity was measured from the decay in absorbance at 340nm following oxidation of nicotinamide adenine dinucleotide (NADH) by LDH. This assay tests for major disruption of cellular membranes occurring during necrosis when cytoplasmic LDH leaches into the culture supernatant. After 16-hour incubations there was no difference in cytoplasmic LDH activity between oxidised LDL, native LDL and untreated samples (Figure 3.15). This result was surprising in view of previously published data on oxidised LDL cytotoxicity. LDH is not a sensitive indicator of more subtle aspects of cellular toxicity such as depressed metabolic function or apoptosis. The LDH assay did not lend itself to high sample throughput (each sample had to have activity measured in a spectrophotometer cuvette over 3 minutes) and because of these concerns annexin V was pursued as a marker of cellular injury. Annexin V is a calcium dependent phospholipid binding protein with a high affinity for the phospholipid phosphatidylserine (PS). PS translocation is the movement of PS from the inner to the outer cellular membrane leaflet and is an early event during apoptosis, also occurring during cell necrosis (Koopman et al 1994).

The binding of FITC-conjugated annexin V to human endothelial cells following incubations with varying concentrations of oxidised LDL was examined (Figure 3.16). Untreated cells and cells incubated with native LDL (100 μg/ml) for 16 hours had levels of annexin V binding below 4%. Hydrogen peroxide was included as a positive control inducing necrosis and etoposide was included as an inducer of apoptosis. These produced rates of annexin V binding of 70.1% and 20.1% respectively. The relatively low rate of annexin V binding for etoposide was in accordance with the microscopic appearance of the cell culture after treatment. There was evidence of cell rounding and lifting although the majority of cells appeared intact. Oxidised LDL exhibited a dose relationship for annexin V staining. A 24 h incubation with 100 μg/ml of oxidised LDL produced 9.3% annexin V

103
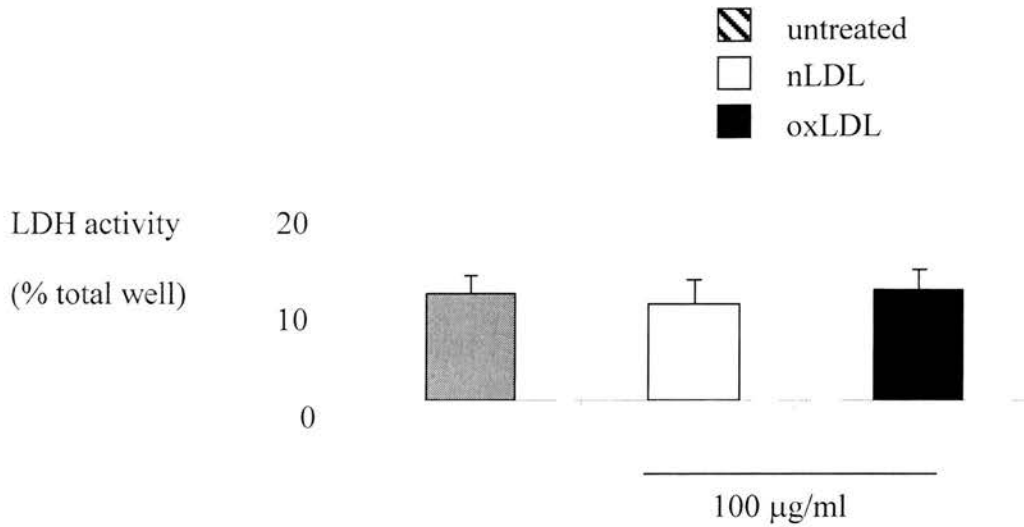
Figure 3.15. Incubation with native LDL or oxidised LDL did not increase HUVEC LDH supernatant activity.

HUVECs were incubated for 24 hours in medium alone or in the presence of native LDL or oxidised LDL at concentrations of 50 μg/ml (not shown) and 100 μg/ml (above). Supernatants were removed after the incubations and LDH activity was recorded. The results are expressed as a percentage rate of absorbance change of wells that had been completely lysed with PBS 1% Triton X. The data are mean and standard deviation from one batch of LDL and a single HUVEC donor performed in quadruplicate.

104

Chapter 3

105
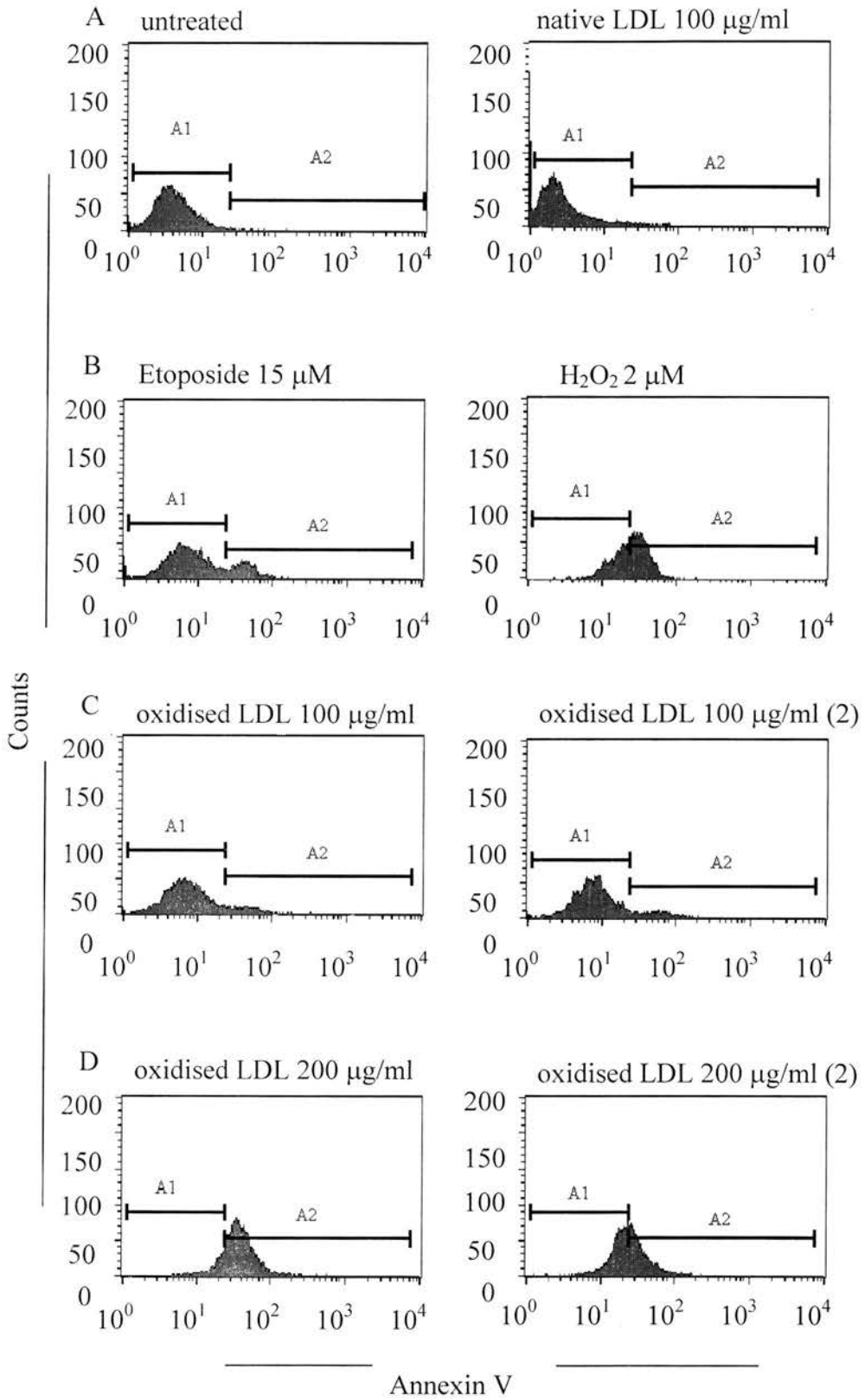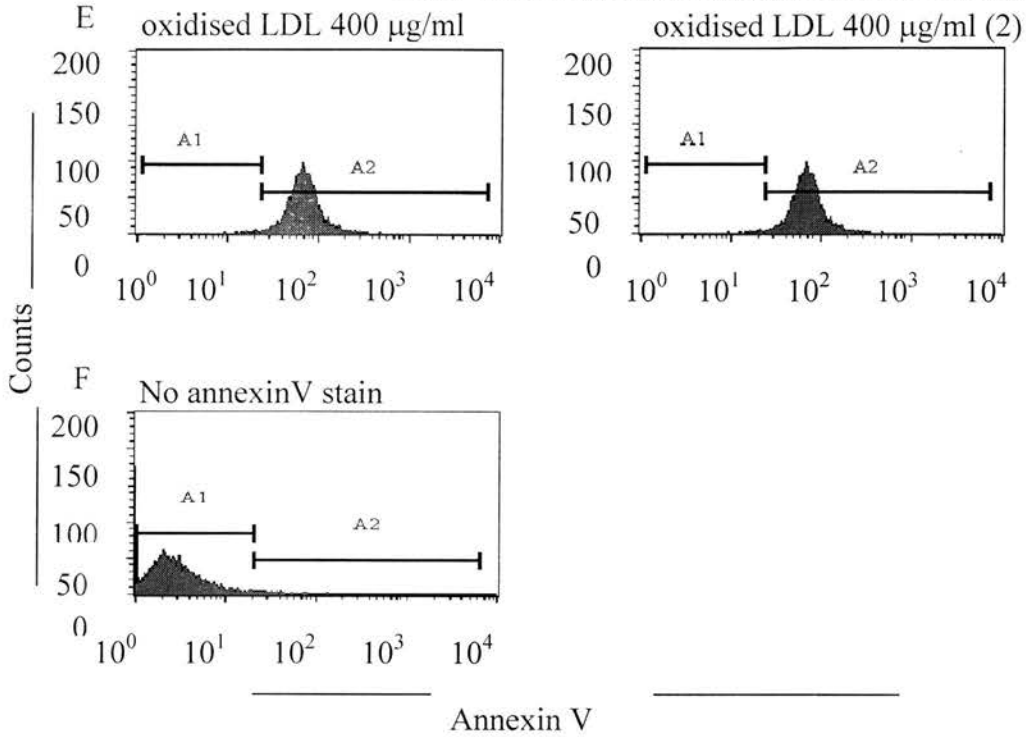
Figure 3.16. The effect of increasing concentrations of oxidised LDL on annexin V staining in HUVECs.

HUVECs were incubated for 16 hours in medium alone or with oxLDL at the concentrations indicated. Etoposide (15 µM) and H_2O_2 (2 µM in PBS) treatments for 6 h were included as positive controls of apoptotic and necrotic stimuli respectively. Following the treatments, supernatants were removed and the cells washed, trypsinised, and resuspended in annexin V binding buffer. The results are presented in histograms representing 5000 counts for each experiment. The percentage of dead or necrotic cells was taken as 100A2/(A1+A2). A. Untreated cells and native LDL (100 µg/ml) produced low levels of annexin V staining (mean 3.20%, and 4.25%). B. Treatment with etoposide and H_2O_2 resulted in cell death at rates of 21.1% and 70.1 % respectively. C-E. Concentrations of 100, 200 and 400 µg/ml oxidised LDL produced mean percentages of annexin V staining of 9.3%, 80.1% and 99.8% respectively after 16 h. F. The background fluorescence in the FL1-H channel in the absence of annexin V was 0.9%.

106

Chapter 3

binding and this increased to almost 100% following incubations with 400 µg/ml. This experiment illustrated the damaging effects of the oxidised LDL on endothelial cells, increasing annexin V binding rates above levels observed with untreated or native LDL treated cells. No firm conclusion could be drawn over the nature of cellular damage, whether it was in the form of necrosis or apoptosis, although the results from LDH supernatant analysis (Figure 3.15) suggested no excess necrosis in the oxidised LDL treated cultures.

3.3. Discussion

The data presented in this chapter demonstrate the isolation of a pure culture of human umbilical vein endothelial cells (HUVECs, Figure 3.1) and characterisation of a preparation of LDL with minimal LPS contamination as a model for inflammatory endothelial injury in atherosclerosis. Mechanisms of oxidised LDL inflammatory injury are also illustrated including release into the culture supernatants of the chemokines IL-8 and MCP-1. For IL-8, part of this increased production was through increased gene transcription and this was associated with activation of the transcription factor NF-κB. The importance of oxidation for LDL's effect was also demonstrated, with native LDL proving to be relatively inert, producing only a small increase in cytokine production above untreated cells. Finally, the damaging effects of oxidised LDL on endothelial cells cultures was examined. Concentrations that produced heightened cytokine production and NF-κB activation also had excessive rates of apoptosis or necrosis compared with native LDL and untreated cultures.

3.3.1. The use of cultured endothelial cells in an *in vitro* model of atherosclerosis

A fundamental question is the validity of venous endothelial cells (HUVECS) in a model of a pathological process affecting arterial vessels. HUVECS remain the most prevalent model for studying human endothelial cells *in vitro*. Advantages include the ability to isolate pure populations of primary cells that can be expanded

107

Chapter 3

in culture prior to freezing for future use. Criticisms of the use of these cells include the fact that venous vessels do not develop atheroma and more appropriate cell populations including human coronary artery endothelial cells (HCAECs) and bovine aortic endothelial cells are available. However, a study comparing HCAECs and HUVECs found qualitatively similar cytokine responses to inflammatory stimuli (Briones et al., 2001). The loss of arterial pressure and turbulent flow effects are more significant deficiencies of *in vitro* models of atheroma. The potential for venous vessels to develop atheroma when exposed to high arterial pressures is also a significant clinical problem following saphenous vein grafting for coronary artery bypass surgery.

HUVECs were chosen as a model owing to the favourable properties outlined above and the extensive international laboratory experience already available on this cell type. Possible cell contaminants in HUVEC cultures that had been passaged following collagenase digestion from umbilical cords included pericytes, fibroblasts and smooth muscle cells from the vessel wall (Gimbrone, Jr. et al 1974; Jaffe et al 1973). The CD31 antigen, platelet endothelial cell adhesion molecule-1 (PECAM-1) was chosen to identify endothelial cells by flow cytometry (Figure 3.1) (Newman 1997). Expression of PECAM-1 is confined to endothelial cells and leucocytes (Newman et al., 1997) and failure of a proportion of the cell population to stain with the antibody would have indicated the presence of a contaminating cell type. Greater that 99% of cells were CD31 positive indicating a relatively pure culture (Figure 3.1).

3.3.2. The inflammatory effects of native and oxidised LDL on endothelial cells

A central tenet of this thesis is the role of oxidised LDL as an inflammatory stimulus, present and bound to matrix within the intimal space, driving the formation of atheroma through interaction with endothelial cells. Having established an endothelial cell culture, a source of both native and oxidised LDL had to be

108

identified and characterised. Professor Riemersma's laboratory was producing LDL and oxidising it against copper sulphate within the University. Native and oxidised LDL preparations could also be bought commercially. An initial experiment demonstrated MCP-1 and IL-8 production by endothelial cells in response to both native and oxidised LDL produced within the University (Figure 3.2). IL-8 and MCP-1 are members of the CXC and CC chemokine families respectively (Rossi et al 2000). They are important chemoattractants for neutrophils and monocytes and have been implicated in a variety of inflammatory diseases. At a concentration of 100 μg/ml, oxidised LDL is a potent inducer of cytokine production with native LDL producing small increases above untreated conditions. A key unknown is the biologically relevant amount of oxidised LDL trapped within the extracellular space of the subendothelium and how this could be translated into a concentration in solution within tissue culture medium. Oxidised LDL is not found in the circulation or lymphatic systems (Steinberg et al 1999) and information on the specific quantities of different components of LDL within atheromatous tissue is not available (Tabas et al 1999). The choice of LDL concentration to use in the initial experiment was therefore heavily influenced by work published by other groups studying oxidised LDL's effects on various cell types in culture. There is a close correlation between *in vitro* observations of oxidised LDL's effects on endothelial cell activation and immunohistochemical examination of endothelial cells from atheromatous vessels demonstrating chemokine production and NF-κB activation (Brand et al 1996; Claise et al 1996; Cominacini et al 2000; Koch et al 1993; Simonini et al 2000). Having demonstrated a clear differential in biological activity between native LDL and oxidised LDL, at concentrations of 100 μg/ml (Figure 3.2) that was in accordance with previously published work with respect to IL-8 production in an endothelial cell line (Claise et al 1996), it was decided to conduct further LDL studies using this concentration.

In order to be sure that it was the inflammatory activity of LDL that was being examined it was important to eliminate any LPS contamination occurring during preparation that might be contributing to cytokine production. Problems with LPS

109

contamination of biological reagents, including LDL have been described frequently in the past (Rickles et al 1979; Sata et al 1998) and significant quantities of LPS ranging up to 1 μg/ml were identified within LDL preparations produced locally or obtained commercially using the Limulus Amebocyte Lysate (LAL) assay (Table 3.1). Specific LPS binding has been demonstrated for all lipoprotein family members (Levels et al 2001) including LDL, very low density lipoprotein (VLDL) and high density lipoprotein (HDL). The levels observed (Table 3.1) were much higher than those quoted for LDL prepared using similar protocols by other workers and suggested contamination during preparation. Grafe et al (1998) and Claise et al (1996) found no evidence of contaminating LPS using the LAL assay within the oxidised LDL in their studies. In contrast, levels as high as 800 pg per mg of lipoprotein have been detected by other workers (Terkeltaub et al 1994). Importantly, the data sheet for the commercial LDL purchased from Intracel © stated that the product was 'prepared aseptically but not guaranteed sterile'. By analysing aliquots of the LDL preparation from each step in the process, the Amicon ultracentrifugation unit was identified as one major source of contamination (Figure 3.3).

The contribution to endothelial cell activation of any LPS contamination was difficult to quantify for two reasons. Firstly, the LAL assay provided no information on LPS serotype, an important variable for determining the magnitude of response (Rietschel et al 1990). However, at the higher concentrations listed in Table 3.1, E Coli 0127b8 LPS, a serotype used within our laboratory, would result in activation of HUVECS and human monocyte derived macrophages (see chapters 5 and 6). Secondly, the biological activity of LPS bound within LDL is reduced (Flegel et al 1993; Netea et al 1996) and this has been proposed as a mechanism whereby lipoproteins facilitate safe clearance from the circulation (Rauchhaus et al 2000). Polymyxin B was pre-incubated with a batch of LDL in an attempt to neutralise the biological activity of any contaminating LPS (Figure 3.4). Polymyxin B is a naturally occurring antibiotic with powerful disrupting properties on cell membranes of gram negative bacteria. Its properties of binding, neutralising and inhibiting inflammatory signalling by LPS has been used by investigators for over 20 years (Pier et al 1981).

110

Chapter 3

Cytokine production to both oxidised and native LDL was significantly reduced following pre-incubation with polymyxin B (Figure 3.4). This was also effective in reducing cytokine production in response to LPS alone and oxidised LDL containing a spiked quantity of LPS (Figure 3.5). The interpretation of these results was clouded by the inhibitory activity of polymyxin B on TNF-α induced cytokine production in an LPS-free control limb of the experiment (Figure 3.5). In eukaryotic cells, polymyxin B has additional effects and has been used specifically as an inhibitor of protein kinase C (Gandhi et al 1992). It is not clear whether protein kinase C inhibition was responsible for attenuating the response to TNF-α but this property prevented any assessment of specific LPS signalling blockade by polymyxin B.

LPS contamination levels within the LDL were measured in fresh preparations after modification of the protocol for LDL production and in particular, introduction of a new method to clean the Amicon ultracentrifugation unit between preparations. LPS content was markedly reduced from previous levels (to less than 100 pg/ml within the LDL preparation, prior to dilution in culture medium for use in experiments, Table 3.2) and compared very favourably with levels of contamination between 80 and 3200 pg/ml reported by some authors: (Fischer et al 2002; Terkeltaub et al 1994). Oxidised LDL prepared with minimal LPS contamination retained the ability to stimulate IL-8 production and after 4 h incubations, IL-8 message was up regulated in oxidised LDL treated cells compared to native LDL or untreated cells (Figure 3.6). IL-8 production has been characterised in a range of cell types including leucocytes, fibroblasts, epithelial and endothelial cells in response to specific inflammatory stimuli (reviewed by Roebuck 1999). IL-8 induction by TNF-α, IL-1β and LPS is primarily at the level of gene transcription (Blease et al 1999; Chaly et al 2000; Yeh et al 2001) and my own observation of oxidised LDL regulation of endothelial cell IL-8 transcription was in accordance with this.

The IL-8 promoter contains binding sites for several inducible transcription factors characterised as pro-inflammatory responsive elements (Mukaida et al 1994).

111

Chapter 3

The increased transcription correlated with increased release of IL-8 protein into the culture supernatants of endothelial cells and oxidised LDL demonstrated a dose effect with respect to IL-8 production (Figure 3.7A). These experiments were conducted using LDL with minimal LPS contamination (Table 3.2) and it was notable that total amounts of cytokine production were reduced compared to levels seen with an earlier lipid batch, prepared using the old protocol (Figure 3.2). This provides further evidence that contaminating LPS may have been contributing to the activity of the old LDL preparations. Oxidised LDL and minimally modified LDL (MM-LDL) have been shown to activate an immortalised endothelial cell line (Claise et al 1996) and human aortic endothelial cells to produce IL-8 (Lee et al 2000a). Claise et al (1996) used oxidised LDL at a concentration of 100 µg/ml to demonstrate increased IL-8 release after 24 h but not at an earlier timepoint of 4 h. MM-LDL is produced using a much shorter incubation with copper and although it attains new biological properties (Berliner et al 1990) it has not undergone the major oxidative changes seen with oxidised LDL and is still recognised by LDL but not by scavenger receptors (Navab et al 1996). In line with the identification of biological activity in minimally or non-modified LDL, 16 h incubations of non-oxidised native LDL with HUVECs produced a non-significant trend towards increased IL-8 release (Figure 3.7A) in contrast to the lack of effect seen on IL-8 transcription after 4 hours.

The literature contains conflicting reports on the biological activity of native LDL. Claise et al (1996) demonstrated a non-significant trend towards heightened IL-8 release in cells incubated with native LDL. Using higher concentrations for 4-day incubations, monocyte adhesiveness towards HUVECs was increased through a mechanism involving increased intercellular adhesion molecule-1 (ICAM-1) expression (Smalley et al 1996). Native LDL activity may arise from oxidation in culture during prolonged incubations (Fang et al 1998; Steinberg et al 1989). However, shorter 5-hour incubations using high concentrations (700 µg/ml) of native LDL have been shown to trigger a transient calcium influx and to increase vascular cell adhesion molecule-1 (VCAM-1) expression in human coronary artery endothelial cells, indicating the possibility of a more direct action (Allen et al 1998).

112

Chapter 3

Prepared with the new protocol, oxidised LDL retained its ability to stimulate HUVEC MCP-1 production (Figure 3.7B) although native LDL had no significant effect. Once again, levels of MCP-1 were less than those seen with earlier LDL preparations (Figure 3.2B). Both MM-LDL (Berliner et al 1990) and oxidised LDL (Li et al 2000) have been shown to increase MCP-1 release from endothelial cell cultures. The finding of elevated IL-8 and MCP-1 production by endothelial cells exposed to oxidised LDL correlates well with pathological studies of human atherosclerotic tissue (Koch et al 1993; Simonini et al 2000) demonstrating heightened production of both chemokines.

Both IL-8 and MCP-1 production are regulated primarily at the level of gene transcription and have regulatory sites for NF-κB. For this reason, experiments were designed to investigate transcriptional events associated with oxidised LDL signalling on HUVECs. IL-8 transcriptional mechanisms for an active oxidised phospholipid moiety found within oxidised LDL and MM-LDL have previously been elicited using reporter plasmids under the control of the IL-8 promoter (Yeh et al 2001). A series of plasmids, containing the luciferase reporter gene, with different components of the IL-8 promoter removed either through truncation or mutation, were obtained (Figure 3.9) in order to perform a similar analysis on our own locally prepared oxidised LDL. A reporter plasmid encoding red fluorescent protein DsRed2 (Baird et al 2000) was used initially to facilitate optimisation of a transfection protocol through rapid quantification of transfection efficiency by fluorescent microscopy. HUVECs have been found to be relatively refractory to transfection techniques with maximal transfection rates as low as 2% being reported for lipofection and electroporation (Teifel et al 1997). Modified protocols have produced improved transfection efficiencies in HUVECs with calcium phosphate (Segura et al 2001) and liposomes (Kaiser et al 2001). The latter transfection methods were compared in HUVECs (Figure 3.10) and lipofectin proved to be a more efficient delivery vehicle giving transfection rates of around 25%. Toxicity as evidenced by cytopathic microscopic appearances was a particular problem with calcium phosphate precipitates and concern about inflammatory activation of endothelial cells

113

Chapter 3

made this protocol an unattractive option for studying oxidised LDL signalling mechanisms.

IL-8 reporter plasmids were transfected into HUVECs that were subsequently incubated with oxidised LDL (Figure 3.11). A vector constitutively expressing luciferase (pGL3) was included as a positive control for luciferase expression. PMA and TNF-α were also included as potent inducers of IL-8 activation and although all three positive controls lead to appreciable increases in luciferase activity, oxidised LDL failed to induce enough luciferase to register on the luminometer (Figure 3.11) with any of the plasmids. This result contrasts with the strong luciferase activity induced in HeLa cells transfected with the same IL-8 promoter-luciferase construct following stimulation with oxidised phospholipid, oxidised 1-palitoyl-2-arachidonoyl-*sn*-glycero-3-phosphorylcholine (OX-PAPC) (Yeh et al 2001). OX-PAPC was found to be a relatively potent stimulus for IL-8 production at the concentration used, leading to IL-8 levels within 50% of those seen with TNF-α in this study. Data comparing HUVEC IL-8 production are presented in chapter 5 and oxidised LDL induced levels of IL-8 production are less than 10% those of TNF-α (Figure 5.12). Similarly, a low concentration of TNF-α (1 ng/ml) was a much more potent stimulus for NF-κB activation in HUVECs than oxidised LDL (Figures 3.13 and 3.14).

It seems likely that the comparatively low potency of oxidised LDL as a stimulus for IL-8 production combined with relatively low levels of transfection in HUVECs (compared to the more readily transfectable HeLa cells) resulted in failure to detect luciferase activity in these experiments. The IL-8 reporter constructs were tested in HUVECs with TNF-α (Figure 3.12) to demonstrate the potential of this approach for elucidating transcriptional mechanisms. In particular, the importance of active NF-κB and AP-1 for IL-8 transcription were illustrated when these sites were mutated in the -133 bp plasmid. This finding corresponds to previous promoter

114

mutation studies in a range of cell types (Roebuck 1999) including HUVECs (Wagner et al 1998). The relatively low luciferase activity in the full length (-1481 bp) IL-8 promoter construct was surprising (Figure 3.12). It suggests the possibility of an active negative regulatory element, requiring the presence of a segment in region –1481 to –561 bp to exert its effect. Following failure to gain information on oxidised LDL transcription mechanisms from the IL-8 promoter constructs, EMSAs were employed to directly examine for NF-κB activation. This was because of the latter's close association with IL-8 transcription and numerous studies demonstrating endothelial cell NF-κB activation in response to oxidised LDL in endothelial cells (Cominacini et al 2000; Parhami et al 1993) and macrophages (Hamilton et al 1998; Janabi et al 2000).

The concentration of active NF-κB within HUVEC nuclear extracts rose significantly following 1 h incubations with oxidised LDL (Figure 3.13). Native LDL had no activating effect within this time period, supporting the view that it was non-inflammatory over shorter incubation periods. Li et al (2000) also demonstrated degradation of inhibitory subunit IκBα and active NF-κB within human coronary artery endothelial cell nuclear extracts following incubation with oxidised LDL. Cominacini et al (2000) demonstrated NF-κB activation in bovine aortic endothelial cells and used a blocking antibody to show that this action was dependent on lectin-like oxidised LDL receptor-1 (LOX-1), originally cloned from this cell type (Sawamura et al 1997). Another scavenger receptor, CD36 also regulates oxidised LDL induced NF-κB activation in peripheral blood monocyte derived macrophages (Janabi et al 2000). Macrophages from patients who are CD36 deficient have diminished NF-κB activation in response to oxidised LDL. The relationship in monocytes may be more complex with short incubations increasing NF-κB activation but longer exposure to oxidised LDL suppressing this response (Brand et al 1997a).

115

Chapter 3

The NF-κB/Rel transcription family has several members including NF-κB1 *p50/p105*, p65 *RelA*, NF-κB2 *p52/p100*, RelB and c-Rel (Chen et al 1999). Most of these proteins can form hetero- or homodimers and the most prevalent activated form of NF-κB is a heterodimer consisting of a p65 and a p50 or p52 subunit (Tak et al 2001). Supershift analysis of the active NF-κB was performed on HUVEC nuclear lysates following oxidised LDL, LPS and TNF-α stimulation. The p50 antibody resulted in complete supershift of NF-κB induced by all three stimuli, suggesting a preponderance of p50 homo- or heterodimers. In contrast, Li et al (2000) performed Western blots demonstrating the presence of active p65 in nuclear lysates but did not search for other NF-κB proteins. Oxidised LDL induced NF-κB complexes in human monocytes could also be supershifted by p50 and p65 antibodies but not an antibody to c-Rel (Brand et al 1997a).

Activated NF-κB has been identified *in situ* in human atherosclerotic plaque endothelial cells but is absent or nearly absent in vessels devoid of atherosclerosis (Brand et al 1996). This observation coupled with the regulatory relationship of this transcription factor with so many genes putatively involved in the atherosclerotic process, including leukocyte adhesion molecules such as ICAM-1 and chemokines such as IL-8, suggest it plays a pivotal role (Brand et al 1997b). The data presented in this chapter support the idea that oxidised LDL located within the subendothelial space acts as a persistent stimulus to endothelial cell NF-κB activation. The parallels between experimental findings from HUVEC cultures and immunohistochemical observations from atherosclerotic specimens lend credence to the *in vitro* model of atherosclerosis introduced in this chapter and continued as a workhorse throughout the remainder of this thesis.

3.3.3. Oxidised LDL effects on endothelial cell survival

One final aspect of LDL's inflammatory effects, its impact on cell survival, required further analysis. Several studies have documented the cytotoxic nature of

116

Chapter 3

oxidised LDL on cultured endothelial cells (Colles et al 2001). Culturing HUVECs with oxidised LDL (25 µg/ml) for 10 hours led to an apoptosis rate of 8% increasing to 16% after 50 hours (Harada-Shiba et al 1998). The corresponding background rates of apoptosis in this study were less than 1% and 5% indicating increased apoptosis induced by oxidised LDL. Incubation with oxidised and native LDL led to no detectable increase in LDH activity in the supernatants of cultured HUVECs (Figure 3.15). LDH release occurs during major cellular disruption and necrosis and this result was in keeping with absence of any gross cytopathy on microscopic examination of the cultures following incubations. FACS analysis for fluorescently labelled annexin V, a marker of apoptosis and necrosis was performed. Following a 16-hour incubation with oxidised LDL at a concentration of 100 µg/ml, 9.3% of cells were annexin positive (Figure 3.16). The rate of cell death increased sharply with increasing concentrations of oxidised LDL to 21.1% (200 µg/ml) and 99.1% (400 µg/ml). These apoptosis levels compared to 3.20 and 4.25% rates of annexin V staining in untreated or native LDL treated cultures respectively. Hydrogen peroxide was included as a positive control inducer of necrosis and it was striking that this produced less cell death (70.1%) albeit for a shorter incubation period than the highest concentration of oxidised LDL. It seems very unlikely that the small differences in cytopathy between native and oxidised LDL at 100 µg/ml was responsible for the observed differences in cytokine release.

No further characterisation was performed to assess the nature or mechanism (apoptotic or necrotic) of cell death leading to annexin V positivity. Other workers have identified apoptotic pathways influenced by oxidised LDL in human endothelial cells including caspase activation, ceramide accumulation (Harada-Shiba et al 1998) and sensitisation to Fas mediated apoptosis (Sata et al 1998). The latter mechanism may be important *in vivo* where endothelial cells are normally relatively resistant to Fas mediated apoptosis.

117

Chapter 3

Taken together, the results of this chapter characterise a model of endothelial injury involving the incubation of oxidised LDL with HUVECs that is pertinent to the study of atherogenesis. The nature of oxidised LDL's inflammatory activation of endothelial cells observed with LDL and HUVECs prepared and set up within our laboratory correlated closely with the behaviour of endothelial cells studied under similar conditions in other laboratories and studies of endothelial cells from atherosclerotic plaque specimens. This provided the necessary proof of principle to proceed towards further characterisation of the system and a model for testing the effects of therapeutic gene augmentation

Chapter 3

Appendix I

Characterisation of oxidised LDL mediated endothelial cell injury.

Explanation of research project- for patient

This study aims to identify new genes responsible for the cause of atherosclerosis ('hardening of the arteries'). This disease is responsible for heart attacks and strokes.

The aim is to establish cultures of endothelial cells (the cells lining the blood vessels) and study their responses to stimuli which model those stimuli occurring during the development of atherosclerosis. These cells can be purified from umbilical cords which form the connection between the baby and placenta during pregnancy.

Normally the cord and placenta are disposed for incineration following childbirth. If you give consent, the cord will be removed for purification of endothelial cells. Neither you nor the baby will require additional tests or treatments as a result of agreeing to release the cord.

It is important for you to know that neither you nor the baby's name will be shown to any researchers, appear on any documents or any publication. Please feel free to discuss any of these aspects with the doctor who gives you this letter or the principal investigator whose name appears at the bottom of this sheet. If you have further queries you may contact an independent advisor listed below. This is a doctor who is independent of the study and can provide additional advice. This study has been approved by the Research Ethics Committee in this hospital, (which has a responsibility for reviewing and approving any research projects that involve patients).

Please understand that you are under no obligation to take part in this study. If you do consent to release of the cord you may change your mind at any time and do not need to give a reason for doing so. Finally whether the cord is released or not the routine care for you and your baby will be unaffected

119

Chapter 4

Gene expression profiling of oxidised LDL stimulated endothelial cells

4.1. Aims

The aim of the work in this chapter is to identify further genes responsible for oxidised LDL endothelial injury by comparing gene expression profiles, using commercial nylon miniarrays.

Expression changes observed in individual genes needed confirmation by separate methods of mRNA quantification such as semiquantitaive RT-PCR and Northern blotting. Demonstrating a correlation of changes in gene expression with translation and protein expression is important in order to interpret functional significance.

The angiogenic factor angiopoietin-2 emerged as a target gene and preliminary array findings correlated with semi-quantitative RT-PCR and ribonuclease protection assays. The remaining work in this chapter is therefore directed towards detecting angiopoietin-2 protein expression in HUVECs and human atherosclerotic coronary arteries.

4.2. Results

4.2.1. Expression profiling of HUVECs under basal conditions and following incubation with oxidised and native LDL.

The nylon human cytokine miniarrays (Sigma Genosys, UK) consist of 375 cDNA sequences of cytokines, growth factors and their receptors printed in dot pairs at specific locations. DNA was printed in 2 dot pairs at the four corners of each array to provide a positive hybridisation control and orientation for design of an analysis grid to determine signal intensity for each dot pair using image analysis software. Nine positive control housekeeping genes including human pyrophosphate phosphoribosyltransferase (HPRT) and glyceraldehyde-3-phosphate dehydrogenase (GAPDH) were included on the array. Housekeeping genes are transcripts that are considered to have constant levels of expression in different physiological conditions.

The relative signal intensity of housekeeping genes between different samples may therefore provide information to facilitate correction for the amount of target (radiolabelled cDNA) used in the hybridisation reaction. Negative controls including chromosomal DNA from *E. Coli*, $1 \times$ TE spotting buffer and the pUC19 plasmid were also printed to provide information about the efficiency of hybridisation and the contribution of any non-specific binding to the observed signal. The broad similarity of signal pattern between different treatment conditions can be seen on visual inspection of the four hybridisations in figure 4.1. The signal from housekeeping genes was similar across the different hybridisations.
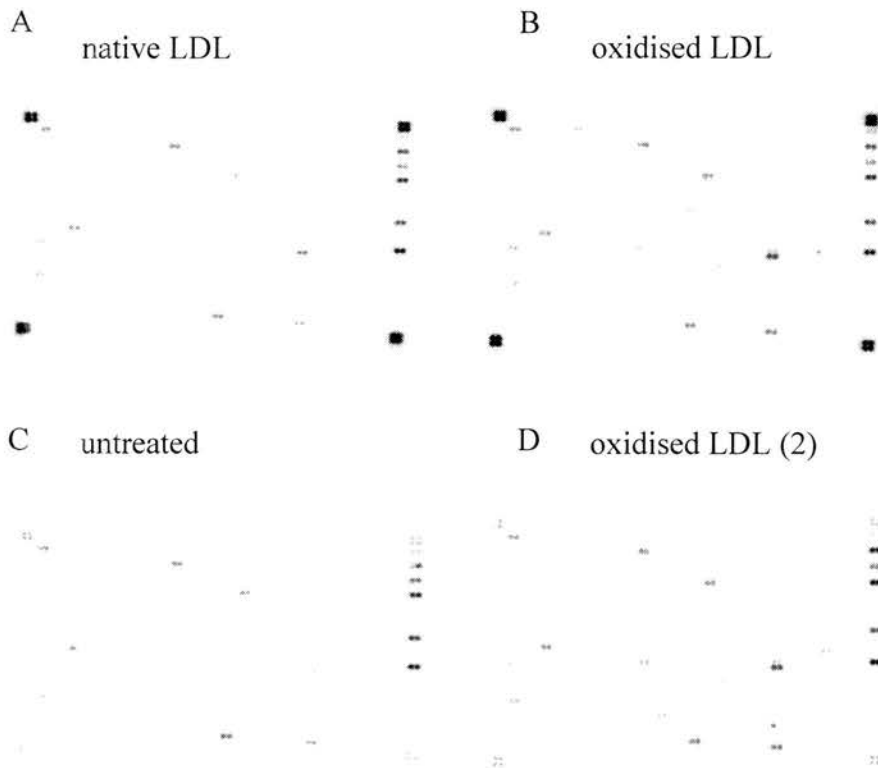
Figure 4.1. Cytokine Miniarray gene expression profiles of HUVECs in basal (untreated) conditions and following incubation with native and oxidised LDL.

mRNA was extracted from HUVECs grown to passage 4 in 6-well Costar plates incubated under basal conditions and following incubations with oxidised LDL (100 μg/ml) and native LDL (100 μg/ml). Two nylon arrays were stripped and reused in two separate hybridisations; A v B and C v D. A: array '1' hybridised with radiolablelled cDNA (2.5 μg) from native LDL treated cells. B: array '2' hybridised with radiolabelled cDNA (2.5 μg) from oxidised LDL treated cells. C: array '2' hybridised with radiolabelled mRNA (2.5 μg) from cells grown under basal (untreated) conditions. D: array '1' hybridised with radiolabelled mRNA (2.5 μg) from cells treated with oxidised LDL.

The mean ratio and standard deviation for 9 paired housekeeping gene signal intensity ratios was 1.01 ± 0.32 (array '1' v array '2') for the first hybridisation and 0.99 ± 0.28 for the second hybridisation. These figures suggested that the quantity of target hybridised to each filter was similar for each experiment. This method of signal normalisation was recommended by the manufacturer although variation in housekeeping gene transcript abundance between samples is possible and the existence of genes whose transcript abundance is truly invariant in different physiological conditions has been questioned (Dheda et al 2004).

Background signal was selected from a clear area of the array and subtracted from each spot. This basic method of normalisation did not account for important differences in hybridisation properties between the two arrays. The signal from the four negative controls (the plasmid pUC19 and 3 bacterial DNAs) was different between miniarray 1 and 2. The negative control signal for array 1 (figure 4.1) was negligible and comparable to signal on non-printed areas of the filter for both hybridisations. In contrast, array 2 had significant signal from all negative control spots following both hybridisations. The net signal (the signal put forward for comparative analysis between hybridisations) from a significant minority of probes on array 2 was nullified following subtraction of the negative control signal. In addition, 'blank' spots that had been printed with TE spotting buffer consistently had signal in some areas of both arrays. The signal from the TE buffer blanks illustrated how factors unrelated to DNA hybridisation, including physical characteristics of the nylon miniarray surface may contribute to signal intensity.

These limitations led to a significant number of probe signals being inconsistent between the two hybridisations demonstrating both up and down-regulation in response to oxidised LDL. The high (background) negative control signal from array 2 was probably responsible although it is conceivable that some of the discrepancy was related to the use of different controls in each hybridisation: native LDL sample and untreated sample. Many probes were therefore excluded and

only genes with high signal (greater than 25000 densitometric units on phosphorimager analysis) were suitable for comparisons between hybridisations. Genes of interest were identified by expressing the corrected signal intensity from the oxidised LDL treated sample as a ratio against native LDL or untreated samples. Genes that exhibited greater than 1.8 fold up or down-regulation reproducibly, in both hybridisations, were selected as genes of interest (Table 4.1). Several genes were reproducibly up regulated in the oxidised LDL treated samples. These included matrix metalloprotease-1 (MMP-1), placental growth factor and angiopoietin-2. The growth factor midkine was down regulated in oxidised LDL treated samples compared to untreated or native LDL treated samples. The vast majority of probes had less than 1.4 fold variation between treatments or, following correction for background, produced insufficient signal. The signals for IL-8 and MCP-1 fell into the latter category, illustrating a potential weakness of expression profiling. It is a useful technique for providing global changes in gene expression with many probes providing strong and reproducible signals but its sensitivity as a tool for following expression changes of a predetermined gene of interest (such as IL-8) will depend on interaction of the IL-8 probe and labelled IL-8 transcripts within a complex hybridisation mixture. One of the strongest signals on the array came from MMP-1 both from native LDL, untreated and oxidised LDL.

	Signal intensity ratios		
	oxidised LDL: native LDL	oxidised LDL: untreated	Mean ratio
Matrix metalloprotease-1	1.59	2.67	2.13
Placental growth factor	2.79	3.47	3.13
Angiopoietin-2	2.11	2.16	2.14
Midkine	0.63	0.40	0.52

Table 4.1. A summary of the results from two miniarray hybridisations.

Signal intensities from target genes in oxidised LDL treated samples were expressed as a ratio of native LDL or untreated samples.

Two genes from Table 4.1 were selected for further study by Northern blotting. Angiopoietin-2 expression was increased and midkine expression decreased following oxidised LDL stimulation. Neither midkine (Figure 4.2) nor angiopoietin-2 (Figure 4.3) could be detected by this technique following electrophoresis of 20 μg of HUVEC RNA. It is important to note that the probes used in the miniarray studies were different from those used for Northern blotting (see Materials and Methods section). The relatively high abundance housekeeping transcript GAPDH was readily detected by Northern blot and could be used to compare sample loading between lanes (Figures 4.2, 4.3).

Angiopoietin-2 cDNA probe (80 ng) was dot blotted onto the nylon filter as a positive control and produced a strong signal following hybridisation. The probe would be expected to hybridise more efficiently to itself than a native angiopoietin-2 sequence although the absence of signal for genes of interest within the samples and the presence of a strong GAPDH signal suggested that low sequence abundance and the relatively weak sensitivity of Northern blotting were the reasons for failure to detect midkine and angiopoietin-2 signal.

The absence of signal on Northern blotting for two target genes that had exhibited high signal intensity on the arrays illustrated the comparably high sensitivity of arrays working on a reverse principle to Northern blotting where the sample is radiolabelled and hybridised to a fixed probe. More sensitive techniques were going to be required to corroborate changes in transcript abundance observed on the arrays and efforts were focused on detecting angiopoietin-2 by semiquantitative RT-PCR and ribonuclease protection assay.

28s (5.0kb)

18s (1.9kb)

GAPDH (1.2kb)
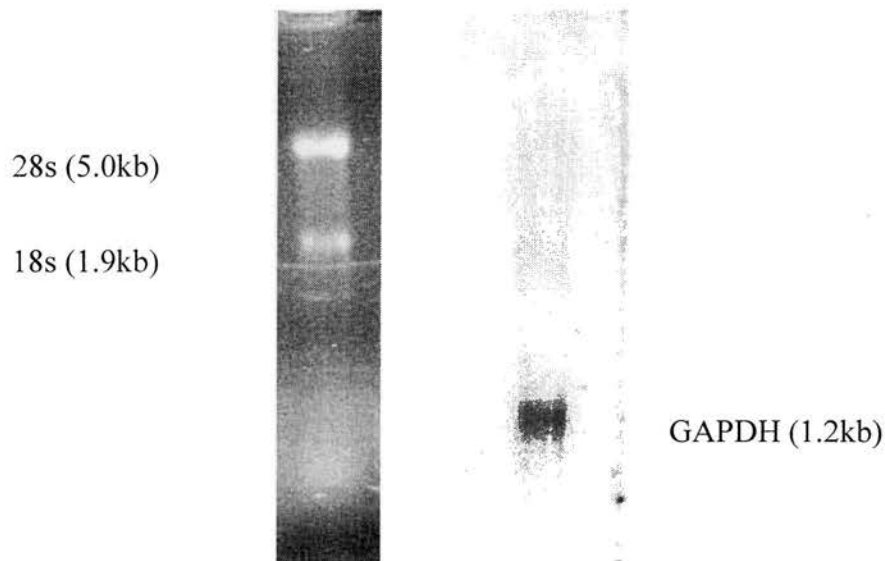
Figure 4.2. Northern blot for midkine and GAPDH

RNA was extracted form HUVECs grown in 6-well Costar plates that had been incubated with oxidised LDL for 4 h using TRIzol according to a protocol outlined in Materials and Methods (section 2.2.4.4). 20 μg of total RNA was loaded onto a denaturing formaldehyde agarose gel and separated by electrophoresis according to the protocol in Materials and Methods. LEFT PANEL: An image taken of the gel following ethidium bromide staining under ultraviolet light prior to RNA blotting and transfer to a nylon filter. 28s and 18s ribosomal subunits are clearly seen in an approximate intensity ratio of 2:1 indicating the absence of any significant RNA degradation. RIGHT PANEL: After blotting the nylon filter was hybridised in Ultrahyb buffer overnight with radiolabelled midkine probe (target transcript size 4.6 kB). Following washes and exposure to a phosphor screen, no signal was seen (exposure not shown) and the filter was then probed without any further washing for GAPDH. In addition to the intense band for GAPDH, faint bands representing non-specific signal from 18s and 28s subunits can be seen.

28s (5.0kb)

18s (1.9kb)

GAPDH (1.2kb)

basal   TNF   native   oxidised
                LDL   LDL
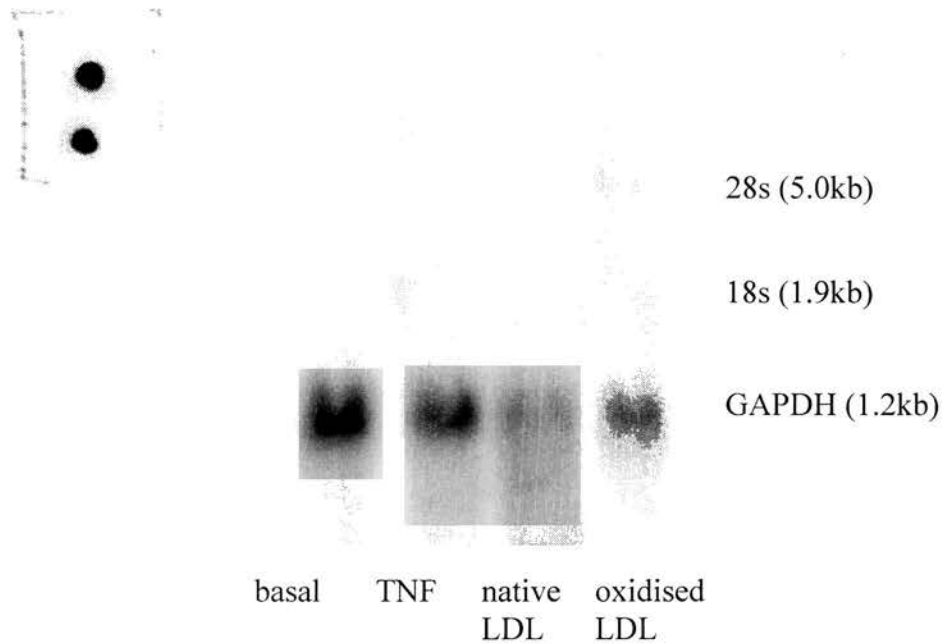
Figure 4.3. Northern blot for angiopoietin-2 and GAPDH

LEFT PANEL: As a positive control for hybridisation around 80 ng of angiopoietin-2 cDNA probe was denatured by boiling at 95°C for 5 min and dot blotted onto a nylon filter. Subsequent hybridisation with radiolabelled angiopoietin-2 cDNA produced a strong signal following exposure on a phosphorimager screen. RIGHT PANEL: HUVECs were grown as for figure 4.2. RNA was extracted from cells grown in basal conditions, after incubation with TNF-α (1ng/ml), a known inducer of angiopoietin-2, and following incubations with oxidised LDL and native LDL (both 100 μg/ml) for 4 h. 20 μg of total RNA was loaded and Northern blotting performed according to the protocol in figure 4.2. The nylon filter was hybridised initially with angiopoietin-2 probe (target transcript size 2.3 kB) and then for GAPDH. The images shown are following the second hybridisation. Position of the 28s and 18s ribosomal subunits are indicated.

Primers were designed for the housekeeping gene HPRT and angiopoietin-2 that produced 300 base pair and 535 base pair PCR products respectively. PCR was performed with a fixed quantity of cDNA and different cycle numbers to ascertain an optimum cycle number for maximum sensitivity without saturation. The effect of increasing PCR cycle number on signal intensity is shown in figure 4.4A. HPRT began to saturate at a lower PCR cycle number consistent with it being a high abundance transcript in comparison to angiopoietin-2. In order to produce non-saturated PCR products that could be used in semi-quantitative comparisons, cycle numbers of 26 and 30 were chosen for HPRT and angiopoietin-2 respectively. Angiopoietin-2 signal was increased in oxidised LDL treated samples compared to native LDL or untreated samples (figure 4.4B).

Further quantification of angiopoietin-2 transcript was performed using a ribonuclease protection assay. This method has no signal amplification step in contrast to quantitative PCR and allows linear quantification of transcript abundance. Compared to hybridisation protocols that rely on RNA bound to solid supports (i.e. Northern blots) low abundance mRNAs are detected more readily by using a solution hybridisation protocol (Lee et al 1987). Riboprobes for angiopoietin-2 and HPRT (for reference) were generated and an initial experiment to determine signal intensity from RNAase protected angiopoietin-2 transcripts for different loading quantities of HUVEC RNA was determined (Figure 4.5). The full length probe (lane 2, Figure 4.5) was demonstrated and protected probe fragments after hybridisation with HUVEC RNA and RNAase digestion could be seen (lanes 3-6, Figure 4.5). A faint band of protected angiopoietin-2 transcript could be seen following loading with 5 µg of HUVEC RNA (Lane 3, Figure 4.5). This result is in contrast to the failure to detect angiopoietin-2 transcript in 20 µg of HUVEC RNA using Northern blotting (Figure 4.3). Protected probe fragments of varied lengths were seen following RNAase digestion (arrows, Figure 4.5). This result may reflect premature termination of transcription during probe synthesis or degradation of the probe. Shorter probe

Chapter 4   129

fragments still hybridise and protect their complement sequences within the sample RNA and the resulting multiple bands have been described previously (Zinn et al 1983). A small increase in angiopoietin-2 signal was seen in RNAase protected samples form oxidised LDL treated cells compared to native LDL and untreated cells (Figure 4.6). HPRT transcript abundance was also quantified to demonstrate equivalent loading between lanes (lanes 3-5, Figure 4.6). Although the data presented for semi-quantiative RT-PCR and ribonuclease protection assay are qualitative, they appear to confirm the original finding from the array indicating increased angiopoietin-2 expression in oxidised LDL treated cells.

Angiopoietin-2 is a member of a novel family of angiogenic factors (Carmeliet 2000). Increased gene expression in the context of oxidised LDL mediated endothelial cell injury would have broad implications for angiogenesis within the atherosclerotic plaque and this gene was selected from the original array findings for further study. The remaining work in this chapter sought to establish any associated increase in HUVEC angiopoietin-2 protein production and whether there was evidence of angiopoietin-2 production within human atherosclerotic specimens.

A

B

1. untreated

2. oxidised LDL 100 µg/ml

3. native LDL 100 µg/ml
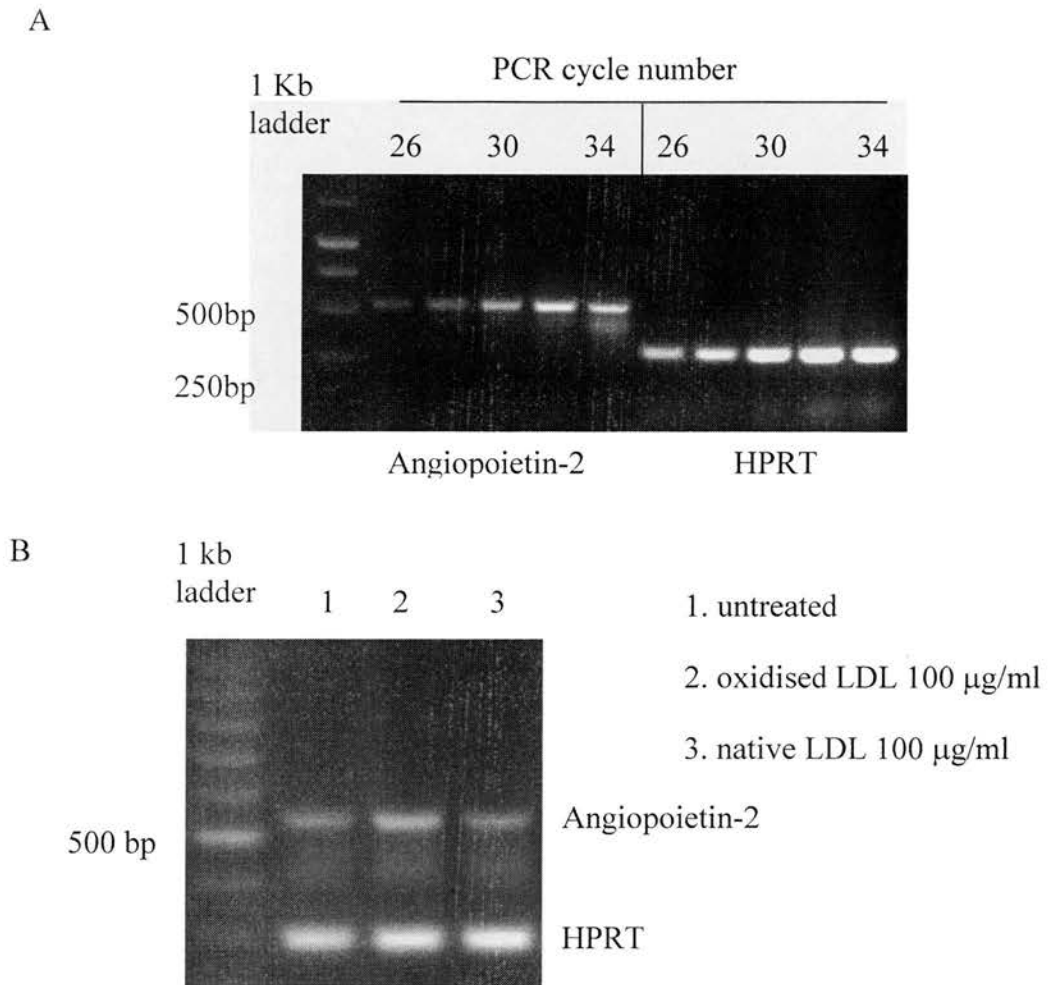
Figure 4.4. Semi-quantitative RT-PCR for angiopoietin-2 gene in HUVECs treated with oxidised LDL.

Semi-quantitative was performed using primers for the housekeeping gene, HPRT and angiopoietin-2. A. Titration of PCR cycle number for HPRT and angiopoietin-2 using 2 µl out of a 20 µl RT reaction performed on 1 µg of HUVEC RNA. RT and PCR were performed according to protocols outlined in the Material and Methods (section 2.2.4.6). Primers for HPRT and angiopoietin-2 produced 300 and 565 base pair products respectively. B. Semiquantitative RT-PCR was performed separately for HPRT (26 PCR cycles) and angiopoietin-2 (30 PCR cycles) using total RNA prepared from HUVECs according to experimental protocol outlined in figure 4.2.
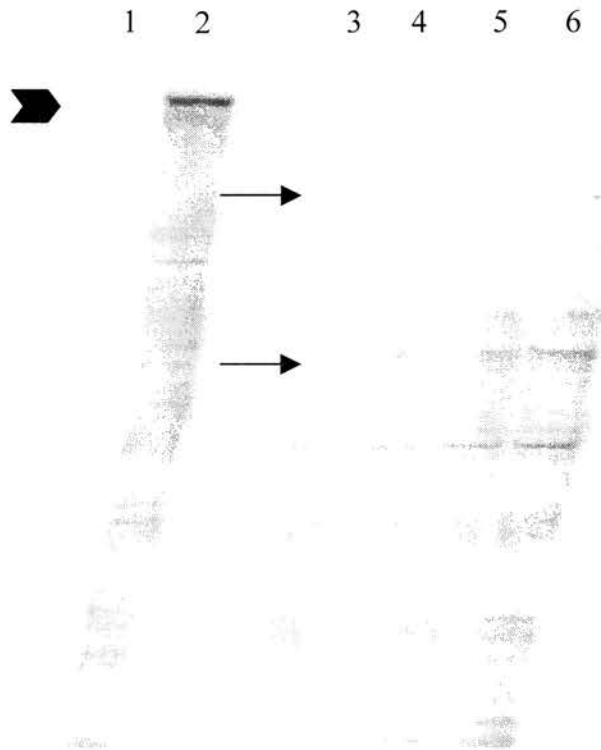
Figure 4.5. Ribonuclease protection assay for angiopoietin-2

HUVECs were grown to passage 4 in 6-well Costar plates and total RNA was extracted using TRIzol. The method for RNAase protection is outlined in Materials and Methods (sections 2.2.4.7-8) and was briefly as follows. An angiopoietin-2 PCR fragment was subcloned into a PGEMT Easy vector and a radiolabelled riboprobe was generated using SP6 RNA polymerase. Probe and sample were co-precipitated and resuspended in hybridisation buffer. After an overnight hybridisation (14 hours) the mix was digested with RNAase, precipitated again and the resulting RNA pellet was resuspended in loading buffer. Samples were run in a polyacrylamide gel (Sequagel) and dried to Whatman paper before exposure on a phosphorimaging screen. 1. 20 µg Yeast RNA and RNAase. 2. Yeast RNA alone (Full length probe). 3. 5 µg HUVEC RNA. 4. 10 µg HUVEC RNA. 5. 20 µg HUVEC RNA. 6. 40 µg HUVEC RNA. The full length undigested probe (arrowhead) and protected angiopoietin-2 riboprobes (arrows) are shown.
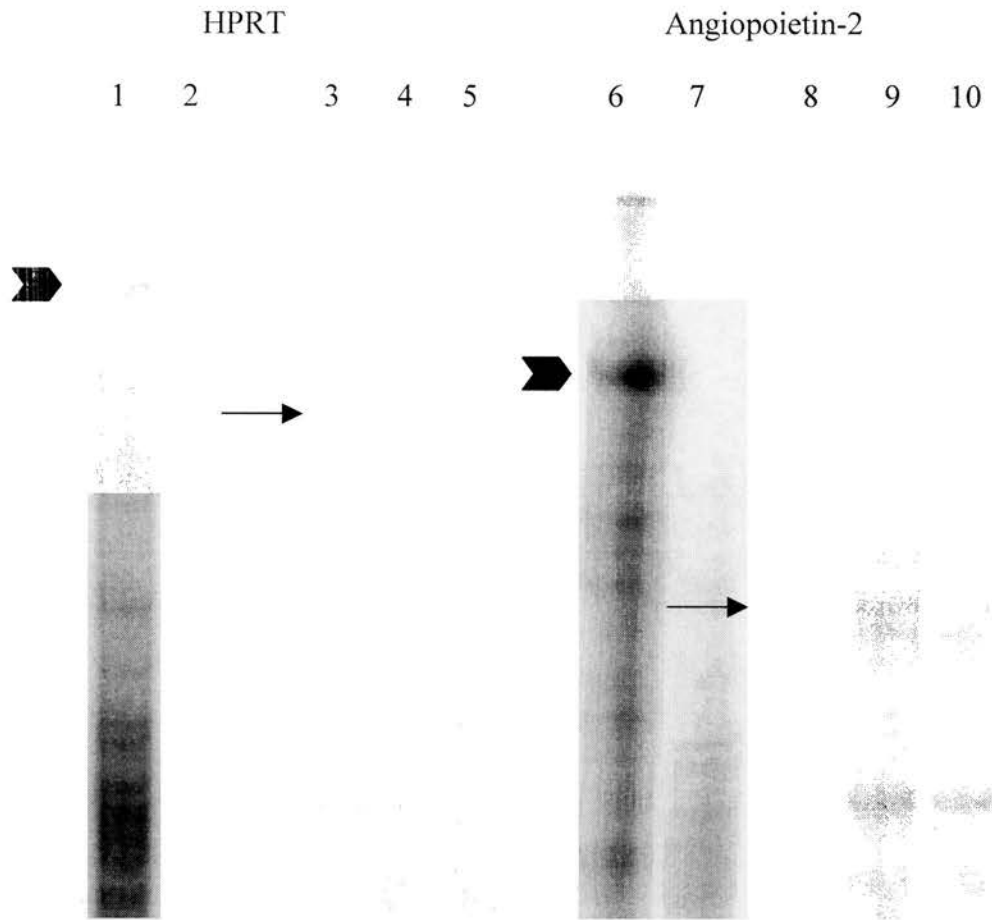
Figure 4.6. Ribonuclease protection assay for angiopoietin-2 gene expression in oxidised LDL treated HUVECs.

HUVEC total RNA was prepared as for Figure 4.2. HUVECs were incubated for 4 h with oxidised LDL (100 µg/ml), native LDL (100 µg/ml) or left untreated in basal conditions. RPAs were performed using 15µg of RNA in each lane, for the housekeeping gene, HPRT (left panel) and angiopoietin-2 (right panel). 1. HPRT probe + 15 µg yeast RNA. 2. HPRT probe + 15 µg yeast RNA + RNAase. 3. Untreated. 4. Oxidised LDL. 5. Native LDL. 6. Angiopoietin-2 probe + 15 µg yeast RNA, 7. Angiopoietin-2 + 15 µg yeast RNA + RNAase, 8. Untreated, 9. Oxidised LDL, 10. Native LDL. Arrowheads; full length probes. Arrows, protected fragments following RNAase digestion.

4.2.2. Characterisation of angiopoietin-2 protein production, by endothelial cells and within human atheroma.

Angiopoietin-2 protein could not be detected in HUVEC supernatants (data not shown) or cell lysates (Figure 4.7) by Western blotting. Previous workers have used concentrators (Witzenbichler et al 1998) or loaded large quantities (50 μg) of cell lysate (Kim et al 2000b) in order to detect HUVEC angiopoietin-2 production suggesting that it is present in low abundance. More recently, angiopoietin-2 signal has been demonstrated with the same Santa Cruz antibody used in the present work in 15 μg of HUVEC cell lysate (Chang et al 2003) indicating that differences in technical aspects relating to the immunoblotting protocol may also explain the absence of signal using a direct approach. An immunoprecipitation protocol was therefore devised in order to detect angiopoietin-2 protein in HUVEC culture supernatants. Angiopoietin-2 activity could be detected in HUVEC supernatants using this approach. Both oxidised LDL and TNF-α, a known stimulus for angiopoietin-2 production (Kim et al 2000b), led to impressive increases in angiopoietin-2 release compared to untreated or native LDL treated cells (Figure 4.8). Production of angiopoietin-2 *in vivo* has been found in pathological states characterised by disordered angiogenesis including the vasculature of tumours (Ahmad et al 2001). New blood vessel formation within the neointima or neointimal angiogenesis is a feature of advanced atherosclerotic plaques (Barger et al 1984) and the *in vitro* data with oxidised LDL, led to the question of whether angiopoietin-2 was present within human atheroma.
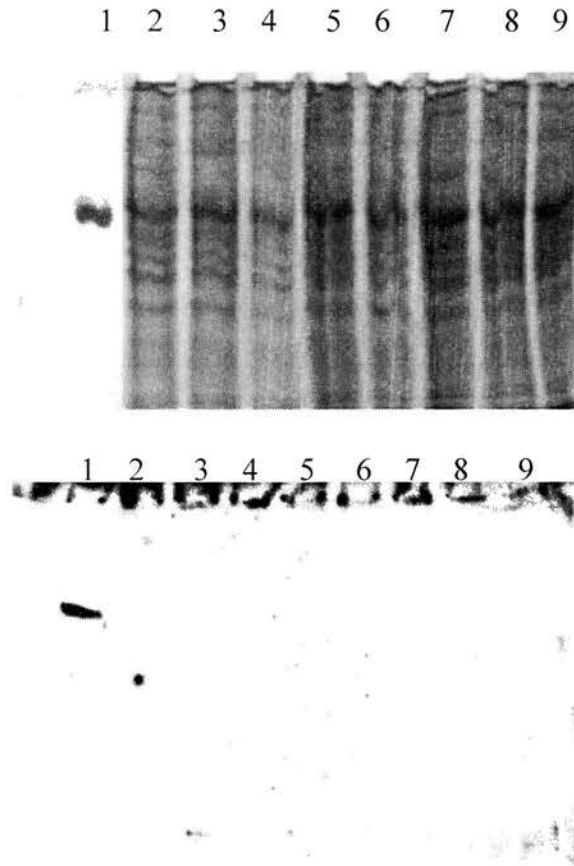
Figure 4.7. Western blot for angiopoietin-2 in HUVEC cell lysates

HUVECs at passage 4 were grown to confluence in 6-well Costar plates and incubated in medium alone (lanes2-3) with oxidised LDL (100 µg/ml, lanes 4-5), native LDL (100 µg/ml, lanes 6-7) and TNF-α (1 ng/ml, lanes 8-9). Cell lysates were extracted with RIPA buffer and equal quantities from each treatment were separated on a 12% SDS polyacrylamide gel according to protocols set out in Materials and Methods (section 2.2.5.5). Recombinant angiopoietin-2 (20 ng) was included as a positive control (lane-1). UPPER PANEL: A Coomasie stain illustrates protein loading and migration of recombinant angiopoietin-2. LOWER PANEL: Angiopoietin-2 immunoblot of the above gel.
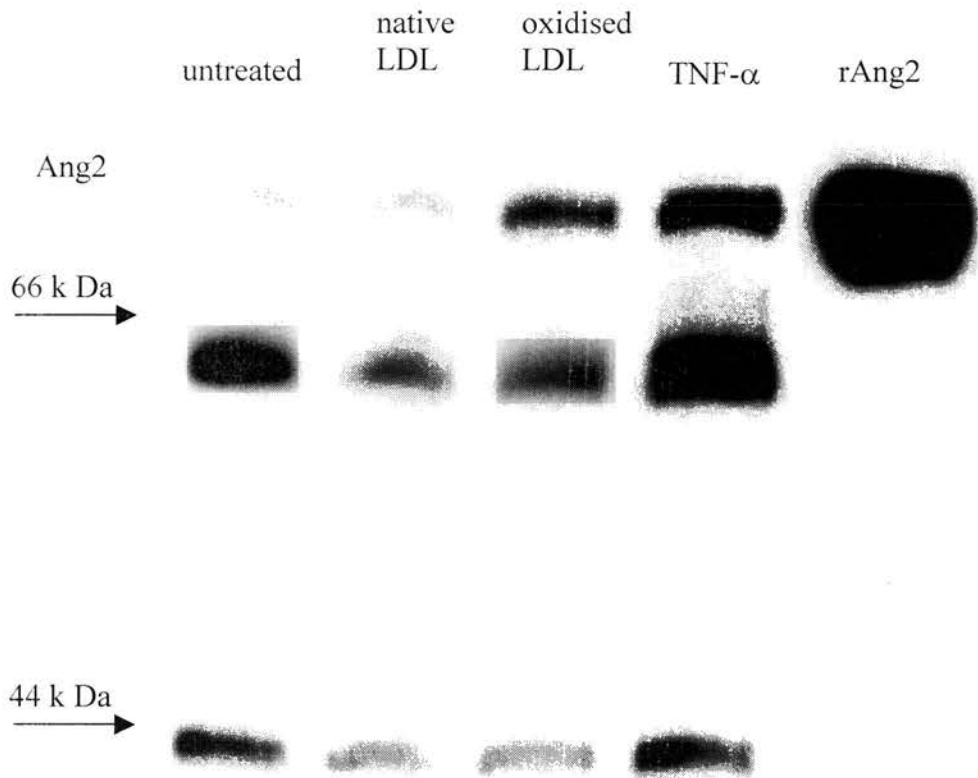
Figure 4.8. Identification of angiopoietin-2 production in HUVECs using immunoprecipitation.

Immunoprecipitation of Angiopoietin-2 from HUVEC supernatants following stimulation with TNF-α (10 ng/ml), oxidised LDL (100 μg/ml) and native LDL (100 μg/ml) for 8 hours. rAng2, recombinant angiopoietin-2 (100 ng). Similar results were seen in 2 independent experiments. The band running in front of angiopoietin-2 is an immunoglobulin chain, the faster migrating band is Protein G.

A series of human tissues including four coronary arteries were obtained from the living (non-post mortem) archive of patients with atherosclerosis undergoing coronary artery bypass surgery from the University of Edinburgh Department of Pathology. Non-diseased renal artery and umbilical vein specimens were also obtained for comparison. Full local research ethics committee approval was received. Angiopoietin-2 expression was limited to the luminal endothelial cells of non-diseased renal artery and umbilical vein samples. These vessels had no neointimal expansion. By contrast, immunohistochemical staining demonstrated strong angiopoietin-2 expression within the cells of human coronary artery atherosclerotic plaque neointima in addition to endothelial cells lining the vascular lumen (Figure 4.9). Staining for the endothelial cell (CD31), lymphocyte (CD3), macrophage (CD68) and vascular smooth muscle cells (Smooth muscle actin, SMA) specific markers was performed on sequential sections (Figure 4.9C-F) and there was significant overlap of expression with Ang2 and CD31 (Figure 4.9C) and the smooth muscle antigen SMA (Figure 4.9F). Angiopoietin-2 expression was frequently seen within cells with smooth muscle morphology that stained for SMA (Figure 4.10). Not all SMA positive smooth muscle cells were positive for Ang2 and variation both within different regions of the same sample and between samples was noted. Angiopoietin-2 staining from a further atherosclerotic coronary artery specimen with a complex plaque is shown in Figure 4.11A. Strong expression from the small capillaries and neointimal vessels can be seen co-localising with CD31 (Figure 4.11B, C). Positive and negative controls for immunoperoxidase staining of SMA, CD31, CD3, CD68 and angiopoietin-2 are given in Figure 4.12.

The immunohistochemistry studies indicated high angiopoietin-2 expression within the neointima of human atherosclerotic plaques. In addition to localisation within the endothelial cells of neointimal vessels, smooth muscle expression was also identified.

Figure 4.9. Immunoperoxidase staining for angiopoietin-2 in human atherosclerotic specimens

Immunohistochemical analysis of atherosclerotic human coronary arteries obtained during cardiac surgery or at autopsy was performed. Immunohistochemistry was performed on paraffin embedded sections according to protocols outlined in Material and Methods (section 2.2.5.2). A. Immunoperoxidase staining for angiopoietin-2 in a human coronary artery with an eccentric atherosclerotic plaque. B. Higher magnification of the boxed region highlighted in slide A. Staining was performed on sequential sections for specific cellular markers. C. CD31 (endothelial cells). D. CD3 (T lymphocytes). E. CD68 (macrophages). F. Smooth muscle cell actin (SMA).

C

CD31

D

CD3

E

CD68

F

SMA
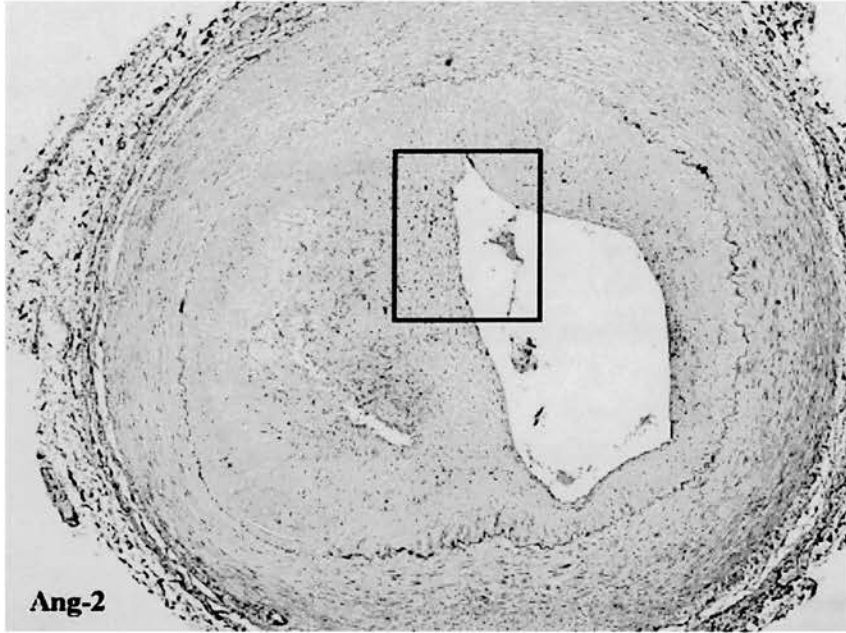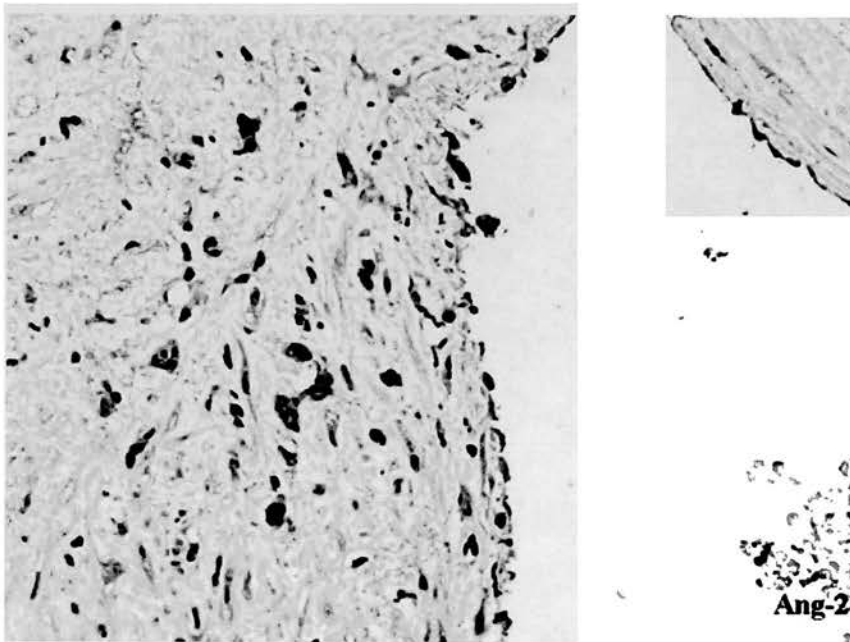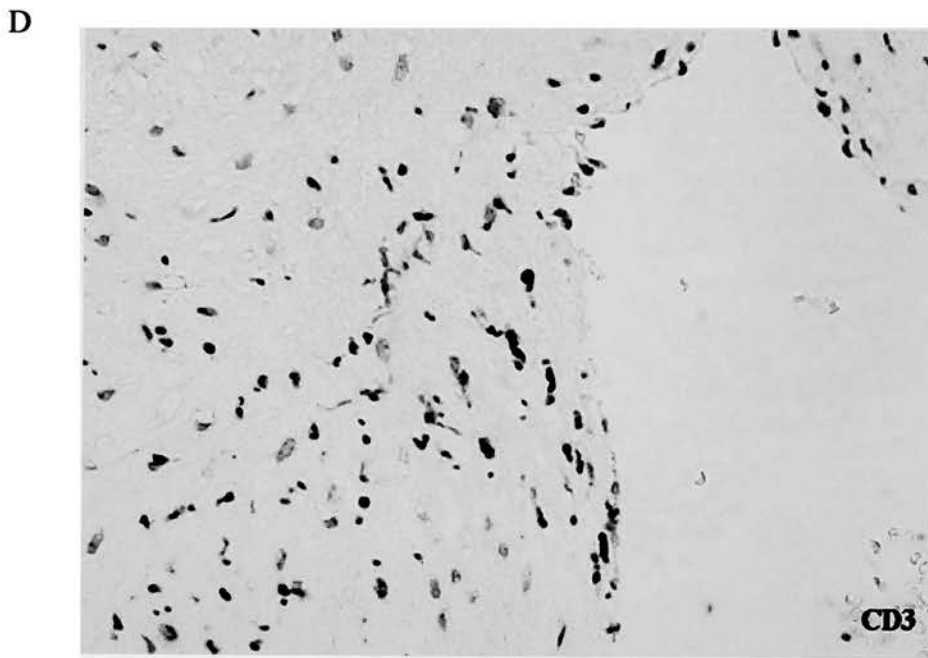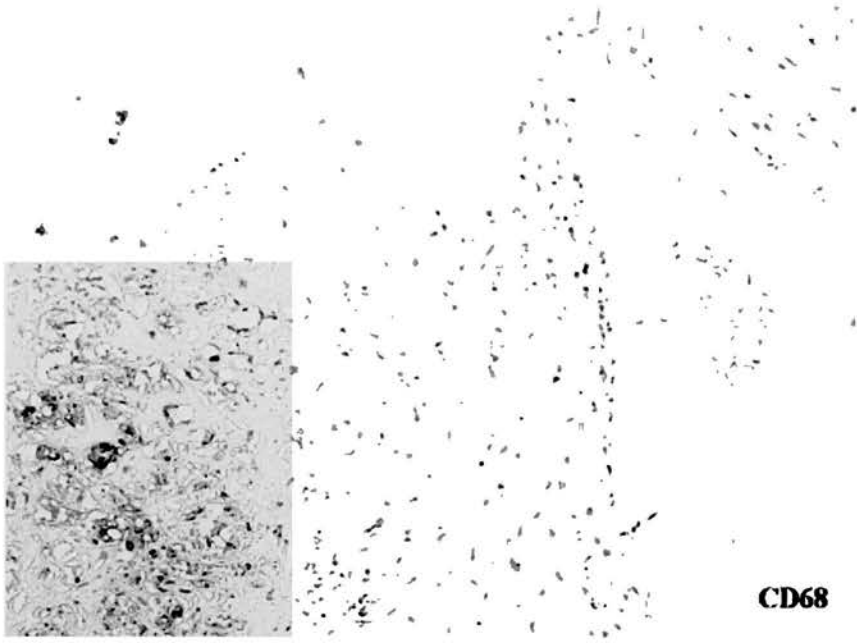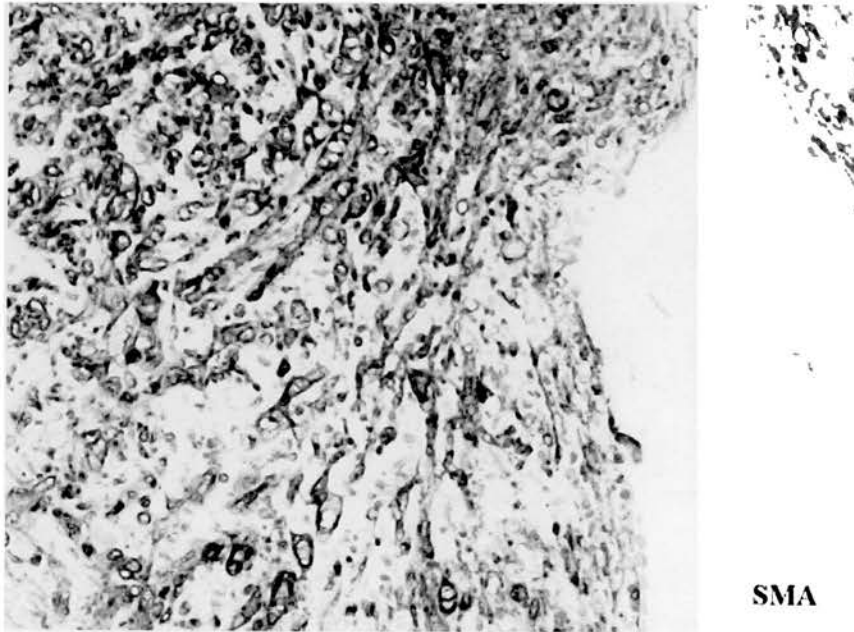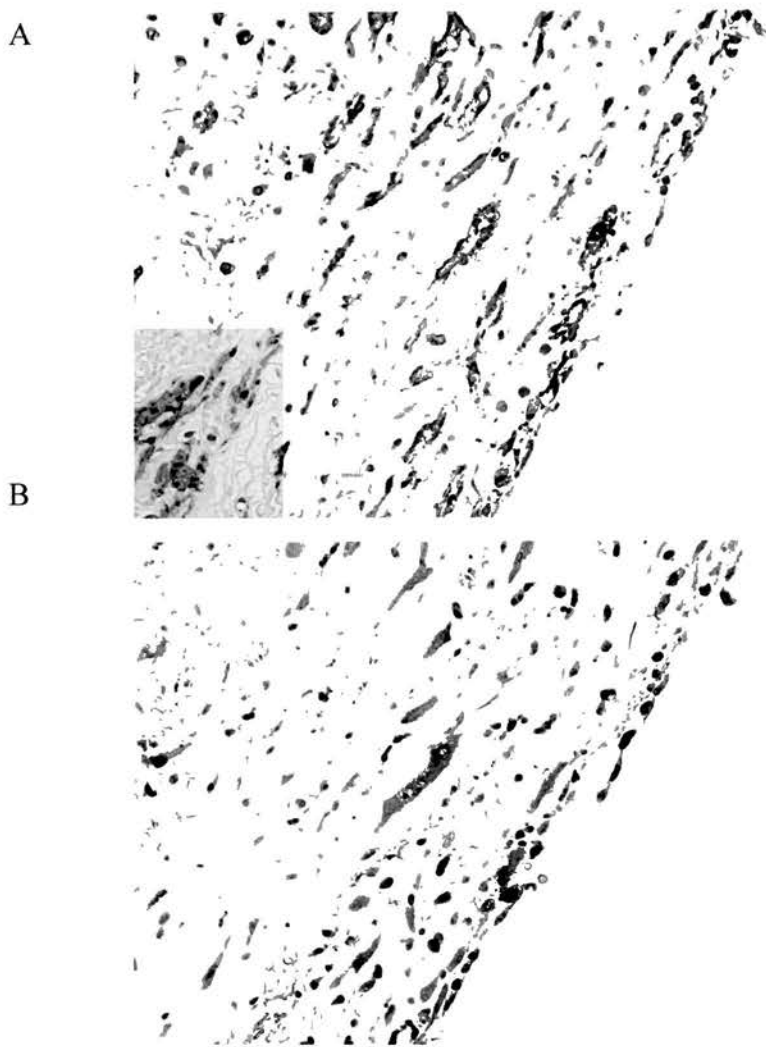
Figure 4.10. Immunostaining of atherosclerotic coronary artery for angiopoietin-2 and SMA.

A. Representative cross section of an atherosclerotic coronary artery stained for angiopoietin-2. B. Sequential slice from the same coronary artery stained for SMA. Results are representative of findings in four diseased human coronary arteries. Magnification × 200
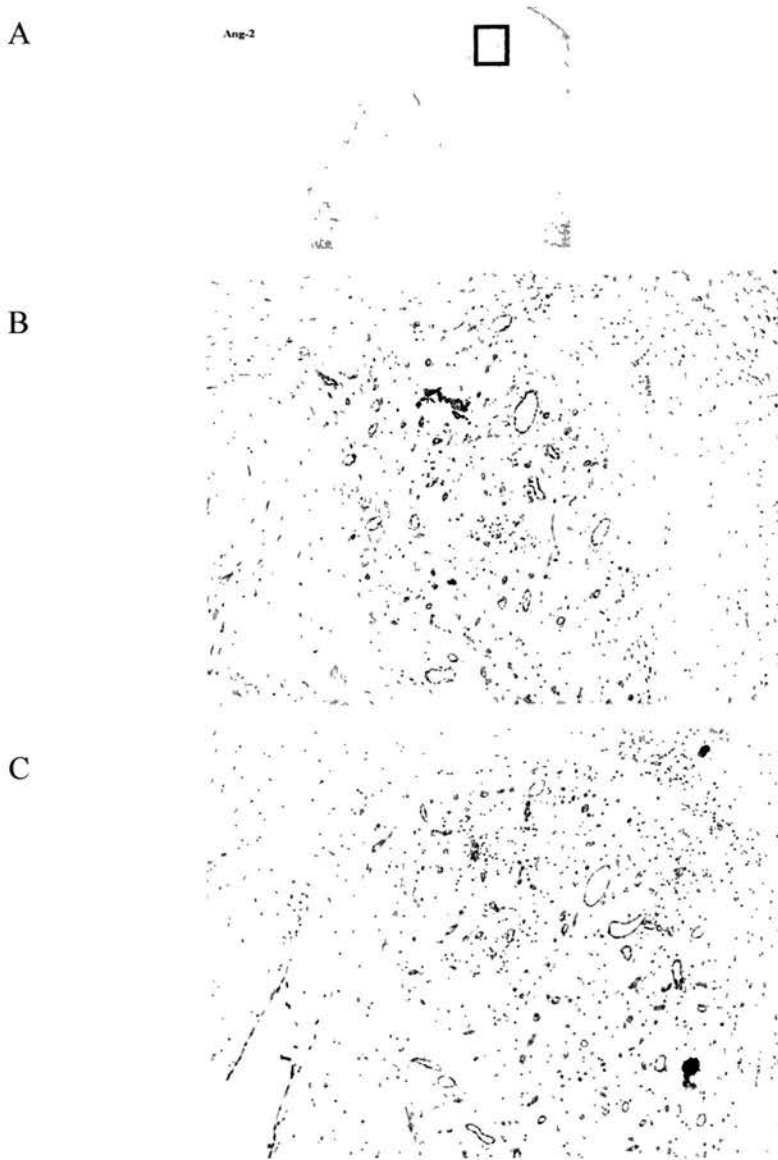
Figure 4.11. Immunoperoxidase staining of angiopoietin-2 in an area of neointimal angiogenesis within a complex human atherosclerotic plaque.

A. Low power view of human coronary artery. B. Representative cross section from region outlined in B stained for angiopoietin-2. Magnification × 100. C. sequential slice from the same coronary artery stained for endothelial CD31 Magnification × 100. Results are representative of findings in four diseased human coronary arteries.
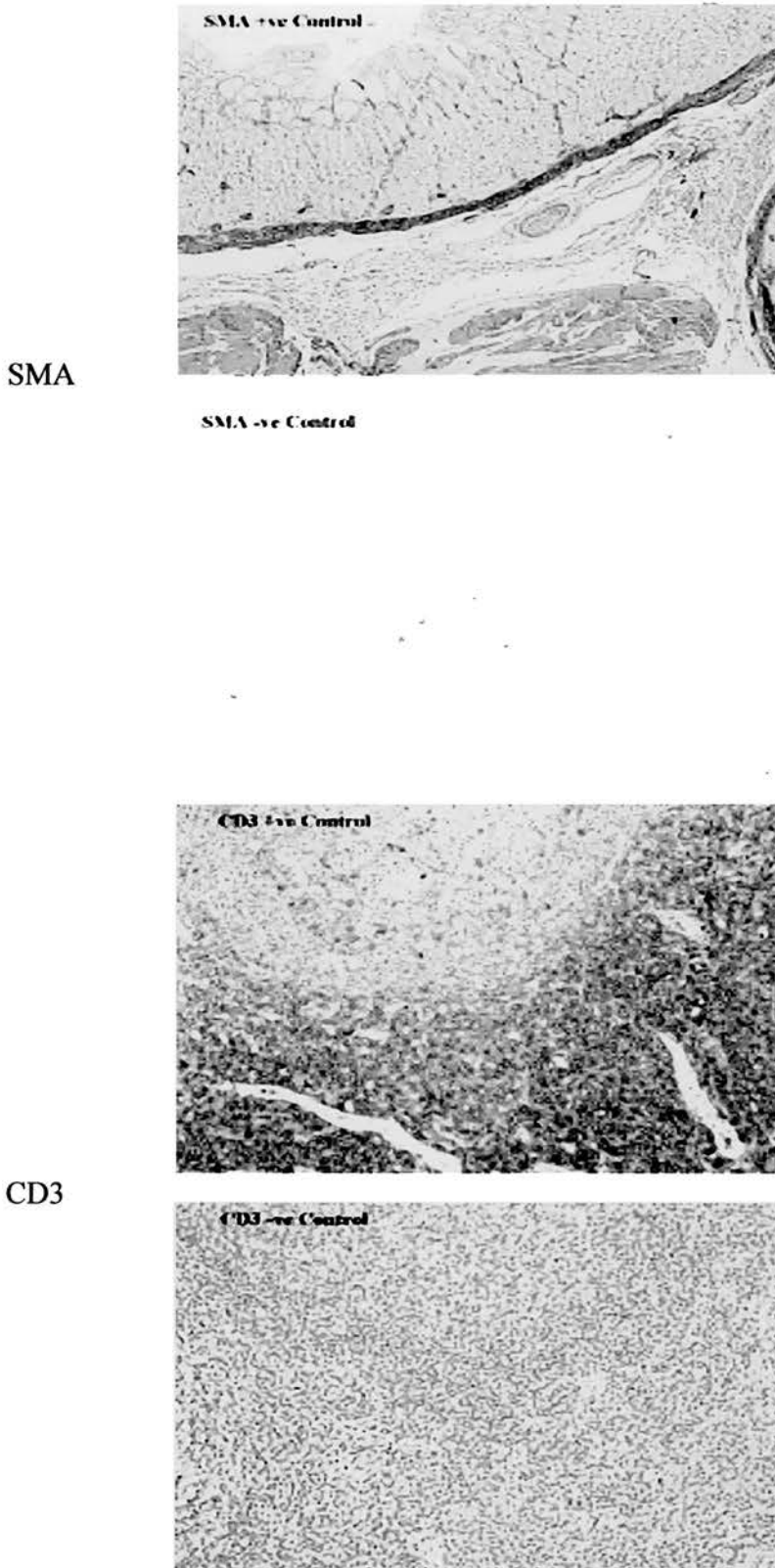
SMA

CD3

Figure 4.12. Positive and negative controls of immunoperoxidase staining for SMA, CD3, CD31, angiopoietin-2 (Ang-2) and CD68.
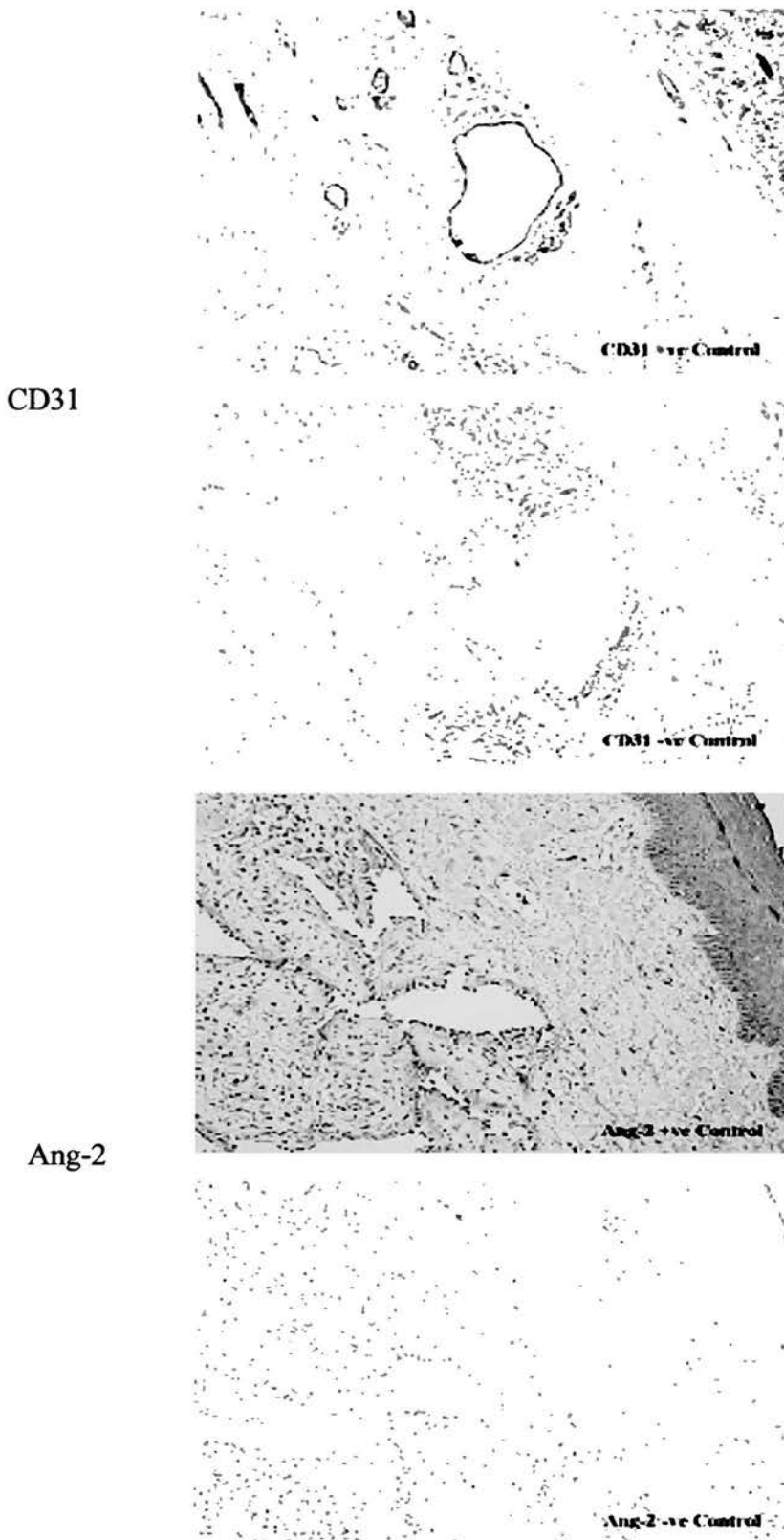
CD31

Ang-2

Figure 4.12. Positive and negative controls of immunoperoxidase staining for SMA, CD3, CD31, angiopoietin-2 (Ang-2) and CD68 (contd)

CD68
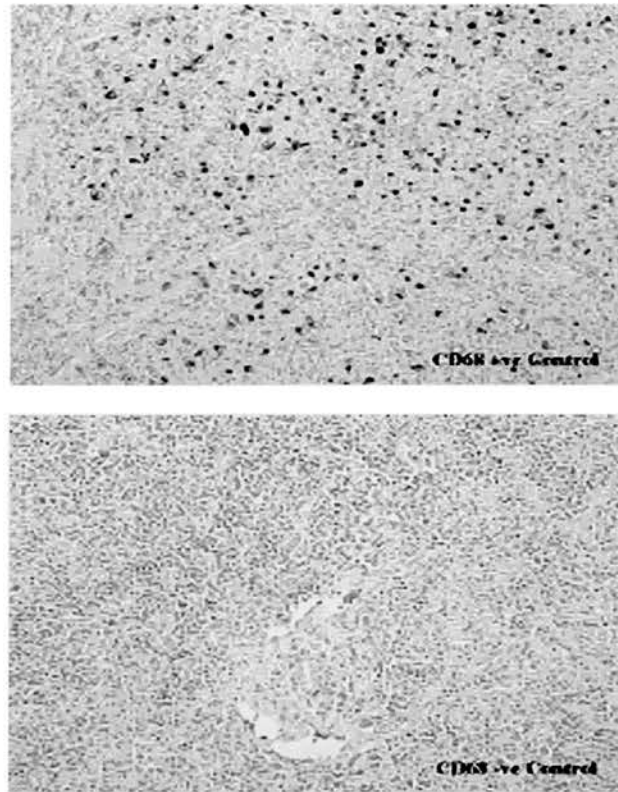
Figure 4.12. Positive and negative controls of immunoperoxidase staining for SMA, CD3, CD31, angiopoietin-2 (Ang-2) and CD68.

Tissue from human trachea (SMA, smooth muscle actin), haemagioendothelioma (angiopoietin-2 and CD31) and lymph node (CD3 and CD68) were used as positive controls. Negative control staining included the secondary peroxidase conjugated antibody only.

Chapter 4   146

4.3. Discussion

The angiogenic factor, angiopoietin-2, displays differential expression in human endothelial cells in response to oxidised LDL. Furthermore, endothelial cell release of angiopoietin-2 is increased in response oxidised LDL and immunohistochemistry demonstrated strong angiopoietin-2 staining in endothelial cells and vascular smooth muscle cells within atherosclerotic neointima.

This line of investigation arose from a gene expression profiling study using nylon miniarrays and the following section will consider practical issues associated with designing, interpreting and following up data from this kind of experiment.

4.3.1. Discussion of miniarray results

The various methods for profiling gene expression including differential display, subtractive hybridisation and microarrays are reviewed in the introduction (section 1.6.1). Miniarrays were chosen because of their relative ease of use compared to the other techniques. In contrast to differential display and subtractive hybridisation the sequence of the target gene is known and although relatively expensive this technique obviates the need for further laborious identification of unknown sequences.

The nylon miniarrays used in this chapter contained 375 different cDNAs from relatively well characterised human cytokines, growth factors and their receptors printed at defined locations as PCR products. An additional modification of the standard array reverse transcription step was to use a mixture of specific primers in place of random primers. The Panorama cDNA labelling mixture had been developed by Sigma Genosys in order to improve cytokine labelling efficiency.

The hybridisations (Figure 4.1) illustrate the potential of this approach for unlocking vast quantities of information. They also reveal problems that can be encountered with respect to background noise and correcting for signal differences arising form extraneous factors such as hybridisation efficiency. An initial observation on visual inspection of the hybridisations was the close similarity following different treatments. This is a common finding in expression profiling studies using cDNA arrays (personal communication from Dr Paul Dickinson, The Scottish Centre for Genome Technology and Informatics, University of Edinburgh) and the vast majority of sequences probed in any array experiment will typically vary in abundance by less than a factor of two.

Visual inspection also revealed a fundamental difference in signal between the two nylon arrays used in these experiments. Array 2 (Figure 4.1B, C) consistently produced signal in more genes compared to array 1 (Figure 4.1A, D). The discrepancy was unlikely to reflect the samples used or hybridisation conditions as it occurred over two hybridisations. Spotting buffer (with no cDNA) and the bacterial DNA plasmid pUC19 were spotted on the arrays as negative controls. Faint signal was detected from the buffer controls on both arrays and some signal was also detected from areas designated as blank (more intense from array 1). There appeared to be a difference in the binding quality of array 2 leading to higher signal even from spots that had no printed cDNA. The signals from these negative controls were quantified by densitometry as being between 1000 and 6000 units and by contrast, the reading from a gene exhibiting a strong signal, angiopoietin-2, was 33027 (untreated sample). This background may have arisen from regional variation in physical qualities of the nylon membrane rather than differences in preparative procedures such as blocking prior to hybridisation. This was supported by the observation that blanks producing signal tended to be the same between hybridisations.

The effect of re-use following washing of the nylon membranes on hybridisation signal is also seen in Figure 4.1. Comparing Figures 4.1A and B with Figures 4.1C and D it can be seen that the genomic DNA signal at the four corners of each array was markedly reduced in the second hybridisation. Following the first hybridisation, both arrays were washed stringently and exposed again. Signal was still present in the genomic controls at each corner indicating failure to remove all bound sample. Further washes to remove remaining signal were not performed owing to a concern that array probes (which had no residual signal following the initial wash) might be damaged by further washes. The decline in genomic signal intensity following the second hybridisation indicated the potential for array sensitivity to fall during re-use.

These findings made decisions on how to correct for background signal difficult. The signal from non-printed regions of the array was very low and this was used to correct signal intensity. It was clear that low gene expression signals would have to be interpreted with care and because of concerns regarding non-specific signal outlined above, interest focused on genes with high expression signals. Comparisons of expression profiles under different conditions were performed following signal normalisation.

The existence of (housekeeping) genes, whose mRNA transcript quantity remains unchanged under different conditions and can therefore be used to compare loading and hybridisation efficiency between different experiments, has been questioned (Dheda et al 2004) although this principle is still widely applied both in quantitative PCR and array analysis. The ratio of signals for each housekeeping gene between hybridisations was calculated and a mean ratio for all eight was used as a correction factor for signal intensities when comparing hybridisations. In practice this correction made little numerical difference to overall results because of the similarity in housekeeping gene signal between hybridisations.

Using a cut off for gene expression change of 1.8 fold, four genes were identified with increased expression following oxidised LDL treatment and one gene had relatively higher expression in native LDL or untreated cells. The use of two different controls is a further criticism of these experiments and native LDL or untreated were assumed to be similar for the purpose of investigating oxidised LDL specific effects. The level of change in gene expression used as a cut off has varied between different investigators. For example 2.5 (Feng et al 1999), 2.0 (Shiffman et al 2000) and 1.8 (Stanton et al 2000) have been used in previous studies. The higher the cut off, the greater the chance that quantitatively small but functionally important gene expression changes will be missed. The lower the cut off, the greater the potential exists for positive or false positive findings. There were too few observations to analyse statistically. In fact, expression changes in all target genes could be confirmed retrospectively by visual inspection of the exposed arrays.

Oxidised LDL has previously been shown to have a positive regulatory effect on MMP-1 transcription in HUVECs and human coronary artery endothelial cells (Huang et al 1999). Its regulatory influence over MMP-1 expression has been used to investigate oxidised LDL signalling mechanisms (Huang et al 1999; Li et al 2003) and the finding that it was also up regulated following oxidised LDL treatment in our system provided further indication that our model was comparable to that used by investigators in other laboratories (see chapter 3). Midkine expression was reduced consistently in samples treated with oxidised LDL in contrast to increased expression observed with two angiogenic factors: angiopoietin-2 and placental growth factor. Midkine is an angiogenic factor (Choudhuri et al 1997) whose production has been identified previously in HUVECs (Sumi et al 2002b). The angiogenic roles of placental growth factor and angiopoietin-2 have been characterised in greater detail and both are associated with angiogenesis in response to tissue injury and pathologies including cancers (Carmeliet 2000; Carmeliet et al 2001).

Initial attempts to confirm expression changes by Northern blotting were unsuccessful for midkine (Figure 4.2), angiopoietin-2 (Figure 4.3) and placental growth factor (data not shown). Angiopoietin-2 expression changes were confirmed using semiquantitaive RT-PCR (Figure 4.4) and following development of a ribonuclease protection assay (Figures 4.5, 4.6). Having demonstrated up regulation of this angiogenic factor in response to oxidised LDL attention focussed on its production in HUVECs and whether it was present in atherosclerotic plaques.

4.3.2. Angiopoietin-2 protein is increased in endothelial cells incubated with oxidised LDL and human atherosclerotic plaques

Efforts to detect angiopoietin-2 directly in culture supernatants by Western blotting were unsuccessful (Figure 4.7). An immunoprecipitation protocol was therefore developed and this demonstrated increased angiopoietin-2 release into the culture medium of endothelial cells incubated with oxidised LDL compared to native LDL or untreated cells (Figure 4.8). TNF-α was also an effective stimulus for angiopoietin-2 release in these cells in keeping with previous studies demonstrating regulation by inflammatory stimuli and vascular endothelial growth factor (Kim et al 2000b; Oh et al 1999).

Angiopoietin-2 and its receptor Tie-2 are closely involved along with the other angiopoietin family members in blood vessel development. Angiopoietin-2 was initially regarded as a natural antagonist of angiopoietin-1 having no activating effect on their shared Tie-2 receptor. More recently, angiopoietin-2 has been shown to exert concentration and context dependent effects on Tie-2. At low concentrations the receptor may be bound but not activated by autophosphorylation (Maisonpierre et al 1997). In this situation it may block Tie-2 activation by other ligands such as angiopoietin-1 and prevent chemotactic, sprouting and pro-survival messages (Papapetropoulos et al 1999; Witzenbichler et al 1998). At high concentrations, angiopoietin-2 binding is conversely associated with Tie-2 phosphorylation and

activation (Kim et al 2000a). In the embryo, over-expression of angiopoietin-2 is associated with disruption of blood vessel development, possibly through antagonising the effects of angiopoietin-1 and during vascular development angiopoietin-2 expression is associated with loosening of peri-endothelial cell contacts and increased permeability prior to new blood vessel formation (Maisonpierre et al 1997).

The angiopoietin system has recently been implicated in the development of atheroma. Angiopoietin-1 was shown to be protective against the apoptotic effects of oxidised LDL on porcine coronary artery endothelium, *in vitro*, at relatively high concentrations (Kim et al 2001). Heightened expression of angiopoietin-2 is seen in diseases characterised by disordered blood vessel formation including the vasculature of tumours and following cerebral infarction (Ahmad et al 2001; Beck et al 2000). New blood vessel formation within the neointima (Barger et al 1984) is also a feature of atherosclerosis and following the demonstration of oxidised LDL as a regulator of angiopoietin-2 expression, immunohistochemical analysis of human atheroma specimens was performed to examine whether angiopoietin-2 expression was associated with neointimal angiogenesis.

Angiopoietin-2 staining of a coronary artery with progressive atherosclerosis is shown in Figure 4.9A. The plaque has an extensive fibroproliferative cap best illustrated by the vascular smooth muscle staining (Figure 4.9F) with evidence of a small necrotic core system and cholesterol clefts. Angiopoietin-2 staining cells can clearly be seen both within the neointima and lining the vascular lumen (Figure 4.9B) in a high power field selected from Figure 4.9A. Sequential sections were taken to stain for endothelial cell, lymphocyte, macrophage and vascular smooth muscle cell markers, the predominant cell types within atheroma. CD31 staining confirmed that the angiopoietin-2 signal from cells lining the vascular lumen was endothelial in origin (Figure 4.9C) although in this section there were no endothelial cells within the neointima. CD3 staining for lymphocytes was relatively scarce from

this fibroproliferative zone (Figure 4.9D) and macrophage CD68 staining (Figure 4.9E) was concentrated around the necrotic core in keeping with studies demonstrating their part in lipid laden foam cell formation and necrosis (Libby, 2001). Although alveolar macrophage angiopoietin-2 expression has been described previously (Kim et al 2000b) co-localisation with plaque leucocytes was not seen.

The predominant cell type within the fibroproliferative cap was vascular smooth muscle (Virmani et al 2000) and comparing Figures 4.9B and 4.9F it seems probable that a subpopulation of vascular smooth muscle cells was responsible for angiopoietin-2 expression observed within the neointima. Although the sequential sections do not provide perfect overlay, the spindle shape morphology of the angiopoietin-2 positive intimal cells (Figure 4.9B) and the virtual absence of markers for other cell types within this zone support this conclusion. High power micrographs from a different donor demonstrated further evidence of smooth muscle expression within the fibroproliferative cap (Figure 4.10). A more advanced and complex atherosclerotic plaque in a coronary vessel from a separate donor is shown, stained for angiopoietin-2, in Figure 4.11. The low power orientation view demonstrates at least two foci of necrosis and cholesterol clefts. The area to the bottom left of the micrograph contained a dense acellular necrotic area and there was associated non-specific uptake of secondary HRP conjugated secondary antibody. The zone examined under high power shows dense staining of small vessels for angiopoietin-2 (Figure 4.11B) and CD31 (Figure 4.11C). In contrast, angiopoietin-2 expression was limited to the luminal endothelial cells of human umbilical veins and non-diseased segments of human renal artery. One caveat to interpretation of the immunohistochemistry was the use of secondary antibody alone as a control. Ideally an isotype matched primary antibody should be used in addition to exclude non-specific staining although this step is frequently missed out in the analysis of clinical specimens (personal communication; Dr Lee Jordan, Department of Pathology, University of Edinburgh). These control tissues had no neointimal formation and coronary artery specimens with varying degrees of plaque development would have been preferable controls. (The work was conducted during a period of upheaval with

respect to the access and use of human tissues in research and access to coronary artery tissue was restricted as a result.)

4.3.3. The role of angiopoietin-2 in atherosclerotic plaque development

Taken together, these findings indicate significant angiopoietin-2 expression within the atherosclerotic plaque, both from a subtype of vascular smooth muscle cells and from endothelial cells within zones of neointimal angiogenesis. During the writing of this thesis, an Italian group published work demonstrating increased angiopoietin-2 gene expression and protein content in extracts from human atherosclerotic plaques (Calvi et al 2004). Immunofluorescence was performed to illustrate angiopoietin-2 localisation within the neointima but surprisingly, the cell types expressing angiopoietin-2 were not identified and in particular, smooth muscle stains were not performed. An earlier study examining non-atheromatous porcine coronary arteries found limited angiopoietin-2 expression within luminal endothelial cells with no evidence of vascular smooth muscle cell expression (Kim et al 2001). In adult tissues, angiopoietin-2 expression tends to be localised to endothelial cells and closely related supporting cells at sites of vascular re-modelling (Maisonpierre et al 1997; Yuan et al 2000b). The original description of angiopoietin-2 documented high expression in murine embryonal vascular smooth muscle (Maisonpierre et al 1997) and others have confirmed smooth muscle specific expression during development (Yuan et al 2000a). The potential for adult vascular smooth muscle cells and fibroblasts to produce angiopoietin-2 has recently been demonstrated (Kelly et al 2003) and angiopoietin-2 protein expression from rat cardiomyocytes was also shown to be increased in an experimental model of myocardial infarction. The variable staining in vascular smooth muscle cells, observed in the present work, is consistent with preferential induction of angiopoietin-2 in these cells by inflammatory signals, possibly at sites of vascular remodelling or injury. Heterogeneity of smooth muscle within atheroma is well described and may reflect differing phenotypes or possibly different sources of smooth muscle cells (Gittenberger-de Groot et al 1999).

Vascular smooth muscle cell expression of angiopoietin-2 may play a role in plaque development. In cancers, high angiopoietin-2 expression by tumour cells is associated with increased invasion and angiogenesis (Hu et al 2003; Ochiumi et al 2004). Angiopoietin-2 was recently shown to regulate the invasiveness of human glioma cells through induction of matrix metalloprotease-2 (Hu et al 2003). A similar action on vascular smooth muscle cells within the plaque might be expected to promote both angiogenesis and plaque instability (Rajavashisth et al 1999a; Rajavashisth et al 1999b).

The extensive network of fine blood vessels within the plaque provides an expansive surface area for the transit of inflammatory cells and mediators. The neointimal vessels are fragile and susceptible to rupture with ensuing haemorrhage, leading to sudden plaque expansion or even rupture (Barger et al 1984). Treatment with angiogenesis inhibitors is effective in reducing plaque burden in murine models of atheroma (Moulton et al 1999; Moulton et al 2003). Recently, adenoviral gene delivery of angiopoietin-1 was shown to reduce arterial wall thickening in a rat model of transplant arteriosclerosis (Nykanen et al 2003). The investigators did not examine angiopoietin-2 in this study but the implication that angiopoietin-1 may be working, at least in part, through antagonism of angiopoietin-2 expression is intriguing.

The possibility that angiopoietin-2 may be acting in synergy with vascular endothelial growth factor (VEGF) was not examined in this chapter. This is an important question for VEGF is present within human atheroma (Calvi et al 2004) and administration of exogenous VEGF has been shown to enhance atherosclerotic plaque progression in apolipoprotein E knockout mice and cholesterol fed rabbits (Celletti et al 2001). Furthermore, VEGF has also been shown to be a facilitator of angiopoietin-2 induced endothelial cell proliferation, migration and capillary

formation (Lobov et al 2002). VEGF is a stimulus for angiopoietin-2 production by endothelial cells (Oh et al 1999) and because it was present in the endothelial cell culture medium, possible co-operativity with oxidised LDL induced angiopoietin-2 production cannot be excluded.

In summary, gene expression profiling identified oxidised LDL as a stimulus for angiopoietin-2 production in human endothelial cells. Subsequent immunohistochemical analysis of human atheroma identified extensive angiopoietin-2 staining within endothelial cells lining neointimal blood vessels and also within vascular smooth muscle cells from human coronary arteries with advanced atheroma. These findings lead to two further questions. Firstly, to what degree does oxidised LDL contribute to angiopoietin-2 production within the plaque? Given the central role of oxidised lipid throughout plaque development and its presence within the earliest lesions its role is likely to be important. Other inflammatory stimuli such as VEGF or TNF-α may also contribute, particularly in more advanced atheroma. Secondly, the association of angiopoietin-2 with pathological angiogenesis and the observation of high expression within zones of neointimal angiogenesis suggest it may be a key mediator and possible therapeutic target for plaque growth. This is an important hypothesis for future study.

Chapter 5

Adenoviral gene delivery of elafin and SLPI attenuates the inflammatory responses of endothelial cells and macrophages to atherogenic stimuli

5.1. Aims

The work in chapter 3 demonstrated that oxidised LDL induced proinflammatory gene expression in endothelial cells through a mechanism involving NF-κB mediated transcription. A fundamental aim of this chapter is to determine whether two homologous endogenous antiproteases, elafin and secretory leucocyte protease inhibitor (SLPI), could attenuate pro-inflammatory signalling in human endothelial cells and macrophages.

Several lines of evidence, described in detail in the introduction, point to an anti-inflammatory role for these peptides that extends beyond inhibition of extracellular proteases. The studies demonstrating blockade of NF-κB activation in a range of tissues following delivery of SLPI (Lentsch et al 1999a; Lentsch et al 1999b) are particularly important in this respect. No such broad ranging anti-inflammatory properties have been identified for elafin although its homology with SLPI indicated this to be a possibility. While the experimental work in this chapter was being performed, members of the laboratory team were characterising the inflammatory responses of elafin transgenic mice and demonstrated reduced inflammatory cytokine production in response to systemically delivered LPS (Sallenave et al 2003).

157

The protective property of elafin against vascular inflammation in elafin transgenic mice targeted to express elafin in vascular tissues under the control of the preproendothelin promoter has been demonstrated by Professor Rabinovitch's group in Toronto (Zaidi et al 1999; Zaidi et al 2000). A human elafin continuous intravenous infusion was also shown to attenuate the intimal thickening and arteriopathy occurring following orthoptic cardiac transplant in rabbits (Cowan et al 1996). The localisation of elafin within human coronary arteries by immunohistochemistry was a further intriguing finding (Sumi et al 2002a) reported while the work described in this chapter was in progress. This study raised the additional possibility that endogenous elafin contributes to vessel wall defences against inflammation in addition to the anti-inflammatory effects of exogenously delivered or genetically overexpressed protein.

The work in this chapter had two objectives. Firstly, to develop techniques for high efficiency gene delivery using adenoviral vectors to endothelial cells and macrophages. Secondly, to examine the effects of overexpression of human elafin and the murine orthologue of SLPI (mSLPI) on inflammatory cytokine production and NF-κB activation in macrophages and endothelial cells.

A gene augmentation strategy was chosen because of evidence indicating that the inhibitory activity of murine SLPI on NF-κB activation was dependent on intracellular expression of the protein (Jin et al 1997; Zhu et al 1999). The requirement for a continuous infusion of peptide to achieve therapeutic delivery of elafin and SLPI *in vivo* was an additional concern. This would be impractical and expensive and development of a gene based treatment that would facilitate targeted and time controlled delivery therefore had additional appeal.

158

Chapter 5

5.2. Results

5.2.1. Development of a protocol to optimise adenoviral infection of HUVECs and macrophages

Staining for β-galactosidase activity and quantification of elafin production by ELISA were the principal methods utilised in the following section to quantify adenovirus infection efficiency and transgene expression following infection with Ad-β-Gal and Ad-elafin respectively. β-galactosidase staining and elafin production were low in HUVECs (Figure 5.1) and macrophages (Figure 5.2) compared to those reported for the A549 epithelial cell line (Simpson 2001) (compare 1.5 ng/ml from HUVECs to 120 ng/ml from A549 cells infected with Ad-elafin at an MOI 50). The latter cell type demonstrates high tropism for adenovirus and previous work within our group at similar multiplicities of infection had produced close to 100 % infection rates measured by β-galactosidase positivity. Elafin supernatant concentrations are in the 100ng/ml range compared to 1-10ng/ml for HUVECs and even less for macrophages. In HUVECs, infection efficiencies (β-galactosidase positive cells) were estimated at 10%, 20%, 50% and 80% for MOIs of 25, 50, 100 and 1000 respectively (Figure 5.1A). For macrophages, infection efficiencies with Ad-β-Gal were estimated at 2%, 5% and 10% for MOIs of 25, 50 and 100 respectively (Figure 5.2A). No elafin was detected in supernatants from uninfected HUVECs. By contrast, an elafin signal was detected from uninfected macrophages (Figures 5.1B, 5.2B). It must be emphasised that the macrophage experiments were performed using autologous human serum that contains elafin (Molhuizen et al 1995). The levels of elafin observed in uninfected macrophage supernatants approximate the 1.7ng/ml quantity described in culture medium containing 10% human serum described by Dr A.J. Simpson (Simpson 2001).

The relatively poor infection efficiency and gene expression levels for HUVECs (at low MOI) and macrophages needed to be improved before the effects of elafin and SLPI gene delivery could be studied. Fasbender et al. (1998) described

159

Chapter 5

a protocol of precomplexing adenovirus with calcium phosphate precipitates (CaPi) to enhance infection efficiency to primary epithelial cells both *in vitro* and *in vivo*. This protocol was adapted for use in human endothelial cells and macrophages (Figures 5.3 and 5.4).

Precomplexing with CaPi dramatically improved infection efficiencies for Ad-β-Gal in HUVECs (Figure 5.3). Infection efficiency was close to 100% at MOI 5 for HUVECS and the increased intensity of β galactosidase staining with MOI 10 was consistent with higher expression levels per cell. There was a dramatic increase in elafin production with an MOI 20 in the presence of CaPi leading to production of over 30-times the levels of elafin observed with an MOI 200 and virus alone. Similar increases in infection efficiency and gene expression levels were seen for macrophages (Figure 5.4). The latter finding was particularly striking given the hitherto reported refractory nature of this cell type to any form of gene delivery (Kaner et al., 1999). Macrophage morphology changed following adenoviral-CaPi gene delivery. Examination with light microscopy demonstrated coalescing and increased giant cell formation. This finding appeared to be more marked for β-galactosidase cells compared to elafin expressing cells although giant cell formation occurred following infection with both adenoviruses. A cytopathic effect consisting of lifting and rounding had been observed in HUVECs following infection with CaPi and higher MOIs of 100 (data not shown). These observations raised the concern that high levels of gene delivery came with the price of cytotoxicity and staining with propidium iodide was performed to elucidate any evidence of cell death (Figures 5.5 and 5.6).

CaPi alone did not produce any increase in propidium iodide staining above basal levels in HUVEC cultures (Figure 5.5, first 2 panels). Propidium iodide staining was increased in adenovirus-CaPi exposed cells and this effect was more pronounced with higher viral MOIs despite the cells appearing viable under light microscopy in terms of shape, confluence and adherence (Figure 5.5). Macrophages

160

Chapter 5

A

MOI 25   MOI 50

MOI 100   MOI 1000

B
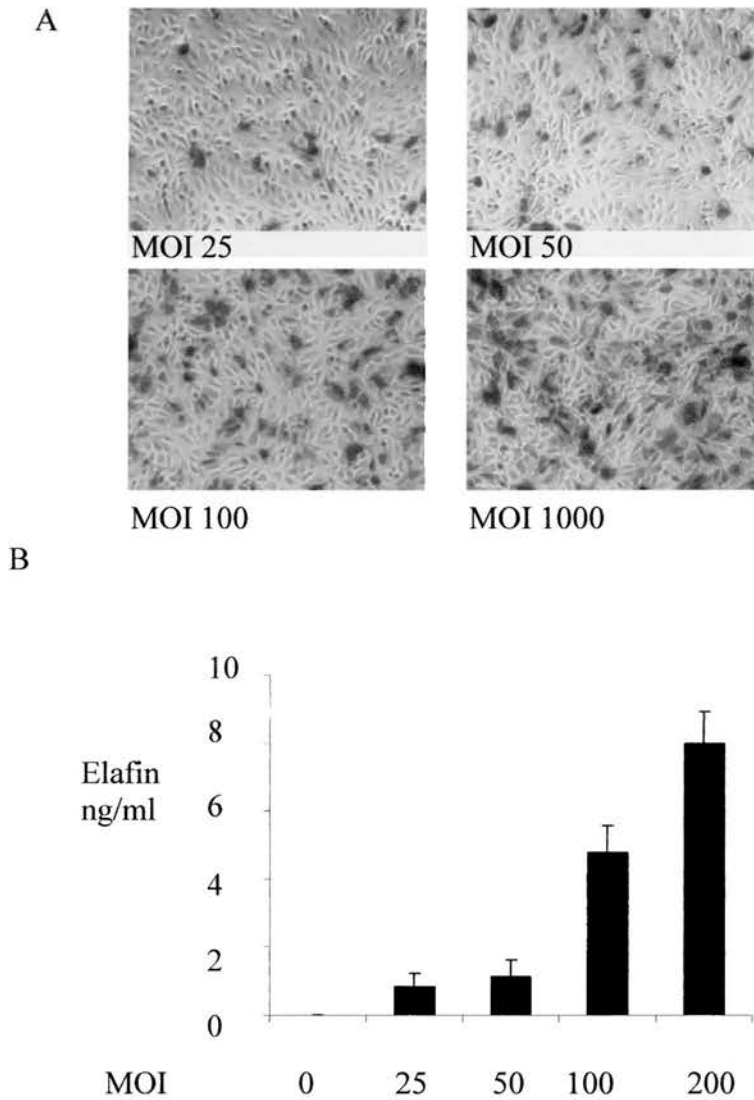
Figure 5.1. β galactosidase staining and elafin production in HUVECs infected with Ad-βgal and Ad-elafin at varying MOI.

Adenovirus was left in contact with cells for 1 h before washing and replenishing with normal growth medium. β galactosidase staining and elafin ELISAs were performed 24 h after infection. A. HUVECs exhibited increasing β-galactosidase positivity with greater viral MOI (multiplicity of infection). B. The effect of viral MOI on elafin production in supernatants from Ad-Elafin infected cells. Results are mean ± SD from one experiment performed in triplicate.

161

Chapter 5
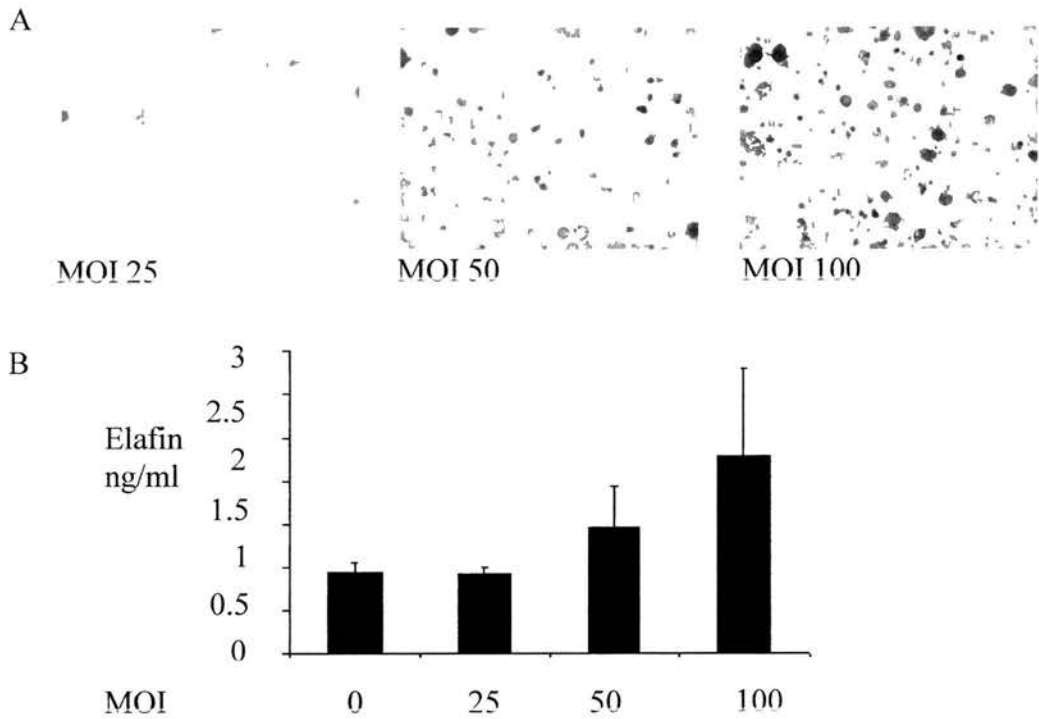
Figure 5.2. β galactosidase staining and elafin production in human peripheral blood monocyte derived macrophages infected with Ad-βgal and Ad-elafin.

Macrophages were prepared as outlined in Materials and Methods (section 2.2.1.2). They were matured on tissue culture plastic in 10% autologous serum for 5 days with a wash on day 2 to remove non-adherent cells. Adenoviral infections were performed in serum-free media for 1 h before replenishing with normal medium. A. Macrophages were infected with Ad-βGal on day 5 and stained for β-galactosidase activity on day 6. Micrographs are representative of two experiments from a single donor. B. Elafin production by Ad-elafin infected macrophages, data are mean ± SD from one experiment performed in triplicate.

Chapter 5

showed a slight increase in propidium iodide staining when exposed to CaPi alone (Figure 5.6) and adenovirus-CaPi led to a large increase in cytotoxic effect.

The levels of propidium iodide staining indicated high rates of cell death in both macrophages and HUVECs. Propidium iodide staining was conducted at the same time interval following infection that the quantifications of elafin and β-galactosidase activity were performed and several conclusions could be drawn with respect to the mechanism of toxicity. Firstly, cell death occurred several hours after viral entry and gene expression had taken place and propidium iodide positive cells also stained strongly for β-galactosidase. Secondly, although there was an impression of higher toxicity with β-galactosidase in macrophages, toxicity did not appear to be transgene specific and was observed with several different adenoviral gene vectors and importantly, an empty vector (Ad-dl703) expressing no transgene (Figure 5.6). Finally, viral dosing (MOI) was a factor with higher adenovirus-CaPi doses giving increased toxicity.

The levels of cell death were too high for this protocol to be used and the effects of altering the calcium concentration for precipitate formation on gene expression and cytotoxicity were therefore examined. Reducing the calcium concentration led to a fall in HUVEC elafin production (Figure 5.7). A similar result was seen for macrophage elafin production (not shown). Cytotoxicity was also reduced in both HUVECs (data not shown) and macrophages (Figure 5.8) with lower calcium concentrations. Increased levels of gene expression (compared to adenovirus alone)

163

Chapter 5
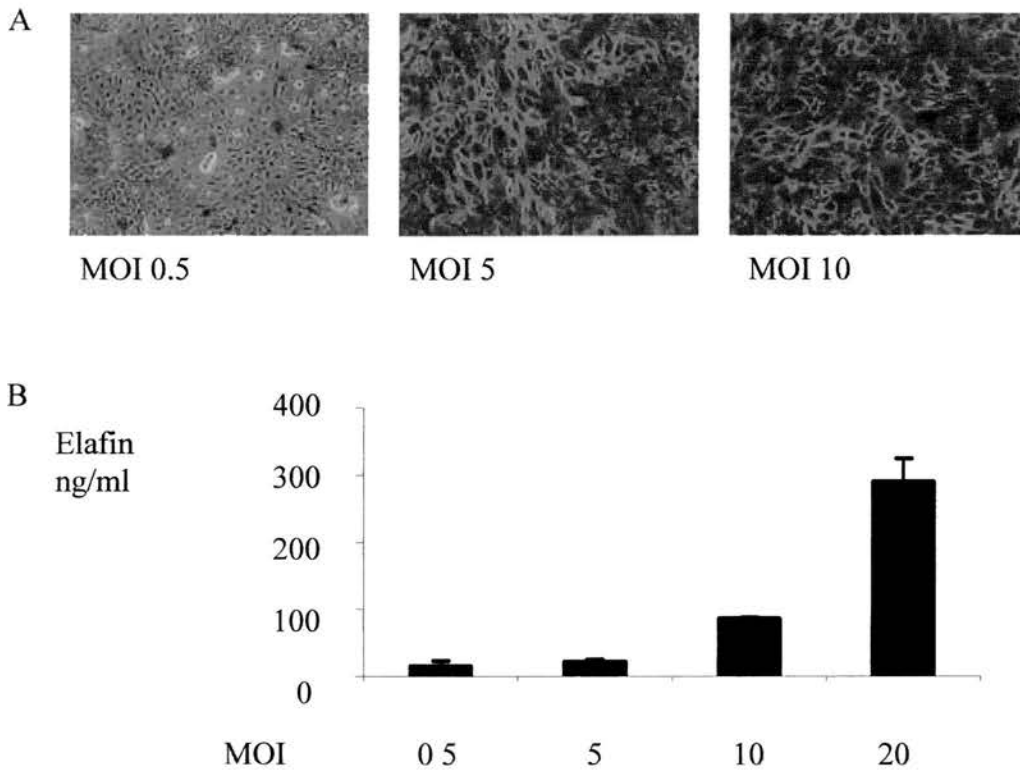
Figure 5.3. The effect on gene expression levels of precomplexing adenovirus with calcium phosphate precipitates prior to infection of HUVECs.

Adenoviral infections were performed in Eagle's minimal essential medium (cat M2770 Sigma) without serum. $CaCl_2$ was added to a final concentration of 8.3mM allowing calcium precipitate (CaPi) formation. Adenovirus was pre-incubated with the CaPi suspension for 20 min prior to addition to the cells at the required MOI. A. β-galactosidase staining of HUVECs following Ad-β-Gal-CaPi delivery. B. Elafin production in the supernatants from HUVECs 24 h after infection with Ad-elafin-CaPi. Results are mean ± SD from one experiment performed in triplicate.

164

Chapter 5
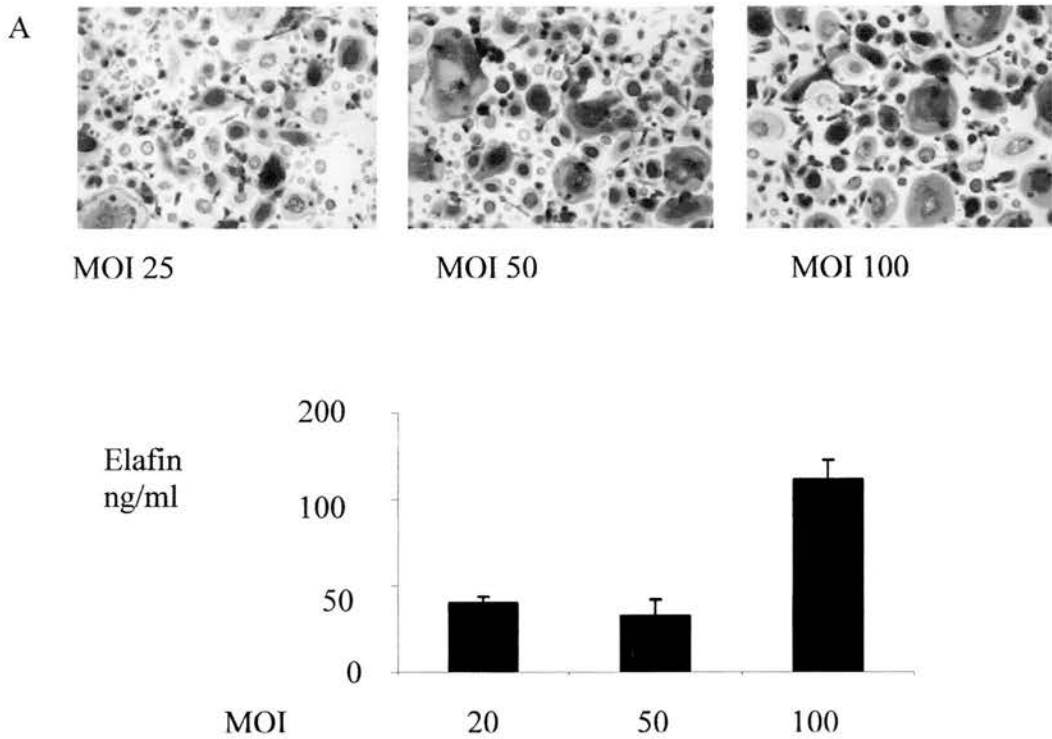
Figure 5.4. The effect on gene expression levels of precomplexing adenovirus with calcium phopshate precipitates prior to infection of macrophages.

Adenoviral infections were performed according to the protocol described in Fig.5.3. A. β-galactosidase staining of macrophages following Ad-β-Gal-CaPi infection. B. Elafin production in the supernatants from macrophages infected with Ad-elafin-CaPi. Results are mean ± SD from one experiment performed in triplicate.
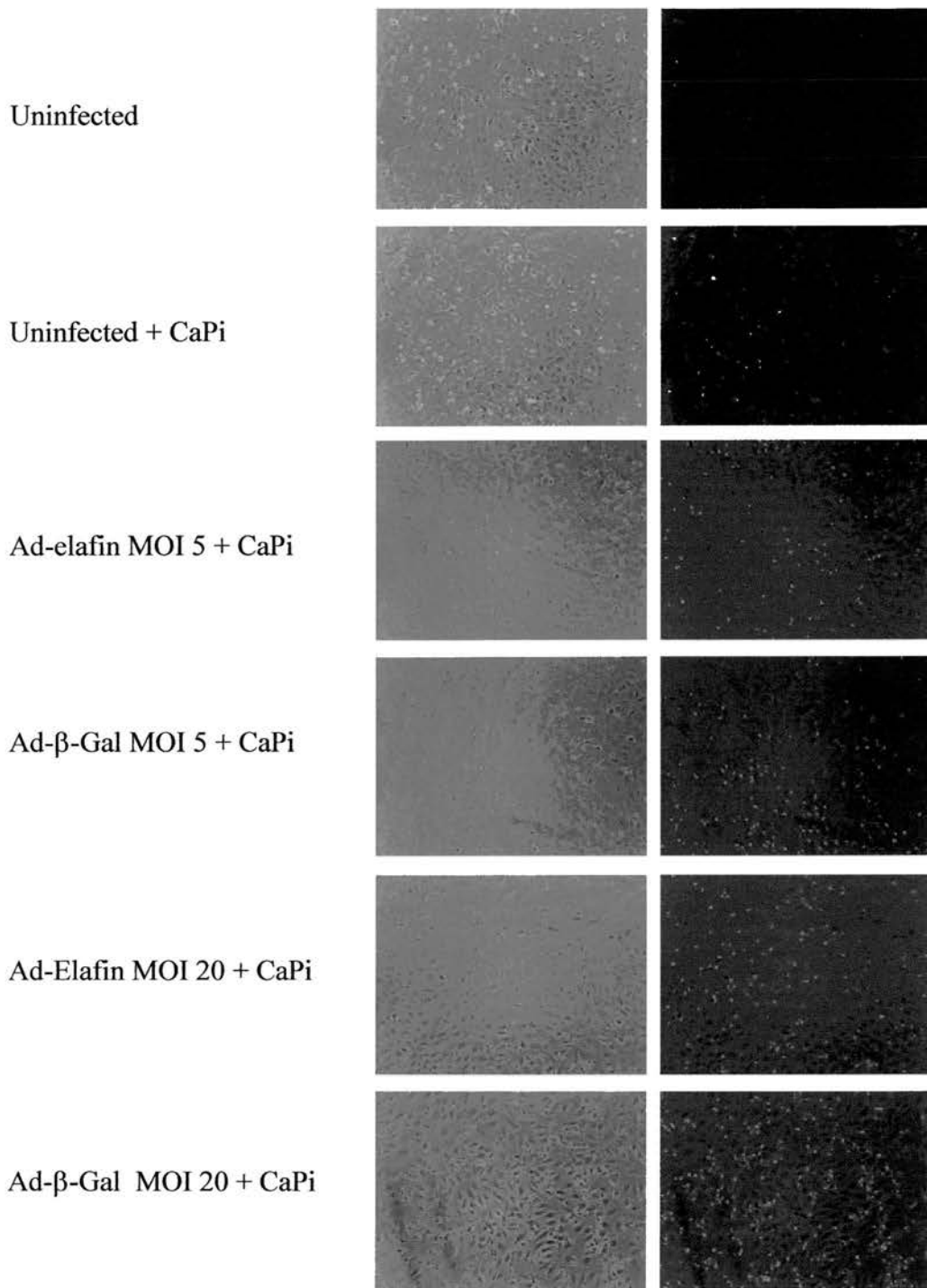
165

Chapter 5

Uninfected

Uninfected + CaPi

Ad-elafin MOI 5 + CaPi

Ad-β-Gal MOI 5 + CaPi

Ad-Elafin MOI 20 + CaPi

Ad-β-Gal MOI 20 + CaPi

Figure 5.5. Propidium iodide staining for cytotoxicity in HUVECs following Adenoviral-CaPi delivery.

166

Chapter 5

Uninfected

Uninfected + CaPi

Ad-Elafin MOI 5 + CaPi

Ad-Elafin MOI 20 + CaPi

Ad-dl703 MOI 20 + CaPi

Ad-IκBα MOI 20 + CaPi

Figure 5.6. Propidium iodide staining for cytotoxicity in macrophages following Adenoviral-CaPi delivery.

167

Chapter 5
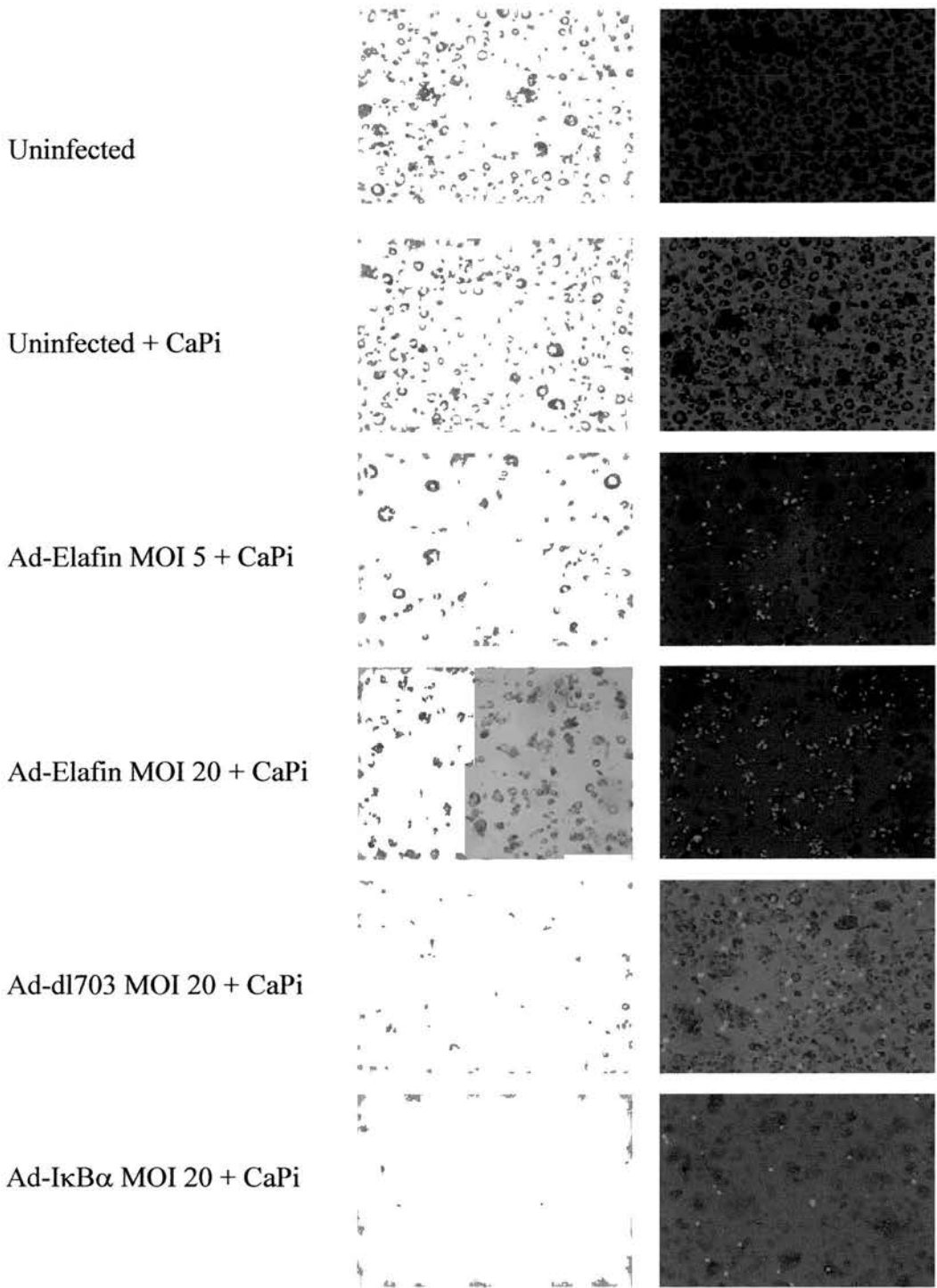
Figure 5.5. Propidium iodide staining for cytotoxicity in HUVECs following Adenoviral-CaPi delivery.

Paired micrographs of HUVECs taken under light (left panels) or green fluorescence (right panels) immediately after adding propidium iodide stain. There were very few propidium iodide positive cells following incubation in medium alone, medium and CaPi and following infection with a high dose of Ad-elafin (MOI 200). Adenoviral-CaPi resulted in more cell death, demonstrating dose dependence with viral MOI increasing with Ad-elafin and Ad-β-Gal at MOI 20.

Figure 5.6. Propidium iodide staining for cytotoxicity in macrophages following Adenoviral-CaPi delivery.

Paired micrographs of day 7 macrophages infected on day 6 and taken under light (left panels) or green fluorescence (right panels) for propidium iodide staining. Increasing MOI of virus together with CaPi resulted in clumping, the formation of more multinucleate giant cells and increased numbers of propidium iodide positive cells.

168

Chapter 5

could be achieved in the absence of overt increases in toxicity by reducing the calcium concentration. The effect of reducing calcium concentration on toxicity and β-galactosidase staining in macrophages is evident in Figure 5.8. A calcium concentration of 4.3 mM (Figure 5.8, middle panel) produced an estimated 70% infection rate with no discernible increase in propidium iodide staining.

Because of the concerns regarding CaPi mediated cytotoxicity, lipofectamine, another cationic adjuvant was assessed. Preliminary studies indicated that this was also effective in boosting adenoviral infection efficiency and microscopic appearances of cytopathy were notably absent in HUVECs at high viral MOIs compared to CaPi. The effects of duration of viral incubation and precomplexing with CaPi and lipofectamine were compared in HUVECs. For the same viral MOI of 100, lipofectamine had a similar effect to CaPi, increasing infection and elafin production (Figure 5.9). Interestingly the action on adenoviral infection was rapid with high levels of transgene expression following only a brief incubation of 30 minutes. There was a trend towards a further increase in elafin production after a 2-hour incubation for both CaPi and lipofectamine. Extending the length of incubation to 24 hours for virus precomplexed with either CaPi or lipofectamine did not increase elafin production in contrast to virus alone (Fig. 5.9). The latter finding was of particular interest indicating that for virus on its own, the length of incubation was a determining factor for successful infection. Previous laboratory protocols with adenovirus receptive cell types such as A549 cells had advocated a 1-hour incubation period but this may be too short for the kinetics of virus-cell interaction in HUVECs.

Precomplexing with lipofectamine similarly enhanced adenoviral infection of macrophages. An adenovirus vector encoding green fluorescent protein (Ad-GFP) was available for these experiments (a kind gift from the laboratory of Professor J. Gauldie, McMaster University, Hamilton, Ontario, Canada) and Ad-GFP was used to

169

Chapter 5
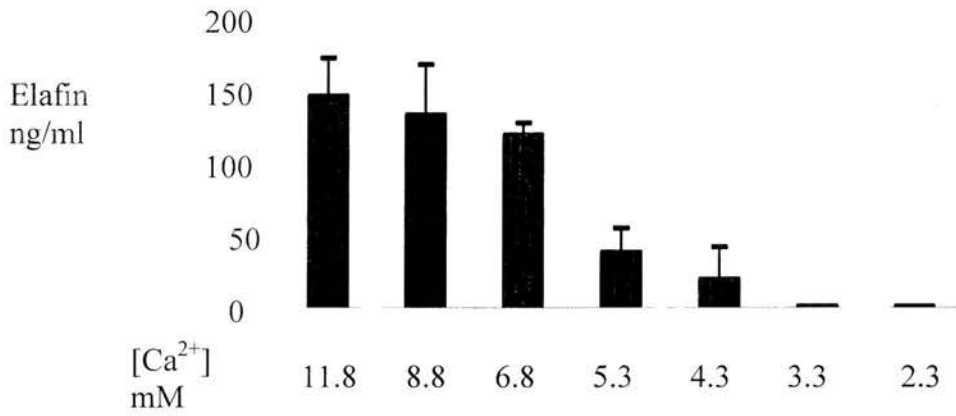
Figure 5.7. The effect of Ca^{2+} concentration on elafin production in HUVECs following Ad-elafin-CaPi infection.

Ad-elafin-CaPi infections were performed as for Fig. 5.3 and the concentration of $CaCl_2$ added to form precipitates was varied as indicated. Elafin levels in supernatants were measured by ELISA 24 h after infection. Results are mean ± SD from one experiment performed in triplicate.

Chapter 5

$[Ca^{2+}]$ mM
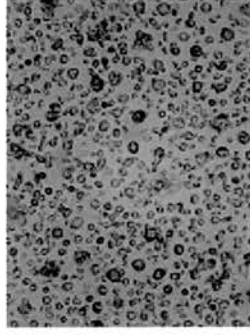
3.3 mM
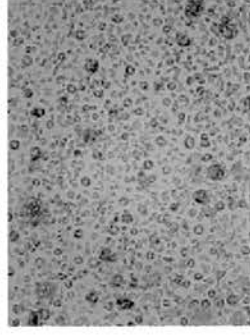
4.3 mM
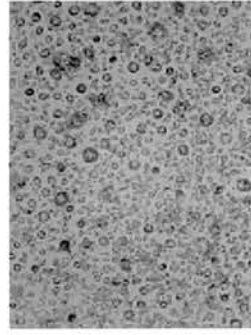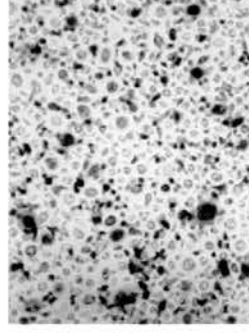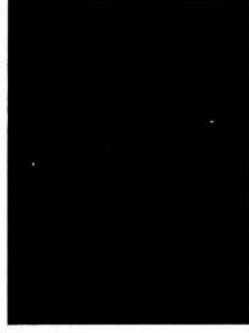
5.3 mM
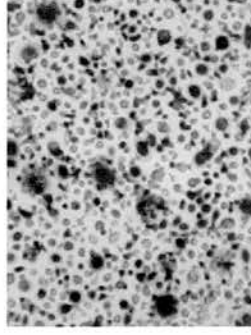
Figure 5.8. Propidium iodide staining examining the effect of varying the Ca^{2+} concentration on cytoxicity and gene expression for adenovirus-CaPi delivery in macrophages.

Ad-β-Gal-CaPi infections were performed at an MOI of 50 with precipitates formed with different Ca^{2+} concentrations according to the protocol in Fig 5.4. Micrographs in light (left panel) and green fluorescence (middle panel) from the same field and following β-galactosidase staining (right panel) from the well were taken.

172

Chapter 5
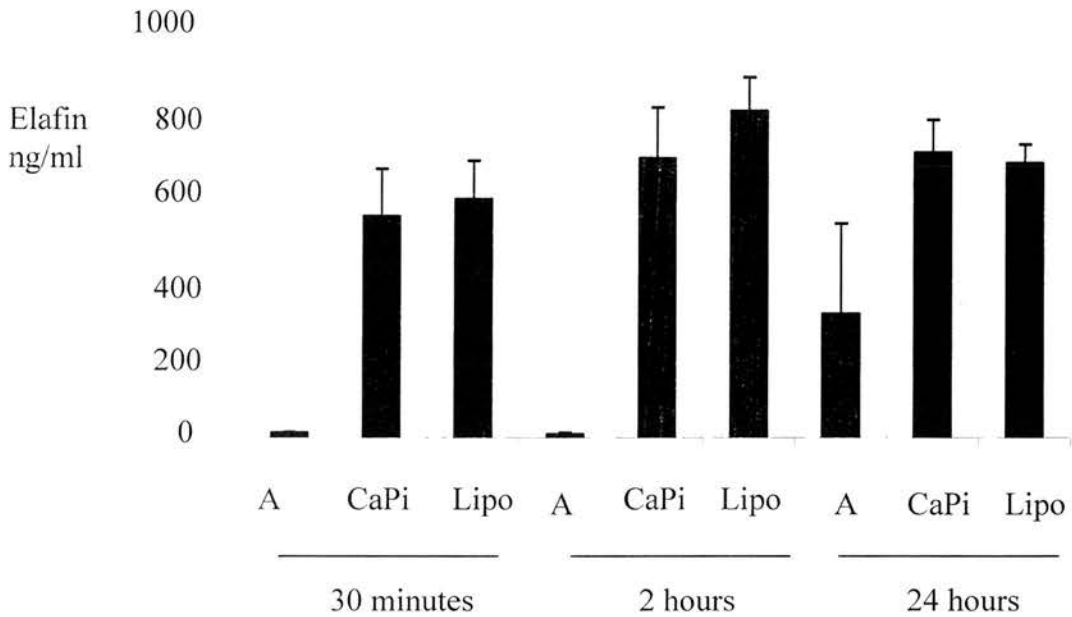
Figure 5.9. A comparison of the effect of duration of viral incubation period and precomplexing virus with cationic liposomes or CaPi on elafin production.

Endothelial cells were infected with Ad-elafin at an MOI 100 alone (A) or following precomplexing with CaPi and lipofectamine according to protocols set out in Materials and Methods (sections 2.2.2.3.1-2). Adenovirus was incubated with HUVECs for the length of time indicated. Virus containing medium was then removed and the cells were incubated in normal culture medium for a further 24 h and supernatant elafin concentrations were quantified by ELISA. Results are the mean ± SD from two HUVEC donors performed in triplicate.

demonstrate infection efficiency directly by green fluorescent protein expression (Fig. 5.10A). Ad-elafin infection and elafin production were affected by varying the ratio of lipofectamine to adenovirus particles. Elafin production increased with increasing lipofectamine ratios with no additional increase above 5×10^4 lipofectamine particles to each adenoviral particle (Fig. 5.10B). The latter ratio was chosen for all further infections involving precomplexing with lipofectamine.

Lipofectamine produced similar augmentation of infection efficiency and transgene expression to CaPi but an important question was whether this was associated with less toxicity. Because macrophages appeared to be most susceptible to CaPi toxicity the effect of lipofectamine precomplexing was evaluated closely on this cell type. There was no increase in propidium iodide uptake in macrophages that had been infected with adenovirus in precomplex with lipofectamine compared to non-infected cells (Fig 5.11). A similar result was observed following infection of HUVECs with adenovirus-lipofectamine. Lipofectamine facilitated efficient non-toxic adenoviral transgene delivery to primary human endothelial cells and macrophages and it was now possible to study the effects of elafin and murine secretory leucocyte protease inhibitor on these cell types.

174

Chapter 5
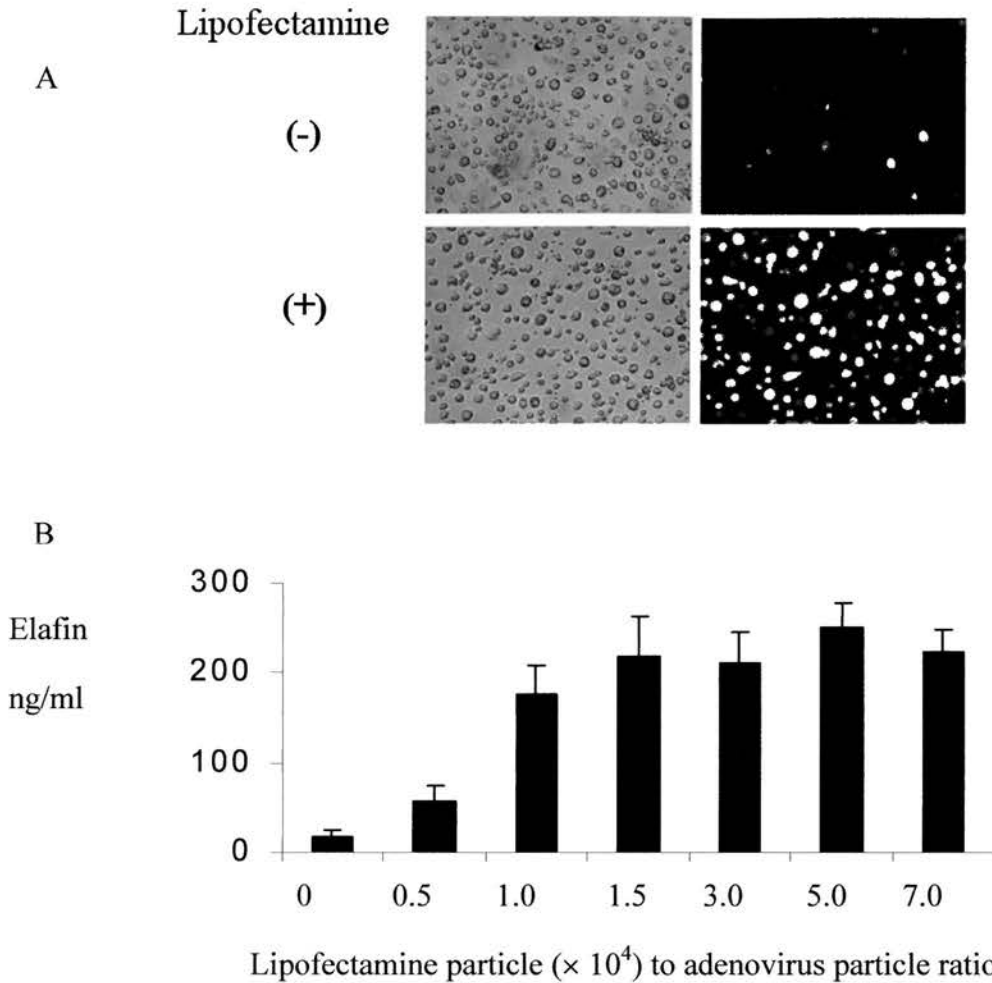
Figure 5.10. Precomplexing adenovirus with lipofectamine improved infection efficiency in macrophages

A. Ad-GFP infection of macrophages. Micrographs comparing the effect of precomplexing adenovirus with lipofectamine on green fluorescent protein expression following infection with virus at an MOI 100. Infections were performed according to protocols in Materials and Methods (section 2.2.2.3.1). The micrographs shown are representative of experiments performed on three separate donors. B. The effect of varying the ratio of lipofectamine to adenoviral particle number on infection efficiency and elafin transgene expression for Ad-elafin MOI 100. Results are mean ± SD from one donor performed in triplicate.

175

Chapter 5
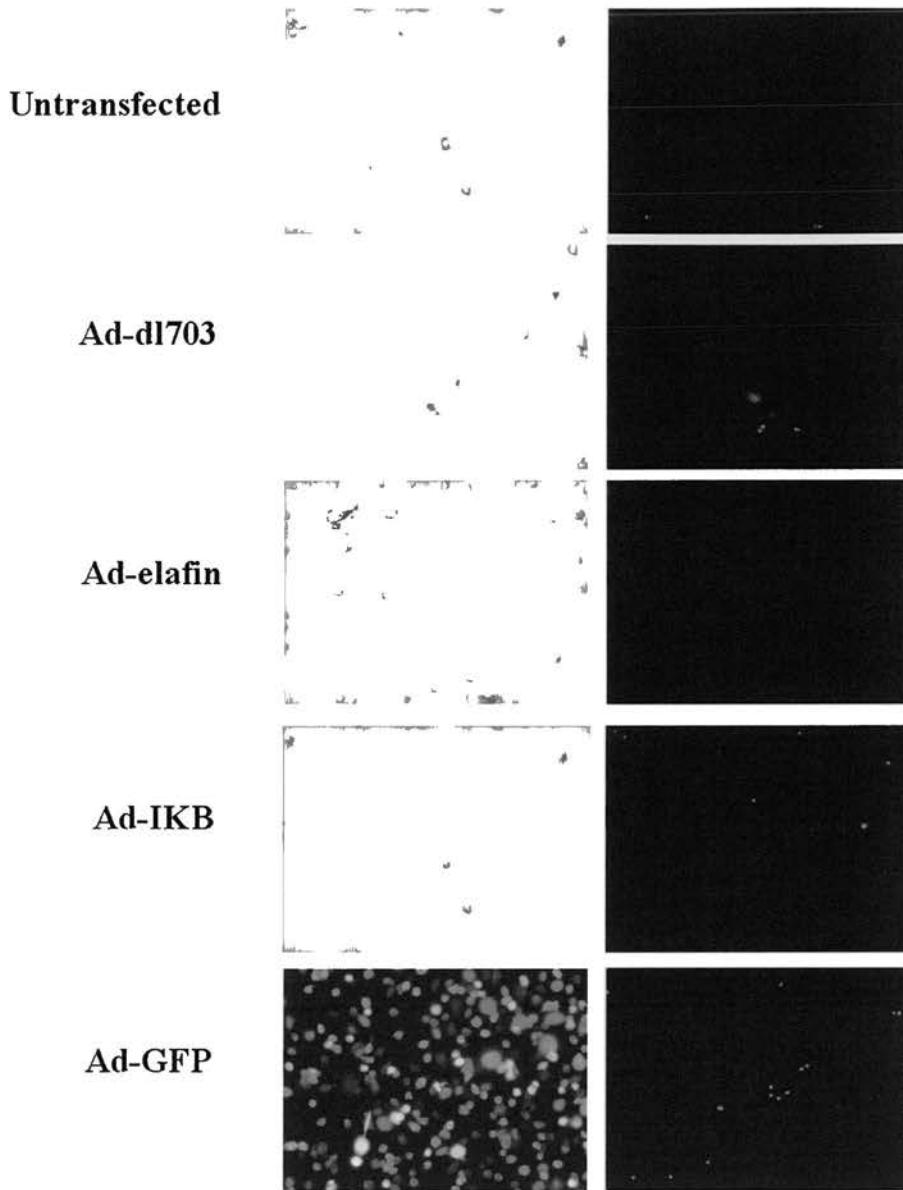
Figure 5.11. Precomplexing adenovirus with lipofectamine facilitates non-toxic high efficiency gene delivery in macrophages

Paired micrographs taken under light (left panel) or green fluorescence for propidium iodide staining (right panel) of day 7 macrophages following infection on day 6 with the different Ad vectors shown at an MOI 100. Ad-GFP infected macrophages were photographed under blue fluorescence to illustrate GFP expression. Macrophages were prepared and infected according to protocols in Figure 5.10.

176

Chapter 5

5.2.2. The effect of elafin and mSLPI overexpression on the inflammatory cytokine responses of human endothelial cells and macrophages to atherogenic stimuli.

The anti-inflammatory activities of elafin and murine secretory leucocyte protease inhibitor (mSLPI) were studied on HUVECs, macrophages and lung alveolar epithelial cell tumour cell line (A549 cells). The mSLPI vector was developed in preference to its human orthologue because the literature indicating anti-inflammatory actions for murine SLPI (Jin et al 1997; Zhu et al 1999) and because of future applicability of this vector in murine models of atheroma. Epithelial cells are not relevant to atherosclerosis (although lung epithelial cells produce both elafin and SLPI) and were included to test whether the potential effect demonstrated cellular specificity. A model of inflammatory activation of endothelial cells in atherosclerosis involving activation of NF-κB and production of IL-8 in response to oxidised LDL has been described in chapter 3. Bacterial lipopolysaccharide (LPS) and TNF-α were included as further stimuli relevant to the development of atheroma (Barath et al 1990; Lehr et al 2001) and both increased endothelial cell IL-8 release (Figure 5.12A). LPS induced TNF-α and IL-8 production were chosen as models of inflammatory activation of macrophages and A549 cells respectively.

The effects of both Ad-elafin and Ad-mSLPI, were examined on responses to LPS, TNF-α and oxidised LDL in HUVECs. In addition to the empty adenovirus construct Ad-dl703 and in order to effect complete control for adenovirus and transgene effects, a further control adenovirus expressing murine eotaxin (Ad-m-eotaxin), a secreted chemokine of similar molecular weight to elafin and mSLPI with no known anti-inflammatory activity in the cell types, was studied.

In HUVECs, Ad-elafin and Ad-mSLPI produced small but significant reductions in basal IL-8 production, an effect not observed in Ad-IκBα infected cells (Figure 5.12B). Ad-elafin and Ad-mSLPI had comparable inhibitory effects to Ad-

177

IκBα following stimulation of HUVECs with LPS and oxidised LDL when compared to control vectors (Figure 5.12D, E). TNF-α stimulation led to a large increase in IL-8 production that was significantly attenuated by Ad-IκBα, Ad-mSLPI and Ad-elafin (Fig. 5.12C). TNF-α was chosen as a marker for the ability of macrophages to respond to LPS. Stimulation of macrophages with LPS produced a response in both non-infected and virally infected cells (Fig. 5.13A). Ad-mSLPI and Ad-elafin significantly reduced the TNF-α response to LPS compared with Ad-dl703 and Ad-m-eotaxin (Fig. 5.12C). In contrast to IL-8 production in HUVECs there was no significant difference in the basal level of TNF-α production among the five adenovirus constructs (Fig. 5.13B).

This result differs from others that have demonstrated inflammatory effects of adenovirus on macrophages with increased TNF-α production following infection. Intratracheal administration of an Ad-βGal in mice resulted in elevated TNF- α message in alveolar macrophages detected by *in situ* hybridisation, 30 minutes after infection (Zsengeller et al 2000). The same workers also demonstrated augmented TNF-α production by the murine RAW264.7 macrophage cell line 2 hours after infection with virus (Zsengeller et al 2000). In contrast, Foxwell et al (1998) did not observe any increase in basal NF-κB activity or TNF-α production 3 days after infection of primary human macrophages with an empty adenoviral vector comparable to Ad-dl703, compared to uninfected cells. The use of a longer time courses in the latter study and the work presented in this chapter may explain the absence of evidence for adenovirus induced inflammation which could represents an early and transient event.

To assess whether the properties of elafin and mSLPI extended to all cell types, similar experiments were conducted on the A549 epithelial tumour cell line. In comparison with their inhibitory effect on stimulated cytokine production in HUVECs and macrophages, Ad-elafin and Ad-mSLPI had no effect on IL-8

5.12. Ad-elafin and Ad-mSLPI reduce IL-8 production in HUVECs in basal conditions and following stimulation with TNF-α, LPS and oxidised LDL.

179

Chapter 5
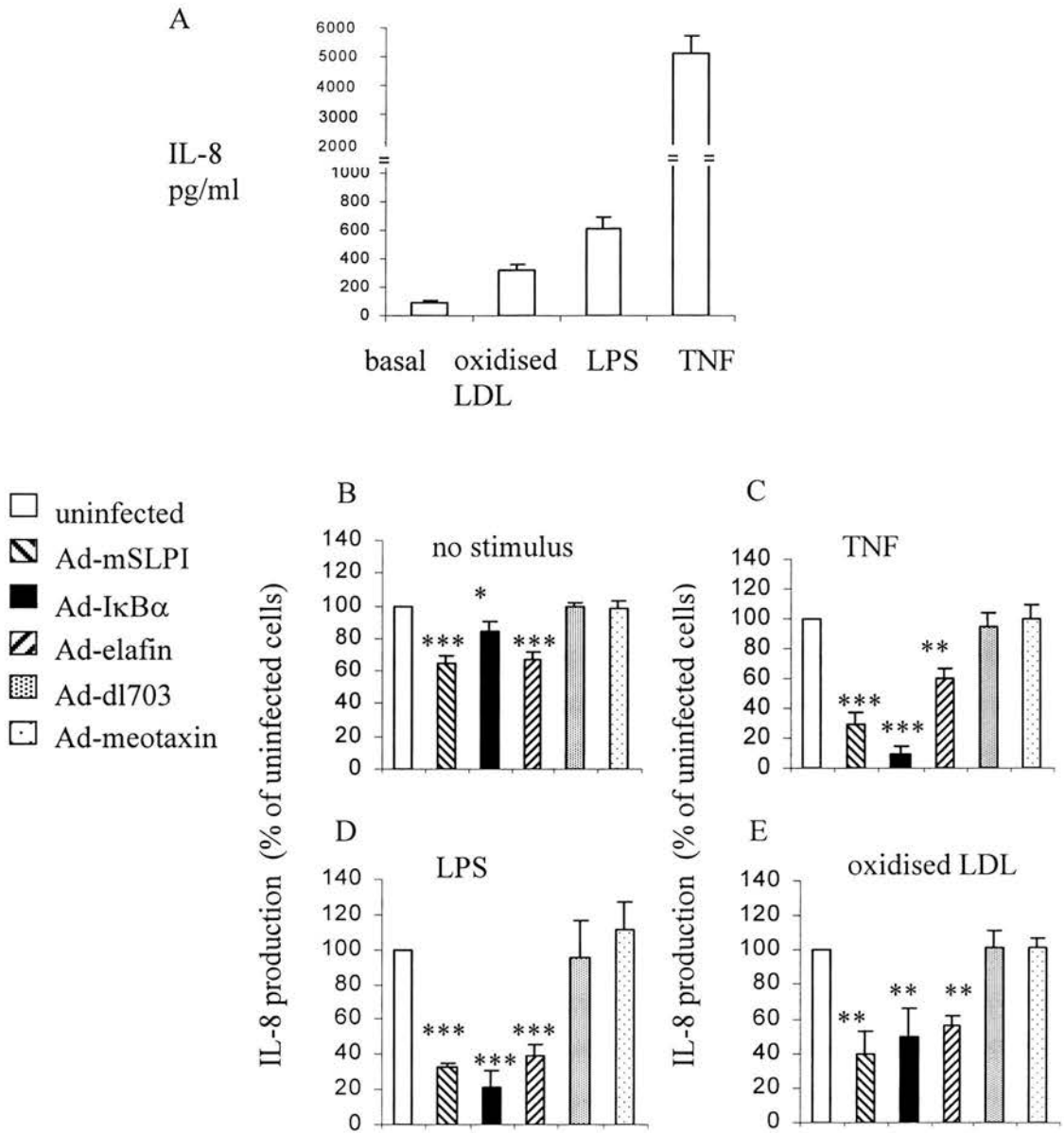
5.12. Ad-elafin and Ad-mSLPI reduce IL-8 production in HUVECs in basal conditions and following stimulation with TNF-α, LPS and oxidised LDL.

Stimuli were applied 24 h after Ad-infection and left for 8 h before removal of conditioned medium for IL-8 ELISA. A. IL-8 response to the three stimuli. B. Ad-elafin, Ad-mSLPI, Ad-dl703, Ad-IκBα and Ad-meotaxin infected cells under basal (untreated) conditions. C. TNF-α 1 ng/ml. D. LPS 100 ng/ml. E. oxidised LDL 100 µg/ml. IL-8 production is expressed as a percentage of uninfected cells. Data in B-E are means and standard deviations from 3 separate donors performed in quadruplicate. *, **, ***, significantly lower than Ad-meotaxin infected cells, $p < 0.05$, 0.01, 0.001.

Chapter 5

A

⦚ no LPS	
☐ uninfected. LPS	
▦ Ad-dl703. LPS	

B no LPS

C LPS

☐ uninfected	
◩ Ad-mSLPI	
■ Ad-IκBα	
▨ Ad-elafin	
▨ Ad-dl703	
⊡ Ad-meotaxin	
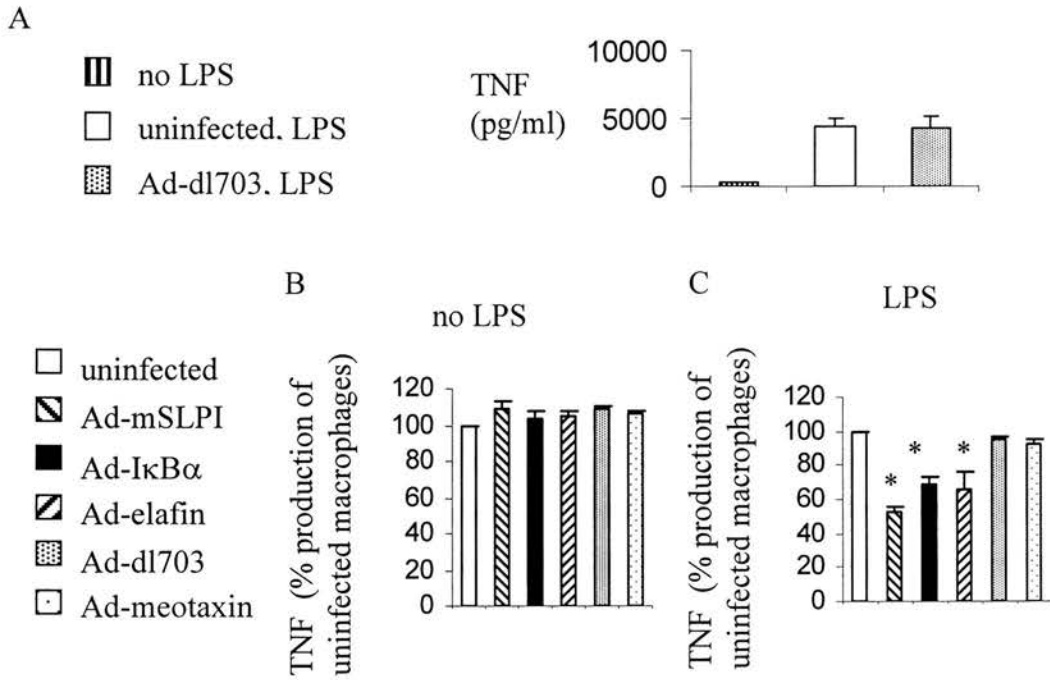
5.13. Ad-elafin and Ad-mSLPI reduced macrophage TNF-α production in response to LPS stimulation.

Adenoviral infections were performed (100 PFU/cell) as described in Materials and Methods and LPS was added on day 7 of culture. Conditioned medium was removed after 3 h for TNF-α ELISA. A. Representative experiment from one donor (mean and standard deviation from triplicate wells) showing TNF-α production from untreated cells and the response following stimulation with LPS (1 ng/ml) in uninfected and Ad-dl703 infected macrophages. B. TNF-α production in infected, non-stimulated cells. C. TNF-α production in response to infected and LPS stimulated macrophages (1 ng/ml). TNF-α production is expressed as a percentage of uninfected cells. Data in B-C are means and standard deviations from 3 donors performed in triplicate. *, significantly less than Ad-m-eotaxin infected cells p < 0.01.

181

Chapter 5
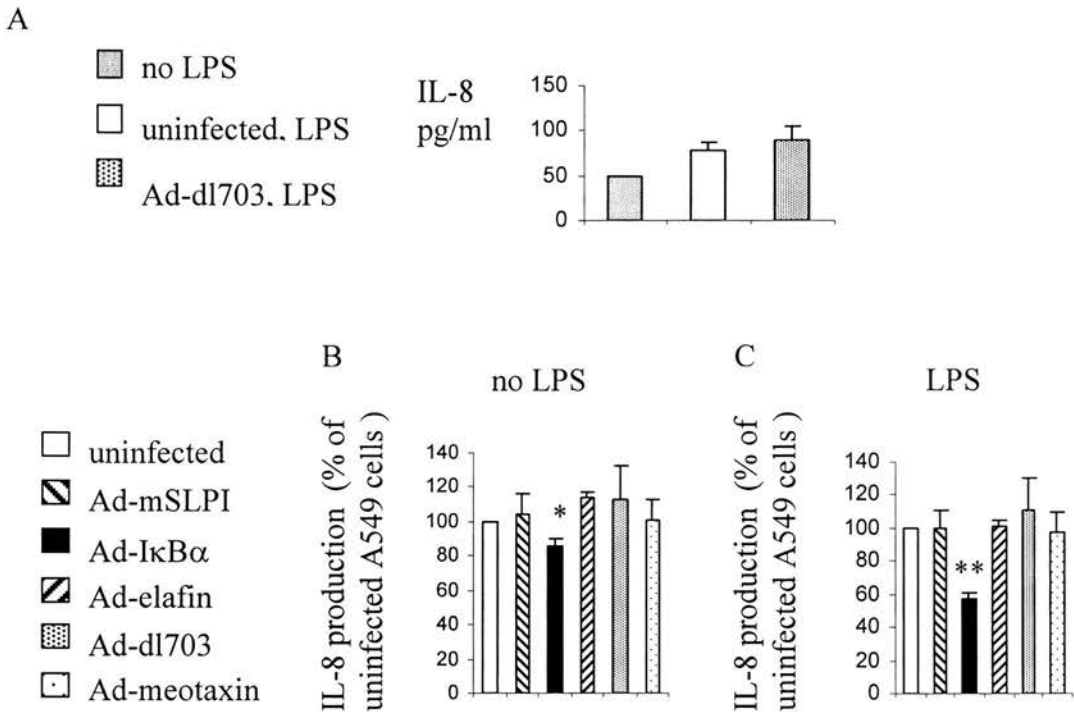
Figure 5. 14 Ad-elafin and Ad-mSLPI had no effect on IL-8 production by A549 epithelial cells in response to LPS stimulation.

A549s were grown to confluence in 48-well Costar plates, infected with adenovirus vectors (100 PFU/cell) and stimulated with LPS using the HUVEC protocol. A. IL-8 production in response to LPS stimulation (100 ng/ml). Data represent the mean and standard deviation from triplicate wells. B. Basal IL-8 release from infected non-stimulated A549s. C. IL-8 production from infected A549s in response to LPS (100 ng/ml). Data represent the means and standard deviations from 3 experiments performed in triplicate. IL-8 concentration is expressed as a percentage of uninfected cells. *,** significantly lower than Ad-meotaxin infected cells p < 0.05, p < 0.001.

182

Chapter 5

production by A549s in basal conditions or following stimulation with LPS (Figs. 5.14B,C).

However, Ad IκBα retained an inhibitory effect, significantly reducing basal IL-8 production and attenuating the response to LPS in A549 cells. This finding was intriguing given that the A549 cell is the only one of the three studied that produces endogenous elafin and SLPI protein in large quantities. This result was expected from previous work conducted on A549 cells in our lab (Dr Sallenave, unpublished data). In seeking a possible explanation for the different response of the A549 cells it is important to consider that they may behave differently as an immortalised cell line and one would need to assess the effect of elafin and mSLPI on primary epithelial cells before concluding that that their effect was cell type specific.

5.2.3. Effect of elafin and mSLPI overexpression on NF-κB activation

IL-8 and TNF-α are strongly regulated by NF-κB transcription in endothelial cells (Roebuck 1999) and macrophages (Foxwell et al 1998). The observation that elafin and mSLPI overexpression inhibited inflammatory cytokine production in response to three different stimuli points to an intracellular mechanism at a point of signalling convergence. NF-κB activity was therefore examined using electromobility shift assays. In HUVECs and macrophages the level of NF-κB activity in unstimulated cells was very low. In preliminary studies, there was no difference between virally infected and uninfected cells. In HUVECs, stimulation with LPS led to an increase in NF-κB activity that was reduced by Ad-elafin and Ad-mSLPI but only at the lowest concentration of LPS used (100 ng/ml) (Fig. 15A). Inhibitory effects disappeared at higher LPS concentrations (1 and 5 μg/ml) by comparison with the inhibitory effect of Ad-IκBα that remained constant (Fig. 5.15A). A similar trend was seen following incubation of HUVECs with oxidised LDL (Fig. 5.16A). Ad-IκBα was most inhibitory, Ad-mSLPI attenuated

183

Chapter 5
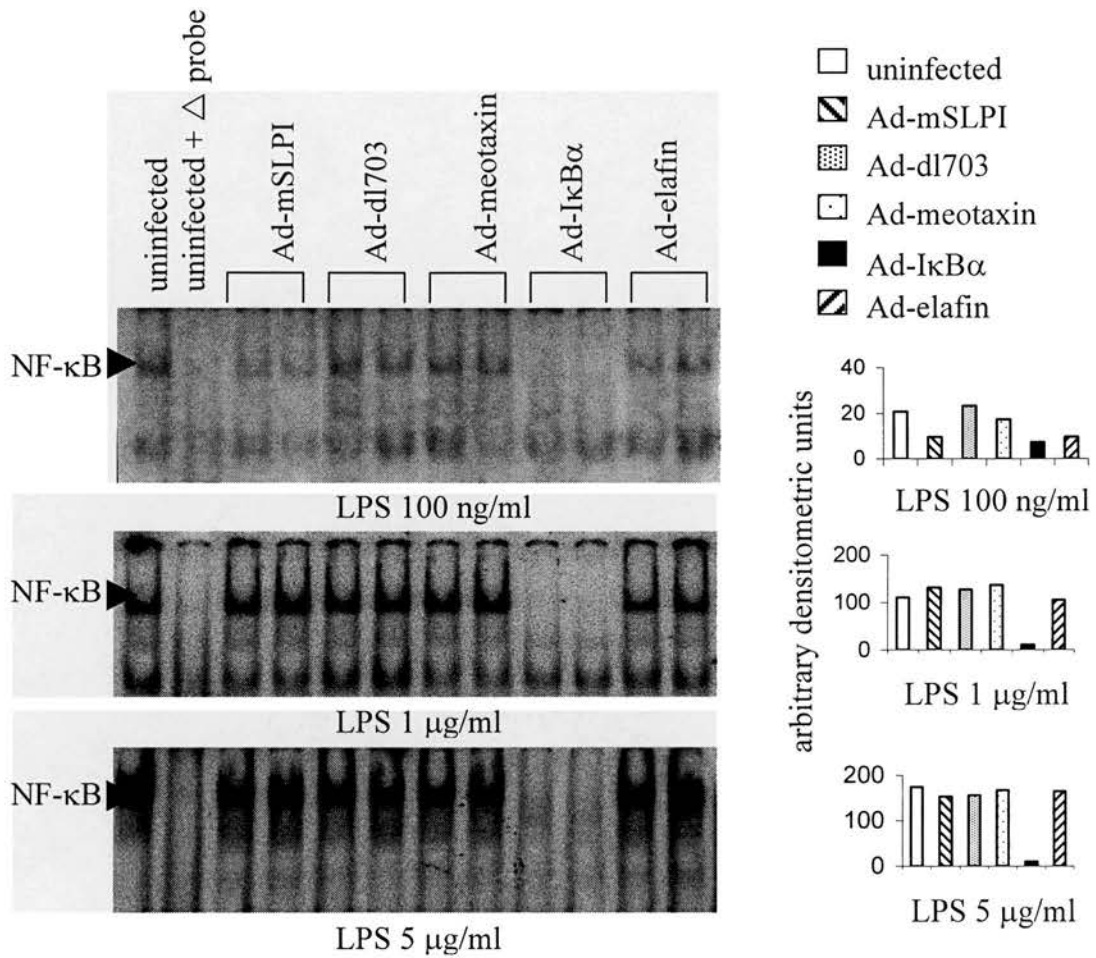
Figure 5.15. Ad-elafin, Ad-mSLPI and Ad-IκBα reduced NF-κB activation in HUVECs following stimulation with LPS.

HUVEC nuclear proteins were prepared for EMSA 1 h after stimulation with LPS. Specificity of binding was demonstrated by disappearance of the NF-κB band with a mutated NF-κB oligo (Δ probe). Nuclear proteins from two separate experiments were run in pairs on the same gel. EMSAs of nuclear proteins (7 μg) from cells infected with Ad-vectors and stimulated with LPS at 100 ng/ml, 1 μg/ml and 5 μg/ml. The mean intensities of the corresponding NF-κB bands for uninfected and adenovirus infected cells were determined using ImageQuant software and expressed as arbitrary densitometric units on the y-axis.

184

Chapter 5

Figure 5.16. Ad-elafin, Ad-mSLPI and Ad-IκBα reduced NF-κB activation in HUVECs following stimulation with oxidised LDL and TNF-α.

185

Chapter 5
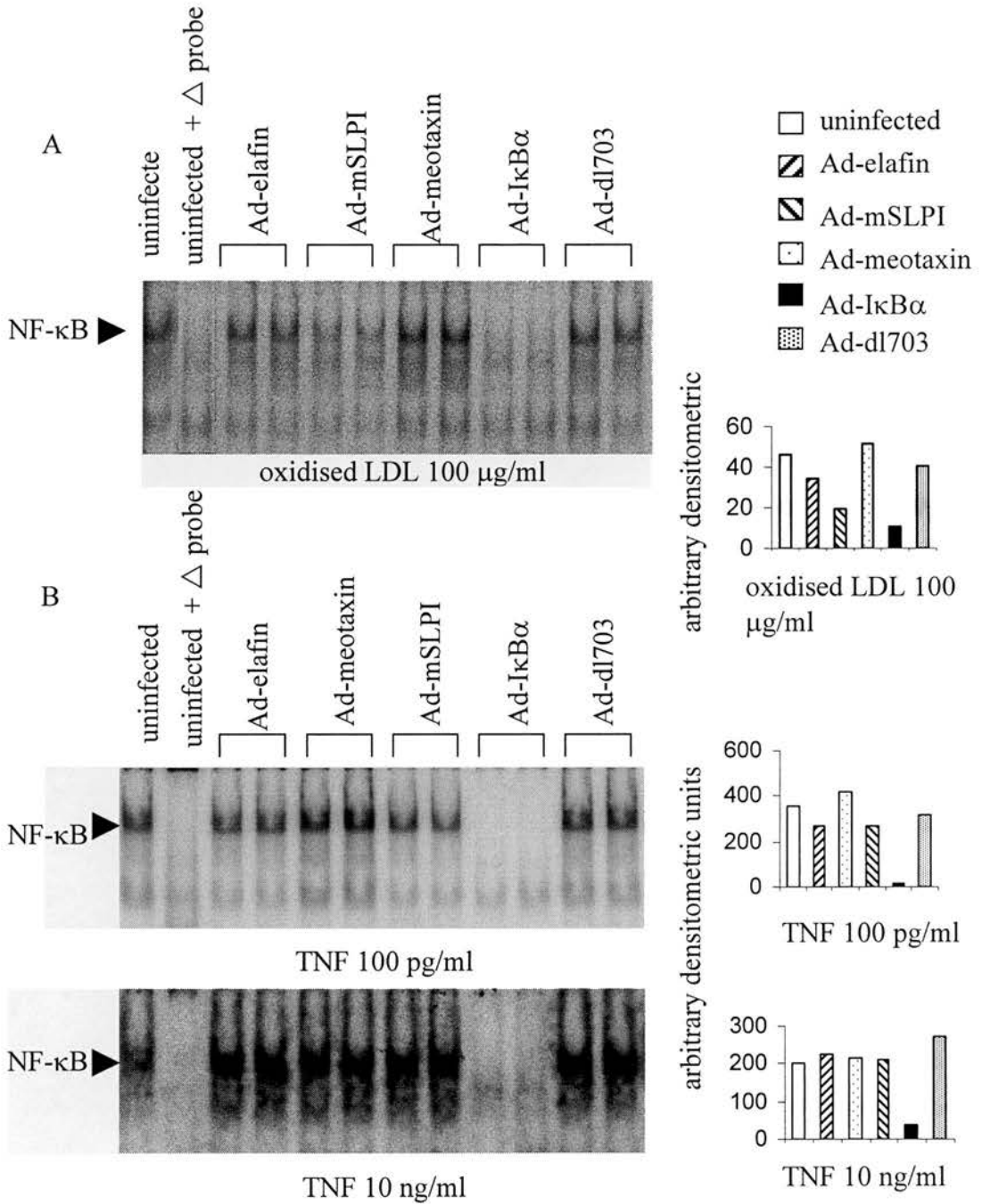
Figure 5.16. Ad-elafin, Ad-mSLPI and Ad-IκBα reduced NF-κB activation in HUVECs following stimulation with oxidised LDL and TNF-α (continued).

EMSAs were performed on nuclear proteins prepared according to protocols in Fig. 5.14 A, oxidised LDL stimulated cells, B, TNF-α stimulated cells. EMSAs are shown with corresponding densitometry.

186

Chapter 5
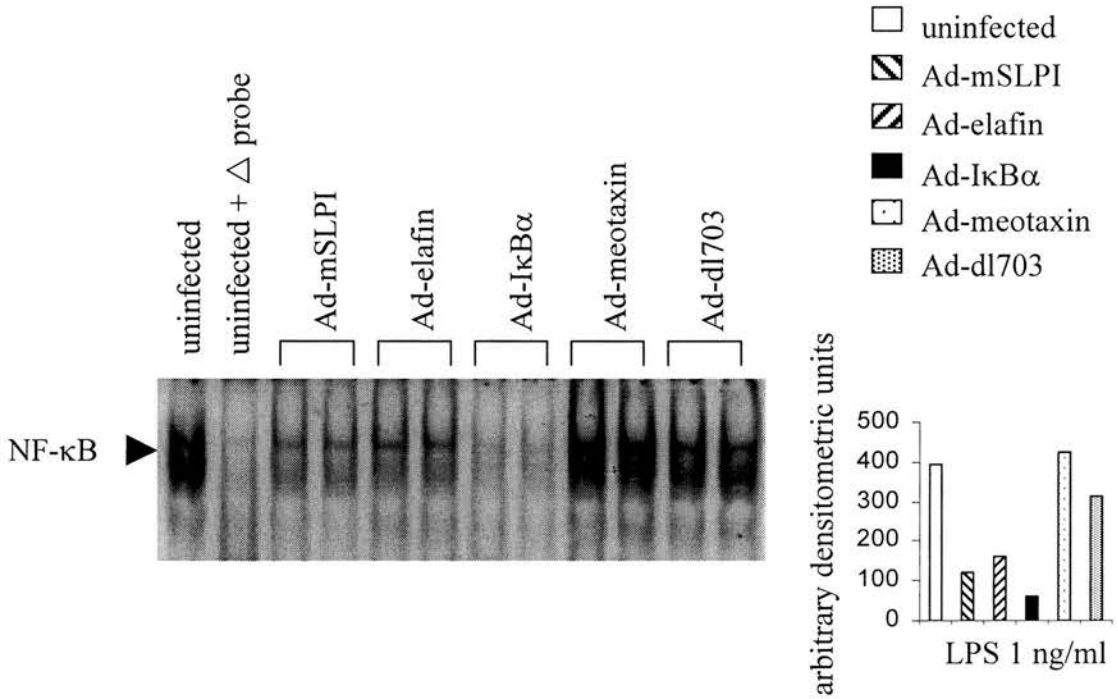
Figure 5.17. Ad-elafin, Ad-mSLPI and Ad-IκBα reduced NF-κB activation in macrophages following stimulation with LPS.

Macrophages were cultured in 12-well Costar plates and infected with adenovirus vectors as for Fig. 5.12. Cells were stimulated with LPS (1 ng/ml) for 1 hour on day 7 and EMSAs performed on nuclear extracts (7 μg) as for Fig. 5.14 (representative gel from an experiment repeated on 2 separate donors). Corresponding densitometry of NF-κB bands is also shown.

187

Chapter 5

NF-κB activation to a lesser degree but the effect of Ad-elafin was marginal compared with control vectors.

Similarly, there was a trend towards reduced NF-κB activity following stimulation with TNF-α (100 pg/ml) in Ad-elafin and Ad-mSLPI infected cells. In parallel with their inhibitory effects on LPS signalling (Fig. 5.15A), this effect disappeared with a higher concentration (1 ng/ml) of TNF-α (Fig. 5.16B). In contrast, the inhibitory effect of Ad-IκBα was much stronger and retained at the higher TNF-α concentration. The observation that the effect of both elafin and mSLPI overexpression could be overridden by higher concentrations of stimulus was intriguing, suggesting that the inhibitory mechanism could be consumed or saturated in contrast to overexpression of mutated IκBα that remains resistant to proteosomal degradation and continues to bind NF-κB at higher concentrations of stimulus.

In macrophages, Ad-elafin and Ad-mSLPI significantly attenuated NF-κB activity following LPS stimulation when compared with control vectors although Ad-IκBα was the most effective (Fig. 5.17).

To investigate the mechanism of NF-κB inhibition by Ad-elafin and Ad-mSLPI further, adenovirus infected HUVECs and macrophages were stimulated with TNF-α and LPS respectively. Total cell lysates were then analysed for IκBα content by Western Blot analysis. Ad-mSLPI and Ad-elafin significantly protected HUVECs and macrophages from TNF-α and LPS-induced IκBα degradation respectively (Figure 5.18). Ad-IκBα produced overexpression of mutated IκBα (as evidenced by its higher molecular weight) but in accordance with other studies (Heimberg et al., 2001) did not completely prevent endogenous IκBα degradation.

188

Chapter 5

To summarise the findings from this section: adenovirus mediated expression of elafin and mSLPI reduced inflammatory cytokine production in human endothelial cells and macrophages in response to several stimuli through a mechanism involving inhibition of the transcription factor NF-κB and preservation of cell IκBα.

189

Chapter 5
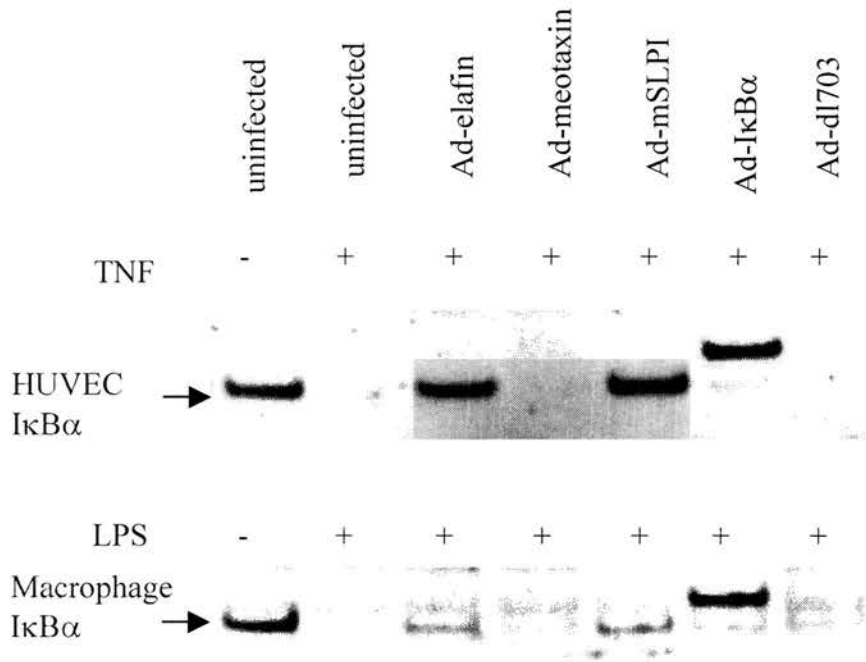
Figure 5.18. Ad-elafin, Ad-mSLPI and Ad-IκBα protected HUVECs and macrophages from IκBα degradation.

HUVECs and macrophages (uninfected or infected with adenovirus constructs) were stimulated with TNF-α (100 pg/ml, upper panel) or LPS (1ng/ml, lower panel) respectively, for 10 min (preliminary experiments were performed to determine optimal timing, not shown). Total cell extracts were obtained and Western Blot analysis was performed for IκBα content as outlined in Materials and Methods (section 2.2.5.5). Ad-derived IκBα migrates slightly higher than endogenous IκBα. Results are representative of experiments performed in duplicate.

190

5.3. Discussion

The principal novel observations arising from this chapter are the development of an inexpensive, non-toxic method to enhance adenoviral gene delivery to HUVECs and facilitate gene delivery to human macrophages, a cell type refractory to gene therapy and the characterisation of elafin and mSLPI as multifaceted innate immunity molecules regulating the inflammatory responses of human endothelial cells and macrophages to atherogenic stimuli. Discussion will focus on the methods used to augment adenoviral gene delivery, the mechanism of effects of elafin and mSLPI on endothelial cell and macrophage inflammatory functioning and the potential of these peptides as targets for gene therapy in atherosclerosis.

5.3.1. Enhancing adenoviral infection of human endothelial cells and macrophages.

HUVECs are receptive to adenoviral infection. They express the coxsackie/adenovirus receptor (CAR) (Jornot et al 2002). Previous workers have demonstrated efficient adenoviral infection and transgene expression (Takahashi et al 1997). A viral MOI of 100 produced an infection efficiency of around 50% estimated by β-galactosidase staining (Figure 5.1A). By contrast, macrophages are less susceptible to adenoviral infection, expressing low levels of CAR (Kaner et al 1999) and in accordance with this, infection efficiency was 10% with a viral MOI of 100 in human macrophages (Figure 5.2A). Improved infection efficiency was therefore deemed to be an important goal, not only to facilitate gene delivery but also to reduce viral dosing, a particular concern in clinical studies. Entry of human adenovirus into host cells involves initial binding of the adenovirus fibre protein to the CAR receptor (Bergelson et al 1997). Following attachment, virus entry into cells is mediated by viral penton base binding to αV integrins (Bai et al 1993). Huang et al (1995) used stimulation with granulocyte macrophage colony-stimulating factor (GM-CSF) to up regulate αV integrin expression on the surface of freshly prepared human monocytes. This modification produced significant increases in transgene expression rates with around 54% infection with a viral MOI of 1000. This approach is relatively costly,

191

Chapter 5

impractical for *in vivo* use and through altering the macrophage phenotype with a growth factor has the potential disadvantage of altering cell function.

The efficiency of adenoviral infection has been improved previously through using a noncovalent complex consisting of a cationic component (calcium precipitates or cationic lipid) and adenovirus in NIH 3T3 cells and murine epithelium *in vivo* (Fasbender et al 1997; Fasbender et al 1998) and human monocytes in suspension (Schleef et al 2001). Calcium precipitates enhanced infection efficiency in HUVECs (Figure 5.3) and dramatically increased infection and gene expression of macrophages (Figure 5.4). The calcium precipitates may be attracted by charge to adenovirus particles that carry a net negative charge (Alemany et al 2000; Mei et al 1995), facilitating attachment to the negatively charged cell membrane. The mechanism of improved infection does not involve fibre knob-CAR or penton base-αV integrin interactions and may occur through non-specific endocytotic pathways (Walters et al 1999). In this regard it is noteworthy that prolonged contact with adenovirus alone, heightened cell infection and transgene expression (Figure 5.9). That the mechanism is receptor independent probably contributes to its success with cell types demonstrating low tropism for adenovirus.

Although gene expression was increased following precomplexing adenovirus with calcium precipitates in HUVECs and macrophages, propidium iodide staining led to the surprise finding of increased cell injury and death (Figures 5.5, 5.6). Calcium precipitates did not account for the toxicity alone and cell death occurred late on, following transgene expression through a mechanism that appeared to be independent of the transgene expressed with similar levels of cell injury being observed in empty vector (Ad-dl703) and Ad-IκBα infected cells (Figure 5.6). The efficiency of gene expression (Figure 5.7) and toxicity (Figure 5.8) were both lowered by reducing the quantity of calcium making the precipitate. No information relating to cell toxicity was presented in the original descriptions of the use of adenovirus-CaPi coprecipitates in the 3T3 cell line and infection was also readily

192

achieved in murine airway epithelium (Fasbender et al 1997; Fasbender et al 1998). Precomplexing with lipofectamine produced similarly high levels of infection in both cell types (Figures 5.9, 5.10) without the associated toxicity (Figure 5.11) suggesting that the CaPi were responsible for the cytotoxic effect. It is postulated that CaPi are internalised along with adenovirus. In an acidic endosome the CaPi may be rendered soluble leading to a damaging influx of calcium (and phosphate) ions (Fasbender et al 1997). The size of cationic polymer and the ratio of polymer to adenovirus have been shown to affect the property of the complexes and resulting infection efficiency (Fasbender et al 1997) and an optimal ratio of lipofectamine to adenoviral particles was established (Figure 5.10).

Other more sophisticated methods have been used to specifically target adenovirus to HUVECs, including bispecific antibodies binding the adenoviral fibre knob protein and epitopes on HUVECs (Nettelbeck et al 2001; Nicklin et al 2000). These elegant approaches may have particular application where specific targeting is necessary or desired *in vivo*.

However precomplexing with lipofectamine proved to be a cheap, simple and effective method for facilitating adenoviral gene transfer *in vitro* and was therefore used in the rest of the studies.

5.3.2. Ad-elafin and Ad-mSLPI reduce inflammatory cytokine production in response to atherogenic stimuli by HUVECs and macrophages.

The mechanisms driving atherosclerotic plaque development have been underpinned by *in vitro* studies demonstrating the inflammatory actions of oxidised LDL on intimal cells (Claise et al 1996; Lei et al 2002). A possible contribution from infectious agents or bacterial components such as LPS has been suggested by detection of *Chlamydia pneumoniae* (Kuo et al 1993b; Kuo et al 1993a) and

193

Chapter 5

increased expression of the LPS receptor Toll like receptor-4 (Vink et al 2002), in atherosclerotic specimens. These results are in agreement with the observation that atheroma formation is accelerated in atheroma prone rabbits treated with LPS (Lehr et al 2001).

Endothelial cells demonstrate increased chemokine expression during plaque development (Koch et al 1993; Simonini et al 2000) and macrophages are the predominant cell of the mononuclear cell infiltrate. Murine models of atheroma have exemplified the importance of chemokine expression in atherogenesis. Indeed, atherosclerosis susceptible, LDL receptor-deficient mice that were irradiated and repopulated with marrow cells lacking the neutrophil chemokine receptor CXCR-2, had reduced atheroma (Boisvert et al 1998). This body of data directed the study towards endothelial cell chemokine production in response to oxidised LDL, TNF-α and LPS. In accordance with previously published work (Claise et al 1996; Roebuck 1999), all three stimuli increased production of the neutrophil chemokine IL-8 in endothelial cells (Figure 5.12A).

The effects of overexpression of elafin, its homologue mSLPI, previously shown to inhibit LPS (Jin et al 1997; Zhu et al 1999) and IκBα were compared in HUVECs, macrophages and A549 cells. Adenoviral infection alone did not induce inflammatory cytokine production. Ad-elafin and Ad-mSLPI along with Ad-IκBα significantly reduced basal cytokine production in HUVECs (Figure 5.12B) whereas only Ad-IκB reduced basal cytokine release in macrophages (Figure 5.13B) and A549 cells (Figure 5.14B). Control vectors had no significant effect on basal cytokine production in any of the cell types. This result conflicts with work that has demonstrated inflammatory activation and TNF-α production following adenoviral delivery in macrophages (Zsengeller et al 2000). There are several explanations for this discrepancy. The macrophage cell type used was a cell line (RAW264.7), TNF-α production was observed very early after infection (2 hours) and the method of infection used virus alone giving very low infection efficiency (Zsengeller et al

194

Chapter 5

2000). The precomplexing protocol used in this thesis involved changing the medium after a 2-hour incubation with the virus and this would cause early TNF-α production to be missed. Adenoviral vectors carrying different genes were employed. Empty viral vectors and a vector expressing a secreted protein (Ad-meotaxin) may be non-inflammatory compared to Ad-βGal which leads to expression and intracellular accumulation of β galactosidase. Finally the studies differed in the method of adenovirus delivery. Foxwell et al (1998) used recombinant GM-CSF treatment of macrophages to increase expression of αV integrin co-receptors and observed no excess basal TNF-α production in control vector cells, although again, this study examined a later time point to that of Zsengeller et al (2000).

The question of inflammatory cytokine production in response to adenovirus is important with respect to controlling safety and immune mediated inhibition of adenoviral vectors and their transgenes. TNF-α is detected shortly after administration of both wild type virus and defective vectors to mice (Ginsberg et al 1991). Interaction of adenovirus penton base with the plasma membrane and cellular integrins leads to mitogen activated protein kinase activation and NF-κB mediated IL-8 production as early as 20 minutes post-infection (Bruder et al 1997). In wild type viruses, viral gene products from the E1 and E3 regions (the regions deleted in the adenoviral vectors used in this thesis) modulate cell defence mechanisms including NF-κB activation and TNF-α induced apoptosis (Russell 2000). E1A gene product from wild type adenovirus can bind to the p65 subunit of NF-κB leading to activation (Pahl et al 1996). The interplay between cellular proteins and (wild type) viral gene products seeking to control cell survival and viral propagation is more complex. E1A proteins may stimulate apoptosis by increasing production and inhibiting proteosomal degradation of the key apoptotic factor p53 (Hale et al 1999). By contrast, gene products from E1B 19K can inactivate members of the family of pro-apoptotic proteins that interact with mitochondria and are involved in caspase induction (Han et al 1996). Reduced *Bax* activity has also been postulated as a mechanism of enhanced survival of cultured human endothelial cells following infection with an E1 deleted replication deficient vector similar to the vectors used in

195

this thesis although the mechanism was not described (Ramalingam et al 1999a). These *in vitro* observations indicate that the outcome of adenoviral infection on cell cytokine production and survival will depend on multiple (non-viral) factors including cell type, stage of cell cycle and the signalling environment e.g. presence of TNF-α or interferon γ produced as part of the immune response to virus *in vivo*. The latter statement is supported by the demonstration of altered signalling and calcium regulated cytoskeletal protein gene expression in HUVECs but not in human dermal fibroblasts or alveolar macrophages (Ramalingam et al 1999b).

Through facilitating adenoviral delivery by an alternative pathway that does not result in increased basal cytokine production, lipofectamine precomplexing provides the additional benefit of reducing the immune response to adenoviral vectors.

In HUVECs, Ad-elafin and Ad-mSLPI significantly reduced IL-8 in response to TNF-α, LPS and oxidised LDL (Figure 5.12C-E). Macrophage TNF-α production in response to LPS was chosen as a model macrophage inflammatory response (Figure 5.13A) and overexpression of elafin, mSLPI and IκBα significantly reduced TNF-α production in response to LPS stimulation (Figure 5.13C-E). The magnitudes of effect for both elafin and mSLPI were impressive compared to IκBα, a model inhibitor of cytokine activation. There was a non-significant trend towards higher degrees of TNF-α inhibition with mSLPI (Figure 5.13C).

mSLPI's antagonistic action on LPS signalling was first identified using differential display to compare two murine macrophage cell lines, one of which (C3H/HeJ) demonstrated hyporesponsiveness to LPS. Transfection with SLPI converted macrophages from an LPS sensitive to LPS hyporesponsive phenotype (Jin et al 1997). Subsequent work demonstrated that whereas transfection of a non-

196

secretory form of mSLPI into HeNC2 macrophages conferred protection form LPS induced TNF-α production, addition of recombinant protein to the culture medium had no inhibitory effect (Zhu et al 1999). Transfection of human cells with mSLPI has not previously been performed although shortly after the original report by Jin et al (1997), human peripheral blood monocytes cultured with exogenous human SLPI were shown to have suppressed production of monocyte prostaglandin H synthase-2 and matrix metalloproteases 1 and 9 but not TNF-α in response to LPS (Zhang et al 1997). Although SLPI has been shown to bind to LPS (Ding et al 1999), SLPI-containing medium is unable to transfer LPS-inhibiting activity to fresh cells, (Dr J McMichael, from our laboratory, unpublished data) suggesting that extracellular SLPI may not be able to interfere with LPS signalling. The different actions of intracellular and extracellular SLPI will be discussed further in the following section

In addition to confirming the previously known anti-LPS activity of mSLPI these data establish for the first time the broad ranging antagonism of both elafin and mSLPI against different stimuli suggesting a general role in dampening inflammation.

Notably, Ad-elafin and Ad-mSLPI had no inhibitory effect on basal or LPS induced IL-8 production by lung A549 epithelial cells, however, Ad-IκBα was inhibitory (Figures 5.14B,C), possibly reflecting a cellular or organ specific action for these antiproteases. Indeed, recent work from our group has demonstrated enhanced neutrophil migration and a trend towards increased chemokine production in murine lungs receiving Ad-elafin prior to LPS exposure (Simpson et al 2001a). One investigative line under development is the possibility that elafin may modulate inflammation differently on endothelial and epithelial surfaces, priming murine lung innate immune responses following an intra-tracheal LPS challenge (Sallenave et al 2003).

197

Chapter 5

5.3.3. Mechanism of anti-inflammatory actions of Ad-elafin and Ad-mSLPI

Both IL-8 and TNF-α production are dependent on NF-κB regulated transcription (Foxwell et al 1998; Mukaida et al 1994). An effect across 2 different cell types against several different stimuli suggested an intracellular mode of action. NF-κB activity is increased within the intimal cells of human plaques and is a possible therapeutic target regulating the expression of many proatherogenic genes (Brand et al 1996). Oxidised LDL increases endothelial cell production of reactive oxygen species and activates NF-κB through interaction with the LOX-1 scavenger receptor (Cominacini et al 2000). Oxidised LDL, LPS and TNF-α stimulation were associated with increased activity of the pro-inflammatory transcription factor in HUVECs (Figures 5.15, 5.16) (Hawiger et al 1999; Zen et al 1998). Following Ad-elafin and Ad-mSLPI infection, NF-κB activity was reduced in LPS (Figure 5.15), oxidised LDL (Figure 5.16A) and TNF-α stimulated HUVECs (Figure 5.16B). This provides evidence for an inhibitory effect prior to or at the level of gene transcription for these stimuli. Ad-elafin and Ad-mSLPI also reduced LPS induced macrophage NF-κB activation in accordance with their inhibitory action on production of the NF-κB regulated pro-inflammatory cytokine TNF-α (Figure 5.17). Ad-IκB was a potent inhibitor of NF-κB activation in endothelial cells and macrophages against all stimuli.

Chapter 5
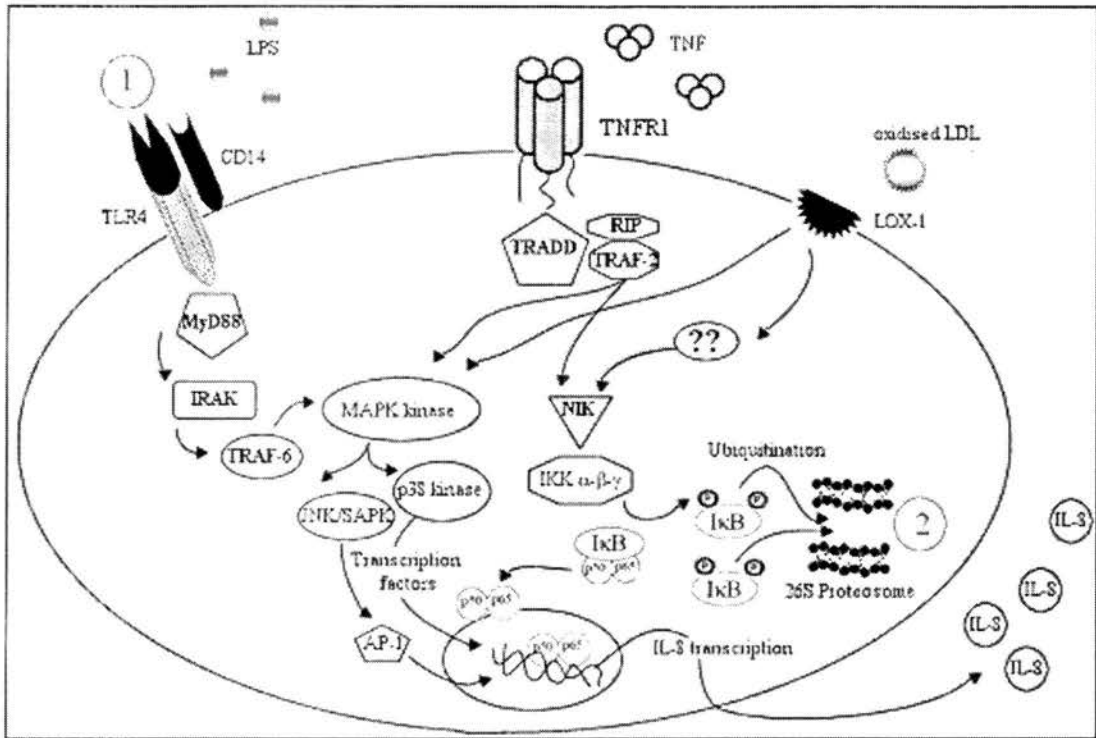
Figure 5.19. Elafin and mSLPI modulate inflammatory signalling by TNF-α, oxidised LDL and LPS.

Key to Figure 5.19. IRAK: Interleukin-1 receptor associated protein kinase. TRAF: tumour necrosis factor receptor associated factors. NIK: NF-κB inducing kinase. MAPK: mitogen activated protein kinases. LOX-1: lectin like oxidised LDL receptor-1 (endothelial cells). TLR4: Toll-like receptor-4. MyD88: myeloid differentiation protein 88. TNFR1: TNF-α receptor type-1. TRADD: TNF receptor-associated death domain protein. RIP: receptor interacting protein. MAPK kinase: mitogen activated protein kinase kinase. IKK: IκB kinase complex consisting of α, β and γ subunits. JNK/SAPK: c-Jun N-terminal kinase/stress activated protein kinase. ??: question marks are used to indicate that the signalling pathways linking oxidised LDL and scavenger receptors to NF-κB have not been identified. This figure was compiled from reviews by (Collins et al 2001) and (Ledgerwood et al 1999)

199

Chapter 5

Figure 5.19. Elafin and mSLPI modulate inflammatory signalling by TNF-α, oxidised LDL and LPS.

Schematic diagram of signalling pathways for oxidised LDL, TNF-α and LPS in endothelial cells leading to transcription factor activation and gene transcription. Potential points where elafin and mSLPI may interact with these pathways are numbered.

Binding of LPS to CD14 leads to association of CD14 with TLR4. Signalling depends on interaction of the intracellular TLR domain with adapter proteins including MyD88. IRAK is phosphorylated and associates with TRAF-6, leading to activation of MAP kinases (p38 and JNK) and IKK. To induce NF-κB activation, IKKs phosphorylate the inhibitory subunit (bound to inactive NF-κB) at its serine residues. This 'targets' IκB for ubiquitination at lysine residues. The polyubiquitinated IκB subunit is then degraded by the 26S proteosome and the active NF-κB p65-p50 heterodimer is free to translocate to the nucleus and initiate transcription. TNF-α signalling, similarly depends on interaction of the intracellular domain of the active TNFR1 with the adapter proteins TRADD. TRAF-2 and RIP are two proteins recruited to the TNFR-1-TRADD complex. This coupling facilitates p38 kinase, JNK and IKK activation. TNFR1 also transduces an apoptotic signal (not shown) depending on the signalling context (other stimuli and the status of the cell). Oxidised LDL binding to LOX-1 is associated with NF-κB and p38 MAPK activation in endothelial cells although the mechanism of LOX-1 intracellular transduction has not been elicited.

The points where elafin and mSLPI may be acting to inhibit signal transduction and cytokine production are shown. The possibilities of an extracellular action (1) or inhibition of protease subunits within the proteosomal machinery (2) are discussed in the text.

Chapter 5

In contrast to their effects in relation to IκBα with respect to cytokine inhibition, elafin and mSLPI were relatively weak inhibitors of NF-κB activation. The inhibitory action was lost with higher doses of LPS and TNF-α (Figures 5.15 and 5.16). Other transcription factors are involved in the regulation of IL-8 transcription and the findings presented here do not exclude the possibility that elafin and mSLPI may interfere with more than one signalling pathway. IL-8 promoter activity is regulated by differential activation and binding of activator protein-1 (AP-1), nuclear factor IL-6 (NF-IL6) and NF-κB (Roebuck 1999). Activator protein-1 (AP-1) is a transcription factor composed of either Jun-Fos heterodimers or Jun-Jun homodimers (Smeal et al 1989) that has been shown to contribute to IL-8 promoter activity in human bronchial epithelial cells (Nakamura et al 1991). AP-1 may interact synergistically with NF-κB (Stein et al 1993) or members of the cyclic AMP response element-binding (CREB) and activating transcription factor-1 (ATF-1) transcription factor families (Rabbi et al 1997) to heighten IL-8 gene expression (Yasumoto et al 1992). Recently, a further transcription factor, signal transducer and activator of transcription 3 (STAT3), was found to act co-operatively with c-src kinase to induce IL-8 transcription in human aortic endothelial cells in response to an oxidised phospholipid component of oxidised LDL (Yeh et al 2004).

The involvement of more than one transcriptional pathway may explain the discrepancy between the magnitude of cytokine and NF-κB inhibition observed following overexpression of elafin and mSLPI. Absolute inhibition of NF-κB activation would be undesirable, rendering the cell vulnerable to apoptotic death (Barkett et al 1999). The latter property may be beneficial by providing a brake against cytokine production rather than complete inhibition. The mechanism of NF-κB inhibition was further studied by Western Blot analysis, which demonstrated that Ad-elafin and Ad-mSLPI reduced TNF-α and LPS induced IκBα degradation (Figure 5.18). In macrophages, IκBα protein content was highest in the Ad-IκBα infected cells (Figure 5.18) mirroring the EMSA results which showed that IκBα was most efficient at down-regulating NF-κB activity (Figure 5.17). By contrast,

201

HUVEC IκBα levels following Ad-IκBα infection were comparable to those following Ad-elafin and Ad-mSLPI infection (Figure 5.18) despite Ad-IκBα being more effective at suppressing NF-κB activation in response to TNF-α (Figure 5.16B, upper panel). Samples for IκBα immunoblots and NF-κB EMSAs were taken at 10 min and 1 h respectively and it is possible that the difference in magnitude between elafin and mSLPI's inhibitory effect on NF-κB and preserving action on IκBα in HUVECs related to different time points in this cell type. Elafin and mSLPI may have different actions on the various NF-κB inhibitory subunits and further studies of IκBβ levels would be helpful (Lentsch et al 1999a, see below).

Consistent with its inhibitory activity on NF-κB demonstrated in the present work, murine SLPI knockout macrophages demonstrate sustained increases in NF-κB activation following LPS stimulation (Ashcroft et al 2000). Accordingly, Lentsch et al (1999a) demonstrated that inhibition of NF-κB activity in a rat immune complex lung injury model, following administration of human SLPI, was associated with increased levels of the IκBβ inhibitory subunit (but not IκBα) in lung homogenates. In that model, mutated human SLPI sequences coding for proteins that lack trypsin inhibitory activity failed to inhibit NF-κB activation (Mulligan et al 2000). More recently, after completion of the work presented in this chapter, human SLPI was demonstrated to reduce NF-κB activation in the human myelomonocytic U937 cell line in response to LPS when added to the extracellular medium (Taggart et al 2002). The anti-inflammatory activity against LPS was associated with protection from LPS induced degradation of interleukin-1 receptor associated kinase (IRAK), IκBα and IκBβ and importantly, was shown to be inhibited by proteasome inhibitors.

Taken together these findings strongly suggest that mSLPI and by inference, elafin inhibit NF-κB activation through an intracellular action involving protection of the IκBα (and possibly IκBβ) from proteolytic degradation. Possible sites of action are illustrated in Figure 5.19. Inhibitor studies have implicated serine proteases in

202

Chapter 5

IκB degradation (Henkel et al 1993). The observation that oxidative inactivation of SLPI's antiprotease activity (Taggart et al 2002) disables its ability to protect against IκB degradation is in agreement with previous observations by Mulligan et al (2000) indicating that the mechanism requires intact protease inhibitory activity. Exogenous serine protease inhibitors have previously been shown to block NF-κB activation through inhibition of proteosomal proteases (Jobin et al 1999) and recently the serine protease inhibitor antithrombin III was shown to block NF-κB activation in response to LPS (Mansell et al 2001).

The findings presented in this chapter identify elafin as an inhibitor of NF-κB activation and add to the literature demonstrating a similar role for the closely related protein mSLPI. Inhibition of cytokine production was more striking than the sole suppression of NF-κB activation (particularly for TNF-α stimulation in HUVECs: Figures 5.12 and 5.16B). As discussed earlier it is important to underline that the results do not exclude elafin and mSLPI interference with parallel pro-inflammatory signalling pathways, a possibility not addressed in the current work.

5.3.4. Elafin and mSLPI are homologous proteins sharing broad innate immunity roles and exhibiting potential as gene therapy targets for atherosclerosis.

In conclusion, the work in this chapter has demonstrated that Ad-elafin and Ad-mSLPI block pro-inflammatory signalling in both endothelial cells and macrophages and can, through NF-κB inhibition, attenuate inflammatory responses to LPS, TNF-α and oxidised LDL.

Several important questions are worthy of further study. Firstly, where is (are) the exact molecular site(s) of action of elafin and mSLPI? Several lines of evidence currently point to an intracellular location of SLPI as a prerequisite for cytokine blockade and inhibitory activity against a wide range of stimuli in the current work

203

Chapter 5

supports this view. NF-κB blockade has also been demonstrated following addition of exogenous SLPI (Lentsch et al 1999a; Lentsch et al 1999b; Taggart et al 2002). In *Drosophila*, LPS signalling involves an extracellular serine protease cascade that is kept in check by serine protease inhibitors (Morisato et al 1994). There is no evidence that such a cascade in mammals exists although Mansell et al (2001) concluded that this was a possibility after observing inhibition of NF-κB activation by LPS with antithrombin III. These data are partly reconciled by the fact that SLPI demonstrates cell membrane binding (McNeely et al 1997; Tseng et al 2000) and may therefore be able to translocate across to the cytosol although no such binding has been demonstrated for elafin. In human neutrophils, the majority of SLPI resides in an active form within the cytoplasm (not within granules or a microsomal subfraction) where there is clear potential for interaction with intracellular proteases (Sallenave et al 1997).

Secondly, the extent to which NF-κB inhibition contributes to the innate immunity role of endogenous elafin and SLPI is not known. The concept of secreted serine protease inhibitors having direct influence on intracellular signalling pathways is entirely novel and would require a reappraisal of their roles. Another secreted microbicidal peptide with no sequence homology to elafin and SLPI, PR-39, has recently been shown to inhibit TNF-α induced IκBα degradation by the proteosomal pathway by binding to the α7 subunit of the 26 S proteasome (Gao et al 2000). Together elafin and SLPI form a paradigm, working as effectors of innate immunity to protect tissues against maladaptive inflammatory responses. Their regulation and multifaceted properties would make them ideal response molecules for checking inflammation. They are up regulated by inflammatory stimuli (TNF-α and IL-1β) and in addition to protease inhibition they both exhibit direct microbicidal activity (Sallenave 2000).

Finally, these data indicate the suitability of elafin and SLPI as therapeutic molecules for the treatment of atherosclerosis. Elafin is present within atherosclerotic

204

Chapter 5

tissue (Sumi et al 2002a) and may therefore have a role in checking endogenous arterial wall inflammation. Although SLPI is produced by macrophages its role within atheroma has not yet been characterised. The potential to focus the inflammation damping properties of these peptides on atherosclerotic tissue through gene therapy is attractive and certainly worthy of further study.

205

Chapter 5

Chapter 6

Gene delivery of elafin reduces HNE mediated endothelial cell injury and protects macrophages from HNE mediated impairment of apoptotic cell recognition.

6.1. Aims

The preceding chapter characterised the antinflammatory role for elafin and murine SLPI against a range of atherogenic stimuli. Elafin was initially characterised as a potent and specific inhibitor of both proteinase 3 and human neutrophil elastase (HNE) (Sallenave et al 1991; Wiedow et al 1990) and SLPI has a broader range of antiprotease activity including HNE, trypsin and chymotrypsin (Fink et al 1986; Ohlsson et al 1976).

Until recently, neutrophils and their granule derived proteases were not considered to play a prominent role in the development of atherosclerosis. The demonstration of elafin within atherosclerotic plaques (Sumi et al 2002a) was surprising given its strong association in the literature with the neutralisation of HNE in acute inflammatory processes not believed to be occurring within atheroma. Recent reports have demonstrated evidence of neutrophil activation and degranulation in patients with advanced atheroma and acute coronary syndromes (Buffon et al 2002). Intriguingly, several neutrophil derived proteins have already been demonstrated within atherosclerotic tissue and one of these, myeloperoxidase, may mediate oxidative modification of low density lipoprotein (Daugherty et al 1994). Professor Libby's group recently extended these findings, demonstrating HNE

206

in both fibrous and atheromatous plaques but not normal coronary arteries (Dollery et al 2003).

The aim of this chapter is to characterise the effects of HNE on the inflammatory responses of human endothelial cells and macrophages. HNE is rapidly inactivated by antiproteases including antitrypsin and macroglobulin contained within the serum used to culture endothelial cells and macrophages (Travis et al 1983). The work in this chapter, examining HNE's actions, was therefore conducted in serum-free conditions. That HNE can similarly function within the atherosclerotic plaque in a microenvironment devoid of neutralising antiproteases is a central assumption underlying the experiments. Myeloperoxidase catalyses inactivation of protease inhibitors including antitrypsin in the low pH microenvironment associated with neutrophil degranulation and inactivation of circulating and locally produced antiproteases is one mechanism whereby HNE activity may persist (Shock et al 1988).

The effect of different concentrations of HNE on the integrity of endothelial monolayers was examined. A further aim was to examine to what degree adenoviral mediated over-expression of elafin could protect endothelial cells and macrophages from HNE injury.

At high concentrations, HNE has been shown to have cytopathic effects on epithelial cells with lower concentrations signalling inflammatory cytokine production (Sallenave et al 1994; Simpson et al 2001b; Walsh et al 2001). The importance of inflammatory activation of endothelial cells with respect to the initiation and progression of atheroma has been emphasised in earlier chapters. Endothelial cell death may also contribute to both development and complications of atheroma (Stoneman et al 2004). Loss of endothelium or denudation exposes a thrombogenic surface (Davies 1994). Factors including HNE that facilitate loosening

207

Chapter 6

of endothelial cell-matrix attachments or endothelial cell death would be expected to contribute to this process.

The work in this chapter confirms previously published observations that monocytes and macrophages remain intact at HNE concentrations that cause detachment and necrosis of epithelial cells and endothelial cells *in vitro* (Le Barillec et al 1999b; Smedly et al 1986). HNE alters monocyte function in a more subtle fashion by cleaving surface receptors responsible for recognition of bacterial lipopolysaccharide (Le Barillec et al 1999) and macrophage recognition of apoptotic cells (Vandivier et al 2002) prior to phagocytic engulfment. The resulting functionally impaired macrophage is unable to mount an inflammatory cytokine response to LPS or clear apoptotic cells from sites of inflammation. HNE is a potent protease cleaving a range of surface receptors and extracellular proteins. The degree to which this enzyme modulates macrophage function within the atherosclerotic plaque is unknown although Dollery et al (2002) have indicated that HNE co-localises and may indeed originate from macrophages in the vulnerable shoulder regions of the plaque prone to rupture.

Work within our own group had already demonstrated the protective effects of both recombinant elafin and adenovirus mediated overexpression of elafin on HNE injury to epithelial monolayers (Simpson et al 2001b). The concept of a protease-antiprotease balance within atherosclerotic plaques has previously been evoked as a mechanism underlying the stability of the shoulder regions of plaques containing a necrotic lipid core (Watanabe et al 2004). Given their presence together within the atherosclerotic plaque, it was important to explore the possibility that elafin provided protection from HNE injury to endothelial cells.

Similarly, apoptotic cell recognition was studied with respect to HNE modulation of macrophage function. Apoptotic cell clearance, in particular, is a central mechanism in the resolution of inflammation (Savill et al 2002) and

208

Chapter 6

impairment of apoptotic cell recognition is a feature of chronic inflammatory pathologies such as cystic fibrosis and chronic obstructive airways disease (Hodge et al 2003; Vandivier et al 2002). The technique of efficient adenoviral gene delivery to macrophages described in chapter 5 was employed to discover whether elafin overexpression could prevent HNE impairment of phagocytic function.

6.2. Results

6.2.1. The effect of Ad-elafin on HNE mediated endothelial cell injury.

HNE produced rounding and lifting of endothelial cells following incubations for 8 hours in serum-free medium (Figure 6.1). The work in chapter 5 demonstrates that Ad-elafin infection in conjunction with lipofectamine generates high concentrations of elafin from HUVECs. Ad-elafin reduced the cytopathic changes in response to HNE when compared to Ad-dl703 and Ad-GFP (Figure 6.1). These adenoviruses were included to demonstrate the specificity of effect for Ad-elafin. Ad-GFP was used in this experiment specifically to visualise both infection efficiency and cell damage following HNE injury. Increasing concentrations of HNE were associated with a decline in viable cell numbers measured by MTS assay (Figure 6.2). Similarly, prolonged incubations with increasing HNE concentrations led to increased LDH release into HUVEC culture supernatants indicating cell lysis (Figure 6.3). HNE had no direct action on the tetrazolium colour indicator used in this assay (data not shown). Ad-elafin was significantly more effective than Ad-GFP or Ad-dl703 at preserving cell viability although both control viruses had significantly higher viable cell counts than uninfected cells (Figure 6.4) following HNE incubation.

HNE also increased endothelial cell IL-8 production during more prolonged incubations at lower concentrations that were associated with less cytopathy (Figure 6.5). The increases in IL-8 production were modest compared to LPS or other inflammatory stimuli (Figure 5.12A). In view of published reports indicating

209
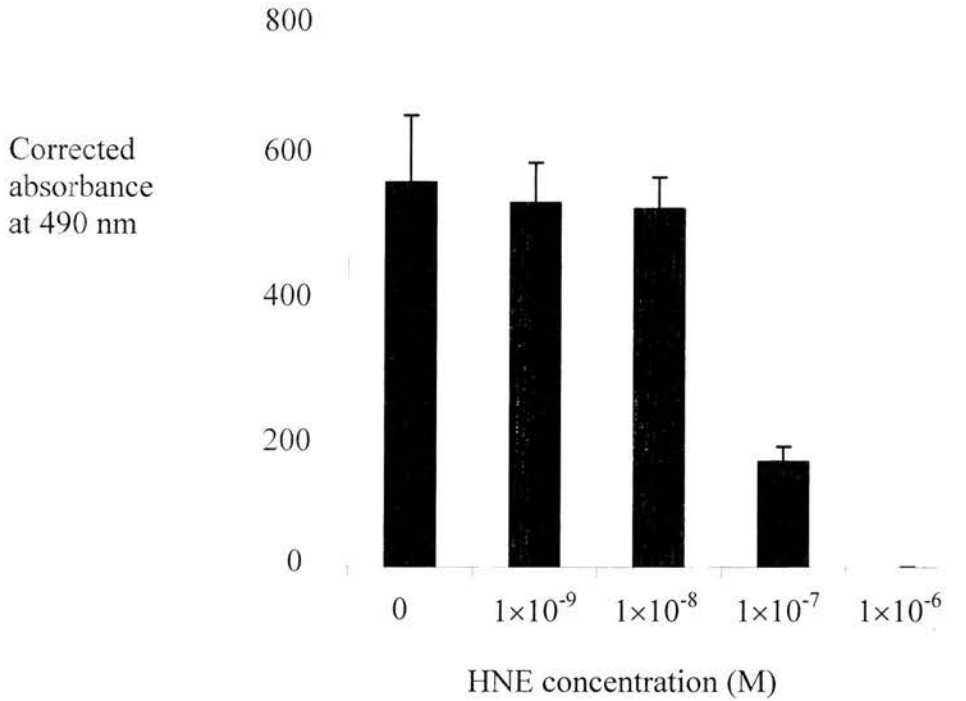
Figure 6.1. Incubation of endothelial cells with HNE led to a reduction in viable cell numbers measured by MTS assay.

HUVECS were cultured in 96-well plates in serum-free conditions and incubated with the concentration of HNE indicated for 24 h. Supernatants were removed following the incubation and 120 μl serum-free endothelial culture medium with 20 μl MTS Cell Titre reagent added according to the manufacturer's protocol. The MTS tetrazolium compound is reduced by cells into a coloured formazan product that is soluble in tissue culture medium. Production of the coloured agent can be measured directly by recording absorbance at 490 nm giving an indirect measure of viable cell number. Cells were incubated for 4 h and cell viability was determined from measuring the absorbance at 490 nm. The absorbance from wells containing only medium and MTS reagent was measured to provide a background for the corrected absorbance shown. Results are mean and standard deviation from one experiment performed in triplicate. Similar results were seen in two donors.

210
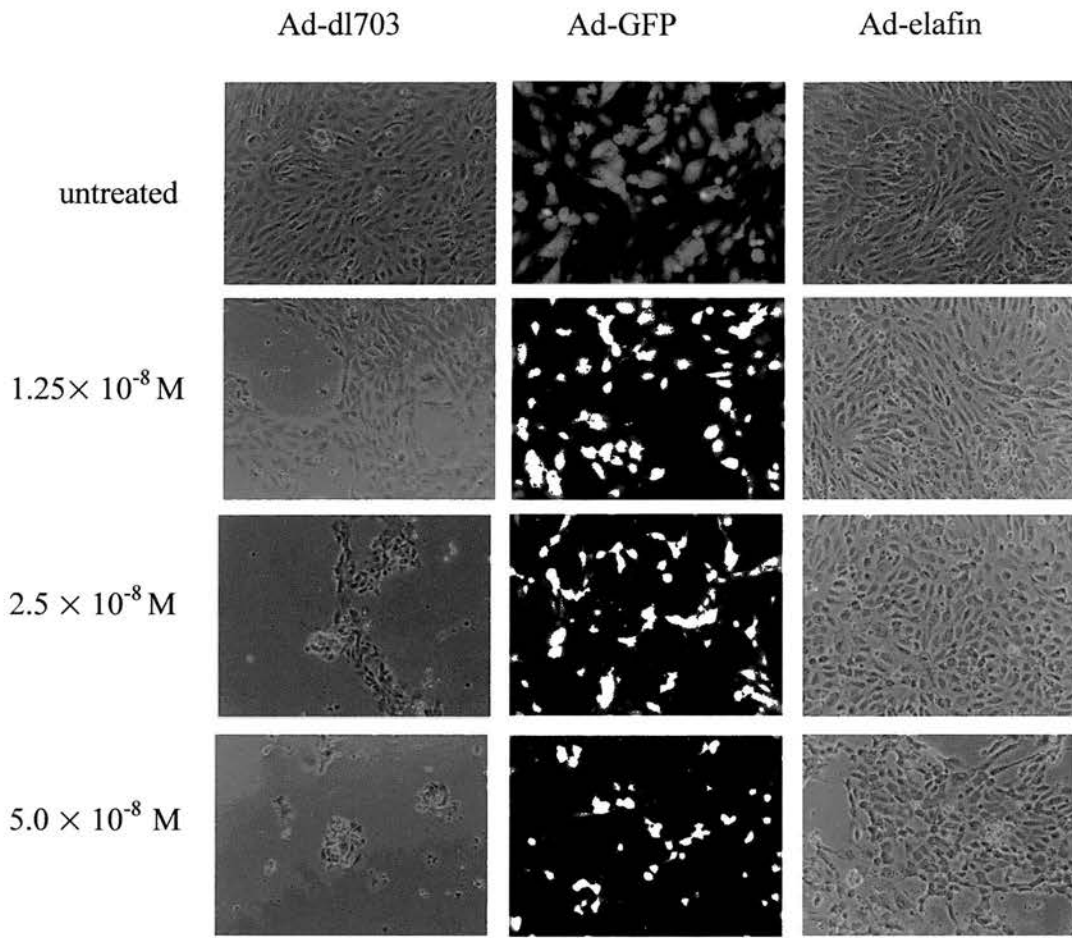
Chapter 6

Figure 6.2. Overexpression of elafin protects HUVEC monolayers against HNE damage

HUVECs were cultured and infected with Ad-dl703, Ad-elafin and Ad-GFP using the lipofectamine protocol outlined in chapter 5. All HNE treatments were performed 24 h after viral infection. Photomicrographs of Ad-dl703, Ad-GFP and Ad-elafin infected cells (all MOI 100), untreated and following incubation for 8 hours in serum-free medium with HNE at the concentrations shown. Appearances of uninfected cells were identical to Ad-dl703 infected cells (not shown).

211

Chapter 6
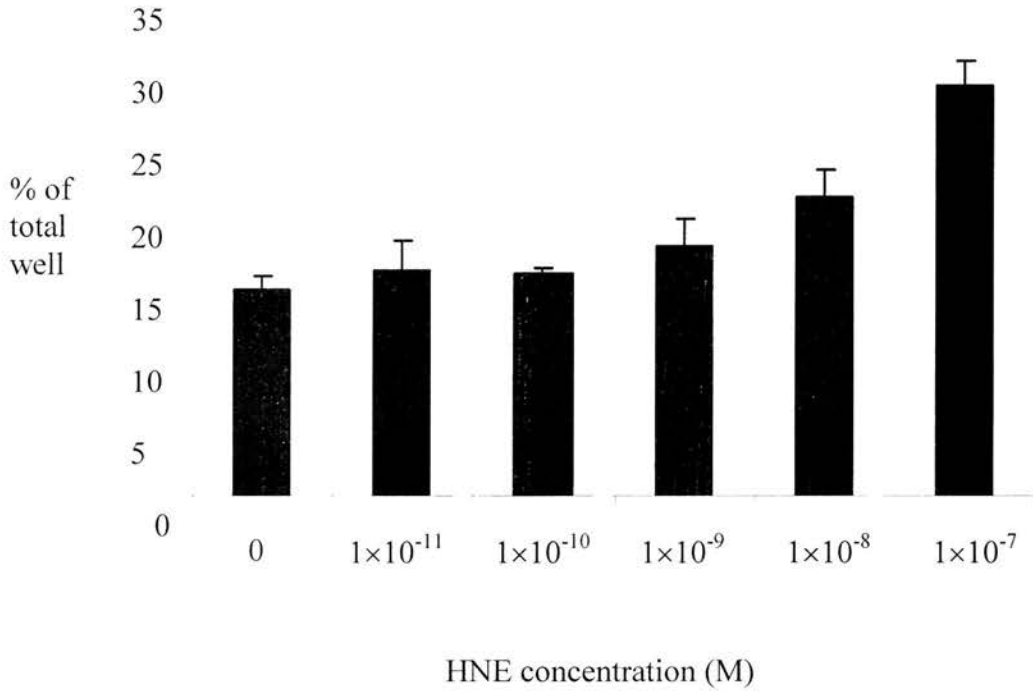
Figure 6.3. HNE induced release of cytosolic LDH into HUVEC culture supernatants is concentration dependent.

HUVECS were cultured in 96-well plates in serum-free conditions and incubated with the concentration of HNE indicated for 24 h. Supernatants were removed following the incubation and supernatant LDH activity was expressed (after correction for background within the culture medium) as a percentage of the activity resulting from total cell lysis produced using 1% Triton X-100. Results are mean and standard deviation from one experiment performed in triplicate.

212

Chapter 6
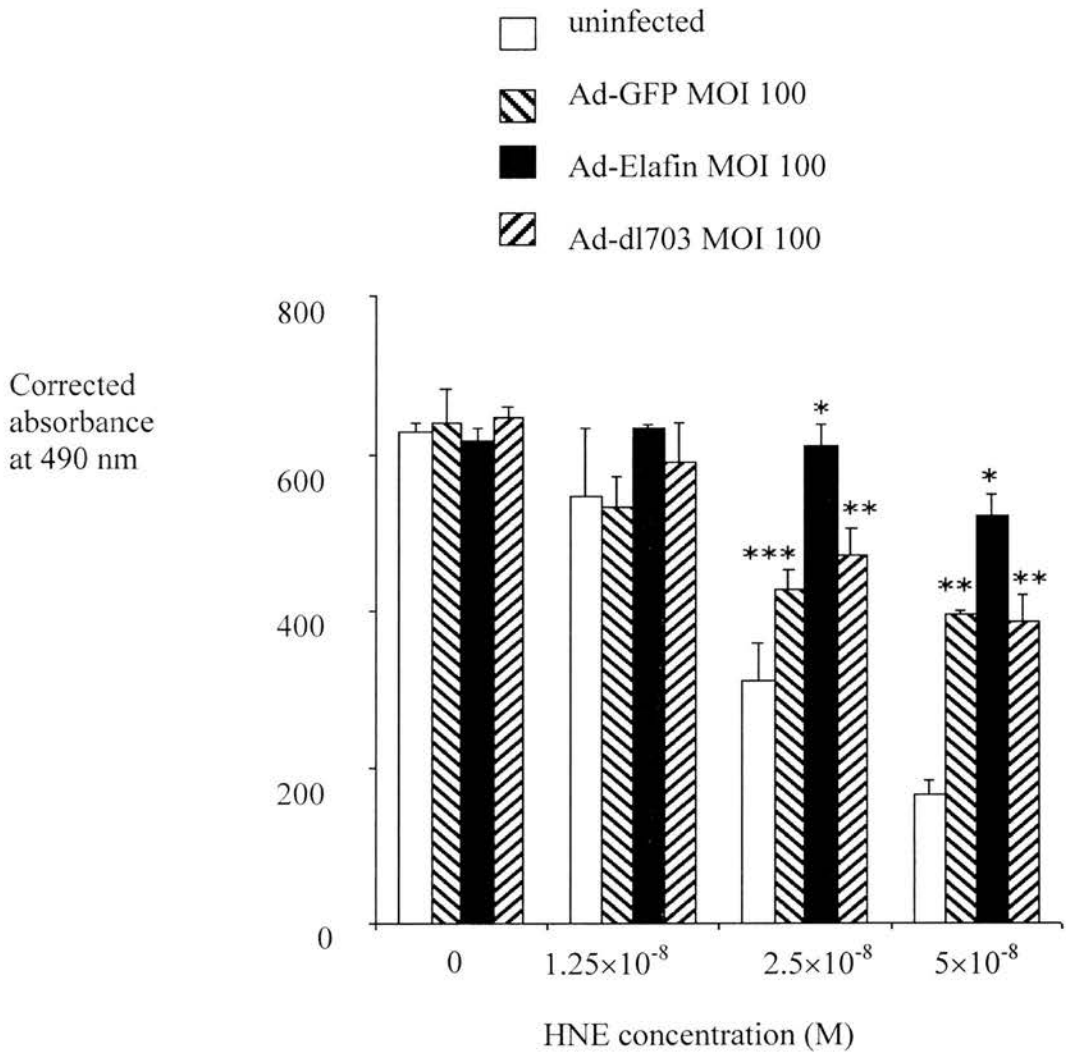
Figure 6.4. The effect of adenoviral overexpression of elafin on HNE mediated endothelial cell death.

Adenoviral infections were performed according to protocols outlined in figure 6.1 in 96-well plates. HNE incubations were set up and Cell Titre assays performed according to protocols in figure 6.2. Data are means and standard deviations of 2 experiments performed in triplicate. *, significantly higher than Ad-GFP and Ad-dl703, $p < 0.01$. **, significantly higher than uninfected cells, $p < 0.01$. ***, significantly higher than uninfected cells, $p < 0.05$.

213

Chapter 6

IL-8 pg/ml

HNE concentration (M)
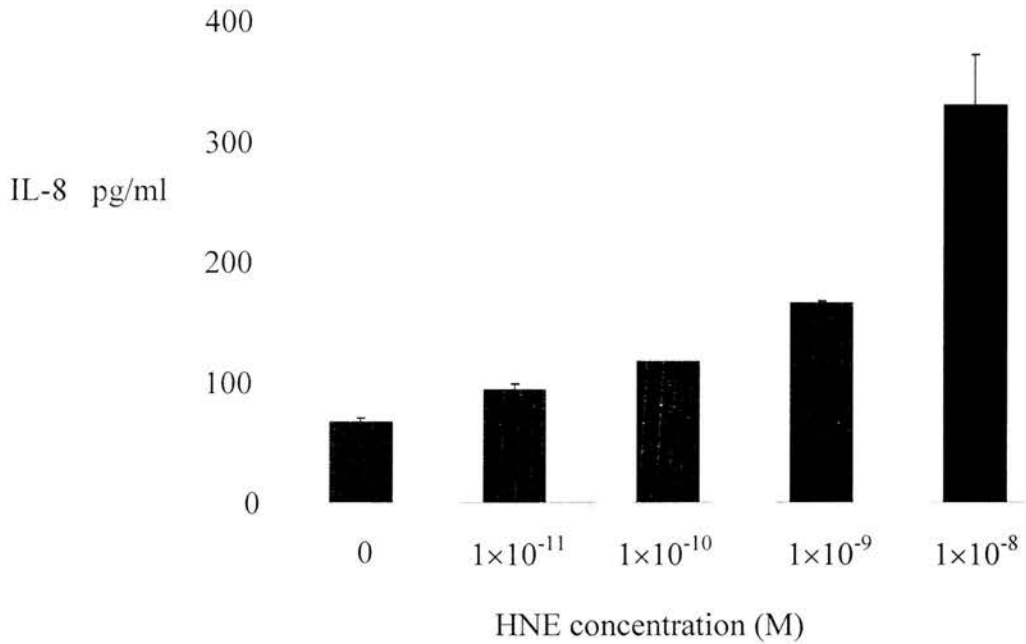
Figure 6.5. IL-8 release by endothelial cells in response to incubation with HNE.

HUVECS were cultured in 96-well plates in serum-free conditions and incubated with the concentration of HNE indicated for 24 h. Following incubation, supernatants were removed and analysed for IL-8 content. Results are mean and standard deviation form one experiment performed in triplicate.

214

HNE mediated disruption of surface receptors and because HNE has been demonstrated within atherosclerotic tissue, an experiment was devised to search for any interaction between HNE and other inflammatory stimuli including oxidised LDL, TNF-α and LPS. Because of the necessity to conduct HNE experiments in serum-free conditions, HUVECs were incubated with HNE for 1 hour after which serum-containing medium with the further stimulus was added.

Pre-incubation with HNE dramatically increased subsequent IL-8 release in response to LPS and oxidised LDL (Figure 6.6). The effect was greater than the summative effects of the individual stimuli (compare HNE alone and in combination with oxidised LDL or LPS; Figures 6.6A, 6.6B and 6.6C) and there appeared to be a dose effect for HNE with increasing preteatment doses leading to more IL-8 production in response to subsequent LPS or oxidised LDL. This suggested a positive interaction or synergy between HNE pretreatment and these two stimuli. In contrast, no such effect was observed for HNE pretreatment followed by TNF-α stimulation. The latter stimulus produced a massive IL-8 response from endothelial cells and this may have masked any effect from HNE pretreatment. Overexpression of elafin led to a significant reduction in IL-8 production in response to HNE, HNE and LPS in combination and, in agreement with results presented in chapter 5, in response to LPS alone (Figure 6.7). Ad-IκBα that was included as a positive control of cytokine inhibition reduced HUVEC IL-8 production in response to all three combinations of stimuli (Figure 6.7).

6.2.2. Experiments examining the effect of Ad-elafin on HNE modulation of macrophage function

HNE readily induced cytopathy and cell death in HUVECs and at lower concentrations it stimulated IL-8 production. Both actions could be attenuated by over-expression of elafin. In contrast, cultured macrophages were resistant to HNE cytopathy at concentrations that would cause immediate lysis of HUVECs in serum-

215

Chapter 6
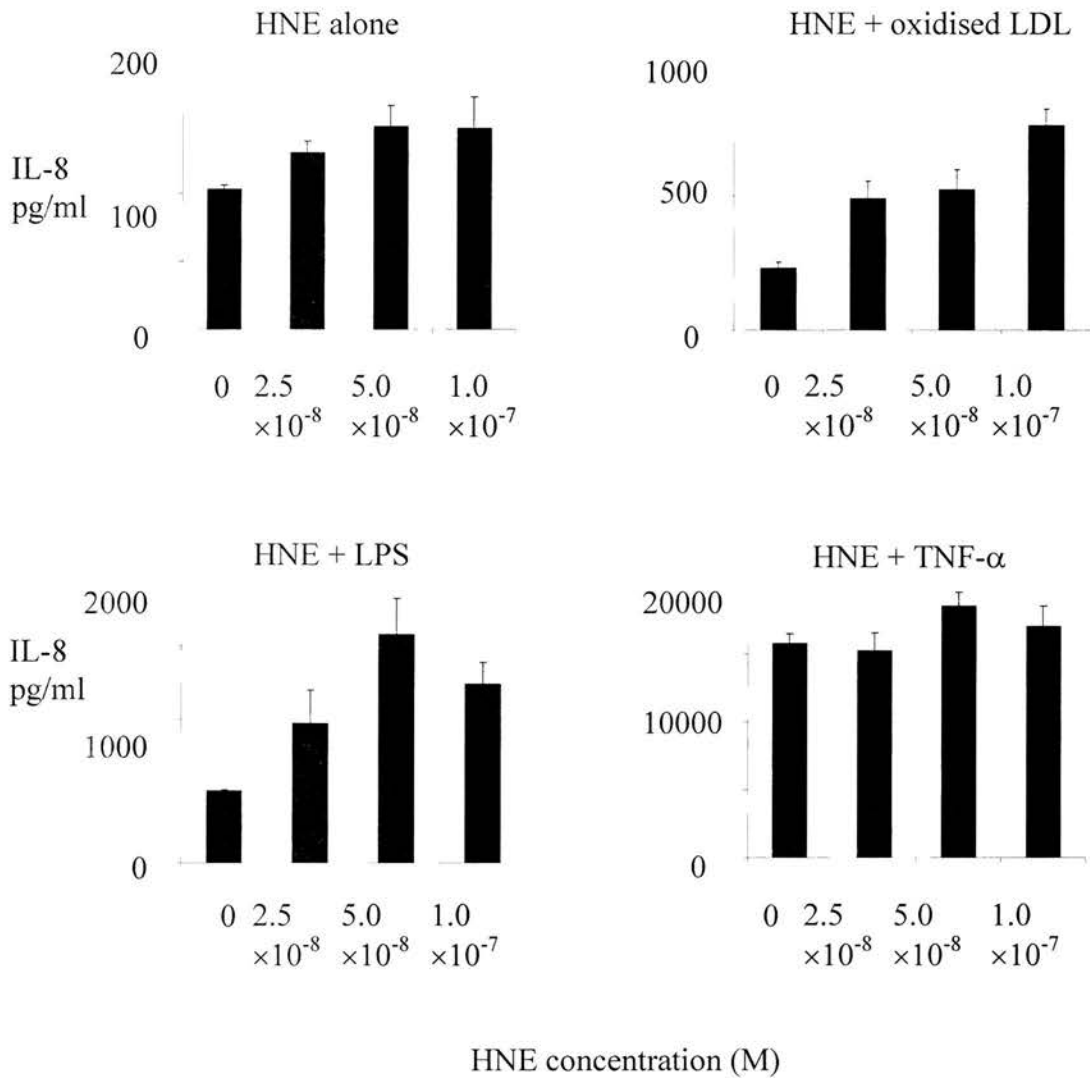
Figure 6.6. The effect of HNE pretreatment on endothelial cell IL-8 production in response to oxidised LDL, LPS and TNF-α.

HUVECs were incubated in serum-free medium with the concentration of HNE indicated for 1 h. Supernatants were removed and replaced with normal serum containing medium alone (HNE alone) or with oxidised LDL (100 µg/ml), LPS (100 ng/ml) and TNF-α (1 ng/ml) for 8 h before supernatants were removed for IL-8 quantification. Data are means and standard deviations from one experiment performed in triplicate.

216

Chapter 6
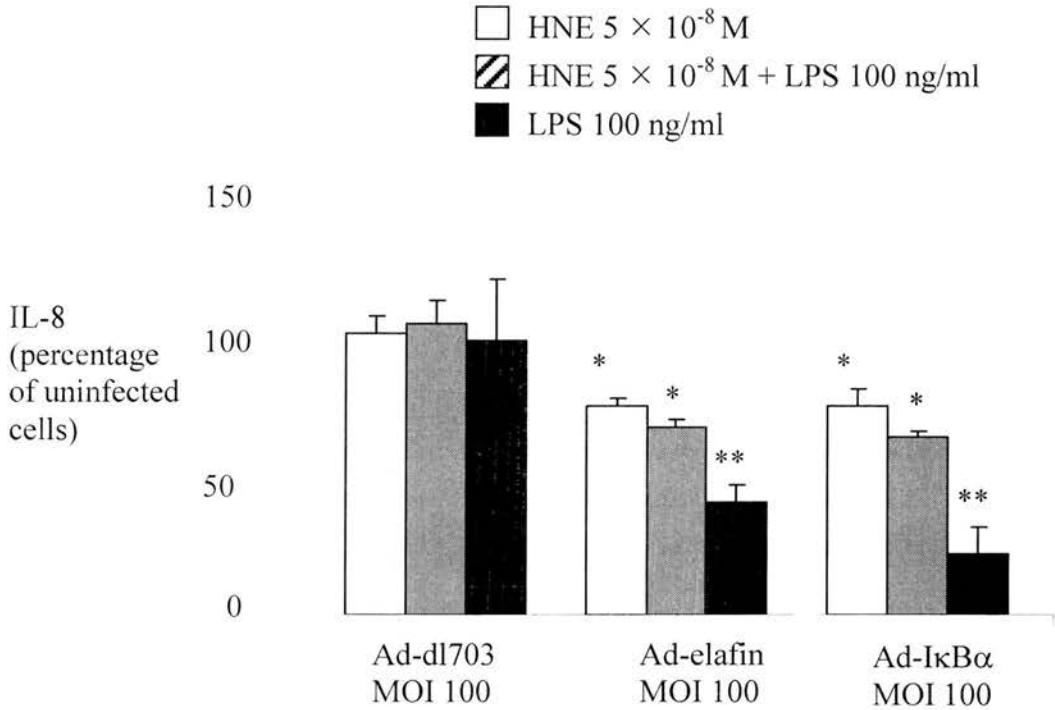
Figure 6.7. The effect of Ad-elafin on endothelial cell IL-8 production following pretreatment with HNE alone, HNE pretreatment in combination with LPS stimulation or LPS stimulation alone.

Adenoviral infections were performed according to the protocol in figure 6.1 and 24 h after infection HNE pretreatments, LPS stimulation and IL-8 assays were conducted as for figure 6.6. Results are means and standard deviation from 3 experiments performed in triplicate. IL-8 production is expressed as a percentage of production in uninfected cells (see Figure 6.6) *,** significantly lower than Ad-dl703 infected cells p< 0.01, p< 0.001.

217
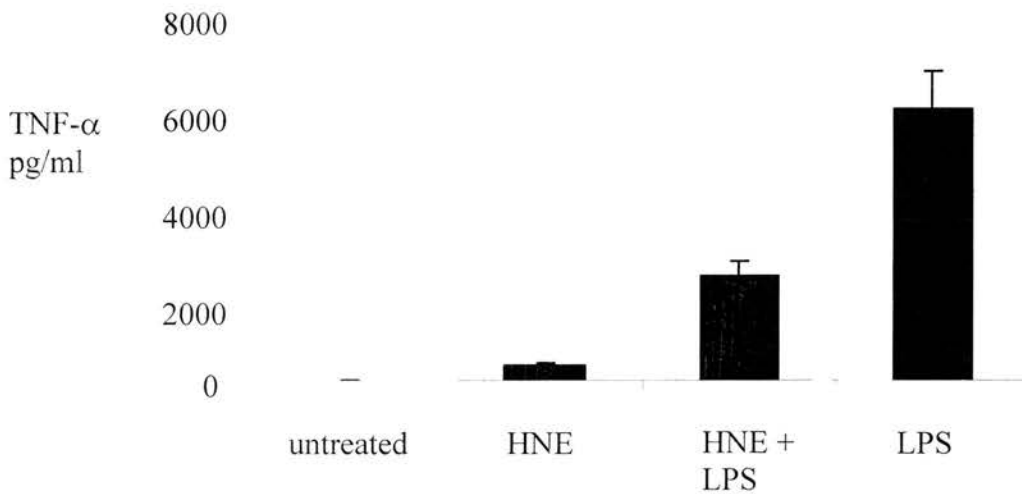
Figure 6.8. The effect of HNE on macrophage production of TNF-α.

Human peripheral blood monocytes were cultured in 6-well plates and matured into macrophages according to protocols described in the Materials and Methods chapter. On culture day 4 macrophages were detached with ice cold PBS and replated (30000 cells/ well) in 96-well plates with serum-free X-vivo 10 medium. Experiments were performed on culture day 7. HNE (1 μM) was added where indicated for 1 h after which culture supernatant was removed and 10% autologous serum-containing medium was introduced. Serum-free medium was also exchanged for serum containing medium in wells that did not receive HNE pretreatments. LPS (100 pg/ml) was added where indicated for a further 4 h and culture supernatants were removed for TNF-α quantification. Results are mean and standard deviation of an experiment from one donor performed in quadruplicate.

218

Chapter 6

free conditions (data not shown). Reports had demonstrated that monocyte responsiveness to HNE was reduced following incubation with HNE through a mechanism involving cleavage of the CD14 receptor (Le Barillec et al 1999). The responsiveness of macrophages to LPS as measured by TNF-α production was reduced following incubation with HNE (Figure 6.8). This result contrasted with HNE's facilitatory action on LPS induced cytokine production in endothelial cells. HNE acted as a weak stimulus for macrophage TNF-α production (Figure 6.8) in line with its effect on endothelial cell inflammatory cytokine production.

Dose finding pilot studies (data not shown) indicated that the minimum HNE concentration (1 µM) required to produce a detectable reduction in macrophage responsiveness after a 1 hour incubation was 100 fold stronger than the concentrations that led to heightened LPS responsiveness in HUVECs.

Flow cytometry for CD14 was performed to assess whether the reduced responsiveness to LPS was associated with disruption of the receptor. HNE reduced surface expression of CD14 (Figure 6.9) and overexpression of elafin significantly attenuated this effect compared to control Ad-dl703 infected cells or uninfected cells (Figure 6.10). This indicated that in addition to inhibiting LPS induced cytokine production in endothelial cells and macrophages (Chapter 5), elafin overexpression may preserve some aspects of CD14 signalling in the context of HNE injury. CD14 expression was not completely restored in elafin expressing macrophages incubated with HNE (mean 43% CD14 expression compared to 66% prior to HNE) following treatment (Figure 6.10E). When macrophages were infected with Ad-elafin/lipofectamine, elafin supernatant levels were increased from 10.4 (± 4.11) ng/ml with Ad-elafin alone to 232 (± 13.1) ng/ml (values are means and SDs derived form a representative experiment performed in triplicate). Elafin was not detected in the supernatant from uninfected cells. These levels of elafin production would not be expected to neutralise the high concentration of HNE used in this experiment. Assuming a molecular weight for elafin of 9.9 kDa, the concentrations of elafin

219
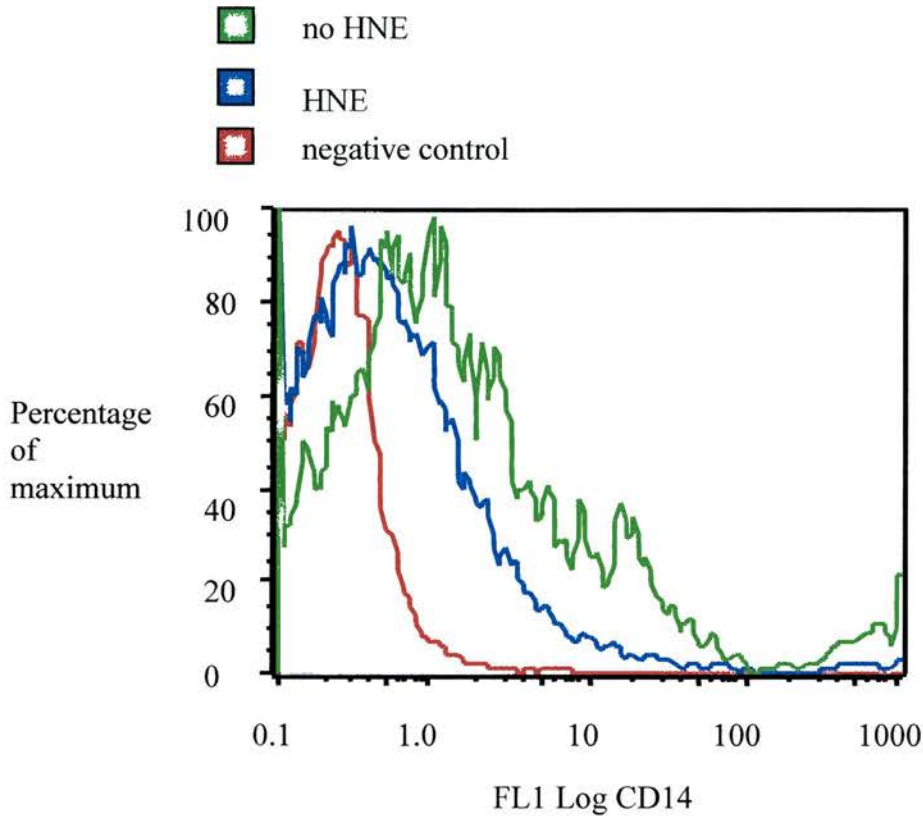
Figure 6.9. FACS analysis of macrophage surface CD14 expression following HNE treatment.

Macrophages were prepared as for figure 6.8 except that on culture day 4 they were transferred to 48-well plates (70000 cells/well). HNE incubations (1 μM) were performed, where indicated, as before (see figure 6.8), supernatants removed and cells washed and resuspended in ice cold PBS. Binding of 61D3 primary antibody was used to determine cell surface CD14 expression. Cells were incubated with 61D3 for 30 min, washed twice and then incubated with phycoerythrin-conjugated goat anti-mouse IgG secondary antibody for 15 min. Washed macrophages were then analysed on a FACScan cytometer (Becton Dickinson and co.). Control cells were incubated with secondary antibody alone. Results are from one donor (5000 counts/condition).

220

Chapter 6
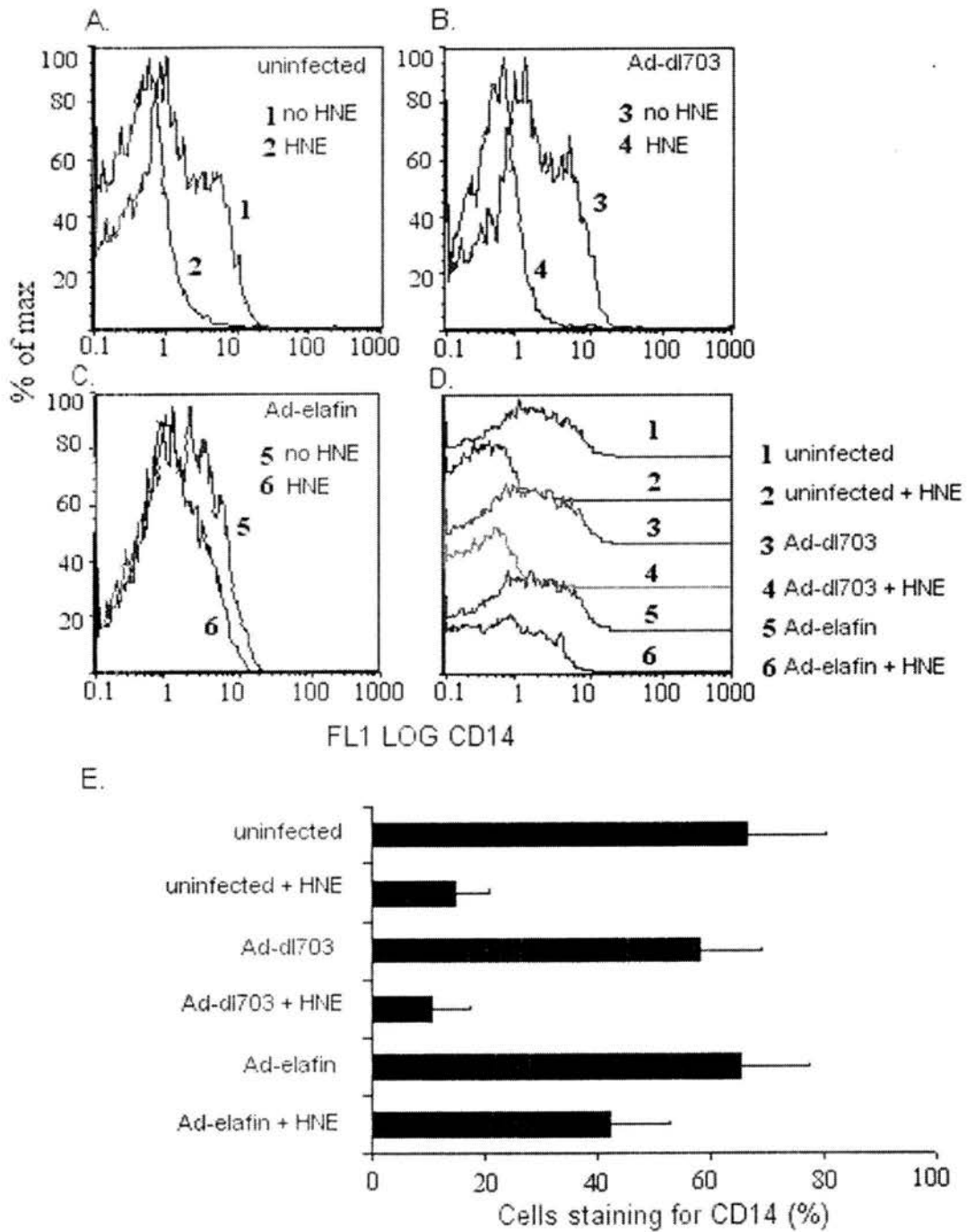
Figure 6.10. Ad-elafin reduces HNE mediated disruption of the macrophage CD14 receptor.

Figure 6.10. Ad-elafin reduces HNE mediated disruption of the macrophage CD14 receptor.

Where indicated, macrophages were incubated with HNE (1 µM) for 1 h prior to removal and binding of 61D3 antibody was analysed according to the protocol described in figure 6.9. Adenovirus infections were performed 24 h prior to the HNE incubation where indicated using the lipofectamine protocol outlined in the methods chapter. A. Uninfected cells B. Ad-dl703 infected cells (MOI 100). C Ad-elafin infected cells (MOI 100). D. Composite figure illustrating 61D3 binding in the different conditions from a separate donor. E: Mean percent of macrophages staining for CD14 ± SD. Data are from experiments performed on 2 separate donors. Data shown are representative from experiments performed on 2 separate donors.

222

Chapter 6

a r-elafin
b r-elafin + HNE
c uninfected
d uninfected + HNE
e Ad-elafin
f Ad-elafin + HNE
g Ad-dl703
h Ad-dl703 + HNE
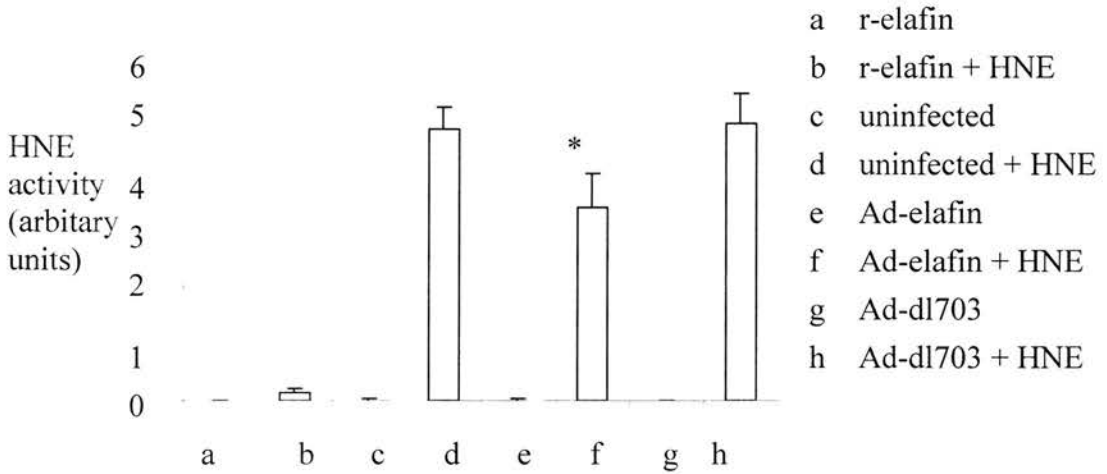
Figure 6.11. A comparison of the HNE inhibitory activity of macrophage culture supernatants.

Macrophages were prepared and infected with adenovirus using the protocols described in figure 6.10. Culture supernatants were removed for determination of residual HNE activity following incubation for 1 h with HNE (1 μM). Supernatants were transferred to a microtitre plate and cleavage of a chromogenic HNE substrate was measured spectrophotometrically over time according to a protocol described in the Methods section. r-elafin: truncated recombinant human elafin (15 μg/ml). Data are mean and standard deviation from experiments performed on 3 separate donors. * significantly less than uninfected cells + HNE or Ad-dl703 infected cells + HNE $p <$ 0.05.

223

produced would be expected to neutralise around 5% of the HNE. Figure 6.11 indicates that although residual supernatant HNE activity was significantly reduced from wells with elafin expressing macrophages compared to control virus and uninfected cells, the magnitude of reduction was modest. In contrast, a saturating concentration of recombinant elafin effectively neutralised residual supernatant HNE activity.

Having demonstrated HNE disruption of surface CD14 on macrophages and partial protection of CD14 through adeno-mediated overexpression of elafin, an *in-vitro* system was devised to investigate the effects of elafin overexpression on macrophage apoptotic cell clearance. CD14 has been identified as a surface recognition receptor for apoptotic cells. HNE impairment of macrophage apoptotic cell recognition through cleavage of apoptotic cell recognition receptors has been demonstrated (Vandivier et al 2002). In agreement with this work, incubation with HNE significantly reduced apoptotic cell interaction with macrophages (Figure 6.12). 61D3, a CD14 antibody with blocking activity against apoptotic cell recognition also reduced macrophage interaction. This effect was increased in the presence of HNE, supporting the possibility that the combined treatments were affecting other apoptotic cell recognition mechanisms in addition to CD14. Apoptotic cell recognition was relatively preserved in Ad-elafin infected macrophages in comparison with viral control and uninfected cells.

224

Chapter 6
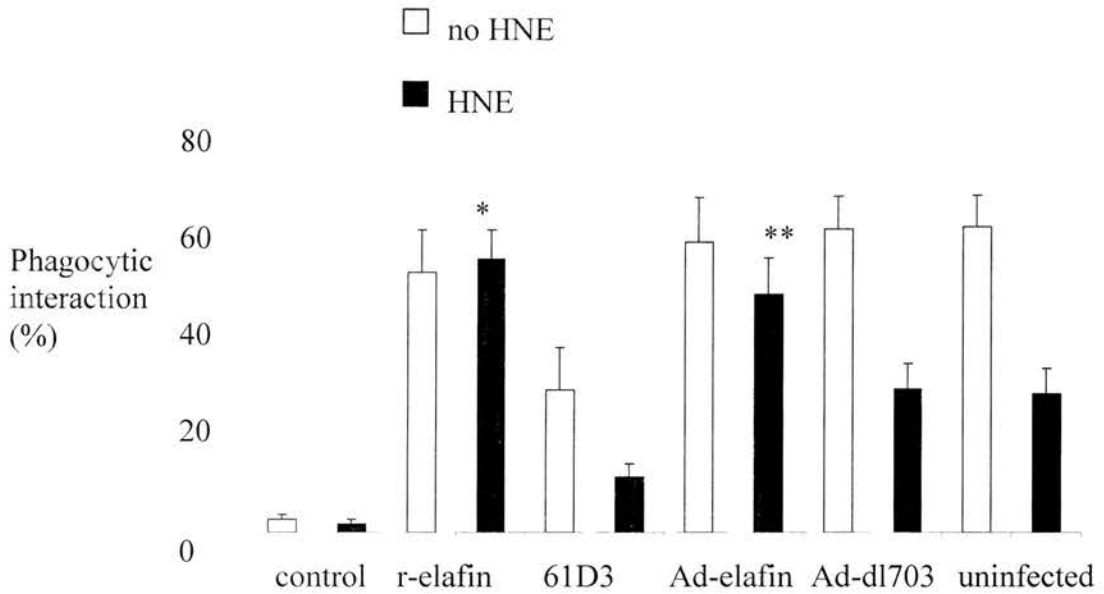
Figure 6.12. Ad-elafin protects macrophages from HNE-mediated impairment of phagocytosis.

Macrophages were cultured and infected with adenovirus according to protocols described in figure 6.10. Where indicated, HNE ($1\mu M$) and r-elafin ($15 \mu g/ml$) were added in serum-free X-vivo 10 medium (Cambrex Bio Science) for 1 h prior to adding the apoptotic Mutu (B cell) target cells with or without 61D3 antibody. After fixing and staining, the percentage of macrophages interacting with apoptotic mutus was calculated (% interaction). Interaction counts performed on macrophages that had not been exposed to mutus (control) are also shown to exclude a significant contribution from apoptotic macrophages originating from the culture. Data are mean and standard deviation from experiments performed in quadruplicate on 3 separate donors. * ,** significantly greater percentage phagocytic interaction than HNE treated uninfected and Ad-dl703 infected cells, $p < 0.05, 0.01$.

225

Chapter 6

6.3. Discussion

The principle finding in this chapter relates to the significant protection against HNE induced cell death, inflammatory activation and impaired cell function conferred by overexpression of elafin. Discussion will focus on the relevance of these findings from in-vitro models to inflammatory events occurring within the atherosclerotic plaque.

6.3.1. Ad-elafin overexpression protects endothelial cells from the inflammatory actions of HNE

The considerable genetic augmentation of elafin described in chapter 5 was sufficient to ameliorate HNE induced cytopathic changes in HUVECs (Figures 6.1, 6.2 and 6.4). HUVEC cell counts were depleted in wells incubated with HNE (Figure 6.2). This reduction was quantified by MTS assay which measures the mitochondrial activity within viable cells (Cory et al 1991). This result was compatible with two possibilities: that HNE induces cell lysis directly or that it causes endothelial cell detachment. The latter mechanism may have resulted in a decline in cell numbers because detached cells were removed during the exchange of medium prior to introducing the MTS reagent. Both detachment and cytolysis have been demonstrated in cultured endothelial cells following incubation with HNE (Ballieux et al 1994) or with degranulating neutrophils (Smedly et al 1986; Westlin et al 1993). Subendothelial extracellular matrix proteins such as fibronectin and thrombospondin are particularly susceptible to HNE cleavage, leading to cell retraction and rounding (Bonnefoy et al 2000). The correlate of this process *in vivo* may be the appearance of circulating endothelial cells and their fragments in various diseases characterised by endothelial injury including atherosclerosis (Makin et al 2004; Mutin et al 1999). In addition to membrane disruption and cytolysis, HNE has also been shown to induce apoptotic cell death in bovine endothelial cells (Yang et al 1996a). As reported by Ballieux et al (1994), it is likely that HNE concentration and period of incubation combine to determine the predominant mechanism. In this work, the increased

226

Chapter 6

supernatant LDH activity (Figure 6.3) and propidium iodide uptake (data not shown) indicated that cell lysis was occurring. The increases in LDH activity at higher concentrations of HNE were modest (around 15% compared to untreated cells, Figure 6.3) compared to the observed disruption of the HUVEC monolayer under light microscopy. This result may reflect mixed mechanisms including cell detachment, apoptosis and lysis. A direct effect of HNE on liberated cytosolic LDH can also not be excluded, possibly leading to reduced LDH activity and an under estimation of cell lysis.

Both Ad-GFP and Ad-dl703 increased cell viability (Figure 6.4) and protected endothelial cells from HNE damage (Figure 6.1) in comparison to uninfected cells. This raised the intriguing possibility that viral infection was leading to upregulation of an endogenous protecting factor against HNE. In contrast to epithelial cells, cultured endothelial cells do not produce elafin (Figure 5.1) or SLPI (SLPI dot blots performed on HUVEC culture supernatants, data not shown). Serine proteinase inhibitory activity from cultured human and bovine endothelial cells has been isolated by others against both HNE and trypsin (Hanley et al 1996; Rao et al 1995) although the mediators involved were not identified and the capacity for the endothelium to protect itself from HNE damage through upregulation of endogenous antiproteases remained unknown. That protection was observed in both GFP expressing cells and Ad-dl703 infected cells indicates that the virus effect was not related to a specific transgene. A similar effect on HNE mediated injury has been observed in epithelial A549 cells in our laboratory following infection with adenovirus expressing B-galactosidase (Simpson 2001).

HNE incubation at concentrations below levels associated with immediate cytopathy led to release of IL-8 into HUVEC culture supernatants (Figure 6.5). HNE has previously been shown to augment IL-8 release from lung epithelial cells (Sallenave et al 1994; Walsh et al 2001) and its ability to positively regulate transcription and production of inflammatory mediators such as tissue factor in

227

Chapter 6

HUVECs has been demonstrated (Haubitz et al 2001). Proteinase 3, another azurophil granule protease, has also been shown to positively regulate interleukin-8 in HUVECs (Berger et al 1996). The effect of HNE pretreatment on HUVEC responses to other inflammatory stimuli was investigated. The presence of several potentially inflammatory stimuli within atherosclerotic tissue including oxidised LDL and HNE (Dollery et al 2003) raises the question of how cells respond when exposed to both stimuli. HNE has been shown to cleave surface CD14 on monocytes (Le Barillec et al 1999) and fibroblasts (Nemoto et al 2000). This action leads to reduced inflammatory cytokine production in response to bacterial LPS (Le Barillec et al 1999; Nemoto et al 2000).The concentrations of HNE used in these studies were relatively high (1 μM) and, whereas fibroblasts and monocytes remain intact in these conditions, HUVECs detach and are lysed rapidly (the disruptive effect of HNE at 5.0×10^{-8} M on HUVECs is shown in Figure 6.1). HUVECs were pretreated with concentrations of HNE previously shown to induce IL-8 production and subsequently exposed to inflammatory stimuli. Even short 1 hour treatments led to significant increases in HUVEC IL-8 production without further inflammatory stimuli (Figure 6.6). Pretreatment with HNE dramatically augmented subsequent IL-8 production in response to oxidised LDL and LPS and there was an overall trend for higher pretreatment concentrations of HNE to lead to greater IL-8 release in response to the same concentration of oxidised LDL or LPS (Figure 6.6). The results indicate that a brief exposure to HNE (in which no morphological damage was observed, as evidenced by absence of lifting and rounding of the HUVEC monolayer) not only led to IL-8 production on its own but also primed the cells for subsequent stimulation by other inflammatory stimuli.

This result contrasts with the negative actions on LPS signalling observed in this work (Figure 6.7) and by others with monocytes (Le Barillec et al 1999) and fibroblasts (Nemoto et al 2000) (with the caveat that the experiments on endothelial cells in this chapter were performed with 100-fold lower concentrations of HNE). The increase in IL-8 production was in excess of the sum of either stimulus alone indicating a synergistic effect. TNF-α produced a massive IL-8 response that was not

increased by HNE treatment (Figure 6.6). This result may have reflected saturation of the cellular IL-8 production machinery by TNF-α. Synergism between HNE, oxidised LDL and LPS would be expected to lead to concentrated IL-8 production and a focusing of the chemotactic signal to regions of atherosclerotic tissue where both stimuli are present. Whereas this may be maladaptive in the context of atherosclerosis and arterial wall inflammation, synergy between HNE and LPS would serve a useful purpose in focusing recruitment of leucocytes to areas of infection where both bacteria and degranulating neutrophils are present.

Having demonstrated the capability of HNE to stimulate HUVEC IL-8 production, the effects of overexpression of elafin (a potent HNE inhibitor) and IκBα (an inhibitor of IL-8 transcription) were examined using adenoviral vectors. Elafin significantly attenuated IL-8 production in response to HNE alone, HNE in combination with LPS and, in agreement with data in chapter 5, in response to LPS alone (Figure 6.7). Ad-IκBα similarly reduced IL-8 production to all three stimuli. This result extends the role of elafin as a suppressor of inflammatory cytokine production outlined in chapter 5. In addition to neutralising the disruptive effects of HNE on cell components and the extracellular matrix (Figures 6.1, 6.4) elafin may also exert anti-inflammatory actions through blocking HNE's facilitatory action on IL-8 production. That IκBα overexpression attenuated IL-8 production in response to HNE, was in keeping with data indicating that HNE mediated IL-8 production in epithelial cells is through a MyD88 IL-1R associated kinase-TNFR-associated-factor-6-NF-κB pathway (Walsh et al 2001).The work presented in this chapter along with recognition of specific cell signalling mechanisms and identification of Toll-like receptor-4 as a receptor for HNE (Devaney et al 2003) broaden the perceived role of this inflammatory mediator from an indiscriminate protease cleaving cellular and matrix proteins to a signalling molecule participating in inflammatory cytokine production.

229

Chapter 6

6.3.2. The inflammatory role of HNE on atherosclerotic plaque development.

It is important to consider the relevance of these in-vitro findings to atherosclerotic plaque biology. The role of a neutrophil derived protein in an inflammatory process, characterised histologically by a paucity of neutrophils, also merits further discussion. Several lines of evidence point to a possible role for the neutrophil and neutrophil derived proteins in the development of atheroma. Epidemiological studies have repeatedly demonstrated a link between the circulating leucocyte count and neutrophil differential and the subsequent development of ischaemic heart disease (Friedman et al 1974; Sweetnam et al 1997). Neutrophils from patients with advanced atheroma are more reactive and prone to degranulation (Mohacsi et al 1996). Circulating concentrations of HNE are higher in patients with coronary artery disease (Amaro et al 1995; Kosar et al 1998). Perhaps the most convincing evidence is the observation of neutrophil derived proteins within atherosclerotic tissue. Large quantities of myeloperoxidase, a major neutrophil protein, have been identified within atheroma. This enzyme may be an important mediator of LDL modification within the plaque (Daugherty et al 1994; Hazen et al 1997). Neutrophil granule derived proteins, HNE and α-defensin, have also been demonstrated directly within human atheroma (Barnathan et al 1997; Dollery et al 2003). The origin of these proteins has not been established. Macrophage production has been proposed and there is some evidence that macrophages may produce myeloperoxidase under certain conditions (Sugiyama et al 2001).

Neutrophil granule derived proteins becoming trapped within the neointima following neutrophil degranulation seems a more likely explanation. Buffon et al (2002) elegantly demonstrated the capacity for neutrophil degranulation with myeloperoxidase depletion of neutrophils passing through an inflamed coronary circulation. HNE is contained within the same azurophil granules as myeloperoxidase and passage of both proteins into the subendothelial space may occur following degranulation (Baldus et al 2001). The mechanism of myeloperoxidase transcytosis across endothelial cells and its dependence on albumin

230

and functioning caveolae has recently been elucidated (Tiruppathi et al 2004). Once trapped within the neointima neutrophil derived proteins may exert their inflammatory potential. In favour of such a hypothesis is the observation that HNE can associate with connective tissue in humans (Watanabe et al 1990) and bound HNE appears to be relatively resistant to inhibition (Morrison et al 1990).

Irrespective of the issues raised above, this chapter provides further evidence for the inflammatory effects of HNE on endothelial cells and demonstrates the protective effect of elafin overexpression. This provided the impetus to examine the effects of HNE injury on monocyte-derived macrophages. The macrophage has a central role in plaque development (Glass et al 2001).

6.3.3. Ad-elafin rescues HNE mediated impairment of macrophage-apoptotic cell recognition

Recognition of inflammatory stimuli and uptake of oxidised LDL or apoptotic bodies within the plaque depend on functioning surface receptors. Previous work has demonstrated cleavage of surface CD14 from HNE treated human peripheral blood monocytes (Le Barillec et al 1999) leading to reduced TNF-α production in response to LPS. Following a 1 hour pretreatment with HNE, the responsiveness of peripheral blood monocyte derived macrophages to LPS was similarly reduced (Figure 6.8). The reduced TNF-α production was not a result of reduction in viable cell number following HNE incubation as evidenced by propidium iodide staining and MTS assay (data not shown). Pretreatment with HNE alone followed by replenishment with serum containing medium produced a modest rise in TNF-α production (Figure 6.8). Inflammatory activation of a rat alveolar macrophage cell line by human pancreatic enzymes including pancreatic elastase has previously been demonstrated (Jaffray et al 2000). Pancreatic elastase increased TNF-α release through a mechanism that involved NF-κB activation and selective degradation of cytoplasmic IκBβ. Taken together, these findings suggest that the effect of HNE on macrophage inflammatory programming is complex, stimulating TNF-α production directly but

231

Chapter 6

reducing TNF-α production in response to a second LPS stimulus in contrast to a facilitatory action on endothelial cells (demonstrated earlier in the chapter albeit at lower concentrations). The evidence presented in this chapter and observations by others that specific transcriptional pathways are activated by HNE in a range of cell types (Walsh et al 2001) indicates the possibility of specific receptor interactions.

It is worth comparing the results of HNE pretreatment on subsequent responses of endothelial cells and macrophages to inflammatory stimuli. HNE facilitation of a subsequent LPS or oxidised LDL stimulus in endothelial cells (Figure 6.6) occurred at concentrations 2 orders less than those associated with cleavage of macrophage CD14 and reduced LPS responsiveness (Figures 6.9, 6.8 respectively). HUVECS have very low levels of CD14 expression (Jersmann et al 2001) and it is possible that HNE's facilitatory action on IL-8 production (at low concentrations) in HUVECs is occurring through a separate signalling pathway. Interest in HNE as a ligand for specific surface receptors has identified several candidates. HNE in a covalently stabilised complex with its inhibitor α1-antitrypsin is recognised by the serpin-enzyme complex (SEC) receptor (Perlmutter et al 1990). The SEC receptor transduces the chemotactic activity of HNE-α1 antitrypsin complexes on neutrophils (Joslin et al 1992). In addition, integrin CD11b/CD18 (Cai et al 1996) on neutrophils and Toll-like receptor 4 (TLR4) on human bronchial epithelial cells (Devaney et al 2003) have been proposed as surface receptors for HNE. Toll-like receptors take part in immune and inflammatory responses recognising microbial components with activation of innate immune responses leading to development of adaptive immune responses (Medzhitov et al 2000). TLR4 has been identified as a receptor for bacterial LPS (Chow et al 1999; Hoshino et al 1999). HNE incubation led to increased IL-8 release from human bronchial epithelial cells and human embryonal kidney cells transfected with TLR4 at a similar concentration (50 nM) to that used on HUVECs in this chapter (Devaney et al 2003). In contrast to the results for HUVECs in Figure 6.6, Dr Devaney found that pretreatment with HNE led to reduced IL-8 production in response to a subsequent LPS stimulus. This was attributed to internalisation or cleavage of TLR4 following interaction with HNE and was

232

Chapter 6
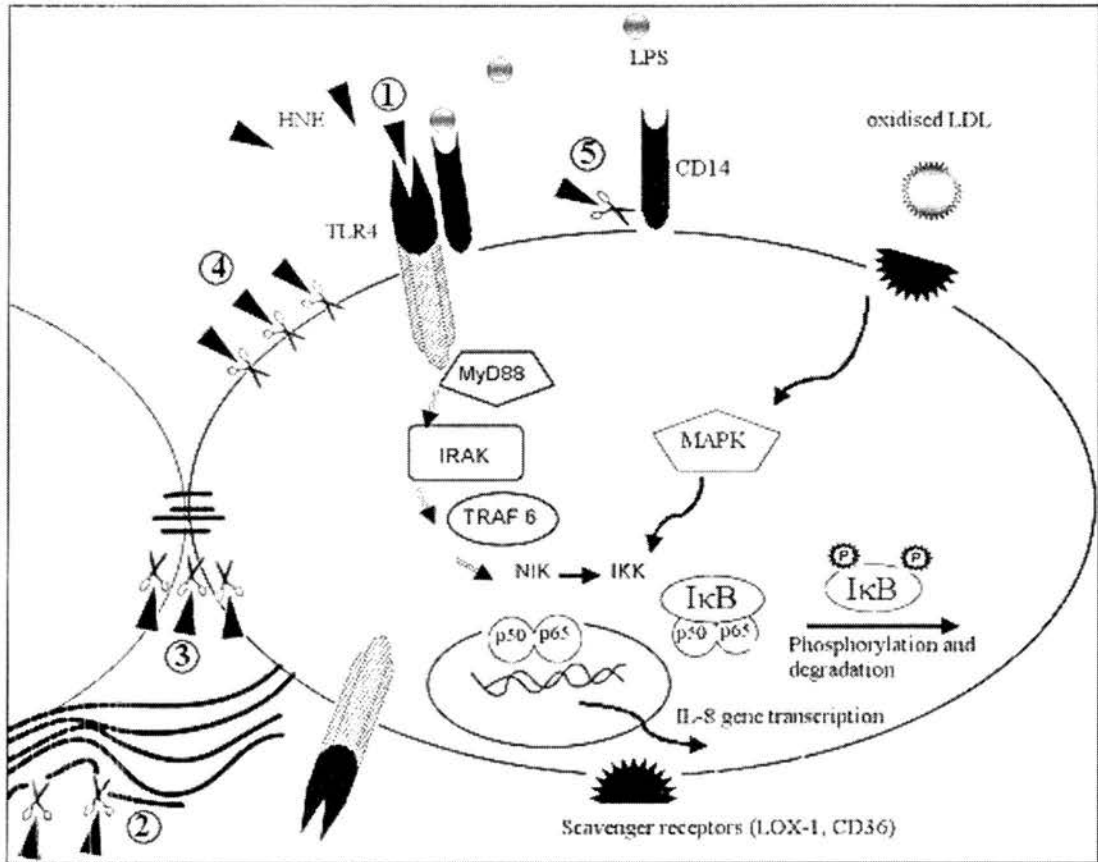
Figure 6.13. Inflammatory mechanisms of HNE, LPS and oxidised LDL

Key to Figure 6.13

IRAK: Interleukin-1 receptor associated protein kinase. TRAF: tumour necrosis factor receptor associated factors. NIK: NF-κB inducing kinase. IKK: IκB Kinase. MAPK: mitogen activated protein kinases. LOX-1: lectin like oxidised LDL receptor-1 (endothelial cells)

233

Chapter 6

Figure 6.13. Inflammatory mechanisms of HNE, LPS and oxidised LDL (continued)

This diagram illustrates the relationship between HNE, LPS and oxidised LDL signalling. HNE may stimulate IL-8 production directly through interaction (1) with TLR4 (Devaney et al 2003) and activation of the Myd88-IRAK-TRAF pathway (Walsh et al 2001). LPS attached to its circulating binding protein (not shown), binds to CD14 and this complex interacts with TLR4 on the membrane surface producing a pro-inflammatory signal (Chow et al 1999). CD14 also participates in apoptotic cell recognition (not shown), an integral process for inflammatory resolution (Devitt et al 1998). Oxidised LDL binds to scavenger receptors and activates NF-κB through up-stream MAP kinases (Li et al 2003). HNE has an extensive list of substrates including extracellular matrix proteins (2) and intercellular cadherins (3) (reviewed by (Lee et al 2001). Disruption of these attachments leads to cell rounding, retraction and lysis (4). HNE also cleaves a range of cell-surface proteins and receptors (5) including CD14 (Lee et al 2001; Vandivier et al 2002). The current work confirms observations by others that pretreatment with HNE reduces LPS responsiveness (Le Barillec et al 1999) and apoptotic cell recognition (Vandivier et al 2002) in monocyte-macrophages. The work in this chapter also demonstrates enhanced IL-8 production in endothelial cells in response to LPS and oxidised LDL following pretreatment with HNE (Figure 6.6). The mechanism involves activation of NF-κB (Figure 6.7), occurs at lower concentrations of HNE than those associated with CD14 cleavage and may involve facilitation of surface or intracellular signalling pathways by HNE or synergy between HNE-TLR4 and oxidised LDL or LPS signals.

234

proposed as a mechanism for desensitisation to LPS signalling (Devaney et al 2003).

The concentrations of LPS used to stimulate HUVECs and human bronchial epithelial cells were different (100 ng/ml and 20 µg/ml respectively) in the two studies. In addition, the duration of HNE pretreatment was longer for human bronchial epithelial cells (4 h compared to 1 h in HUVECs) and this may have resulted in alterations in intracellular signalling such as the inhibition of LPS induced NF-κB activation in monocytes that has been described following pre-incubation with oxidised LDL (Brand et al 1997a). Figure 6.1 summarises putative receptor-signalling pathways for HNE, LPS and oxidised LDL and illustrates the potential for crossover and interaction between these pathways.

HNE reduced surface expression of CD14 on human macrophages (Figure 6.10) in accordance with its action on other cell types (Le Barillec et al 1999; Nemoto et al 2000). CD14 was previously considered only as a receptor for bacterial LPS (Ulevitch et al 1995). More recently CD14 has been shown to be involved in the resolution phase of the inflammatory response, by acting as a cell surface receptor for apoptotic cells (Devitt et al 1998). Macrophages are important phagocytic cells involved in the recognition and removal of apoptotic cells, an integral process in the resolution of the inflammatory response (Savill et al 2002). Recent data have suggested that HNE, through cleaving key receptors, is responsible for the impairment of apoptotic cell recognition by macrophages in inflammatory diseases (Vandivier et al 2002). Although the list of receptors involved in apoptotic cell recognition is increasing rapidly (Savill et al 2000) only the phosphatidylserine receptor and CD14 have previously been shown to be inactivated by HNE (on macrophages and monocytes, respectively). Importantly, Vandivier et al (2002) demonstrated that CD36 and CD32 expression and function were intact following HNE treatment of human monocyte derived macrophages.

235

Chapter 6

Having established the disruptive activity of HNE on macrophage CD14 (Figure 6.9), a gene therapy strategy was devised to protect macrophages from HNE-mediated shedding of CD14 using Ad-elafin. The protocol to facilitate adenoviral gene delivery to macrophages developed in chapter 5 was used to achieve high levels of gene expression. Ad-elafin attenuated the decline in macrophage CD14 levels following HNE treatment compared to uninfected or control virus infected cells (Figure 6.10). The preservation of CD14 expression was striking (Figure 6.10E) although as reported in the results section, the quantities of elafin produced would be expected to neutralise only approximately 5% of the HNE added. Examination of residual supernatant HNE activity following the experiments demonstrated a modest but statistically significant 20% decline in HNE activity from Ad-elafin wells compared to Ad-dl703 or uninfected cells (Figure 6.11, columns d and f). It is possible that elafin was bound to the extracellular matrix (Nara et al 1994) and that the concentration of elafin within the supernatants did not accurately reflect the quantity of active elafin present. This possibility could be explored by examining the elafin content of cell lysates and immunostaining of the macrophage cultures to look for evidence of matrix bound elafin.

An important question following on from these results was whether Ad-elafin could protect macrophages from the HNE mediated impairment of phagocytic function demonstrated previously (Vandivier et al 2002). In order to investigate this further, a model of apoptotic cell clearance had to be established. A variety of cells, such as lymphocytes and neutrophils are routinely used in experimental systems as apoptotic target cells. Group I Burkitt lymphoma cells (Mutu I) were chosen over neutrophils because of the absence of endogenous elastase in the former, which could have interfered with the assay (Henriksen et al 2004). Macrophages were either untreated/uninfected (control) or infected with Ad-elafin (Ad-dl703 as a control) and incubated, where indicated, with HNE. In a variation of these experiments, the CD14 blocking antibody 61D3 (Devitt et al 1998) was used to provide a positive control of CD14 blockade. Figure 6.12 shows that HNE treatment of uninfected cells inhibited Mutu cell recognition by 54%, compared to uninfected cells alone. This level of

236

inhibition was comparable to that of 61D3 treatment. The prominent role of CD14 (the 61D3 antigen) for interaction and initial tethering of apoptotic Mutu cells with human macrophages has previously been characterised (Flora et al 1994). Blocking antibodies and peptides against the $\alpha_v\beta_3$ integrin (Vitronectin receptor) and CD36 produced little if any reduction of apoptotic Mutu cell interaction in this system (Flora et al 1994). Interestingly, when 61D3 and HNE were used in combination (Figure 6.12), a further decrease in recognition occurred, suggesting that the sites of action of 61D3 and HNE are not identical. It is likely that in addition to cleaving CD14 (figure 6.9), HNE is interfering with additional (unidentified) surface receptors in our system and notably the degree of inhibition never approached 100% even with 61D3 and HNE together. HNE cleavage of the phosphatidylserine receptor was associated with reduced ingestion of apoptotic Jurkat cells by human macrophages (Vandivier et al 2002) and the role of phosphatidylserine receptor cleavage in reducing interaction in the experiments in this chapter is unknown.

When recombinant elafin was added extracellularly with HNE, macrophage recognition was restored to normal values. Similarly, when macrophages were transfected with Ad-elafin, prior to HNE challenge, a very significant increase in macrophage recognition of apoptotic cells was obtained, compared to uninfected cells and cells infected with Ad-dl703 demonstrating the elafin transgene specific effect.

These results demonstrate that gene expression of elafin in macrophages partially rescues their capacity to recognise apoptotic cells in the presence of HNE. The mechanism of elafin involves neutralisation of HNE activity and preserved expression of recognition receptors including CD14 (Figure 6.10). The discrepancy between the degree of HNE inhibition (Figure 6.11) and the preservation of CD14 expression and apoptotic cell recognition (Figures 6.10E and 6.12) in Ad-elafin infected macrophages has been discussed earlier. In contrast to Ad-elafin infected macrophages, recombinant elafin produced complete neutralisation of HNE activity

237

Chapter 6

(Figure 6.11) although there was little difference in apoptotic cell recognition activity between Ad-elafin and recombinant elafin treated cells (Figure 6.12). CD14 expression was reduced but still significantly higher in Ad-elafin infected macrophages compared to control cells (Figure 6.10) despite the modest inhibitory effect on supernatant HNE activity (Figure 6.11).

These important discrepancies are not fully explained from the data presented. It may be that measurements of residual HNE supernatant activity do not reflect its activity at the macrophage surface. Elafin's propensity to bind to matrix components (Nara et al 1994) laid down by macrophages may produce an effective 'local' anti-HNE shield. At first sight, Ad-elafin's action on apoptotic cell recognition does not appear to be related to a direct effect of elafin overexpression in macrophages because apoptotic cell recognition was not increased in Ad-elafin infected cells compared to uninfected cells in the absence of HNE (Figure 6.12). This finding does not exclude the possibility that overexpression of elafin with its anti-inflammatory actions, outlined in the earlier chapter, confers a beneficial signal to apoptotic cell recognition in the context of HNE injury.

In addition to removing cells before they undergo lysis, ingestion of apoptotic cells by macrophages results in potent anti-inflammatory and immunosuppressive effects through the production of anti-inflammatory cytokines such as Transforming growth factor (TGF-β1) and Prostaglandin E2 and the suppression of release of pro-inflammatory IL-8, TNF-α and thromboxane A2 (Fadok et al 1998; Voll et al 1997). Elafin and mSLPI overexpression were both shown to suppress LPS induced TNF-α production by macrophages in chapter 5. In restoring apoptotic cell recognition in the context of HNE injury, elafin overexpression would reinforce the endogenous anti-inflammatory phenotype conferred by binding of apoptotic cells (Huynh et al 2002) to macrophages that may otherwise be diminished by HNE.

238

Chapter 6

The recent finding that SLPI production is upregulated following macrophage recognition of apoptotic cells is of particular interest (Odaka et al 2003). The slow kinetics of production after the apoptotic cell recognition event suggests that SLPI is unlikely to act *in vivo* at an autocrine level during the onset of the interaction but rather in a paracrine fashion, during phagocytosis of incoming cells (Odaka et al 2003).

The work presented in this chapter sheds light on the extended pro-inflammatory effects of HNE on endothelial cells and macrophages. The ability of Ad-elafin to rescue endothelial cells from HNE injury and inflammatory signalling has been demonstrated. Ad-elafin also rescues macrophages from an HNE-induced pro-inflammatory to an anti-inflammatory phenotype, favouring apoptotic cell recognition and clearance. These findings raise two exciting possibilities. Firstly, the potential for systemic delivery of macrophages transfected *ex-vivo* with anti-inflammatory genes. This approach has been demonstrated in murine glomerulonephritis (Kluth et al 2001; Zernecke et al 2001) and this methodology may prove useful in inflammatory conditions where direct use of adenovirus gene vectors is precluded because of their intrinsic immunogenicity. Secondly, the data further strengthen the case for targeted overexpression of elafin within arterial vessels as a strategy to reduce inflammation resulting from HNE injury occurring during atherosclerosis.

239

Chapter 6

CONCLUSION AND FUTURE DIRECTIONS

The experiments described in this thesis have illustrated the utility of modelling atherosclerotic endothelial cell injury using cultured human umbilical vein endothelial cells. Incubation with oxidised LDL led to production of the inflammatory chemokines IL-8 and MCP-1 and activation of the inflammatory transcription factor NF-κB. These findings parallel changes observed in endothelial cells within atherosclerotic coronary arteries.

Gene expression profiling using commercial nylon miniarrays was performed on oxidised LDL treated endothelial cells. Limitations of this approach were encountered including the finding that a large majority of genes varied little in expression between different treatment conditions. Reproducibilty between hybridisations was poor for many genes emphasising the importance of a robust array platform and use of repeat hybridisation that was not feasible with the nylon miniarrays.

Angiopoietin-2 was the only target form the array experiments successfully verified using ribonuclease protection assays and semiquantitative PCR. Production of this angiogenic factor was increased in HUVECs incubated with oxidised LDL and TNF-α and intense expression was seen within the neointima of atherosclerotic plaques. Additional possible stimuli for angiopoietin-2 production include VEGF and a relatively hypoxic microenvironment within the plaque. The process of neointimal angiogenesis contributes to plaque growth through providing a plexus of blood vessels facilitating passage of inflammatory cells and mediators within the neointima. Angiopoietin-2 expression might be expected to confer leakiness and these vessels are prone to bleeding. Both properties may give rise to (sudden) plaque expansion or rupture. In animal models, VEGF infusions are associated with accelerated plaque growth and increased plaque density of endothelial cells and macrophages (Celletti et al 2001). Similarly, treatment with angiogenesis inhibitors

240

Chapter 6

attenuates plaque growth (Moulton et al 1999). These findings have led to concerns that attempts to increase angiogenesis within ischaemic tissues using direct or genetic delivery of angiogenic factors may cause plaque expansion or destabilisation. Whereas these concerns have not been realised in the clinical trials, the contribution of neointimal angiogenesis to plaque growth and complications is significant and further understanding of mechanisms driving new vessel formation and factors governing their integrity within the atherosclerotic plaque are important goals.

Gene expression profiling failed to identify a candidate athero-protective mediator and focus therefore turned to elafin, a pleiotropic anti-inflammatory antiprotease previously identified within human atherosclerotic coronary arteries. The effects of adenoviral overexpression of elafin were examined. Development of a simple protocol involving precomplexing adenoviral vectors with lipofectamine enhanced gene delivery to endothelial cells and facilitated gene delivery to human macrophages, a notoriously difficult cell type to transfect. The mechanism of improved gene delivery was not examined in detail but may involve improved uptake of virus. Methods to augment adenoviral gene delivery *in vivo* are attractive through reducing viral dosing and toxicity. Previous work employing adenovirus in complex with calcium precipitates has demonstrated enhanced delivery of adenovirus to the murine airway epithelium and the work here indicates that *in vivo* studies examining the effects of adenovirus in complex with lipofectamine, a relatively non-toxic lipid, would be valuable.

Overexpression of elafin and the related protein SLPI led to reduced inflammatory cytokine production in response to atherogenic stimuli by human endothelial cells and macrophages. This activity was associated with inhibition of NF-κB activation and preservation of the inhibitory IκBα subunit. Overexpression of elafin also protected endothelial cells form HNE mediated injury and inflammatory cytokine production. Elafin protected macrophages from HNE mediated disruption

241

Chapter 6

of surface CD14 expression and this was associated with preserved interaction of apoptotic cells following HNE injury.

These experiments expand our understanding of elafin and SLPI biology, firmly identifying them as powerful modulators of inflammation with properties extending beyond neutralisation of HNE and other proteases. The findings leave several important questions and avenues for further research.

The mechanism of elafin and SLPI upregulation of $I\kappa B\alpha$ has not been identified at the molecular level. Although both proteins have well defined roles as secreted antimicrobial and antiprotease agents, our results identified an additional intracellular mode of action, possibly interfering with $I\kappa B\alpha$ degradation through blockade of the proteosome. This work did not include control experiments with exogenously added elafin and SLPI although similar experiments performed on other cell types within our group failed to show broad ranging cytokine inhibition with addition of recombinant elafin and SLPI to the culture medium. Analysis of mutated proteins has pointed strongly to an intracellular mode of action for SLPI requiring antiprotease activity (Zhu et al 1999) and similar confirmatory experiments with elafin should be performed. The selectivity of elafin and SLPI blockade of inflammatory cytokines following overexpression and whether it is truly cell type specific merits further investigation (indeed, no anti-inflammatory effect was observed in epithelial cells). Study of a potential elafin and SLPI interaction with proteosomal subunits would be a logical starting point.

The ability of elafin overexpression to preserve macrophage surface CD14 expression and interaction with apoptotic cells was striking compared to the relatively modest inhibitory effect against the concentrations of HNE used. Further analysis of cell lysates from elafin infected macrophages may provide information on matrix bound elafin, not measured in the supernatants but contributing to a local

Chapter 6

HNE shield. Although there was no suggestion of heightened apoptotic cell recognition or increased CD14 expression in elafin expressing macrophages, the possibility that elafin confers a pro-apoptotic cell recognition message in the context of HNE injury was not excluded. Future work should examine the expression and activity of other apoptotic cell recognition receptors.

Finally, the *in vitro* biological effects of elafin and SLPI beckon the question of whether gene delivery could modulate the development of atherosclerosis *in vivo*. Several murine models of atherosclerosis exist and a direct extension of this work would be to examine systemic delivery of Ad-elafin and Ad-mSLPI through tail vein delivery in mice. Subsequent hepatic expression would be expected to augment circulating levels of elafin and SLPI and the effect of transient increases in production on atherosclerotic plaque progression could be examined. If the anti-inflammatory effect is dependent on intracellular expression and cannot be achieved by remote production then targeting of viral vectors to atherosclerotic endothelium could be employed. This question could also be addressed with transgenic lines given the availability of mice expressing elafin under the control of the mCMV (Sallenave et al 2003) and endothelin (Zaidi et al 1999) promoters.

In conclusion, the findings described in this thesis have added to our understanding of neointimal angiogenesis by identifying oxidised LDL as a stimulus for endothelial cell production of the angiogenic factor angiopoietin-2 and demonstrating intense expression of this angiogenic factor within human atherosclerotic plaques. An extended role for elafin and SLPI in the innate immune response has been identified. Adenoviral overexpression of these proteins suppressed NF-κB activation and inhibited inflammatory cytokine production in endothelial cells and macrophages. These properties suggest a therapeutic potential for endothelial repair and protection in the treatment of atherosclerosis.

243

Chapter 6

REFERENCES

Ahmad, S. A., Liu, W., Jung, Y. D., Fan, F., Reinmuth, N., Bucana, C. D., and Ellis, L. M. Differential expression of angiopoietin-1 and angiopoietin-2 in colon carcinoma. A possible mechanism for the initiation of angiogenesis. Cancer 92[5], 1138-1143. 2001.

Alemany, R., Suzuki, K., and Curiel, D. T. Blood clearance rates of adenovirus type 5 in mice. J.Gen.Virol. 81[Pt 11], 2605-2609. 2000.

Allaire, E., Hasenstab, D., Kenagy, R. D., Starcher, B., Clowes, M. M., and Clowes, A. W. Prevention of aneurysm development and rupture by local overexpression of plasminogen activator inhibitor-1. Circulation 98[3], 249-255. 1998.

Allen, S., Khan, S., Al Mohanna, F., Batten, P., and Yacoub, M. Native low density lipoprotein-induced calcium transients trigger VCAM-1 and E-selectin expression in cultured human vascular endothelial cells. J.Clin.Invest 101[5], 1064-1075. 1998.

Allison, B. A., Nilsson, L., Karpe, F., Hamsten, A., and Eriksson, P. Effects of native, triglyceride-enriched, and oxidatively modified LDL on plasminogen activator inhibitor-1 expression in human endothelial cells. Arterioscler.Thromb.Vasc.Biol. 19[5], 1354-1360. 1999.

Amaro, A., Gude, F., Gonzalez-Juanatey, R., Iglesias, C., Fernandez-Vazquez, F., Garcia-Acuna, J., and Gil, M. Plasma leukocyte elastase concentration in angiographically diagnosed coronary artery disease. Eur.Heart J. 16[5], 615-622. 1995.

Anderson, R. G., Brown, M. S., and Goldstein, J. L. Role of the coated endocytic vesicle in the uptake of receptor-bound low density lipoprotein in human fibroblasts. Cell 10[3], 351-364. 1977.

Ashcroft, G. S., Lei, K., Jin, W., Longenecker, G., Kulkarni, A. B., Greenwell-Wild, T., Hale-Donze, H., McGrady, G., Song, X. Y., and Wahl, S. M. Secretory leukocyte protease inhibitor mediates non-redundant functions necessary for normal wound healing. Nat.Med. 6[10], 1147-1153. 2000.

Bai, M., Harfe, B., and Freimuth, P. Mutations that alter an Arg-Gly-Asp (RGD) sequence in the adenovirus type 2 penton base protein abolish its cell-rounding activity and delay virus reproduction in flat cells. J.Virol. 67[9], 5198-5205. 1993.

Baird, G. S., Zacharias, D. A., and Tsien, R. Y. Biochemistry, mutagenesis, and oligomerization of DsRed, a red fluorescent protein from coral. Proceedings of the National Academy of Sciences of the United States of America 97[22], 11984-11989. 2000.

Baldus, S., Eiserich, J. P., Mani, A., Castro, L., Figueroa, M., Chumley, P., Ma, W., Tousson, A., White, C. R., Bullard, D. C., Brennan, M. L., Lusis, A. J., Moore, K. P., and Freeman, B. A. Endothelial transcytosis of myeloperoxidase confers specificity to vascular ECM proteins as targets of tyrosine nitration. J.Clin.Invest 108[12], 1759-1770. 2001.

Ballieux, B. E., Hiemstra, P. S., Klar-Mohamad, N., Hagen, E. C., van Es, L. A., van der Woude, F. J., and Daha, M. R. Detachment and cytolysis of human endothelial cells by proteinase 3. Eur.J.Immunol. 24[12], 3211-3215. 1994.

Barath, P., Fishbein, M. C., Cao, J., Berenson, J., Helfant, R. H., and Forrester, J. S. Detection and localization of tumor necrosis factor in human atheroma. Am.J.Cardiol. 65[5], 297-302. 1990.

Barger, A. C., Beeuwkes, R., III, Lainey, L. L., and Silverman, K. J. Hypothesis: vasa vasorum and neovascularization of human coronary arteries. A possible role in the pathophysiology of atherosclerosis. N.Engl.J.Med. 310[3], 175-177. 1984.

Barkett, M. and Gilmore, T. D. Control of apoptosis by Rel/NF-kappaB transcription factors. Oncogene 18[49], 6910-6924. 1999.

Barnathan, E. S., Raghunath, P. N., Tomaszewski, J. E., Ganz, T., Cines, D. B., and Higazi, A. al. Immunohistochemical localization of defensin in human coronary vessels. Am.J.Pathol. 150[3], 1009-1020. 1997.

Baumgartner, I., Pieczek, A., Manor, O., Blair, R., Kearney, M., Walsh, K., and Isner, J. M. Constitutive expression of phVEGF165 after intramuscular gene transfer promotes collateral vessel development in patients with critical limb ischemia. Circulation 97[12], 1114-1123. 1998.

Beck, H., Acker, T., Wiessner, C., Allegrini, P. R., and Plate, K. H. Expression of angiopoietin-1, angiopoietin-2, and tie receptors after middle cerebral artery occlusion in the rat. Am.J.Pathol. 157[5], 1473-1483. 2000.

Bennett, M. R. Apoptosis of vascular smooth muscle cells in vascular remodelling and atherosclerotic plaque rupture. Cardiovasc.Res. 41[2], 361-368. 1999.

Benoit, P., Emmanuel, F., Caillaud, J. M., Bassinet, L., Castro, G., Gallix, P., Fruchart, J. C., Branellec, D., Denefle, P., and Duverger, N. Somatic gene transfer of human ApoA-I inhibits atherosclerosis progression in mouse models. Circulation 99[1], 105-110. 1999.

Bergelson, J. M., Cunningham, J. A., Droguett, G., Kurt-Jones, E. A., Krithivas, A., Hong, J. S., Horwitz, M. S., Crowell, R. L., and Finberg, R. W. Isolation of a common receptor for Coxsackie B viruses and adenoviruses 2 and 5. Science 275[5304], 1320-1323. 1997.

Berger, S. P., Seelen, M. A., Hiemstra, P. S., Gerritsma, J. S., Heemskerk, E., van der Woude, F. J., and Daha, M. R. Proteinase 3, the major autoantigen of Wegener's granulomatosis, enhances IL-8 production by endothelial cells in vitro. J.Am.Soc.Nephrol. 7[5], 694-701. 1996.

Berliner, J. A., Territo, M. C., Sevanian, A., Ramin, S., Kim, J. A., Bamshad, B., Esterson, M., and Fogelman, A. M. Minimally modified low density lipoprotein stimulates monocyte endothelial interactions. J.Clin.Invest 85[4], 1260-1266. 1990.

Berridge, M. V. and Tan, A. S. Characterization of the cellular reduction of 3-(4,5-dimethylthiazol-2-yl)-2,5-diphenyltetrazolium bromide (MTT): subcellular localization, substrate dependence, and involvement of mitochondrial electron transport in MTT reduction. Arch.Biochem.Biophys. 303[2], 474-482. 1993.

Bett, A. J., Haddara, W., Prevec, L., and Graham, F. L. An efficient and flexible system for construction of adenovirus vectors with insertions or deletions in early regions 1 and 3. Proc.Natl.Acad.Sci.U.S.A 91[19], 8802-8806. 1994.

Billingham, M. E. Pathology and etiology of chronic rejection of the heart. Clin.Transplant. 8[3 Pt 2], 289-292. 1994.

Binder, C. J., Chang, M. K., Shaw, P. X., Miller, Y. I., Hartvigsen, K., Dewan, A., and Witztum, J. L. Innate and acquired immunity in atherogenesis. Nat.Med. 8[11], 1218-1226. 2002.

Blease, K., Chen, Y., Hellewell, P. G., and Burke-Gaffney, A. Lipoteichoic acid inhibits lipopolysaccharide-induced adhesion molecule expression and IL-8 release in human lung microvascular endothelial cells. J.Immunol. 163[11], 6139-6147. 1999.

Bode, W., Fernandez-Catalan, C., Grams, F., Gomis-Ruth, F. X., Nagase, H., Tschesche, H., and Maskos, K. Insights into MMP-TIMP interactions. Ann.N.Y.Acad.Sci. 878, 73-91. 1999.

Bode, W. and Maskos, K. Structural basis of the matrix metalloproteinases and their physiological inhibitors, the tissue inhibitors of metalloproteinases. Biol.Chem. 384[6], 863-872. 2003.

Bodzioch, M., Orso, E., Klucken, J., Langmann, T., Bottcher, A., Diederich, W., Drobnik, W., Barlage, S., Buchler, C., Porsch-Ozcurumez, M., Kaminski, W. E., Hahmann, H. W., Oette, K., Rothe, G., Aslanidis, C., Lackner, K. J., and Schmitz, G. The gene encoding ATP-binding cassette transporter 1 is mutated in Tangier disease. Nat.Genet. 22[4], 347-351. 1999.

Boisvert, W. A., Santiago, R., Curtiss, L. K., and Terkeltaub, R. A. A leukocyte homologue of the IL-8 receptor CXCR-2 mediates the accumulation of macrophages in atherosclerotic lesions of LDL receptor- deficient mice. J.Clin.Invest 101[2], 353-363. 1998.

Bonnefoy, A. and Legrand, C. Proteolysis of subendothelial adhesive glycoproteins (fibronectin, thrombospondin, and von Willebrand factor) by plasmin, leukocyte cathepsin G, and elastase. Thromb.Res. 98[4], 323-332. 2000.

Boren, J., Olin, K., Lee, I., Chait, A., Wight, T. N., and Innerarity, T. L. Identification of the principal proteoglycan-binding site in LDL. A single-point mutation in apo-B100 severely affects proteoglycan interaction without affecting LDL receptor binding. J.Clin.Invest 101[12], 2658-2664. 1998.

Brand, K., Eisele, T., Kreusel, U., Page, M., Page, S., Haas, M., Gerling, A., Kaltschmidt, C., Neumann, F. J., Mackman, N., Baeurele, P. A., Walli, A. K., and Neumeier, D. Dysregulation of monocytic nuclear factor-kappa B by oxidized low-density lipoprotein. Arterioscler.Thromb.Vasc.Biol. 17[10], 1901-1909. 1997a.

Brand, K., Page, S., Rogler, G., Bartsch, A., Brandl, R., Knuechel, R., Page, M., Kaltschmidt, C., Baeuerle, P. A., and Neumeier, D. Activated transcription factor nuclear factor-kappa B is present in the atherosclerotic lesion. J.Clin.Invest 97[7], 1715-1722. 1996.

Brand, K., Page, S., Walli, A. K., Neumeier, D., and Baeuerle, P. A. Role of nuclear factor-kappa B in atherogenesis. Exp.Physiol 82[2], 297-304. 1997b.

Breslow, J. L. Mouse models of atherosclerosis. Science 272[5262], 685-688. 1996.

Briles, D. E., Forman, C., Hudak, S., and Claflin, J. L. Anti-phosphorylcholine antibodies of the T15 idiotype are optimally protective against Streptococcus pneumoniae. J.Exp.Med. 156[4], 1177-1185. 1982.

Brophy, C. M., Marks, W. H., Reilly, J. M., and Tilson, M. D. Decreased tissue inhibitor of metalloproteinases (TIMP) in abdominal aortic aneurysm tissue: a preliminary report. J.Surg.Res. 50[6], 653-657. 1991.

Bruder, J. T. and Kovesdi, I. Adenovirus infection stimulates the Raf/MAPK signaling pathway and induces interleukin-8 expression. J.Virol. 71[1], 398-404. 1997.

Buffon, A., Biasucci, L. M., Liuzzo, G., D'Onofrio, G., Crea, F., and Maseri, A. Widespread coronary inflammation in unstable angina. N.Engl.J.Med. 347[1], 5-12. 2002.

Cai, T. Q. and Wright, S. D. Human leukocyte elastase is an endogenous ligand for the integrin CR3 (CD11b/CD18, Mac-1, alpha M beta 2) and modulates polymorphonuclear leukocyte adhesion. J.Exp.Med. 184[4], 1213-1223. 1996.

Calvi, C., Dentelli, P., Pagano, M., Rosso, A., Pegoraro, M., Giunti, S., Garbarino, G., Camussi, G., Pegoraro, L., and Brizzi, M. F. Angiopoietin 2 induces cell cycle arrest in endothelial cells: a possible mechanism involved in advanced plaque neovascularization. Arterioscler.Thromb.Vasc.Biol. 24[3], 511-518. 2004.

Carden, D., Xiao, F., Moak, C., Willis, B. H., Robinson-Jackson, S., and Alexander, S. Neutrophil elastase promotes lung microvascular injury and proteolysis of endothelial cadherins. Am.J.Physiol 275[2 Pt 2], H385-H392. 1998.

Carmeliet, P. Mechanisms of angiogenesis and arteriogenesis. Nat.Med. 6[4], 389-395. 2000.

Carmeliet, P., Moons, L., Dewerchin, M., Mackman, N., Luther, T., Breier, G., Ploplis, V., Muller, M., Nagy, A., Plow, E., Gerard, R., Edgington, T., Risau, W., and Collen, D. Insights in vessel development and vascular disorders using targeted inactivation and transfer of vascular endothelial growth factor, the tissue factor receptor, and the plasminogen system. Ann.N.Y.Acad.Sci. 811, 191-206. 1997.

Carmeliet, P., Moons, L., Luttun, A., Vincenti, V., Compernolle, V., De Mol, M., Wu, Y., Bono, F., Devy, L., Beck, H., Scholz, D., Acker, T., DiPalma, T., Dewerchin, M., Noel, A., Stalmans, I., Barra, A., Blacher, S., Vandendriessche, T., Ponten, A., Eriksson, U., Plate, K. H., Foidart, J. M., Schaper, W., Charnock-Jones, D. S., Hicklin, D. J., Herbert, J. M., Collen, D., and Persico, M. G. Synergism between vascular endothelial growth factor and placental growth factor contributes to angiogenesis and plasma extravasation in pathological conditions. Nat.Med. 7[5], 575-583. 2001.

Cawston, T. E. and Mercer, E. Preferential binding of collagenase to alpha 2-macroglobulin in the presence of the tissue inhibitor of metalloproteinases. FEBS Lett. 209[1], 9-12. 1986.

Celletti, F. L., Waugh, J. M., Amabile, P. G., Brendolan, A., Hilfiker, P. R., and Dake, M. D. Vascular endothelial growth factor enhances atherosclerotic plaque progression. Nat.Med. 7[4], 425-429. 2001.

Chaly, Y. V., Selvan, R. S., Fegeding, K. V., Kolesnikova, T. S., and Voitenok, N. N. Expression of IL-8 gene in human monocytes and lymphocytes: differential regulation by TNF and IL-1. Cytokine 12[6], 636-643. 2000.

Chang, H., Wang, B. W., Kuan, P., and Shyu, K. G. Cyclical mechanical stretch enhances angiopoietin-2 and Tie2 receptor expression in cultured human umbilical vein endothelial cells. Clin.Sci.(Lond) 104[4], 421-428. 2003.

Chang, M. W., Barr, E., Lu, M. M., Barton, K., and Leiden, J. M. Adenovirus-mediated over-expression of the cyclin/cyclin-dependent kinase inhibitor, p21 inhibits vascular smooth muscle cell proliferation and neointima formation in the rat carotid artery model of balloon angioplasty. J.Clin.Invest 96[5], 2260-2268. 1995.

Chen, F. E. and Ghosh, G. Regulation of DNA binding by Rel/NF-kappaB transcription factors: structural views. Oncogene 18[49], 6845-6852. 1999.

Chomczynski, P. A reagent for the single-step simultaneous isolation of RNA, DNA and proteins from cell and tissue samples. Biotechniques 15[3], 532-537. 1993.

Choudhuri, R., Zhang, H. T., Donnini, S., Ziche, M., and Bicknell, R. An angiogenic role for the neurokines midkine and pleiotrophin in tumorigenesis. Cancer Res. 57[9], 1814-1819. 1997.

Chow, J. C., Young, D. W., Golenbock, D. T., Christ, W. J., and Gusovsky, F. Toll-like receptor-4 mediates lipopolysaccharide-induced signal transduction. J.Biol.Chem. 274[16], 10689-10692. 1999.

Claise, C., Edeas, M., Chalas, J., Cockx, A., Abella, A., Capel, L., and Lindenbaum, A. Oxidized low-density lipoprotein induces the production of interleukin- 8 by endothelial cells. FEBS Lett. 398[2-3], 223-227. 1996.

Colles, S. M., Maxson, J. M., Carlson, S. G., and Chisolm, G. M. Oxidized LDL-induced injury and apoptosis in atherosclerosis. Potential roles for oxysterols. Trends Cardiovasc.Med. 11[3-4], 131-138. 2001.

Collins, R. G., Velji, R., Guevara, N. V., Hicks, M. J., Chan, L., and Beaudet, A. L. P-Selectin or intercellular adhesion molecule (ICAM)-1 deficiency substantially protects against atherosclerosis in apolipoprotein E-deficient mice. J.Exp.Med. 191[1], 189-194. 2000.

Collins, T. and Cybulsky, M. I. NF-kappaB: pivotal mediator or innocent bystander in atherogenesis? J.Clin.Invest 107[3], 255-264. 2001.

Cominacini, L., Pasini, A. F., Garbin, U., Davoli, A., Tosetti, M. L., Campagnola, M., Rigoni, A., Pastorino, A. M., Lo, Cascio, V, and Sawamura, T. Oxidized low density lipoprotein (ox-LDL) binding to ox-LDL receptor-1 in endothelial cells induces the activation of NF-kappaB through an increased production of intracellular reactive oxygen species. J.Biol.Chem. 275[17], 12633-12638. 2000.

Cory, A. H., Owen, T. C., Barltrop, J. A., and Cory, J. G. Use of an aqueous soluble tetrazolium/formazan assay for cell growth assays in culture. Cancer Commun. 3[7], 207-212. 1991.

Cotran, R., Kumar, V., and Collins, T. Acute and Chronic Inflammation. In *Robbins Pathological Basis of Disease-6th edition, Chapter 3*. R. A. Cotran ed.W.B Saunders Company, Philadelphia, US., 50-88. 1999.

Cowan, B., Baron, O., Crack, J., Coulber, C., Wilson, G. J., and Rabinovitch, M. Elafin, a serine elastase inhibitor, attenuates post-cardiac transplant coronary arteriopathy and reduces myocardial necrosis in rabbits afer heterotopic cardiac transplantation. J.Clin.Invest 97[11], 2452-2468. 1996.

Cybulsky, M. I. and Gimbrone, M. A., Jr. Endothelial expression of a mononuclear leukocyte adhesion molecule during atherogenesis. Science 251[4995], 788-791. 1991.

Daugherty, A., Dunn, J. L., Rateri, D. L., and Heinecke, J. W. Myeloperoxidase, a catalyst for lipoprotein oxidation, is expressed in human atherosclerotic lesions. J.Clin.Invest 94[1], 437-444. 1994.

Davies, M. J. Pathology of arterial thrombosis. Br.Med.Bull. 50[4], 789-802. 1994.

Davies, M. J., Woolf, N., Rowles, P. M., and Pepper, J. Morphology of the endothelium over atherosclerotic plaques in human coronary arteries. Br.Heart J. 60[6], 459-464. 1988.

de Villiers, W. J. and Smart, E. J. Macrophage scavenger receptors and foam cell formation. J.Leukoc.Biol. 66[5], 740-746. 1999.

Decker, T. and Lohmann-Matthes, M. L. A quick and simple method for the quantitation of lactate dehydrogenase release in measurements of cellular cytotoxicity and tumor necrosis factor (TNF) activity. J.Immunol.Methods 115[1], 61-69. 1988.

Der Thusen, J. H., Kuiper, J., Fekkes, M. L., De Vos, P., Van Berkel, T. J., and Biessen, E. A. Attenuation of atherogenesis by systemic and local adenovirus-mediated gene transfer of interleukin-10 in LDLr-/- mice. FASEB J. 15[14], 2730-2732. 2001.

Devaney, J. M., Greene, C. M., Taggart, C. C., Carroll, T. P., O'Neill, S. J., and McElvaney, N. G. Neutrophil elastase up-regulates interleukin-8 via toll-like receptor 4. FEBS Lett. 544[1-3], 129-132. 2003.

Devitt, A., Moffatt, O. D., Raykundalia, C., Capra, J. D., Simmons, D. L., and Gregory, C. D. Human CD14 mediates recognition and phagocytosis of apoptotic cells. Nature 392[6675], 505-509. 1998.

Dheda, K., Huggett, J. F., Bustin, S. A., Johnson, M. A., Rook, G., and Zumla, A. Validation of housekeeping genes for normalizing RNA expression in real-time PCR. Biotechniques 37[1], 112-119. 2004.

Dichtl, W., Stiko, A., Eriksson, P., Goncalves, I., Calara, F., Banfi, C., Ares, M. P., Hamsten, A., and Nilsson, J. Oxidized LDL and lysophosphatidylcholine stimulate plasminogen activator inhibitor-1 expression in vascular smooth muscle cells. Arterioscler.Thromb.Vasc.Biol. 19[12], 3025-3032. 1999.

Dimmeler, S., Haendeler, J., Galle, J., and Zeiher, A. M. Oxidized low-density lipoprotein induces apoptosis of human endothelial cells by activation of CPP32-like proteases. A mechanistic clue to the 'response to injury' hypothesis. Circulation 95[7], 1760-1763. 1997.

Ding, A., Thieblemont, N., Zhu, J., Jin, F., Zhang, J., and Wright, S. Secretory leukocyte protease inhibitor interferes with uptake of lipopolysaccharide by macrophages. Infect.Immun. 67[9], 4485-4489. 1999.

Dollery, C. M., Owen, C. A., Sukhova, G. K., Krettek, A., Shapiro, S. D., and Libby, P. Neutrophil elastase in human atherosclerotic plaques: production by macrophages. Circulation 107[22], 2829-2836. 2003.

Dong, Z. M., Chapman, S. M., Brown, A. A., Frenette, P. S., Hynes, R. O., and Wagner, D. D. The combined role of P- and E-selectins in atherosclerosis. J.Clin.Invest 102[1], 145-152. 1998.

Duggan, D. J., Bittner, M., Chen, Y., Meltzer, P., and Trent, J. M. Expression profiling using cDNA microarrays. Nat.Genet. 21[1 Suppl], 10-14. 1999.

Dzau, V. J., Mann, M. J., Morishita, R., and Kaneda, Y. Fusigenic viral liposome for gene therapy in cardiovascular diseases. Proc.Natl.Acad.Sci.U.S.A 93[21], 11421-11425. 1996.

Fadok, V. A., Bratton, D. L., Konowal, A., Freed, P. W., Westcott, J. Y., and Henson, P. M. Macrophages that have ingested apoptotic cells in vitro inhibit proinflammatory cytokine production through autocrine/paracrine mechanisms involving TGF-beta, PGE2, and PAF. J.Clin.Invest 101[4], 890-898. 1998.

Falkenberg, M., Tom, C., DeYoung, M. B., Wen, S., Linnemann, R., and Dichek, D. A. Increased expression of urokinase during atherosclerotic lesion development causes arterial constriction and lumen loss, and accelerates lesion growth. Proc.Natl.Acad.Sci.U.S.A 99[16], 10665-10670. 2002.

Fang, X., Weintraub, N. L., Rios, C. D., Chappell, D. A., Zwacka, R. M., Engelhardt, J. F., Oberley, L. W., Yan, T., Heistad, D. D., and Spector, A. A. Overexpression of human superoxide dismutase inhibits oxidation of low-density lipoprotein by endothelial cells. Circ.Res. 82[12], 1289-1297. 1998.

Fasbender, A., Lee, J. H., Walters, R. W., Moninger, T. O., Zabner, J., and Welsh, M. J. Incorporation of adenovirus in calcium phosphate precipitates enhances gene transfer to airway epithelia in vitro and in vivo. J.Clin.Invest 102[1], 184-193. 1998.

Fasbender, A., Zabner, J., Chillon, M., Moninger, T. O., Puga, A. P., Davidson, B. L., and Welsh, M. J. Complexes of adenovirus with polycationic polymers and cationic lipids increase the efficiency of gene transfer in vitro and in vivo. J.Biol.Chem. 272[10], 6479-6489. 1997.

Febbraio, M., Podrez, E. A., Smith, J. D., Hajjar, D. P., Hazen, S. L., Hoff, H. F., Sharma, K., and Silverstein, R. L. Targeted disruption of the class B scavenger receptor CD36 protects against atherosclerotic lesion development in mice. J.Clin.Invest 105[8], 1049-1056. 2000.

Felgner, P. L. Improvements in cationic liposomes for in vivo gene transfer. Hum.Gene Ther. 7[15], 1791-1793. 1996.

Feng, Y., Yang, J. H., Huang, H., Kennedy, S. P., Turi, T. G., Thompson, J. F., Libby, P., and Lee, R. T. Transcriptional profile of mechanically induced genes in human vascular smooth muscle cells. Circ.Res. 85[12], 1118-1123. 1999.

Fink, E., Nettelbeck, R., and Fritz, H. Inhibition of mast cell chymase by eglin c and antileukoprotease (HUSI-I). Indications for potential biological functions of these inhibitors. Biol.Chem.Hoppe Seyler 367[7], 567-571. 1986.

Fischer, B., von Knethen, A., and Brune, B. Dualism of oxidized lipoproteins in provoking and attenuating the oxidative burst in macrophages: role of peroxisome proliferator-activated receptor-gamma. J.Immunol. 168[6], 2828-2834. 2002.

Flegel, W. A., Baumstark, M. W., Weinstock, C., Berg, A., and Northoff, H. Prevention of endotoxin-induced monokine release by human low- and high-density lipoproteins and by apolipoprotein A-I. Infect.Immun. 61[12], 5140-5146. 1993.

Flora, P. K. and Gregory, C. D. Recognition of apoptotic cells by human macrophages: inhibition by a monocyte/macrophage-specific monoclonal antibody. Eur.J.Immunol. 24[11], 2625-2632. 1994.

Fourney, R. M., Miyakoshi, J., Day, R. S., and Paterson, M. C. Northern blotting: Efficient RNA staining and transfer. Focus 10, 5-7. 1988.

Foxwell, B., Browne, K., Bondeson, J., Clarke, C., de Martin, R., Brennan, F., and Feldmann, M. Efficient adenoviral infection with IkappaB alpha reveals that macrophage tumor necrosis factor alpha production in rheumatoid arthritis is NF-kappaB dependent. Proc.Natl.Acad.Sci.U.S.A 95[14], 8211-8215. 1998.

Friedman, G. D., Klatsky, A. L., and Siegelaub, A. B. The leukocyte count as a predictor of myocardial infarction. N.Engl.J.Med. 290[23], 1275-1278. 1974.

Fryer, H. J., Davis, G. E., Manthorpe, M., and Varon, S. Lowry protein assay using an automatic microtiter plate spectrophotometer. Anal.Biochem. 153[2], 262-266. 1986.

Galis, Z. S., Muszynski, M., Sukhova, G. K., Simon-Morrissey, E., Unemori, E. N., Lark, M. W., Amento, E., and Libby, P. Cytokine-stimulated human vascular smooth muscle cells synthesize a complement of enzymes required for extracellular matrix digestion. Circ.Res. 75[1], 181-189. 1994a.

Galis, Z. S., Sukhova, G. K., Kranzhofer, R., Clark, S., and Libby, P. Macrophage foam cells from experimental atheroma constitutively produce matrix-degrading proteinases. Proc.Natl.Acad.Sci.U.S.A 92[2], 402-406. 1995a.

Galis, Z. S., Sukhova, G. K., Lark, M. W., and Libby, P. Increased expression of matrix metalloproteinases and matrix degrading activity in vulnerable regions of human atherosclerotic plaques. J.Clin.Invest 94[6], 2493-2503. 1994b.

Galis, Z. S., Sukhova, G. K., and Libby, P. Microscopic localization of active proteases by in situ zymography: detection of matrix metalloproteinase activity in vascular tissue. FASEB J. 9[10], 974-980. 1995b.

Gandhi, V. C. and Jones, D. J. Protein kinase C modulates the release of [3H]5-hydroxytryptamine in the spinal cord of the rat: the role of L-type voltage-dependent calcium channels. Neuropharmacology 31[11], 1101-1109. 1992.

Gao, Y., Lecker, S., Post, M. J., Hietaranta, A. J., Li, J., Volk, R., Li, M., Sato, K., Saluja, A. K., Steer, M. L., Goldberg, A. L., and Simons, M. Inhibition of ubiquitin-proteasome pathway-mediated I kappa B alpha degradation by a naturally occurring antibacterial peptide. J.Clin.Invest 106[3], 439-448. 2000.

Gerhold, D., Rushmore, T., and Caskey, C. T. DNA chips: promising toys have become powerful tools. Trends Biochem.Sci. 24[5], 168-173. 1999.

Gerszten, R. E., Garcia-Zepeda, E. A., Lim, Y. C., Yoshida, M., Ding, H. A., Gimbrone, M. A., Jr., Luster, A. D., Luscinskas, F. W., and Rosenzweig, A. MCP-1 and IL-8 trigger firm adhesion of monocytes to vascular endothelium under flow conditions. Nature 398[6729], 718-723. 1999.

Gimbrone, M. A., Jr., Cotran, R. S., and Folkman, J. Human vascular endothelial cells in culture. Growth and DNA synthesis. J.Cell Biol. 60[3], 673-684. 1974.

Ginsberg, H. S., Moldawer, L. L., Sehgal, P. B., Redington, M., Kilian, P. L., Chanock, R. M., and Prince, G. A. A mouse model for investigating the molecular pathogenesis of adenovirus pneumonia. Proc.Natl.Acad.Sci.U.S.A 88[5], 1651-1655. 1991.

Gittenberger-de Groot, A. C., DeRuiter, M. C., Bergwerff, M., and Poelmann, R. E. Smooth muscle cell origin and its relation to heterogeneity in development and disease. Arterioscler.Thromb.Vasc.Biol. 19[7], 1589-1594. 1999.

Glass, C. K. and Witztum, J. L. Atherosclerosis. the road ahead. Cell 104[4], 503-516. 2001.

Gosling, J., Slaymaker, S., Gu, L., Tseng, S., Zlot, C. H., Young, S. G., Rollins, B. J., and Charo, I. F. MCP-1 deficiency reduces susceptibility to atherosclerosis in mice that overexpress human apolipoprotein B. J.Clin.Invest 103[6], 773-778. 1999.

Gossen, M. and Bujard, H. Tight control of gene expression in mammalian cells by tetracycline-responsive promoters. Proc.Natl.Acad.Sci.U.S.A 89[12], 5547-5551. 1992.

Graham, F. L. and Prevec, L. Manipulation of adenovirus vectors. In *Methods in Molecular Biology, Vol 7: Gene Transfer and Expression protocols*. Murray E.J., ed. The Humana Press Inc., Clifton, US 109-128. 1991.

Graham, F. L., Smiley, J., Russell, W. C., and Nairn, R. Characteristics of a human cell line transformed by DNA from human adenovirus type 5. J.Gen.Virol. 36[1], 59-74. 1977.

Gravanis. M. B. and Roubin, G. S. Histopathologic phenomena at the site of percutaneous transluminal coronary angioplasty: the problem of restenosis. Hum.Pathol. 20[5], 477-485. 1989.

Grossman, M., Rader, D. J., Muller, D. W., Kolansky, D. M., Kozarsky, K., Clark, B. J., III, Stein, E. A., Lupien, P. J., Brewer, H. B., Jr., Raper, S. E., and . A pilot study of ex vivo gene therapy for homozygous familial hypercholesterolaemia. Nat.Med. 1[11], 1148-1154. 1995.

Gu, L., Okada, Y., Clinton, S. K., Gerard, C., Sukhova, G. K., Libby, P., and Rollins, B. J. Absence of monocyte chemoattractant protein-1 reduces atherosclerosis in low density lipoprotein receptor-deficient mice. Mol.Cell 2[2], 275-281. 1998.

Gurwith, M. J., Horwith, G. S., Impellizzeri, C. A., Davis, A. R., Lubeck, M. D., and Hung, P. P. Current use and future directions of adenovirus vaccine. Semin.Respir.Infect. 4[4], 299-303. 1989.

Guzman, R. J., Lemarchand, P., Crystal, R. G., Epstein, S. E., and Finkel, T. Efficient and selective adenovirus-mediated gene transfer into vascular neointima. Circulation 88[6], 2838-2848. 1993.

Haj-Ahmad, Y. and Graham, F. L. Development of a helper-independent human adenovirus vector and its use in the transfer of the herpes simplex virus thymidine kinase gene. J.Virol. 57[1], 267-274. 1986.

Hale, T. K. and Braithwaite, A. W. The adenovirus oncoprotein E1a stimulates binding of transcription factor ETF to transcriptionally activate the p53 gene. J.Biol.Chem. 274[34], 23777-23786. 1999.

Haley, K. J., Lilly, C. M., Yang, J. H., Feng, Y., Kennedy, S. P., Turi, T. G., Thompson, J. F., Sukhova, G. H., Libby, P., and Lee, R. T. Overexpression of eotaxin and the CCR3 receptor in human atherosclerosis: using genomic technology to identify a potential novel pathway of vascular inflammation. Circulation 102[18], 2185-2189. 2000.

Hamilton, T. A., Major, J. A., Armstrong, D., and Tebo, J. M. Oxidized LDL modulates activation of NFkappaB in mononuclear phagocytes by altering the degradation if IkappaBs. J.Leukoc.Biol. 64[5], 667-674. 1998.

Han, J., Hajjar, D. P., Febbraio, M., and Nicholson, A. C. Native and modified low density lipoproteins increase the functional expression of the macrophage class B scavenger receptor, CD36. J.Biol.Chem. 272[34], 21654-21659. 1997.

Han, J., Sabbatini, P., Perez, D., Rao, L., Modha, D., and White, E. The E1B 19K protein blocks apoptosis by interacting with and inhibiting the p53-inducible and death-promoting Bax protein. Genes Dev. 10[4], 461-477. 1996.

Han, K. H., Han, K. O., Green, S. R., and Quehenberger, O. Expression of the monocyte chemoattractant protein-1 receptor CCR2 is increased in hypercholesterolemia. Differential effects of plasma lipoproteins on monocyte function. J.Lipid Res. 40[6], 1053-1063. 1999.

Hanley, M. E., Terada, L. S., Cheronis, J. C., and Repine, J. E. Endothelial cell associated anti-elastolytic activity. Inflammation 20[3], 327-337. 1996.

Harada-Shiba, M., Kinoshita, M., Kamido, H., and Shimokado, K. Oxidized low density lipoprotein induces apoptosis in cultured human umbilical vein endothelial cells by common and unique mechanisms. J.Biol.Chem. 273[16], 9681-9687. 1998.

Harvey, B. G., Hackett, N. R., El Sawy, T., Rosengart, T. K., Hirschowitz, E. A., Lieberman, M. D., Lesser, M. L., and Crystal, R. G. Variability of human systemic humoral immune responses to adenovirus gene transfer vectors administered to different organs. J.Virol. 73[8], 6729-6742. 1999.

Haubitz, M., Gerlach, M., Kruse, H. J., and Brunkhorst, R. Endothelial tissue factor stimulation by proteinase 3 and elastase. Clin.Exp.Immunol. 126[3], 584-588. 2001.

Hawiger, J., Veach, R. A., Liu, X. Y., Timmons, S., and Ballard, D. W. IkappaB kinase complex is an intracellular target for endotoxic lipopolysaccharide in human monocytic cells. Blood 94[5], 1711-1716. 1999.

Hazen, S. L. and Heinecke, J. W. 3-Chlorotyrosine, a specific marker of myeloperoxidase-catalyzed oxidation, is markedly elevated in low density lipoprotein isolated from human atherosclerotic intima. J.Clin.Invest 99[9], 2075-2081. 1997.

Hedman, M., Hartikainen, J., Syvanne, M., Stjernvall, J., Hedman, A., Kivela, A., Vanninen, E., Mussalo, H., Kauppila, E., Simula, S., Narvanen, O., Rantala, A., Peuhkurinen, K., Nieminen, M. S., Laakso, M., and Yla-Herttuala, S. Safety and feasibility of catheter-based local intracoronary vascular endothelial growth factor gene transfer in the prevention of postangioplasty and in-stent restenosis and in the treatment of chronic myocardial ischemia: phase II results of the Kuopio Angiogenesis Trial (KAT). Circulation 107[21], 2677-2683. 2003.

253

Heery, J. M., Kozak, M., Stafforini, D. M., Jones, D. A., Zimmerman, G. A., McIntyre, T. M., and Prescott, S. M. Oxidatively modified LDL contains phospholipids with platelet-activating factor-like activity and stimulates the growth of smooth muscle cells. J.Clin.Invest 96[5], 2322-2330. 1995.

Hegde, P., Qi, R., Abernathy, K., Gay, C., Dharap, S., Gaspard, R., Hughes, J. E., Snesrud, E., Lee, N., and Quackenbush, J. A concise guide to cDNA microarray analysis. Biotechniques 29[3], 548-4, 556. 2000.

Henkel, T., Machleidt, T., Alkalay, I., Kronke, M., Ben Neriah, Y., and Baeuerle, P. A. Rapid proteolysis of I kappa B-alpha is necessary for activation of transcription factor NF-kappa B. Nature 365[6442], 182-185. 1993.

Henriksen, P. A., Devitt, A., Kotelevtsev, Y., and Sallenave, J. M. Gene delivery of the elastase inhibitor elafin protects macrophages from neutrophil elastase-mediated impairment of apoptotic cell recognition. FEBS Lett. 574[1-3], 80-84. 2004.

Herman, M. P., Sukhova, G. K., Kisiel, W., Foster, D., Kehry, M. R., Libby, P., and Schonbeck, U. Tissue factor pathway inhibitor-2 is a novel inhibitor of matrix metalloproteinases with implications for atherosclerosis. J.Clin.Invest 107[9], 1117-1126. 2001a.

Herman, M. P., Sukhova, G. K., Libby, P., Gerdes, N., Tang, N., Horton, D. B., Kilbride, M., Breitbart, R. E., Chun, M., and Schonbeck, U. Expression of neutrophil collagenase (matrix metalloproteinase-8) in human atheroma: a novel collagenolytic pathway suggested by transcriptional profiling. Circulation 104[16], 1899-1904. 2001b.

Hinek, A., Wrenn, D. S., Mecham, R. P., and Barondes, S. H. The elastin receptor: a galactoside-binding protein. Science 239[4847], 1539-1541. 1988.

Hitt, M., Bett, A. J., Addison, C. L., and Prevec, L. Graham F. L. Techniques for human adenovirus vector construction and characterization. Methods Mol.Genet. 7, 13-30. 1995.

Hochstrasser, K., Reichert, R., Schwarz, S., and Werle, E. [Isolation and characterisation of a protease inhibitor from human bronchial secretion]. Hoppe Seylers.Z.Physiol Chem. 353[2], 221-226. 1972.

Hodge, S., Hodge, G., Scicchitano, R., Reynolds, P. N., and Holmes, M. Alveolar macrophages from subjects with chronic obstructive pulmonary disease are deficient in their ability to phagocytose apoptotic airway epithelial cells. Immunol.Cell Biol. 81[4], 289-296. 2003.

Hornebeck, W., Derouette, J. C., and Robert, L. Isolation, purification and properties of aortic elastase. FEBS Lett. 58[1], 66-70. 1975.

Hoshino, K., Takeuchi, O., Kawai, T., Sanjo, H., Ogawa, T., Takeda, Y., Takeda, K., and Akira, S. Cutting edge: Toll-like receptor 4 (TLR4)-deficient mice are hyporesponsive to lipopolysaccharide: evidence for TLR4 as the Lps gene product. J.Immunol. 162[7], 3749-3752. 1999.

Hu, B., Guo, P., Fang, Q., Tao, H. Q., Wang, D., Nagane, M., Huang, H. J., Gunji, Y., Nishikawa, R., Alitalo, K., Cavenee, W. K., and Cheng, S. Y. Angiopoietin-2 induces human glioma invasion through the activation of matrix metalloprotease-2. Proc.Natl.Acad.Sci.U.S.A 100[15], 8904-8909. 2003.

Huang, Y., Mironova, M., and Lopes-Virella, M. F. Oxidized LDL stimulates matrix metalloproteinase-1 expression in human vascular endothelial cells. Arterioscler.Thromb.Vasc.Biol. 19[11], 2640-2647. 1999.

Huynh, M. L., Fadok, V. A., and Henson, P. M. Phosphatidylserine-dependent ingestion of apoptotic cells promotes TGF-beta1 secretion and the resolution of inflammation. J.Clin.Invest 109[1], 41-50. 2002.

Ishibashi, S., Brown, M. S., Goldstein, J. L., Gerard, R. D., Hammer, R. E., and Herz, J. Hypercholesterolemia in low density lipoprotein receptor knockout mice and its reversal by adenovirus-mediated gene delivery. J.Clin.Invest 92[2], 883-893. 1993.

Jaffe, E. A., Nachman, R. L., Becker, C. G., and Minick, C. R. Culture of human endothelial cells derived from umbilical veins. Identification by morphologic and immunologic criteria. J.Clin.Invest 52[11], 2745-2756. 1973.

Jaffray, C., Mendez, C., Denham, W., Carter, G., and Norman, J. Specific pancreatic enzymes activate macrophages to produce tumor necrosis factor-alpha: role of nuclear factor kappa B and inhibitory kappa B proteins. J.Gastrointest.Surg. 4[4], 370-377. 2000.

Janabi, M., Yamashita, S., Hirano, K., Sakai, N., Hiraoka, H., Matsumoto, K., Zhang, Z., Nozaki, S., and Matsuzawa, Y. Oxidized LDL-induced NF-kappa B activation and subsequent expression of proinflammatory genes are defective in monocyte-derived macrophages from CD36-deficient patients. Arterioscler.Thromb.Vasc.Biol. 20[8], 1953-1960. 2000.

Janciauskiene, S., Moraga, F., and Lindgren, S. C-terminal fragment of alpha1-antitrypsin activates human monocytes to a pro-inflammatory state through interactions with the CD36 scavenger receptor and LDL receptor. Atherosclerosis 158[1], 41-51. 2001.

Janeway, C. A., Jr. and Medzhitov, R. Innate immune recognition. Annu.Rev.Immunol. 20, 197-216. 2002.

Jersmann, H. P., Hii, C. S., Hodge, G. L., and Ferrante, A. Synthesis and surface expression of CD14 by human endothelial cells. Infect.Immun. 69[1], 479-485. 2001.

Jin, F. Y., Nathan, C., Radzioch, D., and Ding, A. Secretory leukocyte protease inhibitor: a macrophage product induced by and antagonistic to bacterial lipopolysaccharide. Cell 88[3], 417-426. 1997.

Jobin, C., Bradham, C. A., Russo, M. P., Juma, B., Narula, A. S., Brenner, D. A., and Sartor, R. B. Curcumin blocks cytokine-mediated NF-kappa B activation and proinflammatory gene expression by inhibiting inhibitory factor I-kappa B kinase activity. J.Immunol. 163[6], 3474-3483. 1999.

Jobin, C., Haskill, S., Mayer, L., Panja, A., and Sartor, R. B. Evidence for altered regulation of I kappa B alpha degradation in human colonic epithelial cells. J.Immunol. 158[1], 226-234. 1997.

Johnson, B. D., Kip, K. E., Marroquin, O. C., Ridker, P. M., Kelsey, S. F., Shaw, L. J., Pepine, C. J., Sharaf, B., Bairey Merz, C. N., Sopko, G., Olson, M. B., and Reis, S. E. Serum amyloid A as a predictor of coronary artery disease and cardiovascular outcome in women: the National Heart, Lung, and Blood Institute-Sponsored Women's Ischemia Syndrome Evaluation (WISE). Circulation 109[6], 726-732. 2004.

255

Jones, C. B., Sane, D. C., and Herrington, D. M. Matrix metalloproteinases: a review of their structure and role in acute coronary syndrome. Cardiovasc.Res. 59[4], 812-823. 2003.

Jornot, L., Morris, M. A., Petersen, H., Moix, I., and Rochat, T. N-acetylcysteine augments adenovirus-mediated gene expression in human endothelial cells by enhancing transgene transcription and virus entry. J.Gene Med. 4[1], 54-65. 2002.

Joslin, G., Griffin, G. L., August, A. M., Adams, S., Fallon, R. J., Senior, R. M., and Perlmutter, D. H. The serpin-enzyme complex (SEC) receptor mediates the neutrophil chemotactic effect of alpha-1 antitrypsin-elastase complexes and amyloid-beta peptide. J.Clin.Invest 90[3], 1150-1154. 1992.

Juan, S. H., Lee, T. S., Tseng, K. W., Liou, J. Y., Shyue, S. K., Wu, K. K., and Chau, L. Y. Adenovirus-mediated heme oxygenase-1 gene transfer inhibits the development of atherosclerosis in apolipoprotein E-deficient mice. Circulation 104[13], 1519-1525. 2001.

Kaiser, S. and Toborek, M. Liposome-mediated high-efficiency transfection of human endothelial cells. J.Vasc.Res. 38[2], 133-143. 2001.

Kaner, R. J., Worgall, S., Leopold, P. L., Stolze, E., Milano, E., Hidaka, C., Ramalingam, R., Hackett, N. R., Singh, R., Bergelson, J., Finberg, R., Falck-Pedersen, E., and Crystal, R. G. Modification of the genetic program of human alveolar macrophages by adenovirus vectors in vitro is feasible but inefficient, limited in part by the low level of expression of the coxsackie/adenovirus receptor. Am.J.Respir.Cell Mol.Biol. 20[3], 361-370. 1999.

Karin, M. The beginning of the end: IkappaB kinase (IKK) and NF-kappaB activation. J.Biol.Chem. 274[39], 27339-27342. 1999.

Kelly, B. D., Hackett, S. F., Hirota, K., Oshima, Y., Cai, Z., Berg-Dixon, S., Rowan, A., Yan, Z., Campochiaro, P. A., and Semenza, G. L. Cell type-specific regulation of angiogenic growth factor gene expression and induction of angiogenesis in nonischemic tissue by a constitutively active form of hypoxia-inducible factor 1. Circ.Res. 93[11], 1074-1081. 2003.

Kienast, J., Padro, T., Steins, M., Li, C. X., Schmid, K. W., Hammel, D., Scheld, H. H., and van de Loo, J. C. Relation of urokinase-type plasminogen activator expression to presence and severity of atherosclerotic lesions in human coronary arteries. Thromb.Haemost. 79[3], 579-586. 1998.

Kim, I., Kim, J. H., Moon, S. O., Kwak, H. J., Kim, N. G., and Koh, G. Y. Angiopoietin-2 at high concentration can enhance endothelial cell survival through the phosphatidylinositol 3'-kinase/Akt signal transduction pathway. Oncogene 19[39], 4549-4552. 2000a.

Kim, I., Kim, J. H., Ryu, Y. S., Jung, S. H., Nah, J. J., and Koh, G. Y. Characterization and expression of a novel alternatively spliced human angiopoietin-2. J.Biol.Chem. 275[24], 18550-18556. 2000b.

Kim, I., Kim, J. H., Ryu, Y. S., Liu, M., and Koh, G. Y. Tumor necrosis factor-alpha upregulates angiopoietin-2 in human umbilical vein endothelial cells. Biochem.Biophys.Res.Commun. 269[2], 361-365. 2000c.

Kim, I., Moon, S. O., Han, C. Y., Pak, Y. K., Moon, S. K., Kim, J. J., and Koh, G. Y. The angiopoietin-tie2 system in coronary artery endothelium prevents oxidized low-density lipoprotein-induced apoptosis. Cardiovasc.Res. 49[4], 872-881. 2001.

Kinscherf, R., Claus, R., Wagner, M., Gehrke, C., Kamencic, H., Hou, D., Nauen, O., Schmiedt, W., Kovacs, G., Pill, J., Metz, J., and Deigner, H. P. Apoptosis caused by oxidized LDL is manganese superoxide dismutase and p53 dependent. FASEB J. 12[6], 461-467. 1998.

Kluth, D. C., Ainslie, C. V., Pearce, W. P., Finlay, S., Clarke, D., Anegon, I., and Rees, A. J. Macrophages transfected with adenovirus to express IL-4 reduce inflammation in experimental glomerulonephritis. J.Immunol. 166[7], 4728-4736. 2001.

Koch, A. E., Kunkel, S. L., Pearce, W. H., Shah, M. R., Parikh, D., Evanoff, H. L., Haines, G. K., Burdick, M. D., and Strieter, R. M. Enhanced production of the chemotactic cytokines interleukin-8 and monocyte chemoattractant protein-1 in human abdominal aortic aneurysms. Am.J.Pathol. 142[5], 1423-1431. 1993.

Kohn, D. B., Sadelain, M., and Glorioso, J. C. Occurrence of leukaemia following gene therapy of X-linked SCID. Nat.Rev.Cancer 3[7], 477-488. 2003.

Koopman, G., Reutelingsperger, C. P., Kuijten, G. A., Keehnen, R. M., Pals, S. T., and van Oers, M. H. Annexin V for flow cytometric detection of phosphatidylserine expression on B cells undergoing apoptosis. Blood 84[5], 1415-1420. 1994.

Kosar, F., Varol, E., Ayaz, S., Kutuk, E., Oguzhan, A., and Diker, E. Plasma leukocyte elastase concentration and coronary artery disease. Angiology 49[3], 193-201. 1998.

Kotin, R. M., Linden, R. M., and Berns, K. I. Characterization of a preferred site on human chromosome 19q for integration of adeno-associated virus DNA by non-homologous recombination. EMBO J. 11[13], 5071-5078. 1992.

Kozarsky, K. F., Jooss, K., Donahee, M., Strauss, J. F., III, and Wilson, J. M. Effective treatment of familial hypercholesterolaemia in the mouse model using adenovirus-mediated transfer of the VLDL receptor gene. Nat.Genet. 13[1], 54-62. 1996.

Kremer, E. J. and Perricaudet, M. Adenovirus and adeno-associated virus mediated gene transfer. Br.Med.Bull. 51[1], 31-44. 1995.

Kuo, C. C., Gown, A. M., Benditt, E. P., and Grayston, J. T. Detection of Chlamydia pneumoniae in aortic lesions of atherosclerosis by immunocytochemical stain. Arterioscler.Thromb. 13[10], 1501-1504. 1993a.

Kuo, C. C., Shor, A., Campbell, L. A., Fukushi, H., Patton, D. L., and Grayston, J. T. Demonstration of Chlamydia pneumoniae in atherosclerotic lesions of coronary arteries. J.Infect.Dis. 167[4], 841-849. 1993b.

Laitinen, M., Hartikainen, J., Hiltunen, M. O., Eranen, J., Kiviniemi, M., Narvanen, O., Makinen, K., Manninen, H., Syvanne, M., Martin, J. F., Laakso, M., and Yla-Herttuala, S. Catheter-mediated vascular endothelial growth factor gene transfer to human coronary arteries after angioplasty. Hum.Gene Ther. 11[2], 263-270. 2000.

Laitinen, M., Zachary, I., Breier, G., Pakkanen, T., Hakkinen, T., Luoma, J., Abedi, H., Risau, W., Soma, M., Laakso, M., Martin, J. F., and Yla-Herttuala, S. VEGF gene transfer reduces intimal thickening via increased production of nitric oxide in carotid arteries. Hum.Gene Ther. 8[15], 1737-1744. 1997.

Le Barillec, K., Si-Tahar, M., Balloy, V., and Chignard, M. Proteolysis of monocyte CD14 by human leukocyte elastase inhibits lipopolysaccharide-mediated cell activation. Journal of Clinical Investigation 103[7], 1039-1046. 1999.

Ledgerwood, E. C., Pober, J. S., and Bradley, J. R. Recent advances in the molecular basis of TNF signal transduction. Lab Invest 79[9], 1041-1050. 1999.

Lee, H., Shi, W., Tontonoz, P., Wang, S., Subbanagounder, G., Hedrick, C. C., Hama, S., Borromeo, C., Evans, R. M., Berliner, J. A., and Nagy, L. Role for peroxisome proliferator-activated receptor alpha in oxidized phospholipid-induced synthesis of monocyte chemotactic protein-1 and interleukin-8 by endothelial cells. Circ.Res. 87[6], 516-521. 2000a.

Lee, J. J. and Costlow, N. A. A molecular titration assay to measure transcript prevalence levels. Methods Enzymol. 152, 633-648. 1987.

Lee, M. L., Kuo, F. C., Whitmore, G. A., and Sklar, J. Importance of replication in microarray gene expression studies: statistical methods and evidence from repetitive cDNA hybridizations. Proc.Natl.Acad.Sci.U.S.A 97[18], 9834-9839. 2000b.

Lee, R. T. and Libby, P. The unstable atheroma. Arterioscler.Thromb.Vasc.Biol. 17[10], 1859-1867. 1997.

Lee, S. W., Trapnell, B. C., Rade, J. J., Virmani, R., and Dichek, D. A. In vivo adenoviral vector-mediated gene transfer into balloon-injured rat carotid arteries. Circ.Res. 73[5], 797-807. 1993.

Lee, W. L. and Downey, G. P. Leukocyte elastase - Physiological functions and role in acute lung injury. American Journal of Respiratory and Critical Care Medicine 164[5], 896-904. 2001.

Lehr, H. A., Sagban, T. A., Ihling, C., Zahringer, U., Hungerer, K. D., Blumrich, M., Reifenberg, K., and Bhakdi, S. Immunopathogenesis of atherosclerosis: endotoxin accelerates atherosclerosis in rabbits on hypercholesterolemic diet. Circulation 104[8], 914-920. 2001.

Lei, Z. B., Zhang, Z., Jing, Q., Qin, Y. W., Pei, G., Cao, B. Z., and Li, X. Y. OxLDL upregulates CXCR2 expression in monocytes via scavenger receptors and activation of p38 mitogen-activated protein kinase. Cardiovasc.Res. 53[2], 524-532. 2002.

Lentsch, A. B., Jordan, J. A., Czermak, B. J., Diehl, K. M., Younkin, E. M., Sarma, V., and Ward, P. A. Inhibition of NF-kappaB activation and augmentation of IkappaBbeta by secretory leukocyte protease inhibitor during lung inflammation. Am.J.Pathol. 154[1], 239-247. 1999a.

Lentsch, A. B., Yoshidome, H., Warner, R. L., Ward, P. A., and Edwards, M. J. Secretory leukocyte protease inhibitor in mice regulates local and remote organ inflammatory injury induced by hepatic ischemia/reperfusion. Gastroenterology 117[4], 953-961. 1999b.

Levels, J. H., Abraham, P. R., van den, Ende A., and van Deventer, S. J. Distribution and kinetics of lipoprotein-bound endotoxin. Infect.Immun. 69[5], 2821-2828. 2001.

Lewin, M. H., Arthur, J. R., Riemersma, R. A., Nicol, F., Walker, S. W., Millar, E. M., Howie, A. F., and Beckett, G. J. Selenium supplementation acting through the induction of thioredoxin reductase and glutathione peroxidase protects the human endothelial cell line EAhy926 from damage by lipid hydroperoxides. Biochim.Biophys.Acta 1593[1], 85-92. 2002.

258

Li, D., Liu, L., Chen, H., Sawamura, T., Ranganathan, S., and Mehta, J. L. LOX-1 mediates oxidized low-density lipoprotein-induced expression of matrix metalloproteinases in human coronary artery endothelial cells. Circulation 107[4], 612-617. 2003.

Li, D. and Mehta, J. L. Antisense to LOX-1 inhibits oxidized LDL-mediated upregulation of monocyte chemoattractant protein-1 and monocyte adhesion to human coronary artery endothelial cells. Circulation 101[25], 2889-2895. 2000.

Li, E., Stupack, D., Klemke, R., Cheresh, D. A., and Nemerow, G. R. Adenovirus endocytosis via alpha(v) integrins requires phosphoinositide-3-OH kinase. J.Virol. 72[3], 2055-2061. 1998.

Lieber, M., Smith, B., Szakal, A., Nelson-Rees, W., and Todaro, G. A continuous tumor-cell line from a human lung carcinoma with properties of type II alveolar epithelial cells. Int.J.Cancer 17[1], 62-70. 1976.

Lin, H., Parmacek, M. S., Morle, G., Bolling, S., and Leiden, J. M. Expression of recombinant genes in myocardium in vivo after direct injection of DNA. Circulation 82[6], 2217-2221. 1990.

Lin, K. F., Chao, J., and Chao, L. Atrial natriuretic peptide gene delivery attenuates hypertension, cardiac hypertrophy, and renal injury in salt-sensitive rats. Hum.Gene Ther. 9[10], 1429-1438. 1998.

Lin, K. F., Chao, L., and Chao, J. Prolonged reduction of high blood pressure with human nitric oxide synthase gene delivery. Hypertension 30[3 Pt 1], 307-313. 1997.

Lobov, I. B., Brooks, P. C., and Lang, R. A. Angiopoietin-2 displays VEGF-dependent modulation of capillary structure and endothelial cell survival in vivo. Proc.Natl.Acad.Sci.U.S.A 99[17], 11205-11210. 2002.

Losordo, D. W., Isner, J. M., and Diaz-Sandoval, L. J. Endothelial recovery: the next target in restenosis prevention. Circulation 107[21], 2635-2637. 2003.

Maisonpierre, P. C., Suri, C., Jones, P. F., Bartunkova, S., Wiegand, S. J., Radziejewski, C., Compton, D., McClain, J., Aldrich, T. H., Papadopoulos, N., Daly, T. J., Davis, S., Sato, T. N., and Yancopoulos, G. D. Angiopoietin-2, a natural antagonist for Tie2 that disrupts in vivo angiogenesis. Science 277[5322], 55-60. 1997.

Maizel, J. V., Jr., White, D. O., and Scharff, M. D. The polypeptides of adenovirus. I. Evidence for multiple protein components in the virion and a comparison of types 2, 7A, and 12. Virology 36[1], 115-125. 1968.

Makin, A. J., Blann, A. D., Chung, N. A., Silverman, S. H., and Lip, G. Y. Assessment of endothelial damage in atherosclerotic vascular disease by quantification of circulating endothelial cells. Relationship with von Willebrand factor and tissue factor. Eur.Heart J. 25[5], 371-376. 2004.

Mansell, A., Reinicke, A., Worrall, D. M., and O'Neill, L. A. The serine protease inhibitor antithrombin III inhibits LPS-mediated NF- kappaB activation by TLR-4. FEBS Lett. 508[3], 313-317. 2001.

McCutcheon, J. C., Hart, S. P., Canning, M., Ross, K., Humphries, M. J., and Dransfield, I. Regulation of macrophage phagocytosis of apoptotic neutrophils by adhesion to fibronectin. J.Leukoc.Biol. 64[5], 600-607. 1998.

McNeely, T. B., Shugars, D. C., Rosendahl, M., Tucker, C., Eisenberg, S. P., and Wahl, S. M. Inhibition of human immunodeficiency virus type 1 infectivity by secretory leukocyte protease inhibitor occurs prior to viral reverse transcription. Blood 90[3], 1141-1149. 1997.

Medzhitov, R. and Janeway, C., Jr. Innate immunity. N.Engl.J.Med. 343[5], 338-344. 2000.

Medzhitov, R. and Janeway, C. A., Jr. Decoding the patterns of self and nonself by the innate immune system. Science 296[5566], 298-300. 2002.

Mei, Y. F. and Wadell, G. Molecular determinants of adenovirus tropism. Curr.Top.Microbiol.Immunol. 199 (Pt 3), 213-228. 1995.

Miller, A. D. Retroviral vectors. Curr.Top.Microbiol.Immunol. 158, 1-24. 1992.

Mochizuki, S., Brassart, B., and Hinek, A. Signaling pathways transduced through the elastin receptor facilitate proliferation of arterial smooth muscle cells. J.Biol.Chem. 277[47], 44854-44863. 2002.

Mohacsi, A., Kozlovszky, B., Kiss, I., Seres, I., and Fulop, T., Jr. Neutrophils obtained from obliterative atherosclerotic patients exhibit enhanced resting respiratory burst and increased degranulation in response to various stimuli. Biochim.Biophys.Acta 1316[3], 210-216. 1996.

Molhuizen, H. O. and Schalkwijk, J. Structural, biochemical, and cell biological aspects of the serine proteinase inhibitor SKALP/elafin/ESI. Biol.Chem.Hoppe Seyler 376[1], 1-7. 1995.

Moreau, M., Brocheriou, I., Petit, L., Ninio, E., Chapman, M. J., and Rouis, M. Interleukin-8 mediates downregulation of tissue inhibitor of metalloproteinase-1 expression in cholesterol-loaded human macrophages: relevance to stability of atherosclerotic plaque. Circulation 99[3], 420-426. 1999.

Morel, D. W., DiCorleto, P. E., and Chisolm, G. M. Endothelial and smooth muscle cells alter low density lipoprotein in vitro by free radical oxidation. Arteriosclerosis 4[4], 357-364. 1984.

Morisato, D. and Anderson, K. V. The spatzle gene encodes a component of the extracellular signaling pathway establishing the dorsal-ventral pattern of the Drosophila embryo. Cell 76[4], 677-688. 1994.

Moriwaki, H., Kume, N., Sawamura, T., Aoyama, T., Hoshikawa, H., Ochi, H., Nishi, E., Masaki, T., and Kita, T. Ligand specificity of LOX-1, a novel endothelial receptor for oxidized low density lipoprotein. Arterioscler.Thromb.Vasc.Biol. 18[10], 1541-1547. 1998.

Morris, A. D. Considerations in assessing effectiveness and costs of diabetes care: lessons from DARTS. Diabetes Metab Res.Rev. 18 Suppl 3, S32-S35. 2002.

Morrison, H. M., Welgus, H. G., Stockley, R. A., Burnett, D., and Campbell, E. J. Inhibition of human leukocyte elastase bound to elastin: relative ineffectiveness and two mechanisms of inhibitory activity. Am.J.Respir.Cell Mol.Biol. 2[3], 263-269. 1990.

Moulton, K. S., Heller, E., Konerding, M. A., Flynn, E., Palinski, W., and Folkman, J. Angiogenesis inhibitors endostatin or TNP-470 reduce intimal neovascularization and plaque growth in apolipoprotein E-deficient mice. Circulation 99[13], 1726-1732. 1999.

Moulton, K. S., Vakili, K., Zurakowski, D., Soliman, M., Butterfield, C., Sylvin, E., Lo, K. M., Gillies, S., Javaherian, K., and Folkman, J. Inhibition of plaque neovascularization reduces macrophage accumulation and progression of advanced atherosclerosis. Proc.Natl.Acad.Sci.U.S.A 100[8], 4736-4741. 2003.

Mukaida, N., Okamoto, S., Ishikawa, Y., and Matsushima, K. Molecular mechanism of interleukin-8 gene expression. J.Leukoc.Biol. 56[5], 554-558. 1994.

Mulligan, M. S., Lentsch, A. B., Huber-Lang, M., Guo, R. F., Sarma, V., Wright, C. D., Ulich, T. R., and Ward, P. A. Anti-inflammatory effects of mutant forms of secretory leukocyte protease inhibitor. Am.J.Pathol. 156[3], 1033-1039. 2000.

Muruve, D. A., Barnes, M. J., Stillman, I. E., and Libermann, T. A. Adenoviral gene therapy leads to rapid induction of multiple chemokines and acute neutrophil-dependent hepatic injury in vivo. Hum.Gene Ther. 10[6], 965-976. 1999.

Mutin, M., Canavy, I., Blann, A., Bory, M., Sampol, J., and Dignat-George, F. Direct evidence of endothelial injury in acute myocardial infarction and unstable angina by demonstration of circulating endothelial cells. Blood 93[9], 2951-2958. 1999.

Muzyczka, N. Use of adeno-associated virus as a general transduction vector for mammalian cells. Curr.Top.Microbiol.Immunol. 158, 97-129. 1992.

Naghavi, M., Libby, P., Falk, E., Casscells, S. W., Litovsky, S., Rumberger, J., Badimon, J. J., Stefanadis, C., Moreno, P., Pasterkamp, G., Fayad, Z., Stone, P. H., Waxman, S., Raggi, P., Madjid, M., Zarrabi, A., Burke, A., Yuan, C., Fitzgerald, P. J., Siscovick, D. S., de Korte, C. L., Aikawa, M., Airaksinen, K. E., Assmann, G., Becker, C. R., Chesebro, J. H., Farb, A., Galis, Z. S., Jackson, C., Jang, I. K., Koenig, W., Lodder, R. A., March, K., Demirovic, J., Navab, M., Priori, S. G., Rekhter, M. D., Bahr, R., Grundy, S. M., Mehran, R., Colombo, A., Boerwinkle, E., Ballantyne, C., Insull, W., Jr., Schwartz, R. S., Vogel, R., Serruys, P. W., Hansson, G. K., Faxon, D. P., Kaul, S., Drexler, H., Greenland, P., Muller, J. E., Virmani, R., Ridker, P. M., Zipes, D. P., Shah, P. K., and Willerson, J. T. From vulnerable plaque to vulnerable patient: a call for new definitions and risk assessment strategies: Part II. Circulation 108[15], 1772-1778. 2003a.

Naghavi, M., Libby, P., Falk, E., Casscells, S. W., Litovsky, S., Rumberger, J., Badimon, J. J., Stefanadis, C., Moreno, P., Pasterkamp, G., Fayad, Z., Stone, P. H., Waxman, S., Raggi, P., Madjid, M., Zarrabi, A., Burke, A., Yuan, C., Fitzgerald, P. J., Siscovick, D. S., de Korte, C. L., Aikawa, M., Juhani Airaksinen, K. E., Assmann, G., Becker, C. R., Chesebro, J. H., Farb, A., Galis, Z. S., Jackson, C., Jang, I. K., Koenig, W., Lodder, R. A., March, K., Demirovic, J., Navab, M., Priori, S. G., Rekhter, M. D., Bahr, R., Grundy, S. M., Mehran, R., Colombo, A., Boerwinkle, E., Ballantyne, C., Insull, W., Jr., Schwartz, R. S., Vogel, R., Serruys, P. W., Hansson, G. K., Faxon, D. P., Kaul, S., Drexler, H., Greenland, P., Muller, J. E., Virmani, R., Ridker, P. M., Zipes, D. P., Shah, P. K., and Willerson, J. T. From vulnerable plaque to vulnerable patient: a call for new definitions and risk assessment strategies: Part I. Circulation 108[14], 1664-1672. 2003b.

Nakamura, H., Yoshimura, K., Jaffe, H. A., and Crystal, R. G. Interleukin-8 gene expression in human bronchial epithelial cells. J.Biol.Chem. 266[29], 19611-19617. 1991.

Napoli, C., D'Armiento, F. P., Mancini, F. P., Postiglione, A., Witztum, J. L., Palumbo, G., and Palinski, W. Fatty streak formation occurs in human fetal aortas and is greatly enhanced by maternal hypercholesterolemia. Intimal accumulation of low density lipoprotein and its oxidation precede monocyte recruitment into early atherosclerotic lesions. J.Clin.Invest 100[11], 2680-2690. 1997.

261

Nara, K., Ito, S., Ito, T., Suzuki, Y., Ghoneim, M. A., Tachibana, S., and Hirose, S. Elastase inhibitor elafin is a new type of proteinase inhibitor which has a transglutaminase-mediated anchoring sequence termed "cementoin". J.Biochem.(Tokyo) 115[3], 441-448. 1994.

Navab, M., Berliner, J. A., Watson, A. D., Hama, S. Y., Territo, M. C., Lusis, A. J., Shih, D. M., Van Lenten, B. J., Frank, J. S., Demer, L. L., Edwards, P. A., and Fogelman, A. M. The Yin and Yang of oxidation in the development of the fatty streak. A review based on the 1994 George Lyman Duff Memorial Lecture. Arterioscler.Thromb.Vasc.Biol. 16[7], 831-842. 1996.

Nemoto, E., Sugawara, S., Tada, H., Takada, H., Shimauchi, H., and Horiuchi, H. Cleavage of CD14 on human gingival fibroblasts cocultured with activated neutrophils is mediated by human leukocyte elastase resulting in down-regulation of lipopolysaccharide-induced IL-8 production. Journal of Immunology 165[10], 5807-5813. 2000.

Netea, M. G., Demacker, P. N., Kullberg, B. J., Boerman, O. C., Verschueren, I., Stalenhoef, A. F., and van der Meer, J. W. Low-density lipoprotein receptor-deficient mice are protected against lethal endotoxemia and severe gram-negative infections. J.Clin.Invest 97[6], 1366-1372. 1996.

Nettelbeck, D. M., Miller, D. W., Jerome, V., Zuzarte, M., Watkins, S. J., Hawkins, R. E., Muller, R., and Kontermann, R. E. Targeting of adenovirus to endothelial cells by a bispecific single-chain diabody directed against the adenovirus fiber knob domain and human endoglin (CD105). Mol.Ther. 3[6], 882-891. 2001.

Newby, D. E. and Fox, K. A. Invasive assessment of the coronary circulation: intravascular ultrasound and Doppler. Br.J.Clin.Pharmacol. 53[6], 561-575. 2002.

Newman, P. J. The biology of PECAM-1. J.Clin.Invest 100[11 Suppl], S25-S29. 1997.

Ng, P., Parks, R. J., Cummings, D. T., Evelegh, C. M., Sankar, U., and Graham, F. L. A high-efficiency Cre/loxP-based system for construction of adenoviral vectors. Hum.Gene Ther. 10[16], 2667-2672. 1999.

Nicklin, S. A., White, S. J., Watkins, S. J., Hawkins, R. E., and Baker, A. H. Selective targeting of gene transfer to vascular endothelial cells by use of peptides isolated by phage display. Circulation 102[2], 231-237. 2000.

No, D., Yao, T. P., and Evans, R. M. Ecdysone-inducible gene expression in mammalian cells and transgenic mice. Proc.Natl.Acad.Sci.U.S.A 93[8], 3346-3351. 1996.

Numaguchi, Y., Naruse, K., Harada, M., Osanai, H., Mokuno, S., Murase, K., Matsui, H., Toki, Y., Ito, T., Okumura, K., and Hayakawa, T. Prostacyclin synthase gene transfer accelerates reendothelialization and inhibits neointimal formation in rat carotid arteries after balloon injury. Arterioscler.Thromb.Vasc.Biol. 19[3], 727-733. 1999.

Nykanen, A. I., Krebs, R., Saaristo, A., Turunen, P., Alitalo, K., Yla-Herttuala, S., Koskinen, P. K., and Lemstrom, K. B. Angiopoietin-1 protects against the development of cardiac allograft arteriosclerosis. Circulation 107[9], 1308-1314. 2003.

O'Blenes, S. B., Zaidi, S. H., Cheah, A. Y., McIntyre, B., Kaneda, Y., and Rabinovitch, M. Gene transfer of the serine elastase inhibitor elafin protects against vein graft degeneration. Circulation 102[19 Suppl 3], III289-III295. 2000.

Ochiumi, T., Tanaka, S., Oka, S., Hiyama, T., Ito, M., Kitadai, Y., Haruma, K., and Chayama, K. Clinical significance of angiopoietin-2 expression at the deepest invasive tumor site of advanced colorectal carcinoma. Int.J.Oncol. 24[3], 539-547. 2004.

Odaka, C., Mizuochi, T., Yang, J., and Ding, A. Murine macrophages produce secretory leukocyte protease inhibitor during clearance of apoptotic cells: implications for resolution of the inflammatory response. J.Immunol. 171[3], 1507-1514. 2003.

Oh, H., Takagi, H., Suzuma, K., Otani, A., Matsumura, M., and Honda, Y. Hypoxia and vascular endothelial growth factor selectively up-regulate angiopoietin-2 in bovine microvascular endothelial cells. J.Biol.Chem. 274[22], 15732-15739. 1999.

Ohlsson, K. and Tegner, H. Inhibition of elastase from granulocytes by the low molecular weight bronchial protease inhibitor. Scand.J.Clin.Lab Invest 36[5], 437-445. 1976.

Ohta, K., Nakajima, T., Cheah, A. Y., Zaidi, S. H., Kaviani, N., Dawood, F., You, X. M., Liu, P., Husain, M., and Rabinovitch, M. Elafin-overexpressing mice have improved cardiac function after myocardial infarction. Am.J.Physiol Heart Circ.Physiol 287[1], H286-H292. 2004.

Okamoto, Y., Kihara, S., Ouchi, N., Nishida, M., Arita, Y., Kumada, M., Ohashi, K., Sakai, N., Shimomura, I., Kobayashi, H., Terasaka, N., Inaba, T., Funahashi, T., and Matsuzawa, Y. Adiponectin reduces atherosclerosis in apolipoprotein E-deficient mice. Circulation 106[22], 2767-2770. 2002.

Okura, Y., Brink, M., Itabe, H., Scheidegger, K. J., Kalangos, A., and Delafontaine, P. Oxidized low-density lipoprotein is associated with apoptosis of vascular smooth muscle cells in human atherosclerotic plaques. Circulation 102[22], 2680-2686. 2000.

Owen, C. A., Campbell, M. A., Boukedes, S. S., and Campbell, E. J. Cytokines regulate membrane-bound leukocyte elastase on neutrophils: a novel mechanism for effector activity. Am.J.Physiol 272[3 Pt 1], L385-L393. 1997.

Padrines, M., Wolf, M., Walz, A., and Baggiolini, M. Interleukin-8 processing by neutrophil elastase, cathepsin G and proteinase-3. FEBS Lett. 352[2], 231-235. 1994.

Pahl, H. L., Sester, M., Burgert, H. G., and Baeuerle, P. A. Activation of transcription factor NF-kappaB by the adenovirus E3/19K protein requires its ER retention. J.Cell Biol. 132[4], 511-522. 1996.

Papapetropoulos, A., Garcia-Cardena, G., Dengler, T. J., Maisonpierre, P. C., Yancopoulos, G. D., and Sessa, W. C. Direct actions of angiopoietin-1 on human endothelium: evidence for network stabilization, cell survival, and interaction with other angiogenic growth factors. Lab Invest 79[2], 213-223. 1999.

Parhami, F., Fang, Z. T., Fogelman, A. M., Andalibi, A., Territo, M. C., and Berliner, J. A. Minimally modified low density lipoprotein-induced inflammatory responses in endothelial cells are mediated by cyclic adenosine monophosphate. J.Clin.Invest 92[1], 471-478. 1993.

Perlmutter, D. H., Glover, G. I., Rivetna, M., Schasteen, C. S., and Fallon, R. J. Identification of a serpin-enzyme complex receptor on human hepatoma cells and human monocytes. Proc.Natl.Acad.Sci.U.S.A 87[10], 3753-3757. 1990.

Pier, G. B., Markham, R. B., and Eardley, D. Correlation of the biologic responses of C3H/HEJ mice to endotoxin with the chemical and structural properties of the lipopolysaccharides from Pseudomonas aeruginosa and Escherichia coli. J.Immunol. 127[1], 184-191. 1981.

Pitas, R. E. Expression of the acetyl low density lipoprotein receptor by rabbit fibroblasts and smooth muscle cells. Up-regulation by phorbol esters. J.Biol.Chem. 265[21], 12722-12727. 1990.

Poole, J. C. and Florey, H. W. Changes in the endothelium of the aorta and the behaviour of macrophages in experimental atheroma of rabbits. J.Pathol.Bacteriol. 75[2], 245-251. 1958.

Poston, R. N., Haskard, D. O., Coucher, J. R., Gall, N. P., and Johnson-Tidey, R. R. Expression of intercellular adhesion molecule-1 in atherosclerotic plaques. Am.J.Pathol. 140[3], 665-673. 1992.

Quarck, R., De Geest, B., Stengel, D., Mertens, A., Lox, M., Theilmeier, G., Michiels, C., Raes, M., Bult, H., Collen, D., Van Veldhoven, P., Ninio, E., and Holvoet, P. Adenovirus-mediated gene transfer of human platelet-activating factor-acetylhydrolase prevents injury-induced neointima formation and reduces spontaneous atherosclerosis in apolipoprotein E-deficient mice. Circulation 103[20], 2495-2500. 2001.

Quinn, M. T., Parthasarathy, S., Fong, L. G., and Steinberg, D. Oxidatively modified low density lipoproteins: a potential role in recruitment and retention of monocyte/macrophages during atherogenesis. Proc.Natl.Acad.Sci.U.S.A 84[9], 2995-2998. 1987.

Quinn, M. T., Parthasarathy, S., and Steinberg, D. Lysophosphatidylcholine: a chemotactic factor for human monocytes and its potential role in atherogenesis. Proc.Natl.Acad.Sci.U.S.A 85[8], 2805-2809. 1988.

Rabbi, M. F., Saifuddin, M., Gu, D. S., Kagnoff, M. F., and Roebuck, K. A. U5 region of the human immunodeficiency virus type 1 long terminal repeat contains TRE-like cAMP-responsive elements that bind both AP-1 and CREB/ATF proteins. Virology 233[1], 235-245. 1997.

Rabinovitch, M. EVE and beyond, retro and prospective insights. Am.J.Physiol 277[1 Pt 1], L5-12. 1999.

Rajavashisth, T. B., Andalibi, A., Territo, M. C., Berliner, J. A., Navab, M., Fogelman, A. M., and Lusis, A. J. Induction of endothelial cell expression of granulocyte and macrophage colony-stimulating factors by modified low-density lipoproteins. Nature 344[6263], 254-257. 1990.

Rajavashisth, T. B., Liao, J. K., Galis, Z. S., Tripathi, S., Laufs, U., Tripathi, J., Chai, N. N., Xu, X. P., Jovinge, S., Shah, P. K., and Libby, P. Inflammatory cytokines and oxidized low density lipoproteins increase endothelial cell expression of membrane type 1-matrix metalloproteinase. J.Biol.Chem. 274[17], 11924-11929. 1999a.

Rajavashisth, T. B., Xu, X. P., Jovinge, S., Meisel, S., Xu, X. O., Chai, N. N., Fishbein, M. C., Kaul, S., Cercek, B., Sharifi, B., and Shah, P. K. Membrane type 1 matrix metalloproteinase expression in human atherosclerotic plaques: evidence for activation by proinflammatory mediators. Circulation 99[24], 3103-3109. 1999b.

Ramalingam, R., Rafii, S., Worgall, S., Brough, D. E., and Crystal, R. G. E1(-)E4(+) adenoviral gene transfer vectors function as a "pro-life" signal to promote survival of primary human endothelial cells. Blood 93[9], 2936-2944. 1999a.

Ramalingam, R., Rafii, S., Worgall, S., Hackett, N. R., and Crystal, R. G. Induction of endogenous genes following infection of human endothelial cells with an E1(-) E4(+) adenovirus gene transfer vector. J.Virol. 73[12], 10183-10190. 1999b.

Randi, A. M., Biguzzi, E., Falciani, F., Merlini, P., Blakemore, S., Bramucci, E., Lucreziotti, S., Lennon, M., Faioni, E. M., Ardissino, D., and Mannucci, P. M. Identification of differentially expressed genes in coronary atherosclerotic plaques from patients with stable or unstable angina by cDNA array analysis. J.Thromb.Haemost. 1[4], 829-835. 2003.

Rao, C. N., Gomez, D. E., Woodley, D. T., and Thorgeirsson, U. P. Partial characterization of novel serine proteinase inhibitors from human umbilical vein endothelial cells. Arch.Biochem.Biophys. 319[1], 55-62. 1995.

Rauchhaus, M., Coats, A. J., and Anker, S. D. The endotoxin-lipoprotein hypothesis. Lancet 356[9233], 930-933. 2000.

Rauma, T., Tuukkanen, J., Bergelson, J. M., Denning, G., and Hautala, T. rab5 GTPase regulates adenovirus endocytosis. J.Virol. 73[11], 9664-9668. 1999.

Rickles, F. R., Rick, P. D., Armstrong, P. B., and Levin, J. Binding studies of radioactive lipopolysaccharide with Limulus amebocytes. Prog.Clin.Biol.Res. 29, 203-207. 1979.

Ridker, P. M. and Morrow, D. A. C-reactive protein, inflammation, and coronary risk. Cardiol.Clin. 21[3], 315-325. 2003.

Riessen, R., Rahimizadeh, H., Blessing, E., Takeshita, S., Barry, J. J., and Isner, J. M. Arterial gene transfer using pure DNA applied directly to a hydrogel-coated angioplasty balloon. Hum.Gene Ther. 4[6], 749-758. 1993.

Rietschel, E. T., Brade, L., Schade, U., Seydel, U., Zahringer, U., Brandenburg, K., Helander, I., Holst, O., Kondo, S., Kuhn, H. M., and . Bacterial lipopolysaccharides: relationship of structure and conformation to endotoxic activity, serological specificity and biological function. Adv.Exp.Med.Biol. 256, 81-99. 1990.

Robert, L., Robert, A. M., and Jacotot, B. Elastin-elastase-atherosclerosis revisited. Atherosclerosis 140[2], 281-295. 1998.

Roebuck, K. A. Regulation of interleukin-8 gene expression. J.Interferon Cytokine Res. 19[5], 429-438. 1999.

Ross, R. The pathogenesis of atherosclerosis--an update. N.Engl.J.Med. 314[8], 488-500. 1986.

Ross, R. Atherosclerosis--an inflammatory disease. N.Engl.J.Med. 340[2], 115-126. 1999.

Rossi, D. and Zlotnik, A. The biology of chemokines and their receptors. Annu.Rev.Immunol. 18, 217-242. 2000.

Rouis, M., Adamy, C., Duverger, N., Lesnik, P., Horellou, P., Moreau, M., Emmanuel, F., Caillaud, J. M., Laplaud, P. M., Dachet, C., and Chapman, M. J. Adenovirus-mediated overexpression of tissue

inhibitor of metalloproteinase-1 reduces atherosclerotic lesions in apolipoprotein E-deficient mice. Circulation 100[5], 533-540. 1999.

Russell, W. C. Update on adenovirus and its vectors. J.Gen.Virol. 81[Pt 11], 2573-2604. 2000.

Sallenave, J. M. The role of secretory leukocyte proteinase inhibitor and elafin (elastase-specific inhibitor/skin-derived antileukoprotease) as alarm antiproteinases in inflammatory lung disease. Respir.Res. 1[2], 87-92. 2000.

Sallenave, J. M., Cunningham, G. A., James, R. M., McLachlan, G., and Haslett, C. Regulation of pulmonary and systemic bacterial lipopolysaccharide responses in transgenic mice expressing human elafin. Infect.Immun. 71[7], 3766-3774. 2003.

Sallenave, J. M., Morgan K, Gauldie J, and Kalsheker N. Elastase Inhibitors in the lung: Expression and Functional Relationships. In *Molecular Biology of the Lung, Vol 1: Emphysema and Infection.* R. A. Stockley, ed. Birkhauser Verlag, Basel, Switzerland. pp 69-94. 1999.

Sallenave, J. M. and Ryle, A. P. Purification and characterization of elastase-specific inhibitor. Sequence homology with mucus proteinase inhibitor. Biol.Chem.Hoppe Seyler 372[1], 13-21. 1991.

Sallenave, J. M., Shulmann, J., Crossley, J., Jordana, M., and Gauldie, J. Regulation of secretory leukocyte proteinase inhibitor (SLPI) and elastase-specific inhibitor (ESI/elafin) in human airway epithelial cells by cytokines and neutrophilic enzymes. Am.J.Respir.Cell Mol.Biol. 11[6], 733-741. 1994.

Sallenave, J. M., Si, Tahar M., Cox, G., Chignard, M., and Gauldie, J. Secretory leukocyte proteinase inhibitor is a major leukocyte elastase inhibitor in human neutrophils. J.Leukoc.Biol. 61[6], 695-702. 1997.

Sallenave, J. M. and Silva, A. Characterization and gene sequence of the precursor of elafin, an elastase-specific inhibitor in bronchial secretions. Am.J.Respir.Cell Mol.Biol. 8[4], 439-445. 1993.

Sallenave, J. M., Xing, Z., Simpson, A. J., Graham, F. L., and Gauldie, J. Adenovirus-mediated expression of an elastase-specific inhibitor (elafin): a comparison of different promoters. Gene Ther. 5[3], 352-360. 1998.

Sata, M. and Walsh, K. Oxidized LDL activates fas-mediated endothelial cell apoptosis. J.Clin.Invest 102[9], 1682-1689. 1998.

Savill, J., Dransfield, I., Gregory, C., and Haslett, C. A blast from the past: Clearance of apoptotic cells regulates immune responses. Nature Reviews Immunology 2[12], 965-975. 2002.

Savill, J. and Fadok, V. Corpse clearance defines the meaning of cell death. Nature 407[6805], 784-788. 2000.

Sawamura, T., Kume, N., Aoyama, T., Moriwaki, H., Hoshikawa, H., Aiba, Y., Tanaka, T., Miwa, S., Katsura, Y., Kita, T., and Masaki, T. An endothelial receptor for oxidized low-density lipoprotein. Nature 386[6620], 73-77. 1997.

Schena, M., Shalon, D., Davis, R. W., and Brown, P. O. Quantitative monitoring of gene expression patterns with a complementary DNA microarray. Science 270[5235], 467-470. 1995.

Schleef, R. R., Olman, M. A., Miles, L. A., and Chuang, J. L. Modulating the fibrinolytic system of peripheral blood mononuclear cells with adenovirus. Hum.Gene Ther. 12[4], 439-445. 2001.

Schneiderman, J., Sawdey, M. S., Keeton, M. R., Bordin, G. M., Bernstein, E. F., Dilley, R. B., and Loskutoff, D. J. Increased type 1 plasminogen activator inhibitor gene expression in atherosclerotic human arteries. Proc.Natl.Acad.Sci.U.S.A 89[15], 6998-7002. 1992.

Schwenke, D. C. and Carew, T. E. Initiation of atherosclerotic lesions in cholesterol-fed rabbits. I. Focal increases in arterial LDL concentration precede development of fatty streak lesions. Arteriosclerosis 9[6], 895-907. 1989a.

Schwenke, D. C. and Carew, T. E. Initiation of atherosclerotic lesions in cholesterol-fed rabbits. II. Selective retention of LDL vs. selective increases in LDL permeability in susceptible sites of arteries. Arteriosclerosis 9[6], 908-918. 1989b.

Segura, I., Gonzalez, M. A., Serrano, A., Abad, J. L., Bernad, A., and Riese, H. H. High transfection efficiency of human umbilical vein endothelial cells using an optimized calcium phosphate method. Anal.Biochem. 296[1], 143-147. 2001.

Senior, R. M., Griffin, G. L., Mecham, R. P., Wrenn, D. S., Prasad, K. U., and Urry, D. W. Val-Gly-Val-Ala-Pro-Gly, a repeating peptide in elastin, is chemotactic for fibroblasts and monocytes. J.Cell Biol. 99[3], 870-874. 1984.

Sharif, F., Daly, K., Crowley, J., and O'Brien, T. Current status of catheter- and stent-based gene therapy. Cardiovasc.Res. 64[2], 208-216. 2004.

Shaw, P. X., Horkko, S., Chang, M. K., Curtiss, L. K., Palinski, W., Silverman, G. J., and Witztum, J. L. Natural antibodies with the T15 idiotype may act in atherosclerosis, apoptotic clearance, and protective immunity. J.Clin.Invest 105[12], 1731-1740. 2000.

Shi, G. P., Villadangos, J. A., Dranoff, G., Small, C., Gu, L., Haley, K. J., Riese, R., Ploegh, H. L., and Chapman, H. A. Cathepsin S required for normal MHC class II peptide loading and germinal center development. Immunity. 10[2], 197-206. 1999.

Shiffman, D., Mikita, T., Tai, J. T., Wade, D. P., Porter, J. G., Seilhamer, J. J., Somogyi, R., Liang, S., and Lawn, R. M. Large scale gene expression analysis of cholesterol-loaded macrophages. J.Biol.Chem. 275[48], 37324-37332. 2000.

Shock, A. and Baum, H. Inactivation of alpha-1-proteinase inhibitor in serum by stimulated human polymorphonuclear leucocytes. Evidence for a myeloperoxidase-dependent mechanism. Cell Biochem.Funct. 6[1], 13-23. 1988.

Silence, J., Collen, D., and Lijnen, H. R. Reduced atherosclerotic plaque but enhanced aneurysm formation in mice with inactivation of the tissue inhibitor of metalloproteinase-1 (TIMP-1) gene. Circ.Res. 90[8], 897-903. 2002.

Silence, J., Lupu, F., Collen, D., and Lijnen, H. R. Persistence of atherosclerotic plaque but reduced aneurysm formation in mice with stromelysin-1 (MMP-3) gene inactivation. Arterioscler.Thromb.Vasc.Biol. 21[9], 1440-1445. 2001.

Simonini, A., Moscucci, M., Muller, D. W., Bates, E. R., Pagani, F. D., Burdick, M. D., and Strieter, R. M. IL-8 is an angiogenic factor in human coronary atherectomy tissue. Circulation 101[13], 1519-1526. 2000.

Simpson, A. J. The Effects of Elafin Gene Augmentation on Acute Pulmonary Inflammation. PhD Thesis. University of Edinburgh. 2001.

Simpson, A. J., Cunningham, G. A., Porteous, D. J., Haslett, C., and Sallenave, J. M. Regulation of adenovirus-mediated elafin transgene expression by bacterial lipopolysaccharide. Hum.Gene Ther. 12[11], 1395-1406. 2001a.

Simpson, A. J., Maxwell, A. I., Govan, J. R., Haslett, C., and Sallenave, J. M. Elafin (elastase-specific inhibitor) has anti-microbial activity against gram-positive and gram-negative respiratory pathogens. FEBS Lett. 452[3], 309-313. 1999.

Simpson, A. J., Wallace, W. A., Marsden, M. E., Govan, J. R., Porteous, D. J., Haslett, C., and Sallenave, J. M. Adenoviral augmentation of elafin protects the lung against acute injury mediated by activated neutrophils and bacterial infection. J.Immunol. 167[3], 1778-1786. 2001b.

Sjoland, H., Eitzman, D. T., Gordon, D., Westrick, R., Nabel, E. G., and Ginsburg, D. Atherosclerosis progression in LDL receptor-deficient and apolipoprotein E-deficient mice is independent of genetic alterations in plasminogen activator inhibitor-1. Arterioscler.Thromb.Vasc.Biol. 20[3], 846-852. 2000.

Skalen, K., Gustafsson, M., Rydberg, E. K., Hulten, L. M., Wiklund, O., Innerarity, T. L., and Boren, J. Subendothelial retention of atherogenic lipoproteins in early atherosclerosis. Nature 417[6890], 750-754. 2002.

Smalley, D. M., Lin, J. H., Curtis, M. L., Kobari, Y., Stemerman, M. B., and Pritchard, K. A., Jr. Native LDL increases endothelial cell adhesiveness by inducing intercellular adhesion molecule-1. Arterioscler.Thromb.Vasc.Biol. 16[4], 585-590. 1996.

Smeal, T., Angel, P., Meek, J., and Karin, M. Different requirements for formation of Jun: Jun and Jun: Fos complexes. Genes Dev. 3[12B], 2091-2100. 1989.

Smedly, L. A., Tonnesen, M. G., Sandhaus, R. A., Haslett, C., Guthrie, L. A., Johnston, R. B., Jr., Henson, P. M., and Worthen, G. S. Neutrophil-mediated injury to endothelial cells. Enhancement by endotoxin and essential role of neutrophil elastase. J.Clin.Invest 77[4], 1233-1243. 1986.

Smithies, O. and Maeda, N. Gene targeting approaches to complex genetic diseases: atherosclerosis and essential hypertension. Proc.Natl.Acad.Sci.U.S.A 92[12], 5266-5272. 1995.

Staal, F. J., Roederer, M., Herzenberg, L. A., and Herzenberg, L. A. Intracellular thiols regulate activation of nuclear factor kappa B and transcription of human immunodeficiency virus. Proc.Natl.Acad.Sci.U.S.A 87[24], 9943-9947. 1990.

Stanton, L. W., Garrard, L. J., Damm, D., Garrick, B. L., Lam, A., Kapoun, A. M., Zheng, Q., Protter, A. A., Schreiner, G. F., and White, R. T. Altered patterns of gene expression in response to myocardial infarction. Circ.Res. 86[9], 939-945. 2000.

Stein, B., Baldwin, A. S., Jr., Ballard, D. W., Greene, W. C., Angel, P., and Herrlich, P. Cross-coupling of the NF-kappa B p65 and Fos/Jun transcription factors produces potentiated biological function. EMBO J. 12[10], 3879-3891. 1993.

Steinberg, D., Parthasarathy, S., Carew, T. E., Khoo, J. C., and Witztum, J. L. Beyond cholesterol. Modifications of low-density lipoprotein that increase its atherogenicity. N.Engl.J.Med. 320[14], 915-924. 1989.

Steinberg, D. and Witzum, J. L. Lipoproteins, Lipoprotein Oxidation and Atherogenesis. In *Molecular Basis of Cardiovascular Disease, Chapter 21.* K. R. Chien, ed. W.B. Saunders Company, Philadelphia, US. pp 458-475. 1999.

Stiko-Rahm, A., Hultgardh-Nilsson, A., Regnstrom, J., Hamsten, A., and Nilsson, J. Native and oxidized LDL enhances production of PDGF AA and the surface expression of PDGF receptors in cultured human smooth muscle cells. Arterioscler.Thromb. 12[9], 1099-1109. 1992.

Stoneman, V. E. and Bennett, M. R. Role of apoptosis in atherosclerosis and its therapeutic implications. Clin.Sci.(Lond) 107[4], 343-354. 2004.

Strayer, M. S., Guttentag, S. H., and Ballard, P. L. Targeting type II and Clara cells for adenovirus-mediated gene transfer using the surfactant protein B promoter. Am.J.Respir.Cell Mol.Biol. 18[1], 1-11. 1998.

Sugiyama, S., Okada, Y., Sukhova, G. K., Virmani, R., Heinecke, J. W., and Libby, P. Macrophage myeloperoxidase regulation by granulocyte macrophage colony-stimulating factor in human atherosclerosis and implications in acute coronary syndromes. Am.J.Pathol. 158[3], 879-891. 2001.

Sukhova, G. K., Shi, G. P., Simon, D. I., Chapman, H. A., and Libby, P. Expression of the elastolytic cathepsins S and K in human atheroma and regulation of their production in smooth muscle cells. J.Clin.Invest 102[3], 576-583. 1998.

Sukhova, G. K., Zhang, Y., Pan, J. H., Wada, Y., Yamamoto, T., Naito, M., Kodama, T., Tsimikas, S., Witztum, J. L., Lu, M. L., Sakara, Y., Chin, M. T., Libby, P., and Shi, G. P. Deficiency of cathepsin S reduces atherosclerosis in LDL receptor-deficient mice. J.Clin.Invest 111[6], 897-906. 2003.

Sumi, Y., Inoue, N., Azumi, H., Seno, T., Okuda, M., Hirata, K., Kawashima, S., Hayashi, Y., Itoh, H., and Yokoyama, M. Expression of tissue transglutaminase and elafin in human coronary artery: implication for plaque instability. Atherosclerosis 160[1], 31-39. 2002a.

Sumi, Y., Muramatsu, H., Takei, Y., Hata, K., Ueda, M., and Muramatsu, T. Midkine, a heparin-binding growth factor, promotes growth and glycosaminoglycan synthesis of endothelial cells through its action on smooth muscle cells in an artificial blood vessel model. J.Cell Sci. 115[Pt 13], 2659-2667. 2002b.

Suzuki, H., Kurihara, Y., Takeya, M., Kamada, N., Kataoka, M., Jishage, K., Ueda, O., Sakaguchi, H., Higashi, T., Suzuki, T., Takashima, Y., Kawabe, Y., Cynshi, O., Wada, Y., Honda, M., Kurihara, H., Aburatani, H., Doi, T., Matsumoto, A., Azuma, S., Noda, T., Toyoda, Y., Itakura, H., Yazaki, Y.,

269

Kodama, T., and . A role for macrophage scavenger receptors in atherosclerosis and susceptibility to infection. Nature 386[6622], 292-296. 1997.

Sweetnam, P. M., Thomas, H. F., Yarnell, J. W., Baker, I. A., and Elwood, P. C. Total and differential leukocyte counts as predictors of ischemic heart disease: the Caerphilly and Speedwell studies. Am.J.Epidemiol. 145[5], 416-421. 1997.

Tabas, I. and Krieger, M. Lipoprotein Receptors and Cellular Cholesterol Metabolism in Health and Disease. In *Molecular Basis of Cardiovascular Disease, Chapter 20.* K. R. Chien, ed. W.B. Saunders Company, Philadelphia, US. pp 428-457. 1999.

Taggart, C. C., Greene, C. M., McElvaney, N. G., and O'Neill, S. Secretory Leucoprotease Inhibitor prevents LPS-induced Ikappa Balpha degradation without affecting phosphorylation or Ubiquitination. J.Biol.Chem. 2002.

Tak, P. P. and Firestein, G. S. NF-kappaB: a key role in inflammatory diseases. J.Clin.Invest 107[1], 7-11. 2001.

Takahashi, J. C., Saiki, M., Miyatake, S., Tani, S., Kubo, H., Goto, K., Aoki, T., Takahashi, J. A., Nagata, I., and Kikuchi, H. Adenovirus-mediated gene transfer of basic fibroblast growth factor induces in vitro angiogenesis. Atherosclerosis 132[2], 199-205. 1997.

Tall, A. R., Dammerman, M., and Breslow, J. L. Disorders of Lipoprotein Metabolism. In *Molecular Basis of Cardiovascular Disease, Chapter 19.* K. R. Chien, ed. W.B. Saunders Company, Philadelphia, US. pp 413-427. 1999.

Talmud, P. J., Martin, S., Steiner, G., Flavell, D. M., Whitehouse, D. B., Nagl, S., Jackson, R., Taskinen. M. R., Frick, M. H., Nieminen, M. S., Kesaniemi, Y. A., Pasternack, A., Humphries, S. E., and Syvanne, M. Progression of atherosclerosis is associated with variation in the alpha1-antitrypsin gene. Arterioscler.Thromb.Vasc.Biol. 23[4], 644-649. 2003.

Taniguchi. M., Miura, K., Iwao, H., and Yamanaka, S. Quantitative assessment of DNA microarrays-- comparison with Northern blot analyses. Genomics 71[1], 34-39. 2001.

Teifel, M., Heine, L. T., Milbredt, S., and Friedl, P. Optimization of transfection of human endothelial cells. Endothelium 5[1], 21-35. 1997.

Terkeltaub, R., Banka, C. L., Solan, J., Santoro, D., Brand, K., and Curtiss, L. K. Oxidized LDL induces monocytic cell expression of interleukin-8, a chemokine with T-lymphocyte chemotactic activity. Arterioscler.Thromb. 14[1], 47-53. 1994a.

Thompson, K. and Rabinovitch, M. Exogenous leukocyte and endogenous elastases can mediate mitogenic activity in pulmonary artery smooth muscle cells by release of extracellular-matrix bound basic fibroblast growth factor. J.Cell Physiol 166[3], 495-505. 1996b.

Tiruppathi, C., Naqvi, T., Wu, Y., Vogel, S. M., Minshall, R. D., and Malik, A. B. Albumin mediates the transcytosis of myeloperoxidase by means of caveolae in endothelial cells. Proc.Natl.Acad.Sci.U.S.A 101[20], 7699-7704. 2004.

Topper, J. N., Cai, J., Falb, D., and Gimbrone, M. A., Jr. Identification of vascular endothelial genes differentially responsive to fluid mechanical stimuli: cyclooxygenase-2, manganese superoxide

dismutase, and endothelial cell nitric oxide synthase are selectively up-regulated by steady laminar shear stress. Proc.Natl.Acad.Sci.U.S.A 93[19], 10417-10422. 1996.

Travis, J. and Salvesen, G. S. Human plasma proteinase inhibitors. Annu.Rev.Biochem. 52, 655-709. 1983.

Tripathy, S. K., Svensson, E. C., Black, H. B., Goldwasser, E., Margalith, M., Hobart, P. M., and Leiden, J. M. Long-term expression of erythropoietin in the systemic circulation of mice after intramuscular injection of a plasmid DNA vector. Proc.Natl.Acad.Sci.U.S.A 93[20], 10876-10880. 1996.

Tseng, C. C. and Tseng, C. P. Identification of a novel secretory leukocyte protease inhibitor-binding protein involved in membrane phospholipid movement. FEBS Lett. 475[3], 232-236. 2000.

Ulevitch, R. J. and Tobias, P. S. Receptor-Dependent Mechanisms of Cell Stimulation by Bacterial-Endotoxin. Annual Review of Immunology 13, 437-457. 1995.

van Ginkel, F. W., McGhee, J. R., Liu, C., Simecka, J. W., Yamamoto, M., Frizzell, R. A., Sorscher, E. J., Kiyono, H., and Pascual, D. W. Adenoviral gene delivery elicits distinct pulmonary-associated T helper cell responses to the vector and to its transgene. J.Immunol. 159[2], 685-693. 1997.

Vandivier, R. W., Fadok, V. A., Hoffmann, P. R., Bratton, D. L., Penvari, C., Brown, K. K., Brain, J. D., Accurso, F. J., and Henson, P. M. Elastase-mediated phosphatidylserine receptor cleavage impairs apoptotic cell clearance in cystic fibrosis and bronchiectasis. Journal of Clinical Investigation 109[5], 661-670. 2002.

Vanin, E. F., Kaloss, M., Broscius, C., and Nienhuis, A. W. Characterization of replication-competent retroviruses from nonhuman primates with virus-induced T-cell lymphomas and observations regarding the mechanism of oncogenesis. J.Virol. 68[7], 4241-4250. 1994.

Varenne, O., Pislaru, S., Gillijns, H., Van Pelt, N., Gerard, R. D., Zoldhelyi, P., Van de, Werf F., Collen, D., and Janssens, S. P. Local adenovirus-mediated transfer of human endothelial nitric oxide synthase reduces luminal narrowing after coronary angioplasty in pigs. Circulation 98[9], 919-926. 1998.

Vermes, I., Haanen, C., Steffens-Nakken, H., and Reutelingsperger, C. A novel assay for apoptosis. Flow cytometric detection of phosphatidylserine expression on early apoptotic cells using fluorescein labelled Annexin V. J.Immunol.Methods 184[1], 39-51. 1995.

Vink, A., Schoneveld, A. H., van der Meer, J. J., van Middelaar, B. J., Sluijter, J. P., Smeets, M. B., Quax, P. H., Lim, S. K., Borst, C., Pasterkamp, G., and de Kleijn, D. P. In vivo evidence for a role of toll-like receptor 4 in the development of intimal lesions. Circulation 106[15], 1985-1990. 2002.

Virmani, R., Kolodgie, F. D., Burke, A. P., Farb, A., and Schwartz, S. M. Lessons from sudden coronary death: a comprehensive morphological classification scheme for atherosclerotic lesions. Arterioscler.Thromb.Vasc.Biol. 20[5], 1262-1275. 2000.

Visse, R. and Nagase, H. Matrix metalloproteinases and tissue inhibitors of metalloproteinases: structure, function, and biochemistry. Circ.Res. 92[8], 827-839. 2003.

Voll, R. E., Herrmann, M., Roth, E. A., Stach, C., Kalden, J. R., and Girkontaite, I. Immunosuppressive effects of apoptotic cells. Nature 390[6658], 350-351. 1997.

von Asmuth, E. J., Leeuwenberg, J. F., Ceska, M., and Buurman, W. A. LPS and cytokine-induced endothelial cell IL-6 release and ELAM-1 expression; involvement of serum. Eur.Cytokine Netw. 2[4], 291-297. 1991.

Wagner, M., Klein, C. L., van Kooten, T. G., and Kirkpatrick, C. J. Mechanisms of cell activation by heavy metal ions. J.Biomed.Mater.Res. 42[3], 443-452. 1998.

Walsh, D. E., Greene, C. M., Carroll, T. P., Taggart, C. C., Gallagher, P. M., O'Neill, S. J., and McElvaney, N. G. Interleukin-8 up-regulation by neutrophil elastase is mediated by MyD88/IRAK/TRAF-6 in human bronchial epithelium. J.Biol.Chem. 276[38], 35494-35499. 2001.

Walter, D. H., Cejna, M., Diaz-Sandoval, L., Willis, S., Kirkwood, L., Stratford, P. W., Tietz, A. B., Kirchmair, R., Silver, M., Curry, C., Wecker, A., Yoon, Y. S., Heidenreich, R., Hanley, A., Kearney, M., Tio, F. O., Kuenzler, P., Isner, J. M., and Losordo, D. W. Local gene transfer of phVEGF-2 plasmid by gene-eluting stents: an alternative strategy for inhibition of restenosis. Circulation 110[1], 36-45. 2004.

Walters, R. and Welsh, M. Mechanism by which calcium phosphate coprecipitation enhances adenovirus-mediated gene transfer. Gene Ther. 6[11], 1845-1850. 1999.

Wang, J. C., Normand, S. L., Mauri, L., and Kuntz, R. E. Coronary artery spatial distribution of acute myocardial infarction occlusions. Circulation 110[3], 278-284. 2004.

Wang, L., Nichols, T. C., Read, M. S., Bellinger, D. A., and Verma, I. M. Sustained expression of therapeutic level of factor IX in hemophilia B dogs by AAV-mediated gene therapy in liver. Mol.Ther. 1[2], 154-158. 2000.

Watanabe, H., Hattori, S., Katsuda, S., Nakanishi, I., and Nagai, Y. Human neutrophil elastase: degradation of basement membrane components and immunolocalization in the tissue. J.Biochem.(Tokyo) 108[5], 753-759. 1990.

Watanabe, N. and Ikeda, U. Matrix metalloproteinases and atherosclerosis. Curr.Atheroscler.Rep. 6[2], 112-120. 2004.

Westlin, W. F. and Gimbrone, M. A., Jr. Neutrophil-mediated damage to human vascular endothelium. Role of cytokine activation. Am.J.Pathol. 142[1], 117-128. 1993.

Wickham, T. J. Ligand-directed targeting of genes to the site of disease. Nat.Med. 9[1], 135-139. 2003.

Wickham, T. J., Mathias, P., Cheresh, D. A., and Nemerow, G. R. Integrins alpha v beta 3 and alpha v beta 5 promote adenovirus internalization but not virus attachment. Cell 73[2], 309-319. 1993.

Wickham, T. J., Segal, D. M., Roelvink, P. W., Carrion, M. E., Lizonova, A., Lee, G. M., and Kovesdi, I. Targeted adenovirus gene transfer to endothelial and smooth muscle cells by using bispecific antibodies. J.Virol. 70[10], 6831-6838. 1996.

Wiedow, O., Harder, J., Bartels, J., Streit, V., and Christophers, E. Antileukoprotease in human skin: an antibiotic peptide constitutively produced by keratinocytes. Biochem.Biophys.Res.Commun. 248[3], 904-909. 1998.

Wiedow, O., Schroder, J. M., Gregory, H., Young, J. A., and Christophers, E. Elafin: an elastase-specific inhibitor of human skin. Purification, characterization, and complete amino acid sequence. J.Biol.Chem. 265[25], 14791-14795. 1990.

Winzeler, E. A., Shoemaker, D. D., Astromoff, A., Liang, H., Anderson, K., Andre, B., Bangham, R., Benito, R., Boeke, J. D., Bussey, H., Chu, A. M., Connelly, C., Davis, K., Dietrich, F., Dow, S. W., El Bakkoury, M., Foury, F., Friend, S. H., Gentalen, E., Giaever, G., Hegemann, J. H., Jones, T., Laub, M., Liao, H., Davis, R. W., and . Functional characterization of the S. cerevisiae genome by gene deletion and parallel analysis. Science 285[5429], 901-906. 1999.

Witzenbichler, B., Maisonpierre, P. C., Jones, P., Yancopoulos, G. D., and Isner, J. M. Chemotactic properties of angiopoietin-1 and -2, ligands for the endothelial-specific receptor tyrosine kinase Tie2. J.Biol.Chem. 273[29], 18514-18521. 1998.

Wulff, C., Wilson, H., Dickson, S. E., Wiegand, S. J., and Fraser, H. M. Hemochorial placentation in the primate: expression of vascular endothelial growth factor, angiopoietins, and their receptors throughout pregnancy. Biol.Reprod. 66[3], 802-812. 2002.

Xiao, Q., Danton, M. J., Witte, D. P., Kowala, M. C., Valentine, M. T., and Degen, J. L. Fibrinogen deficiency is compatible with the development of atherosclerosis in mice. J.Clin.Invest 101[5], 1184-1194. 1998.

Xing, Z., Ohkawara, Y., Jordana, M., Graham, F., and Gauldie, J. Transfer of granulocyte-macrophage colony-stimulating factor gene to rat lung induces eosinophilia, monocytosis, and fibrotic reactions. J.Clin.Invest 97[4], 1102-1110. 1996.

Xu, X. P., Meisel, S. R., Ong, J. M., Kaul, S., Cercek, B., Rajavashisth, T. B., Sharifi, B., and Shah, P. K. Oxidized low-density lipoprotein regulates matrix metalloproteinase-9 and its tissue inhibitor in human monocyte-derived macrophages. Circulation 99[8], 993-998. 1999.

Yang, J. J., Kettritz, R., Falk, R. J., Jennette, J. C., and Gaido, M. L. Apoptosis of endothelial cells induced by the neutrophil serine proteases proteinase 3 and elastase. Am.J.Pathol. 149[5], 1617-1626. 1996a.

Yang, Y., Ertl, H. C., and Wilson, J. M. MHC class I-restricted cytotoxic T lymphocytes to viral antigens destroy hepatocytes in mice infected with E1-deleted recombinant adenoviruses. Immunity. 1[5], 433-442. 1994.

Yang, Y., Su, Q., and Wilson, J. M. Role of viral antigens in destructive cellular immune responses to adenovirus vector-transduced cells in mouse lungs. J.Virol. 70[10], 7209-7212. 1996b.

Yang, Z. Y., Simari, R. D., Perkins, N. D., San, H., Gordon, D., Nabel, G. J., and Nabel, E. G. Role of the p21 cyclin-dependent kinase inhibitor in limiting intimal cell proliferation in response to arterial injury. Proc.Natl.Acad.Sci.U.S.A 93[15], 7905-7910. 1996c.

Yasumoto, K., Okamoto, S., Mukaida, N., Murakami, S., Mai, M., and Matsushima, K. Tumor necrosis factor alpha and interferon gamma synergistically induce interleukin 8 production in a human

gastric cancer cell line through acting concurrently on AP-1 and NF-kB-like binding sites of the interleukin 8 gene. J.Biol.Chem. 267[31], 22506-22511. 1992.

Yeh, M., Gharavi, N. M., Choi, J., Hsieh, X., Reed, E., Mouillesseaux, K. P., Cole, A. L., Reddy, S. T., and Berliner, J. A. Oxidized phospholipids increase interleukin 8 (IL-8) synthesis by activation of the c-src/signal transducers and activators of transcription (STAT)3 pathway. J.Biol.Chem. 279[29], 30175-30181. 2004.

Yeh, M., Leitinger, N., de Martin, R., Onai, N., Matsushima, K., Vora, D. K., Berliner, J. A., and Reddy, S. T. Increased transcription of IL-8 in endothelial cells is differentially regulated by TNF-alpha and oxidized phospholipids. Arterioscler.Thromb.Vasc.Biol. 21[10], 1585-1591. 2001.

Ying, Q. L. and Simon, S. R. Kinetics of the inhibition of human leukocyte elastase by elafin, a 6-kilodalton elastase-specific inhibitor from human skin. Biochemistry 32[7], 1866-1874. 1993.

Yla-Herttuala, S., Palinski, W., Butler, S. W., Picard, S., Steinberg, D., and Witztum, J. L. Rabbit and human atherosclerotic lesions contain IgG that recognizes epitopes of oxidized LDL. Arterioscler.Thromb. 14[1], 32-40. 1994.

Yuan, H. T., Suri, C., Landon, D. N., Yancopoulos, G. D., and Woolf, A. S. Angiopoietin-2 is a site-specific factor in differentiation of mouse renal vasculature. J.Am.Soc.Nephrol. 11[6], 1055-1066. 2000a.

Yuan, H. T., Yang, S. P., and Woolf, A. S. Hypoxia up-regulates angiopoietin-2, a Tie-2 ligand, in mouse mesangial cells. Kidney Int. 58[5], 1912-1919. 2000b.

Yuan, J., Gao, R., Shi, R., Song, L., Tang, J., Li, Y., Tang, C., Meng, L., Yuan, W., and Chen, Z. Intravascular local gene transfer mediated by protein-coated metallic stent. Chin Med.J.(Engl.) 114[10], 1043-1045. 2001.

Zaidi, S. H., Hui, C. C., Cheah, A. Y., You, X. M., Husain, M., and Rabinovitch, M. Targeted overexpression of elafin protects mice against cardiac dysfunction and mortality following viral myocarditis. J.Clin.Invest 103[8], 1211-1219. 1999.

Zaidi, S. H., You, X. M., Ciura, S., Husain, M., and Rabinovitch, M. Overexpression of the serine elastase inhibitor elafin protects transgenic mice from hypoxic pulmonary hypertension. Circulation 105[4], 516-521. 2002.

Zaidi, S. H., You, X. M., Ciura, S., O'Blenes, S., Husain, M., and Rabinovitch, M. Suppressed smooth muscle proliferation and inflammatory cell invasion after arterial injury in elafin-overexpressing mice. J.Clin.Invest 105[12], 1687-1695. 2000.

Zaltsman, A. B., George, S. J., and Newby, A. C. Increased secretion of tissue inhibitors of metalloproteinases 1 and 2 from the aortas of cholesterol fed rabbits partially counterbalances increased metalloproteinase activity. Arterioscler.Thromb.Vasc.Biol. 19[7], 1700-1707. 1999.

Zen, K., Karsan, A., Eunson, T., Yee, E., and Harlan, J. M. Lipopolysaccharide-induced NF-kappaB activation in human endothelial cells involves degradation of IkappaBalpha but not IkappaBbeta. Exp.Cell Res. 243[2], 425-433. 1998.

Zernecke, A., Weber, K. S. C., Erwig, L. P., Kluth, D. C., Schroppel, B., Rees, A. J., and Weber, C. Combinatorial model of chemokine involvement in glomerular monocyte recruitment: Role of CXC chemokine receptor 2 in infiltration during nephrotoxic nephritis. Journal of Immunology 166[9], 5755-5762. 2001.

Zhang, Y., DeWitt, D. L., McNeely, T. B., Wahl, S. M., and Wahl, L. M. Secretory leukocyte protease inhibitor suppresses the production of monocyte prostaglandin H synthase-2, prostaglandin E2, and matrix metalloproteinases. J.Clin.Invest 99[5], 894-900. 1997.

Zhu, J., Nathan, C., and Ding, A. Suppression of macrophage responses to bacterial lipopolysaccharide by a non-secretory form of secretory leukocyte protease inhibitor. Biochim.Biophys.Acta 1451[2-3], 219-223. 1999.

Zhu, L., Wigle, D., Hinek, A., Kobayashi, J., Ye, C., Zuker, M., Dodo, H., Keeley, F. W., and Rabinovitch, M. The endogenous vascular elastase that governs development and progression of monocrotaline-induced pulmonary hypertension in rats is a novel enzyme related to the serine proteinase adipsin. J.Clin.Invest 94[3], 1163-1171. 1994.

Zinn, K., DiMaio, D., and Maniatis, T. Identification of two distinct regulatory regions adjacent to the human beta-interferon gene. Cell 34[3], 865-879. 1983.

Zsengeller, Z., Otake, K., Hossain, S. A., Berclaz, P. Y., and Trapnell, B. C. Internalization of adenovirus by alveolar macrophages initiates early proinflammatory signaling during acute respiratory tract infection. J.Virol. 74[20], 9655-9667. 2000.

Zureik, M., Robert, L., Courbon, D., Touboul, P. J., Bizbiz, L., and Ducimetiere, P. Serum elastase activity, serum elastase inhibitors, and occurrence of carotid atherosclerotic plaques: the Etude sur le Vieillissement Arteriel (EVA) study. Circulation 105[22], 2638-2645. 2002.

Review

Application of gene expression profiling to cardiovascular disease

P.A. Henriksen, Y. Kotelevtsev*

Division of Bio-Medical Sciences, Room 323a, Hugh Robson Building, University of Edinburgh, George Square, Edinburgh EH8 9XD, UK

Abstract

The number of cardiovascular publications featuring gene expression profiling technologies is growing rapidly. This article introduces four profiling techniques; serial analysis of gene expression, differential display, subtractive hybridisation and DNA microarrays. Illustrations of their application towards cardiovascular research are given and their potential for gene discovery and improving our understanding of gene function is discussed. © 2002 Elsevier Science B.V. All rights reserved.

Keywords: Gene expression; Sequence (DNA/RNA/prot)

1. Introduction

Despite intensive studies, the mechanisms behind common cardiovascular diseases such as hypertension and atherosclerosis are poorly understood. The precise combination of environmental and genetic factors responsible for these disorders may vary between patients, producing phenotypically similar manifestations but requiring different interventions to correct them. More detailed characterisation of pathological processes at the molecular and cellular levels will enhance understanding of underlying mechanisms. Cellular phenotype is determined to a large extent (although not completely) by the set of proteins that are expressed in the cell. Ideally a description of cellular phenotype would include information on every protein expressed, its intracellular localisation, and biological activity. This task is beyond the reach of current experimental techniques. New methodologies have provided the opportunity to analyse and in some cases to quantify simultaneously, thousands of messenger RNA (mRNA) transcripts. This type of analysis has been termed gene expression profiling [1]. Databases generated by genome sequencing programs, have facilitated the identification of genes by relatively short sequences within their transcripts and global expression profiling in simple organisms like

yeast has yielded information on the regulation of gene expression in response to different stimuli [2]. Medical researchers are now using expression profiling to systematically characterise molecular events pertaining to complex multifactorial diseases. Serial analysis of gene expression (SAGE), differential display, subtraction suppression hybridisation, and DNA microarrays are four major methods used for expression profiling.

This review aims to provide an introduction to these methods and gives illustrations of their application towards cardiovascular research. We examine the potential for gene discovery and highlight the limitations. The number of cardiovascular publications describing expression profiling strategies is growing rapidly and some of these have been reviewed recently [3–5].

2. Methods used for expression profiling

2.1. Serial analysis of gene expression

SAGE is a technique for determining mRNA expression levels by sequencing cDNA molecules produced by reversed transcription [6]. The method is based on tagging sequences inside cDNA with specific oligonucleotides bearing recognition sequences for a restriction enzyme that

*Corresponding author. Tel.: +44-131-651-1194; fax: +44-131-650-6527.

E-mail address: yuri.kotelevtsev@ed.ac.uk (Y. Kotelevtsev).

Time for primary review 28 days.

cuts DNA 9–13 bases away from its recognition site. The next step involves joining these short fragments together in concatamers. Sequencing several thousand cloned concatamers comprising 20–30 tags and scoring the sequences corresponding to each mRNA provides a direct measure of mRNA abundance in a given sample.

For known genes, the 9–10 base pair oligos are often sufficient for identifying the cDNA of origin using Gen-Bank. Although SAGE can be performed with small amounts of starting mRNA, the quantity of sequencing required and difficulty in reproducing protocols for concatamer formation have limited its uptake as an expression profiling technique. A detailed review of SAGE methodology is given elsewhere [7].

2.2. Differential display

Differential display will detect mRNA sequences that are absent or expressed at very low levels in one sample in comparison with another. This technique is therefore limited to detecting large variations in the amount of mRNA present. The first step involves reverse transcription with an oligo (dT) primer ending with C, G or A at the 3′ end [8]. This splits the resulting cDNA sample into three pools according to the final primer nucleotide and these are amplified in a polymerase chain reaction (PCR) with a mix of arbitrary 5′ primers designed to yield several hundred PCR products. Radionucleotides are incorporated during the reaction and the PCR products are resolved by electrophoresis on a polyacrylamide gel. Bands present in one sample that are absent from another are candidates for differentially expressed genes. This method is relatively simple and has the advantage of facilitating comparison of most cDNAs from a given cell type using several 5′ arbitrary primer combinations and small samples of mRNA. Detected bands are anonymous and therefore require purification, subcloning and sequencing. The PCR step generates a significant rate of false positives based on Northern blot analysis and although modifications may reduce this problem [9], differential display has largely been superseded by the development of more sensitive techniques below.

2.3. Subtraction suppression hybridisation

This approach improves sensitivity for low abundance transcripts by 'equalising' their concentration with high abundance transcripts through a hybridisation step [10,11]. Two cDNA populations termed 'tester' and 'driver' are made using reverse transcription from the two mRNA samples to be compared. The tester cDNA is split further into two pools and two different oligos containing motifs that can be recognised by special primers are ligated onto the 5′ ends. Through a serious of hybridisation steps, sequences equally represented in the 'tester' and 'driver' populations are subtracted out leaving differentially ex-

pressed sequences that can be amplified by PCR using primers complementary to the attached oligos. As with differential display the final PCR product may be subcloned for sequencing and compared to Gen-Bank deposited sequences. The technique is not demanding in terms of resources and can lead to identification of novel genes. It is not however, suited to systematic profiling owing to difficulties in standardising the hybridisation steps and the high rate of false positives [12].

2.4. Microarrays

Microarrays facilitate parallel quantification of thousands of specific mRNAs in a sample through hybridisation to complementary sequences placed at specified positions on glass or silicon supports [1,13]. In contrast to differential display and subtractive hybridisation the sequence of the target gene or expressed sequence tag (EST) is known. Recently, two different techniques for high density spotting of DNA molecules on glass or silicone surfaces became available. One format involves robotic deposition of PCR fragments amplified from cDNA clones and was developed at Stanford University [13]; 10 000 genes may be arrayed on a compact area of 3.6 cm^2. Affymetrix apply an alternative approach based on photolithographic synthesis of oligonucleotides in situ. Ultraviolet light is used to direct base by base synthesis, in parallel, for up to 400 000 oligos on one silicone chip [14]. Specific oligo design allows the user to avoid regions of repetitive or homologous sequence between different genes. Microarrays work on a reverse principle to Northern blot analysis. Instead of labelling a specific cDNA probe and hybridising to a pool of mRNAs immobilised on a membrane, a pool of labelled mRNAs is hybridised to numerous cDNA probes immobilised on a solid support in specific positions. The cDNA populations from two experimental samples are labelled with different fluorescent dyes and hybridised to the same microarray allowing direct comparison of signal intensity. Smaller amounts of RNA are required for the analysis of a greater number of genes than is possible with Northern blotting without a big loss of sensitivity. In one study comparing the two methods, a microarray was able to detect 90% of the expression changes demonstrated in one sample by Northern blotting [15]. Microarray technology is expensive to set up but expression profiling has become possible for many research groups through the development of centralised facilities within academic institutions and the availability of commercial microarrays.

The array fabrication technique is critical for producing high resolution and minimising background 'noise' and cross hybridisation signals. For cDNA arrays, signals vary depending on the slide surface and spotting buffer and the temperature and humidity during array printing [16]. Robotic systems for microarraying are commercially available and the design of the original robot at Stanford

University is available online (http://cmgm.stanford.edu.p-brown/mguide/index.html). Following hybridisation and image processing the data must be normalised to adjust for labelling and detection efficiencies for different fluorescent labels and differences in the quantity of starting RNA between samples. Normalisation strategies (reviewed in Ref. [16]) include correcting for total intensity by assuming that although fluorescence varies between individual transcripts, this should even out over many thousands and be identical for the same quantity of RNA labelled with two different fluorescent markers. A second approach utilises the signal ratio of the gene of interest to that of housekeeping genes (the expression levels of which are assumed not to vary between samples). A third uses the fact that the predicted slope of a scatterplot of housekeeping and added equimolar controls for the two probes should be unity. The data can be rescaled using this slope with regression analysis.

The data of hybridisation experiments with cDNA arrays can be presented as a matrix of fluorescent intensities, each value corresponding to a spot on the microarray. In a given matrix, rows may represent genes and columns may represent cDNA samples. In a simple analysis there will be only two columns comparing gene expression in two different samples. This is the commonest form of data presentation, particularly for clinical specimens. Experiments in cell culture may involve different treatments with extended time points. More detailed analysis of the resulting vast data sets may help to uncover common mechanisms of gene regulation or improve functional understanding by grouping expression changes in terms of time and magnitude or according to designated gene function groups. Algorithms comparing the data between rows (genes) and columns (samples) have been developed. Once a measure of similarity (or distance) between individual gene profiles has been assigned, these may be divided into groups or clusters. Brazma et al. [17] have provided a comprehensive review of clustering algorithms in the analysis of expression data. Clustering was first described by DeRisi et al. [2], who discovered that genes with similar expression profiles during metabolic shift in yeasts were functionally related and shared transcription factor binding sites in their promoter regions.

3. Applications of gene expression profiling to cardiovascular disease

An overview of recent cardiovascular publications using gene expression profiling is provided in Table 1 where studies are classified according to disease model, experimental sample and profiling method.

3.1. Atherosclerosis and endothelial dysfunction

3.1.1. Cell culture models

The above techniques have wide applications in the study of developmental and pathophysiological processes in the cardiovascular system. Difficulties may arise in the interpretation of gene profiles from tissues containing multiple cell types and this may be circumvented in part by using cell culture models described below.

Gimbrone's group used differential display to isolate genes that are up-regulated in cultured endothelial cells (ECs) in response to laminar or turbulent flow shear stress [18]. The genes for manganese superoxide dismutase and cyclooxygenase-2 (COX-2) were up-regulated in cells exposed to laminar shear stress and these findings were confirmed by Northern blotting. Importantly, the investigators confirmed that enhanced gene expression was translated into increased protein synthesis by immunoblotting. The contribution of turbulent flow to endothelial dysfunction and atheromatous plaque development at 'lesion prone areas', such as arterial bifurcations and curvatures, is well established. The putative protective effects of an antioxidant enzyme and prostacyclin (the major product of endothelial COX-2), induced by laminar shear stress are particularly interesting in this regard. The failure of differential display to detect enhanced expression of endothelial cell nitric oxide synthase (demonstrated by Northern analysis) in ECs exposed to laminar flow illustrated the limited sensitivity of this technique. The influence of mechanical stimuli has also been studied on vascular smooth muscle cells grown on fibronectin coated supports using cDNA microarrays [19]. Only a handful of the 5000 genes monitored at two time points after the onset of mechanical stretch varied by more than the 2.5-fold threshold change in expression set by the investigators. Applying this threshold may facilitate more reproducible results although the majority of genes varied by less than 2-fold in their expression and quantitatively small but functionally important changes in expression may have been overlooked. Plasminogen activator inhibitor-1 (PAI-1) and Tenascin-C were induced following stretch. These findings were confirmed with Northern blotting, ELISA and Western blotting for corresponding changes in mRNA and protein production. PAI-1 secreted within the vascular wall may regulate extracellular matrix proteolysis and vascular repair. Tenascin-C is also prominent in remodelling tissues and has anti-adhesive properties. The functional impact of these mediators on the atherosclerotic plaque is harder to predict. Expression of PAI-1 may act to strengthen the surrounding extracellular matrix and could render a fibrous cap less prone to rupture. It may also favour the accumulation of matrix and subsequent plaque growth. Whether a stretch stimulus applied to ECs growing in a monolayer reproduces the mechanical environment of a vessel wall is also questionable and studies on ex vivo vessel preparations would be instructive.

Oxidised low density lipoprotein (Ox-LDL) is another central influence in atherosclerotic plaque development. Monocytes become engorged with cholesterol within the plaque forming foam cells and this process has been modelled by incubating the monocytic THP-1 cell line

Table 1
Summary of recent applications of expression profiling to cardiovascular disease

	Examples of genes identified by expression profiling	Sample type and method of expression profiling			Ref.
		Tissue culture	In vivo	Human derived	
Atherosclerosis	Early growth response gene-1 (Egr-1) and Egr-1 inducible genes: ICAM-1, CD44, TNFα, IL-2, PDGFα, TGF-β1 and TGF-β2 were more highly expressed within the fibrous cap compared to the adjacent media.		LDLR−/− mice demonstrated increased aortic Egr-1 expression on a high cholesterol diet.	DNA array analysis of human carotid endarterectomy tissue.	[25]
	↑ expression of IL-8, MCP-1, VCAM-1, PAI-1, VE-cadherin and Gro-α in activated compared to quiescent ECs	SAGE analysis of human ECs activated with conditioned monocyte medium.			[39]
	↑ expression following incubation with oxidised LDL: adipophilin, heparin-binding epidermal growth factor like growth actor, thrombomodulin, CD73 and nuclear receptors LXRα, RXRα and PPARγ. ↓ expression: CD 64, carbonic anhydrase, cytochrome b-245 and Rnase A2	The human THP-1 macrophage cell line response to oxidised LDL was characterised using a DNA array.			[20]
	↑ expression of plasminogen activator inhibitor 2 in both monocytes from patients with Lipoprotein (a) hyperlipidaemia and healthy donor monocytes incubated with plasma lipoprotein (a).	Corroborative experiment examining healthy donor monocytes incubated in medium containing high Lp(a).		Microarray analysis of monocytes from patients with lipoprotein (a) hyperlipidaemia.	[40]
Endothelial dysfunction	↑ expression in Chlamydia-infected cells: IL-8, IL-1β, bFGF, PDGF-β, MCP-1 and IFN-α receptor.	DNA array analysis of a human micovascular endothelial cell line response to infection with Chlamydia pneumoniae.			[41]
	↑ expression of the chemokine, eotaxin following TNFα treatment.	The response of cultured human aortic smooth muscle cells to TNFα characterised using a microarray.		Confirmatory immuno-histochemical work performed on atherosclerotic tissue.	[21]
Restenosis	↑ expression: manganese superoxide dismutase and cyclooxygenase-2 in response to laminar shear stress.	Differential display analysis of ECs exposed to laminar shear stress.			[18]
	↑ expression with strain: cyclooxygenase-1, tenascin-C and plasminogen activator-1. ↓ expression of matrix metalloprotease-1 and thrombomodulin.	DNA array analysis of human VSMC responses to biaxial cyclic strain.			[19]
	Identification and cloning of gene 2A3-2, homologous to human translational elongation factor in highly proliferating vascular smooth muscle cells.	Subtractive hybridisation analysis was employed to compare a highly proliferating rat VSMC line with primary VSMC in culture.	Northern blot confirmation of 2A3-2 expression in balloon injured rat carotid arteries.		[22]
	↑ expression in restenotic tissue: thrombospondin-1, heat shock protein B, cyclooxygenase-1 and FK506 binding protein-12. ↓ expression of desmin and mammary derived growth inhibitor.			DNA array study of atherectomy tissue from human in-stent restenosis samples.	[24]
Myocardial infarction	↑expression following ischaemia–reperfusion: inhibitor of apoptosis (IAP), PAI-1, PAI 2, heat shock proteins 70, 28 and 22, elongation Factor 1α and connective tissue growth factor.		Subtractive hybridisation analysis of ischaemia reperfusion injury in swine myocardium.		[30]
	↑ expression following myocardial infarction: fibronectin, laminin, fibrillin, fibulin and decorin. TIMP 2 and osteoblast-specific factor 2. ↓ expression: CD36, lipoprotein lipase and long chain acyl-CoA synthase.		DNA array analysis of a rat model of MI.		[29]
	The ACE inhibitor captopril, normalised the increased expression of monoamine oxidase and cytochrome P450 following myocardial infarction and reduced the induction of thrombospondin-4 and TGF binding protein-2 like protein.		DNA array investigation of ACE inhibition following MI in rats.		[42]
	↑ embryonal expression compared to healthy adult myocardium: ANP, BNP, fibronectin and collagen III, osteopontin, superoxide dismutase. ↑ expression in infarcted myocardium: ANP, BNP, osteopontin, collagen III and fibronectin.		DNA array comparison of rat embryonal and neonatal hearts with tissue from infarcted hearts.		[31]

Table 1. Continued

	Examples of genes identified by expression profiling	Sample type and method of expression profiling			Ref.
		Tissue culture	In vivo	Human derived	
Heart failure	↑ expression in failing hearts: Gelsolin, myomesin and ubiquitin. ↓ expression in failing hearts: striated muscle LIM protein-1 (SLIM-1) and α1 Antichymotrypsin.			DNA array comparison of myocardium from heart failure patients with normal myocardium.	[26]
Cardiac hypertrophy	↑ expression during induction of hypertrophy: JAK 3 protein tyrosine kinase, vasopressin receptor and SPARC cystine rich glycoprotein. ↓ during hypertrophy: PAI-2 and desmoplakin. ↑ expression during regression of hypertrophy: NADH dehydrogenase-1 and MEK kinase.		DNA array analysis of pharmacological induction and reversal of cardiac hypertrophy in mice.		[43]

with Ox-LDL and comparing expression profiles to untreated cells using microarrays [20]. Of the 6805 genes arrayed, 268 (4%) altered their expression, a minimum of 2-fold, at one of the time points ranging up to 4 days. Data was presented in clusters according to temporal expression patterns and results were confirmed using quantitative real time PCR. In this method, reverse transcribed mRNA is PCR-amplified with gene specific primers in the presence of a probe containing a quenched fluorescent dye. The 5′ exonuclease activity of the polymerase is utilised to release fluorescent dye from the target probe facilitating continuous monitoring of the reaction against a reference probe such as 18S RNA. Genes previously demonstrated to be responsive to Ox-LDL loading of macrophages such as thrombomodulin, were induced in the THP-1 cells, offering some validation of the model. The scavenger receptors A and CD 36 involved in Ox-LDL uptake were up-regulated along with nuclear receptors that control lipid metabolism reflecting a lipid storage phenotype similar to maturing adipocytes. Vascular smooth muscle cell (VSMC) behaviour in an atheromatous plaque has been modeled by treating cultured VSMCs with the cytokine, tumor necrosis factor α [21]. Eotaxin, a chemokine characterised by its chemotactic properties for eosinophils, was induced more than 20-fold on a cDNA microarray. Eosinophils are not present within atherosclerotic plaques and the finding prompted immunohistochemical studies to localise eotaxin, which was expressed in plaque smooth muscle cells and its receptor, present on plaque macrophages and mast cells. This study demonstrated how transcriptional profiling can complement traditional, hypothesis driven research through producing unexpected findings, in this case the presence of a signalling pathway in atherosclerotic plaques.

The above studies illustrate the contribution expression profiling can make to the molecular dissection of cellular responses to specific stimuli. Comparison between different cell lines or cells grown in different matrix environments has also provided valuable information. Primary rat VSMCs were compared to a transformed proliferating rat VSMC line using differential display [22] in an ingenious

model of smooth muscle cell proliferation occurring during restenosis. Differential up-regulation of one of the isolated clones was confirmed by in situ hybridisation in rat carotid arteries following angioplasty but the full gene could not be identified from the 3′ sequence alone. Further cloning steps were required to determine the full sequence that had homology with human translational elongation factor, coding for a protein involved in protein synthesis.

Finally, coordinating expression profiling with gene mapping led to the identification of the Tangier disease gene coding for the ABC1 transporter [23]. Cells from subjects with Tangier disease are defective in the process of apolipoprotein mediated removal of cholesterol and phospholipids. Microarrays were used to compare gene expression in fibroblasts from Tangier patients with healthy controls under conditions known to induce cholesterol efflux. Probing of samples from three patients identified several under expressed genes including one that mapped to a large genetic locus independently characterised by positional cloning. The confirmation of point mutations in this gene in Tangier patients, the absence of mutations in healthy controls and the observation that overexpression of ABC1 resulted in enhanced cholesterol efflux indicated that ABC1 is the Tangier genetic defect.

3.1.2. Analysis of atherosclerotic tissue

Expression profiles from cell culture models of restenosis and atherosclerosis have led to the identification of novel genes and the demonstration of their expression in clinical specimens and tissue samples from animal models of these diseases. However, complex interactions between multiple cell types and matrix are lost with in vitro systems and further information may be gained by summative expression profiles obtained directly from animal model tissues or clinical specimens. The complexity of expression profiling of patient tissue samples is compounded by the additional variables of different genetic backgrounds, aetiology of underlying disease and preceding drug treatments.

Profiling of human atherosclerotic plaques is limited by the availability of tissue. To overcome the technical problem of limited mRNA, novel methods of cDNA amplification have been applied [24] to use cDNA arrays to probe neointimal tissue obtained following atherectomy of in-stent restenosis. This study highlighted the problem of choosing an appropriate control tissue to compare against neointimal tissue. Tunica media samples form coronary and gastrointestinal arteries were taken as controls and observed differences may therefore not be specific to the process of restenosis that was the target of the study. Carotid endarterectomy samples consist of larger pieces of tunica media gouged from the arterial wall during revascularisation. cDNA array profiling identified heightened activity of the Early growth response gene-1 (Egr-1) transcriptional pathway in these lesions compared to media from non-diseased arteries [25]. Egr-1 modulates a group of stress responsive genes including platelet-derived growth factor and transforming growth factor β that may contribute to plaque growth and smooth muscle cell recruitment. A fundamental role for this pathway in atheroma development was suggested by the additional finding of Egr-1 activation in early atherosclerotic lesions from cholesterol fed LDL receptor knockout mice.

3.2. Heart failure

The heart is an organ with areas of regional specialisation, composed of multiple cell types including cardiomyocytes, fibroblasts, endothelial and neuroendocrine cells. Expression profiles from diseased myocardium will therefore reflect the response from these different cells types as well as leucocytes recruited during inflammatory processes. Yang et al. [26] compared expression profiles from end stage heart failure patients suffering from ischaemic cardiomyopathy and dilated cardiomyopathy to non-diseased myocardium. The authors argued that comparing end-stage heart failure myocardium with different underlying aetiologies would identify shared expression profiles that may be fundamental to the failing myocardium. Only 12 of 7000 arrayed genes were identified with similar expression changes in both types of heart failure in addition to five genes expressed uniquely in failing and two genes expressed in non-failing hearts. Shared changes included functional themes such as reduced expression of the structural and contractile proteins β-actin and striated muscle LIM protein-1. It is not clear to what degree the lack of similarity between heart failure specimens represented different underlying disease aetiology, severity or other variables. Expression profiles are meaningful only in the context of experimental conditions in which they have been measured. In order to apply this technology to human specimens, new methods of detailed characterisation and annotation of the clinical background will be needed to compare results between centres.

3.3. Cardiac hypertrophy

Cardiac hypertrophy is characterised by alterations in cardiomyocyte metabolism, contractile proteins and the extracellular matrix. It may result from a familial disorder or occur as an adaptive response, following stresses such as haemodynamic overload and myocardial infarction (MI). Hwang et al. [27] compared EST frequency between three pooled human hypertrophic ventricle cDNA libraries with more than 70 000 myocardial ESTs generated from human fetal, adult and hypertrophied hearts. The established association with high levels of natriuretic peptide expression (atrial natriuretic peptide and brain natriuretic peptide) was observed in all three hypertrophic samples. In addition there was a striking up-regulation of genes associated with the cellular response to injury including a heat shock protein, α-β-crystallin, not previously implicated in hypertrophy. Only 64 genes were identified as being potentially overexpressed, demonstrating the limitation of large scale EST sequencing to detecting statistically significant changes only in moderately abundant transcripts. The Toronto group used this extensive EST library to create a large 'Cardiochip' cDNA array to probe samples from patients with hereditary hypertrophic obstructive cardiomyopathy [28]. Genes for tropomyosin and thymosin beta4, a regulator of actin polymerization, were differentially expressed in keeping with disruption of the sarcomere and cytoskeleton in this disorder. Although the contribution of these expression changes to function and phenotype remains to be elucidated the potential for detailed characterisation of patients with this disorder was demonstrated.

3.4. Myocardial infarction

Rodent models of MI result in inflammatory and fibrotic repair responses within necrotic myocardium in addition to compensatory hypertrophy of the remaining viable ventricle. Stanton et al. [29] examined expression of 7000 cDNAs in the infarcted left ventricular (LV) free wall and interventricular septum at five different time points after surgical induction of MI in the rat. Approximately 7000 clones were isolated from a rat LV cDNA library and probed with fluorescently labelled cDNA from both sites, at each time point in infarction and sham operated animals. The authors chose an arbitrary threshold of 1.8-fold increase or decrease in expression and sub-arrayed these genes for repeat analysis. Over 700 genes were shown to have reproducible patterns of differential expression. In addition to identifying genes previously described as having altered expression in myocardial infarction, new genes were implicated in the processes of repair and remodelling. That no gene exhibited unique changes in expression within the interventricular septum compared to the LV free wall was surprising considering that they were

subjected to different stress environments. The effectiveness of clustering expression profiles in time and magnitude of response to provide clues to the roles of poorly characterised genes was demonstrated. Osteoblast-specific factor-2 was thought to be unique to osteoblasts. This gene had heightened expression in a cluster with collagen, laminin and fibronectin suggesting a role in the matrix deposition and remodelling occurring after infarction. Finally, the reduced expression of several enzymes involved in the β-oxidation pathway provided a possible insight into the metabolism of injured myocardium, moving away from fatty acid substrates. Models of reversible ischaemia or ischaemia–reperfusion injury allow assessment of early changes occurring before the onset of necrosis. An intriguing theme of cytoprotective gene expression was demonstrated using subtractive hybridisation within the myocardium following transient coronary occlusion in pigs [30]. Anti-apoptotic factors and heat shock proteins were expressed along with growth factors that may act as survival signals. The profile is no more than a catalogue of expression events but it provides insight into the critical balance that exists between life and death following ischaemia–reperfusion and begs the question whether augmentation of survival factors improve functional outcome following ischaemia.

Models of cardiac hypertrophy and failure are characterised by reexpression of fetal genes. However, the consequences of gene expression during development are very different from those initiated following injury. Sehl et al. [31] used microarrays to compare expression profiles during myocardial development and infarction. The arrays consisted mainly of cDNA clones produced by subtractive hybridisation of sham operated and MI samples. This approach has the advantage of enriching the array for differentially expressed genes, decreasing the examination of multiple housekeeping or 'non varying' genes [32]. In addition, the subtractive technique generates clones from any part of the mRNA and allows identification of differentially expressed genes that have not been cloned previously. For developmental profiling, embryonic and 1-day old neonatal myocardial samples were compared with healthy adult rat myocardium. Ventricular tissue was harvested at multiple time points after coronary artery ligation and compared to sham operated tissue for stress response profiling. The greatest contrast was seen when comparing neonatal with adult myocardium and, as expected, this reflected higher expression of signal transduction and growth regulatory proteins such as p21 in the developing heart. Twelve genes previously described as being expressed during myocardial development were identified together with ten uncharacterised ESTs and 36 genes not previously associated with cardiac development. Although the array consisted largely of cDNA clones derived by subtractive hybridisation of infarcted myocardium only 63 of the 989 clones representing 14 different genes had demonstrable differential expression following myocardial infarction. Previously described shared gene

expression patterns between cardiac development and injury, including increased atrial natriuretic peptide, fibronectin and collagen III expression were confirmed. However, these were in a small subset and the discordant regulation of the majority of genes suggested that a shift to the fetal gene program is not a general characteristic in failing hearts.

No information was given on the structural or inflammatory cell types contributing to the changes in gene expression within the myocardial tissue in these models of myocardial ischaemia and infarction. In addition, the array used by Stanton et al. [29] was biased against genes expressed in infiltrating leucocytes or genes with very low basal expression levels because the arrayed genes were taken from a normal LV cDNA library that would not represent genes from these cell populations. This could be why monocyte expression of cathepsin B following MI was detected by Sehl et al. [31] but not in the former study.

Expression profiles from specific cell types, harvested from tissues, can be obtained using laser capture microdissection [33,34]. Laser capture allows precise identification, dissection and retrieval of pure cell populations that are more reflective of the disease process in vivo. Luo et al. [34] compared gene expression in large and small neurons within rat dorsal root ganglia with RNA extracted from 1000 captured neurons of each size. The small quantity of RNA generated required further linear amplification with T7 RNA polymerase before hybridisation. The investigators were able to demonstrate reproducible patterns of gene expression, using microarrays that were subsequently confirmed by immunohistochemistry. One possible application in the cardiovascular field would be the selection of macrophage foam cells from atherosclerotic plaque specimens.

4. Conclusions: cautious optimism

The interpretation of data from any expression profiling technique requires caution. The risk of false positive signals or bands is high. In microarray studies this may arise through cross hybridisation of homologous or conserved repeat sequences. Lee et al. [35] demonstrated that for a specified cDNA sample the ability of a DNA chip to distinguish correctly the presence of any sequence was 90% per run. Costly repeat analysis of the same sample is therefore required and ideally all findings should be confirmed in a separate system such as Northern blotting. Secondly, attaching functional significance to changes in gene expression level alone is difficult. No information is provided on post-translational modifications or the rate of protein degradation. An alteration in expression and protein synthesis of any given gene may represent an adaptive, compensatory response or contribute to disease progression. Profiling merely provides a further level of charac-

terisation for pathophysiological processes without offering information on the role of individual genes. Finally, levels of mRNA do not always correlate with protein synthesis. Studies in yeast indicate that expression of important growth regulatory genes may not vary between quiescent and proliferative conditions [36]. Expression analysis is complicated further by the fact that functionality and not protein level is the critical issue. If receptors or ligands are expressed but not functional, the value of gene expression and protein analysis is disputable and may be misleading.

Bearing these caveats in mind, the potential uses for systematic expression profiling on a genome wide scale in cardiovascular research are clear. Further studies will enhance our understanding of the relationship between expression level and functional consequence for individual genes. Computational approaches such as clustering, outlined above, will allow some degree of functional interpretation through linking the expression of unknown or poorly characterised genes with better known ones and through identifying patterns of genes regulating certain functions such as signalling or metabolic pathways. Profiling information provides a rich source of additional questions and hypotheses. Further experiments are often required to examine whether expression profiles translate from in vitro to in vivo models or from transgenic mice with a certain disease phenotype to diseased human tissue. Association of particular profiles with specific disease phenotypes may have future diagnostic [37] or prognostic value as well as allowing the design of specific experiments to examine in detail, the functional roles of individual genes within these profiles. The enormous amount of data produced by profiling studies poses challenges for publication and journals frequently use supplemental web pages to fully release data. The development of expression databanks akin to the sequence databanks already available will facilitate more rapid comparisons between cells and tissues in health and disease. The Stanford Microarray Database is endeavouring to provide an online, searchable, public interface for the dissemination of microarray studies [38]. Such enhanced facilities for the comparison and pattern recognition of gene expression profiles will give researchers powerful tools for gaining further insights into gene function.

Acknowledgements

References

[1] Duggan DJ, Bittner M, Chen Y, Meltzer P, Trent JM. Expression profiling using cDNA microarrays. Nat Genet 1999;21(Suppl 1):10–14.

[2] DeRisi JL, Iyer VR, Brown PO. Exploring the metabolic and genetic control of gene expression on a genomic scale. Science 1997;278:680–686.

[3] Shiffman D, Porter JG. Gene expression profiling of cardiovascular disease models. Curr Opin Biotechnol 2000;11:598–601.

[4] Rubin EM, Tall A. Perspectives for vascular genomics. Nature 2000;407:265–269.

[5] Stanton LW. Methods to profile gene expression. Trends Cardiovasc Med 2001;11:49–54.

[6] Velculescu VE, Zhang L, Vogelstein B, Kinzler KW. Serial analysis of gene expression. Science 1995;270:484–487.

[7] Yamamoto M, Wakatsuki T, Hada A, Ryo A. Use of serial analysis of gene expression (SAGE) technology. J Immunol Methods 2001;250:45–66.

[8] Livesey FJ, Hunt SP. Identifying changes in gene expression in the nervous system: mRNA differential display. Trends Neurosci 1996;19:84–88.

[9] Sompayrac L, Jane S, Burn TC, Tenen DG, Danna KJ. Overcoming limitations of the mRNA differential display technique. Nucleic Acids Res 1995;23:4738–4739.

[10] Lisitsyn N, Lisitsyn N, Wigler M. Cloning the differences between two complex genomes. Science 1993;259:946–951.

[11] Diatchenko L, Lau YF, Campbell AP et al. Suppression subtractive hybridization: a method for generating differentially regulated or tissue-specific cDNA probes and libraries. Proc Natl Acad Sci USA 1996;93:6025–6030.

[12] Gurskaya NG, Diatchenko L, Chenchik A et al. Equalizing cDNA subtraction based on selective suppression of polymerase chain reaction: cloning of Jurkat cell transcripts induced by phytohemaglutinin and phorbol 12-myristate 13-acetate. Anal Biochem 1996;240:90–97.

[13] Schena M, Shalon D, Davis RW, Brown PO. Quantitative monitoring of gene expression patterns with a complementary DNA microarray. Science 1995;270:467–470.

[14] Gerhold D, Rushmore T, Caskey CT. DNA chips: promising toys have become powerful tools. Trends Biochem Sci 1999;24:168–173.

[15] Taniguchi M, Miura K, Iwao H, Yamanaka S. Quantitative assessment of DNA microarrays — comparison with Northern blot analyses. Genomics 2001;71:34–39.

[16] Hegde P, Qi R, Abernathy K et al. A concise guide to cDNA microarray analysis. Biotechniques 2000;29:548–556.

[17] Brazma A, Vilo J. Gene expression data analysis. FEBS Lett 2000;480:17–24.

[18] Topper JN, Cai J, Falb D, Gimbrone Jr. MA. Identification of vascular endothelial genes differentially responsive to fluid mechanical stimuli: cyclooxygenase-2, manganese superoxide dismutase, and endothelial cell nitric oxide synthase are selectively upregulated by steady laminar shear stress. Proc Natl Acad Sci USA 1996;93:10417–10422.

[19] Feng Y, Yang JH, Huang H et al. Transcriptional profile of mechanically induced genes in human vascular smooth muscle cells. Circ Res 1999;85:1118–1123.

[20] Shiffman D, Mikita T, Tai JT et al. Large scale gene expression analysis of cholesterol-loaded macrophages. J Biol Chem 2000;275:37324–37332.

[21] Haley KJ, Lilly CM, Yang JH et al. Overexpression of eotaxin and the CCR3 receptor in human atherosclerosis: using genomic technology to identify a potential novel pathway of vascular inflammation. Circulation 2000;102:2185–2189.

[22] Zibara K, Bourdillon MC, Chignier E, Covacho C, McGregor JL. Identification and cloning of a new gene (2A3-2), homologous to human translational elongation factor, upregulated in a proliferating rat smooth muscle cell line and in carotid hyperplasia. Arterioscler Thromb Vasc Biol 1999;19:1650–1657.

[23] Lawn RM, Wade DP, Garvin MR et al. The Tangier disease gene product ABC1 controls the cellular apolipoprotein-mediated lipid removal pathway. J Clin Invest 1999;104:R25–R31.

[24] Zohlnhofer D, Klein CA, Richter T et al. Gene expression profiling

of human stent-induced neointima by cDNA array analysis of microscopic specimens retrieved by helix cutter atherectomy: Detection of FK506-binding protein 12 upregulation. Circulation 2001;103:1396–1402.

[25] McCaffrey TA, Fu C, Du B et al. High-level expression of Egr-1 and Egr-1-inducible genes in mouse and human atherosclerosis. J Clin Invest 2000;105:653–662.

[26] Yang J, Moravec CS, Sussman MA et al. Decreased SLIM1 expression and increased gelsolin expression in failing human hearts measured by high-density oligonucleotide arrays. Circulation 2000;102:3046–3052.

[27] Hwang DM, Dempsey AA, Lee CY, Liew CC. Identification of differentially expressed genes in cardiac hypertrophy by analysis of expressed sequence tags. Genomics 2000;66:1–14.

[28] Barrans JD, Stamatiou D, Liew C. Construction of a human cardiovascular cDNA microarray: portrait of the failing heart. Biochem Biophys Res Commun 2001;280:964–969.

[29] Stanton LW, Garrard LJ, Damm D et al. Altered patterns of gene expression in response to myocardial infarction. Circ Res 2000;86:939–945.

[30] Depre C, Tomlinson JE, Kudej RK et al. Gene program for cardiac cell survival induced by transient ischemia in conscious pigs. Proc Natl Acad Sci USA 2001;98:9336–9341.

[31] Sehl PD, Tai JT, Hillan KJ et al. Application of cDNA microarrays in determining molecular phenotype in cardiac growth, development, and response to injury. Circulation 2000;101:1990–1999.

[32] Yang GP, Ross DT, Kuang WW, Brown PO, Weigel RJ. Combining SSH and cDNA microarrays for rapid identification of differentially expressed genes. Nucleic Acids Res 1999;27:1517–1523.

[33] Ohyama H, Zhang X, Kohno Y et al. Laser capture microdissection-generated target sample for high-density oligonucleotide array hybridization. Biotechniques 2000;29:530–536.

[34] Luo L, Salunga RC, Guo H et al. Gene expression profiles of laser-captured adjacent neuronal subtypes. Nat Med 1999;5:117–122.

[35] Lee ML, Kuo FC, Whitmore GA, Sklar J. Importance of replication in microarray gene expression studies: statistical methods and evidence from repetitive cDNA hybridizations. Proc Natl Acad Sci USA 2000;97:9834–9839.

[36] Winzeler EA, Shoemaker DD, Astromoff A et al. Functional characterization of the S. cerevisiae genome by gene deletion and parallel analysis. Science 1999;285:901–906.

[37] Golub TR, Slonim DK, Tamayo P et al. Molecular classification of cancer: class discovery and class prediction by gene expression monitoring. Science 1999;286:531–537.

[38] Sherlock G, Hernandez-Boussard T, Kasarskis A et al. The Stanford Microarray Database. Nucleic Acids Res 2001;29:152–155.

[39] de Walk V, van den Berg BM, Veken J et al. Serial analysis of gene expression to assess the endothelial cell response to an atherogenic stimulus. Gene 1999;226:1–8.

[40] Buechler C, Ullrich H, Ritter M et al. Lipoprotein (a) up-regulates the expression of the plasminogen activator inhibitor 2 in human blood monocytes. Blood 2001;97:981–986.

[41] Coombes BK, Mahony JB. cDNA array analysis of altered gene expression in human endothelial cells in response to Chlamydia pneumoniae infection. Infect Immun 2001;69:1420–1427.

[42] Jin H, Yang R, Awad TA et al. Effects of early angiotensin-converting enzyme inhibition on cardiac gene expression after acute myocardial infarction. Circulation 2001;103:736–742.

[43] Friddle CJ, Koga T, Rubin EM, Bristow J. Expression profiling reveals distinct sets of genes altered during induction and regression of cardiac hypertrophy. Proc Natl Acad Sci USA 2000;97:6745–6750.

Adenoviral Gene Delivery of Elafin and Secretory Leukocyte Protease Inhibitor Attenuates NF-κB-Dependent Inflammatory Responses of Human Endothelial Cells and Macrophages to Atherogenic Stimuli[1]

Peter A. Henriksen,*[†] Mary Hitt,[‡] Zhou Xing,[‡] Jun Wang,[‡] Chris Haslett,* Rudolph A. Riemersma,[†§] David J. Webb,[†] Yuri V. Kotelevtsev,[†] and Jean-Michel Sallenave[2]*

Atherosclerosis is a chronic inflammatory disease affecting arterial vessels. Strategies to reduce the inflammatory responses of endothelial cells and macrophages may slow lesion development and prevent complications such as plaque rupture. The human protease human neutrophil elastase (HNE), oxidized low density lipoprotein, LPS, and TNF-α were chosen as model stimuli of arterial wall inflammation and led to production of the chemokine IL-8 in endothelial cells. To counteract the activity of HNE, we have examined the effects of adenoviral gene delivery of the anti-elastases elafin, previously demonstrated within human atheroma, and murine secretory leukocyte protease inhibitor (SLPI), a related molecule, on the inflammatory responses of human endothelial cells and macrophages to atherogenic stimuli. We developed a technique of precomplexing adenovirus with cationic lipid to augment adenoviral infection efficiency in endothelial cells and to facilitate infection in macrophages. Elafin overexpression protected endothelial cells from HNE-induced IL-8 production and cytotoxicity. Elafin and murine SLPI also reduced endothelial IL-8 release in response to oxidized low density lipoprotein, LPS, and TNF-α and macrophage TNF-α production in response to LPS. This effect was associated with reduced activation of the inflammatory transcription factor NF-κB, through up-regulation of IκBα, in both cell types. Our work suggests a novel and extended anti-inflammatory role for these HNE inhibitors working as effectors of innate immunity to protect tissues against maladaptive inflammatory responses. Our findings indicate that elafin and SLPI may be gene therapy targets for the treatment of atheroma. *The Journal of Immunology,* 2004, 172: 4535–4544.

Early atherosclerotic lesion development results from entrapment and subsequent oxidation of low density lipoprotein (LDL)[3] within the intimal space of arterial vessel walls. Atherosclerosis may be considered a chronic disease caused by inflammatory interactions among oxidized LDL, inflammatory cells recruited to the lesions, and the normal cellular elements of the vessel wall, namely endothelial cells and smooth muscle cells (1). Cytokines such as TNF-α have an established role in plaque inflammation (2) and, more recently, bacterial components including LPS have been implicated as causative agents (3–5).

The neutrophil chemokine IL-8 is increased in atheroma (6, 7), and neutrophils from patients with multiple atherosclerotic plaques and widespread coronary inflammation demonstrate evidence of increased degranulation, becoming depleted of myeloperoxidase (8). Human neutrophil elastase (HNE) is contained in and released from the same azurophil granules as myeloperoxidase, and its damaging effects on endothelial monolayers have been described previously (9). Therefore, we have chosen to study HNE, in addition to oxidized LDL, TNF-α, and LPS, as model stimuli of endothelial cell injury in atherosclerosis.

Elafin, a specific HNE inhibitor, has been identified within human coronary artery intima (10). Recent work has suggested extended anti-inflammatory roles for murine secretory leukocyte protease inhibitor (mSLPI), an inhibitor of HNE sharing homology with elafin (11). Murine SLPI has been shown to attenuate inflammatory cytokine production by macrophages in response to bacterial LPS (12, 13). Human SLPI has been demonstrated to prevent activation of the inflammatory transcription factor NF-κB (14, 15). Therefore, we hypothesized that overexpression of elafin and mSLPI using adenoviral vectors may reduce the inflammatory responses of endothelial cells and macrophages to atherogenic stimuli.

The relative accessibility of vessels affected by atherosclerotic disease makes gene therapy attractive, and strategies directed at reducing inflammation within the vessel wall may slow plaque progression and prevent rupture and ensuing coronary thrombosis. We developed a technique to increase adenoviral gene delivery in human endothelial cells and to facilitate infection of macrophages, a cell type lacking natural tropism for adenovirus.

Our studies show for the first time that: 1) overexpression of elafin protects human endothelial cells from HNE-induced damage and 2) both elafin and mSLPI have broad-ranging anti-inflammatory

---

*Rayne Laboratory. Medical Research Council Centre for Inflammation Research, Medical School, and †Centre for Cardiovascular Science, University of Edinburgh, Edinburgh, United Kingdom; ‡Centre for Gene Therapeutics and Department of Pathology and Molecular Medicine, McMaster University, Hamilton, Ontario, Canada; and §University of Tromso, Tromso, Norway

[2] Address correspondence and reprint requests to Dr. Jean-Michel Sallenave, Rayne Laboratory, Medical School, University of Edinburgh, Edinburgh EH8 9AG, U.K. E-mail address: j.sallenave@ed.ac.uk

[3] Abbreviations used in this paper: LDL, low density lipoprotein; HNE, human neutrophil elastase; mSLPI, murine secretory leukocyte protease inhibitor; EBM2, endothelial basal medium-2; m-eotaxin, murine eotaxin; RT, reverse transcription; Ad, adenovirus; Ad-mSLPI, E1, E3-deleted Ad encoding mSLPI cDNA; Ad-GFP, Ad expressing green fluorescent protein; Ad-dl703, E1, E3-deleted empty adenoviral vector.

activity, reducing endothelial cell IL-8 production in response to TNF-α, LPS, and oxidized LDL and TNF-α production by human macrophages in response to LPS. It is noteworthy that both of these anti-inflammatory actions were associated with reduced activation of the transcription factor NF-κB and concomitant increase in IκBα protein. Our findings extend the observed potential of elafin augmentation in models of arterial wall inflammation, including vein graft degeneration (16) and transplant arteriosclerosis (17). They indicate that gene augmentation of both elafin and mSLPI may have therapeutic potential in the treatment of atherosclerosis.

Materials and Methods

Reagents

HNE was obtained from Elastin Products (Owensville, MO). LPS was from *Escherichia coli* serotype 0127:B8 (Difco Laboratories, Detroit, MI). Endothelial basal medium-2 (EBM2) and growth supplements were obtained from Clonetics (BioWhittaker, Wokingham, U.K.). Penicillin G, streptomycin sulfate, DMEM, and IMDM were obtained from Life Technologies (Paisley, U.K.). Falcon tissue culture material was from A. & J. Beveridge (Edinburgh, U.K.). ELISAs for IL-8, TNF-α, and murine eotaxin (m-eotaxin) were obtained from R&D Systems Europe (Abingdon, U.K.). All other chemicals were purchased from Sigma-Aldrich (Poole, U.K.).

LDL: isolation and oxidation

Human plasma was obtained from the Department of Transfusion Medicine, Royal Infirmary of Edinburgh (U.K.). LDL was isolated by sequential ultracentrifugation, followed by dialysis against PBS and 0.2 g/L chelex (pH 7.4). The LDL was oxidized against CuCl$_2$ and the degree of oxidation was monitored by the formation of conjugated dienes at 234 nm (18). At maximum absorbance (usually 60–90 min after initiation), oxidation was terminated by the addition of 10% excess EDTA. Both native and oxidized LDL were concentrated in an ultrafiltration unit (Amicon 52; Millipore, Watford, U.K.) using polyethersulfone membranes (diameter, 44.5 mm; nominal molecular weight limit, 30,000; Millipore) to yield 5 ml of concentrated material. Traces of Cu^{2+} were then removed by gel filtration chromatography over a Sephadex G25 column (PD-10; Amersham Pharmacia, Uppsala, Sweden). Protein concentrations were measured by the Lowry method (19). The endotoxin concentration of native and oxidized LDL at working dilutions was measured by the *Limulus* amebocyte lysate assay (Chromogenix, Charleston, SC) and was found to be <100 pg/ml or 0.01 endotoxin U/ml.

Murine SLPI oligonucleotides

Murine SLPI oligonucleotides were obtained from MWG Biotech (Milton Keynes, U.K.). A forward oligonucleotide (5'-GCTCTAGAGCTTCAC-CATGAAGTCCTGCGG-3') was engineered to contain an *Xba*l site (5'-GCTCTAGAG-3') and oligonucleotides 6–26 from the mSLPI cDNA sequence containing the endogenous Kozak's sequence and coding for the first 4 aa (20). The reverse oligonucleotide (5'-GGAATTCCTTTGCATA-GAGAAATGAATGCG-3') was designed to contain an *Eco*RI site (5'-GGAATTCC-3') and oligonucleotides 634–655 from the cDNA sequence. The two oligonucleotides were designed to span introns and to amplify a 667-bp product (containing a poly(A) signal and 265 bp of 3' untranslated region).

RNA preparation and cloning of mSLPI

A fresh lung from a murine C57BL6/CBA hybrid was obtained and snap-frozen in liquid nitrogen, and total RNA was prepared using TRIzol reagent (21). RNA was quantified in the final solution (0.29 μg/μl) and used as a template for reverse transcription (RT) and PCR (all reagents from Promega, Southampton, U.K.). Briefly, 1 μg of total RNA was used in the RT reaction (37°C for 45 min) with 5 ng/μl reverse primer, 0.5 mM dNTPs, 10 U/μl reverse transcriptase (Moloney murine leukemia virus), and 2 U/μl RNasin in PCR buffer containing 3 mM MgCl$_2$. After a 5-min incubation at 95°C, the RT mixture was added for PCR (final volume, 100 μl of PCR buffer: 1 ng/μl reverse and forward primers, 0.03 U/μl *Taq* polymerase, and 0.5 mM MgCl$_2$). Thirty cycles of amplification were conducted in a thermal cycler (DNA Engine; MJ Research, Cambridge, MA) using the following conditions for each cycle: 94°C for 30 s, 55°C for 30 s, and 72°C for 1 min. Amplified products were then analyzed on 0.8% agarose gels, cut from the gel, purified, and ligated by conventional methods into pGEM

T-easy (Promega). An *Eco*RI mSLPI cDNA digest was then subcloned into pDK6. The correct orientation was assessed and sequencing was performed to rule out any unwanted mutagenesis. Further directional cloning was performed by subcloning the *Xba*l-*Eco*RV mSLPI cDNA fragment into *Nhe*l-*Eco*RV digested pIRESGFP2 (gift from F. Graham and R. Marr, Department of Biology, McMaster University, Hamilton, Ontario, Canada) to generate pIRESmSLPI-GFP2.

RNA preparation and cloning of m-eotaxin

Murine eotaxin cDNA was amplified by RT-PCR from total RNA extracted from female BALB/c murine lung that had been subjected to induced allergic airway eosinophilia (22). RT was conducted with random hexamers and PCR was performed (as above) using a primer pair containing restriction sites *Eco*RI and *Bam*HI on forward and reverse primers, respectively (forward, 5'-CGGAATTCCGGTAACTTCCATCTGTCTCC-3'; reverse, 5'-CGGGATCCCGGTCCCTGTTTCAA ACAAGC-3'). An 800-bp *Eco*RI/*Bam*HI fragment of full-length m-eotaxin was isolated from a 1% agarose gel and ligated into the multicloning site of the shuttle vector pDK6 to generate pDK6-m-eotaxin (23).

Adenovirus (Ad) constructs

E1, E3-deleted Ad encoding mSLPI cDNA (Ad-mSLPI). pIRES-mSLPI-GFP2 and pBHGloxΔE1,3Cre were used to cotransfect 293 cells. Cre-mediated, site-specific recombination (24) resulted in the generation of Ad-mSLPI. Ad-mSLPI was purified and titered by conventional methods (23). The integrity of mSLPI and its activity in HUVECs were assessed by dot blot analysis (using anti-mSLPI polyclonal Abs) and anti-HNE activity, respectively (data not shown).

Ad-m-eotaxin. The pDK6m-eotaxin plasmid was cotransfected into 293 cells along with the rescuing vector pBHG10. Homologous recombination resulted in the generation of Ad-m-eotaxin. HUVECs were infected with Ad-m-eotaxin, and m-eotaxin production was verified by ELISA (data not shown). The Ad-m-eotaxin virus was purified, titered, and stored as above (23).

Ad-IκBα. Construction of the vector expressing a mutant form of IκBα protein (in which serines 32 and 36 are replaced by alanine residues, therefore preventing inducible IκBα phosphorylation) has been described before (25).

Ad-elafin. The Ad vector encoding for the 95-aa elafin molecule has been described before (26). E1, E3-deleted empty adenoviral vector (Ad-dl703) coding for no transgene was described before (27).

Ad expressing green fluorescent protein (Ad-GFP) was a gift from F. Graham and R. Marr.

Cell isolation and culture

HUVECs. Ethical approval was obtained from Lothian Research and Ethics Committee (2001/R/UO/01) for the procurement of human umbilical veins from healthy term pregnancies during elective cesarean sections. Human umbilical cord was digested using collagenase type IV according to published protocols (28), and HUVECs were grown in EBM2 culture medium containing growth supplements at 37°C, 5% CO$_2$. Cells were not grown beyond six passages.

PBMC-derived macrophages. Mononuclear cells were isolated from peripheral blood as described (29). Freshly citrated blood was centrifuged at 400 × g for 20 min, and the platelet-rich plasma supernatant was used to prepare autologous serum by addition of CaCl$_2$ (10 mM final concentration). Leukocytes were isolated after removal of erythrocytes by sedimentation using 6% (w/v) dextran T500 in saline by fractionation on a discontinuous gradient of isotonic Percoll solutions made in Ca^{2+}/Mg^{2+}-free PBS. Percoll concentrations of 55, 68, and 79% were used, and the leukocytes were centrifuged at 700 × g for 20 min. Mononuclear cells were aspirated from the 55/68% interface and were washed three times in Ca^{2+}/Mg^{2+}-free PBS before culture. Monocytes were enriched from the mononuclear fraction by selectively attaching them to 48- or 12-well plates for 40 min at 37°C. Nonadherent lymphocytes were removed and adherent monocytes were washed twice in PBS. Monocytes were then cultured in IMDM containing 10% autologous serum, penicillin G (final concentration 100 U/ml), and streptomycin sulfate (final concentration 100 μg/ml) at 37°C in a 5% CO$_2$ atmosphere. Maturation into macrophages with this culture protocol has previously been demonstrated using myeloid-specific markers, including CD16 and CD51/CD61 (29).

A549 lung epithelial cells. A549 lung epithelial cells (30) were incubated in DMEM containing 10% FCS, penicillin G (final concentration 100 U/ml), and streptomycin sulfate (final concentration 100 μg/ml) and were grown to confluence in 48-well plates 37°C in a 5% CO$_2$ atmosphere.

Incubations with HNE, TNF-α, LPS, and oxidized LDL

For HNE-mediated injury experiments, HUVECs were washed with PBS to remove serum (because of the presence of HNE inhibitors in serum) and were incubated in serum-free EBM2 containing HNE for 8 h, after which photomicrographs were taken. For HNE pretreatment studies, HUVECs were washed in PBS and preincubated with HNE for 1 h before replenishment with serum-containing EBM2 containing the second LPS or oxidized LDL stimulus. All incubations with TNF-α and oxidized LDL were for 8 h. When LPS was the sole stimulus, it was incubated with HUVECs and A549s for 8 h and with macrophages for 3 h.

Ad infection protocols

To augment adenoviral gene transfer in HUVECs, we adapted a protocol involving precomplexing adenoviral vectors with the cationic liposome lipofectamine (31). We also tested this protocol for gene delivery on human monocyte-derived macrophages, a notoriously difficult cell type to transfect (32). HUVECs and A549 cells were grown to confluency and one well was used for cell count determination. Ad was dosed for each experiment at 100 PFU/cell. Ad vectors were preincubated for 15 min at room temperature in OptiMEM I reduced serum medium (Invitrogen, Paisley, U.K.) with lipofectamine (Invitrogen) at a ratio of 5×10^4 lipofectamine molecules to each adenovirus particle. Ad particle concentration was determined from absorbance at 260 nm for each Ad construct, according to published protocols (33). HUVECs, peripheral blood-derived macrophages, and A549s were incubated in the virus-containing medium for 2 h before replenishment with their respective normal growth media.

Preparation of nuclear extracts and EMSAs

Nuclear extracts were prepared after 1-h treatments from HUVECs and macrophages according to the method of Staal et al. (34). Briefly, cells were scraped and lysed in 400 μl of buffer A (10 mM HEPES, 10 mM KCl, 2 mM MgCl₂ 1 mM DTT, 0.1 mM EDTA, 0.4 mM PMSF, 0.2 mM NaF, 0.2 mM Na₃VO₄, and 1 μg/ml leupeptin), to which was added 25 μl of buffer B (10% Nonidet P-40), and the nuclei were collected by centrifugation (10,000 $\times$ g for 2 min). Nuclei were resuspended in 50 μl of buffer C (50 mM HEPES, 50 mM KCl, 10% glycerol, 0.2 mM NaF, and 0.2 mM Na₃VO₄) and agitated for 20 min at 4°C, followed by centrifugation (10,000 $\times$ g for 5 min). Nuclear proteins (7 μg) were incubated with 5× binding buffer (50 mM Tris-HCl, 0.5 M KCl, 5 mM EDTA, 2.5 mM MgCl₂, 40% glycerol) and [γ-³²P]-labeled NF-κB consensus oligonucleotide and were electrophoresed on a 6% nondenaturing polyacrylamide gel. The NF-κB (5'-AGTTGAGGGGACTTTCCCAGGC-3') oligonucleotide was obtained from Promega. DNA binding was assessed by autoradiography. Quantitative analysis was performed with a Storm 860 PhosphorImager using ImageQuant software (Molecular Dynamics, Buckinghamshire, U.K.). A mutant NF-κB oligonucleotide (ΔNF-κB) with a "G" → "C" substitution in the NF-κB/Rel DNA binding motif (Santa Cruz Biotechnology, Santa Cruz, CA) was used to establish the specificity of the sample nuclear protein binding to NF-κB.

Western blot analysis for IκB protein content in HUVECs and macrophages

Total cell (HUVECs and macrophages) extracts were prepared with cell lysate buffer (10% glycerol, 2% SDS, 62.5 mM Tris-Cl, 2 μg/ml leupeptin, 2 μg/ml aprotinin, and 1 mM PMSF) after 10 min of LPS (100 ng/ml) or TNF-α (100 pg/ml) stimulation. Cell extracts were analyzed for IκBα protein content by SDS-PAGE. Briefly, equal volumes were loaded onto a 12% Bis-Tris/MES polyacrylamide gel (Invitrogen) and electrophoresis was performed. Electroblotting was conducted on nitrocellulose (Amersham Pharmacia, Buckingham, U.K.), and membranes were treated with rabbit anti-IκBα Ab, 1/1000 dilution (Cell Signaling Technology, New England Biolabs, Hitchin, U.K.), for either 16 h at 4°C or 2 h at room temperature and subsequently with goat anti-rabbit, 1/2000 dilution (DAKO, Ely, U.K.) for 1.5 h at room temperature. The Western blots were then developed with ECL (Western Lightning Chemiluminescence Reagent Plus; Perkin-Elmer Life Sciences, Cambridge, U.K.) according to the manufacturer's instructions.

Statistics

Results are presented as mean ± SD, and differences between treatments were tested using the Student t test.

Results

The effects of oxidized LDL, LPS, TNF-α, and HNE on IL-8 production by HUVECs

To validate our in vitro model, HNE, LPS, oxidized LDL, and TNF-α were chosen as stimuli relevant to endothelial injury occurring during the development of atherosclerosis. HUVECs produced the chemotactic cytokine IL-8 (pg/ml) as follows: 92.7 ± 7.05 (untreated), 126 ± 9.65 (post 100 μg/ml native LDL), 317 ± 38.2 (post 100 μg/ml oxidized LDL), 608 ± 144 (post 100 ng/ml LPS), 5144 ± 721 (post 1 ng/ml TNF-α), 126 ± 8.45 (post 2.5 × 10^{-8} M HNE), 145 ± 14.4 (post 5.0 × 10^{-8} M HNE). Nonoxidized, native LDL was included as a control and in agreement with the literature (35) produced a small increase in IL-8 production over untreated cells. This increase was considered negligible compared with the 3-fold increase over basal levels observed with oxidized LDL (36). Results pertaining to native LDL therefore are not shown in the rest of the manuscript. Addition of low concentrations of HNE for 1 h followed by replacement of the HNE-containing medium with serum-containing medium led to a small increase in IL-8 production. In addition, a 1-h HNE pretreatment led to increased IL-8 response after subsequent stimulation with both LPS and oxidized LDL. The data, expressed as a percentage of non-HNE-pretreated cells (Table 1), show a dose-dependent effect for HNE pretreatment. Our results indicate that a brief exposure to HNE (in which no morphological damage was observed, as evidenced by absence of lifting and rounding of the HUVEC monolayer; data not shown) not only induced IL-8 production on its own but also primed cells to further stimulation by LPS and oxidized LDL.

Precomplexing Ad with cationic liposomes dramatically enhanced infection efficiency in HUVECs and macrophages

As a marker for our Ad-lipofectamine infection method, we chose to measure levels of the HNE inhibitor elafin. Endogenous elafin could not be detected in the supernatants from uninfected HUVECs or macrophages in the presence or absence of stimuli (data not shown). In contrast, elafin levels in the supernatants from HUVECs and macrophages as measured by ELISA (37) were dramatically increased after infection with Ad-elafin that had been precomplexed with lipofectamine compared with infection with Ad-elafin alone. Indeed, HUVEC elafin production, after infection with Ad-elafin at an multiplicity of infection of 100 in the absence and presence of lipofectamine, was 61.7 (±6.82) ng/ml and 782 (±27.5) ng/ml, respectively. Lipofectamine also had a facilitatory

Table I. *HUVEC IL-8 response to LPS and oxidized LDL after HNE pretreatment[a]*

HNE Pretreatment Concentration	IL-8 Production (% of Non-HNE-Pretreated Cells)	
	LPS (100 ng/ml)	oxidized LDL (100 μg/ml)
0	100	100
2.5 × 10^{-8} M	193 (45.9)	213 (27.8)
5 × 10^{-8} M	316 (50.0)[b]	228 (32.6)
1 × 10^{-7} M	248 (29.4)	332 (26.3)[c]

[a] HUVECs were grown to confluency in 48-well Costar plates (Cambridge, MA). HNE stimulations were performed in serum-free EBM2 for 1 h, after which the HNE-containing medium was replaced with EBM2 containing 2.5% FCS. LPS or oxidized LDL was added in serum-containing medium and supernatants were harvested for IL-8 determination after 8 h. Data are means and SD, from three separate experiments performed in triplicate. IL-8 is expressed as a percentage of production in non-HNE-pretreated cells.
[b] Significantly higher than 2.5 × 10^{-8} M HNE/LPS; $p < 0.05$.
[c] Significantly higher compared with 2.5 × 10^{-8} M HNE/oxidized LDL; $p < 0.001$.

effect on Ad infection of macrophages, increasing production from 17.1 ($\pm$3.71) ng/ml to 250 ($\pm$18.3) ng/ml. A549 elafin production was 571 ($\pm$23.1) ng/nl, increasing to 893 ($\pm$34.1) ng/ml with lipofectamine (all values are means and SDs derived from one representative experiment performed in quadruplicate).

Ad-elafin reduced HNE induced injury and cytokine production by HUVECs

Having demonstrated the inflammatory effects of oxidized LDL, LPS, and HNE on HUVECs and having established an efficient Ad-infection method (see above), we hypothesized that elafin may modulate the responses to these stimuli by both inhibiting HNE activity and interfering with LPS signaling in a similar fashion to mSLPI (13). Ad-mediated overexpression of elafin reduced the rounding and lifting observed in HUVEC monolayers after an 8-h incubation with HNE (2.5 $\times$ 10^{-8} M) (Fig. 1a). Ad-dl703 and Ad-GFP were included to demonstrate the specificity of effect for Ad-elafin. Ad-GFP was used in this experiment specifically to visualize both infection efficiency and cell damage after HNE injury (Fig. 1a) and was not used further in our study. Ad-IκBα was included as a positive control of cytokine inhibition and reduced HUVEC IL-8 production in response to HNE, HNE and LPS in combination, and LPS alone (Fig. 1b). Ad-elafin also inhibited
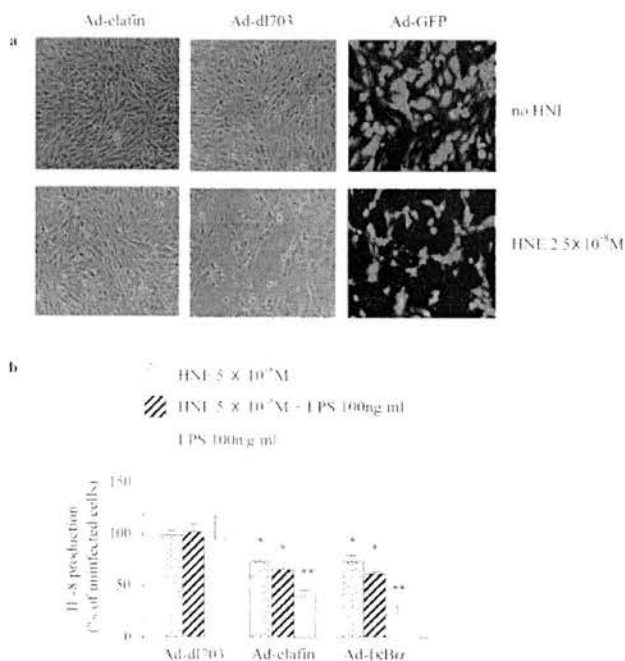

FIGURE 1. Overexpression of elafin protected HUVEC monolayers against HNE damage and inhibited HNE- and LPS-induced IL-8 production. HUVECs were cultured and infected with Ad-elafin, Ad-dl703 (an empty viral construct containing no transgene), and Ad-GFP (100 PFU/cell) according to the protocols in *Materials and Methods*. All experiments were performed 24 h after Ad infection. *a*, Photomicrographs of Ad-elafin-, Ad-dl703-, and Ad-GFP-infected cells untreated (*upper panel*) and after incubation for 8 h with HNE (*lower panel*) in serum-free medium. Appearances of uninfected cells were identical with those of Ad-dl703-infected cells (data not shown). *b*, HUVEC IL-8 production after pretreatment with HNE alone, HNE pretreatment in combination with LPS stimulation, or LPS stimulation alone. HNE pretreatments were conducted as in Table I, and cells were replenished with serum-containing medium after HNE pretreatment. Results are means and SD of three experiments each performed in triplicate. IL-8 production is expressed as a percentage of production in uninfected cells (see Table I). *, $p < 0.01$; **, $p < 0.001$; significantly lower than Ad-dl703-infected cells,.

IL-8 production after a brief exposure to HNE alone (5 $\times$ 10^{-8} M for 1 h), after HNE pretreatment followed by LPS, and, most notably, after LPS stimulation in isolation (Fig. 1b). An extended anti-inflammatory role for elafin was suggested by its disruptive effect on LPS signaling, and the remainder of the study focused on investigation of this property.

Ad-elafin and Ad-mSLPI reduced cytokine production by endothelial cells and macrophages, but not lung epithelial cells

The anti-inflammatory activities of elafin were further studied on HUVECs, macrophages, and lung alveolar epithelial cells (A549 cells). Epithelial cells are not relevant to atherosclerosis and were included to test whether the inhibitory effect demonstrated cellular specificity. The effects of both Ad-elafin and Ad-mSLPI, a closely related antiprotease, were examined on responses to LPS, TNF-α, and oxidized LDL. In addition to the empty Ad construct Ad-dl703, we included a further control Ad expressing m-eotaxin (Ad-m-eotaxin), a secreted chemokine of similar molecular mass to elafin and mSLPI (38), with no known anti-inflammatory activity in the cell types studied. In HUVECs, Ad-elafin and Ad-mSLPI produced small but significant reductions in basal IL-8 production, an effect not observed in Ad-IκBα-infected cells (Fig. 2b). Ad-elafin and Ad-mSLPI had comparable inhibitory effects to Ad-IκBα after stimulation of HUVECs with LPS (Fig. 2d, same data as Fig. 1b) and oxidized LDL (Fig. 2e) when compared with control vectors. TNF-α stimulation led to a large increase in IL-8 production that was significantly attenuated by Ad-IκBα, Ad-mSLPI, and Ad-elafin (Fig. 2c). TNF-α was chosen as a marker for the ability of macrophages to respond to LPS, and stimulation of macrophages with LPS produced a response in both uninfected and virally infected cells (Fig. 3a). In contrast with IL-8 production in HUVECs (Fig. 1b), there was no significant difference in the basal level of TNF-α production among the five adenovirus constructs (Fig. 3b). Ad-mSLPI and Ad-elafin significantly reduced the TNF-α response to LPS compared with Ad-dl703 and Ad-m-eotaxin (Fig. 3c).

In comparison with their inhibitory effect on stimulated cytokine production in HUVECs and macrophages, Ad-elafin and Ad-mSLPI had no effect on IL-8 production by A549s in basal conditions or after stimulation with LPS (Fig. 4, b and c). However, Ad-IκBα retained an inhibitory effect, significantly reducing basal IL-8 production and attenuating the response to LPS in A549 cells.

Ad-elafin and Ad-mSLPI reduced NF-κB activation in HUVECs and macrophages by reducing IκBα degradation

In HUVECs and macrophages, the level of NF-κB activity in unstimulated cells was very low. There was no difference between virally infected and uninfected cells (data not shown). In HUVECs, stimulation with LPS led to an increase in NF-κB activity that was significantly reduced by Ad-elafin and Ad-mSLPI, but only at the lowest concentration of LPS used (100 ng/ml) (Fig. 5a). Inhibitory effects disappeared at higher LPS concentrations (1–5 μg/ml) by comparison with the inhibitory effect of Ad-IκBα, which remained constant (Fig. 5a).

A similar result was seen after incubation of HUVECs with oxidized LDL (Fig. 6a). Ad-IκBα was most inhibitory, but both Ad-elafin and Ad-mSLPI attenuated NF-κB activation significantly compared with control vectors. Similarly, the rise in NF-κB activity after stimulation with TNF-α (100 pg/ml) was reduced in Ad-elafin- and Ad-mSLPI-infected cells. In parallel with their inhibitory effects on LPS signaling (Fig. 5a), this effect disappeared with a higher concentration (1 ng/ml) of TNF-α (Fig. 6b). In contrast, the inhibitory effect of Ad-IκBα was retained at the higher TNF-α concentration.

FIGURE 2. Ad-elafin and Ad-mSLPI reduced IL-8 production in HUVECs in basal (untreated) conditions and after stimulation with TNF-α, LPS, and oxidized LDL. HUVECs were grown to confluency in 48-well plates and were infected with Ad as in Fig. 1. Stimuli were applied 24 h after infection and left for 8 h before removal of conditioned medium for IL-8 ELISA. Ad-m-eotaxin and the empty viral construct containing no transgene (Ad-dl703) were included as controls for the effects of adenoviral infection. Ad-IκB was included as a positive control of cytokine inhibition. *a*, IL-8 response to the three stimuli (see *Results*). *b*, Ad-elafin, Ad-mSLPI, Ad-dl703, Ad-IκBα, and Ad-m-eotaxin-infected cells under basal (untreated) conditions. *c*, TNF-α, 1 ng/ml. *d*, LPS, 100 ng/ml (Ad-elafin/LPS data are the same as in Fig. 1*b*). *e*, Oxidized LDL, 100 μg/ml. IL-8 production is expressed as a percentage of uninfected cells. Data in *b–e* are means and SDs from three separate donors performed in quadruplicate. *, $p < 0.05$; **, $p < 0.01$; ***, $p < 0.001$; significantly lower than Ad-m-eotaxin infected cells.
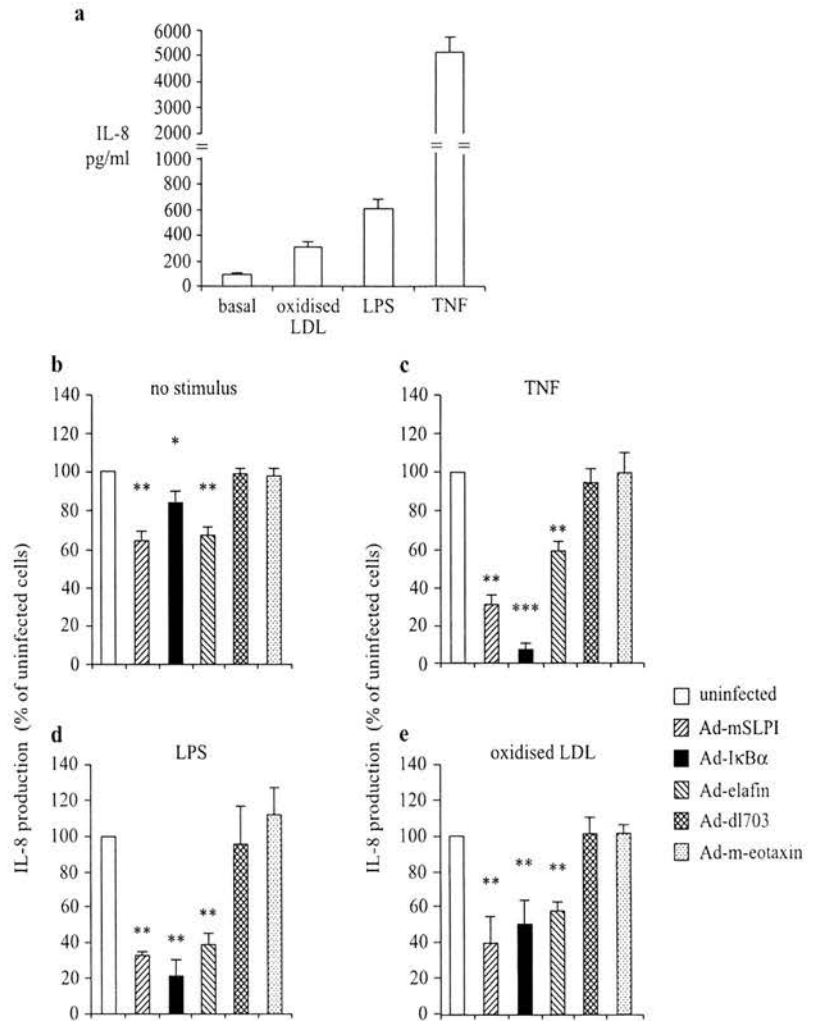
In macrophages, Ad-elafin and Ad-mSLPI significantly attenuated NF-κB activity after LPS stimulation when compared with control vectors, although Ad-IκBα was the most effective (Fig. 7).

The mechanism of NF-κB inhibition by Ad-elafin and Ad-mSLPI was further studied by stimulating Ad-infected HUVECs and macrophages with TNF-α and LPS, respectively. Total cell lysates were then analyzed for IκBα content by Western blot analysis.

Fig. 8 shows that Ad-mSLPI and Ad-elafin significantly protected HUVECs and macrophages from TNF-α- and LPS-induced IκBα degradation, respectively. Ad-IκBα produced overexpression of mutated IκBα (as evidenced by its higher m.w.), but in accordance with other studies it did not completely prevent endogenous IκBα degradation.

Discussion

The mechanisms driving atherosclerotic plaque development have been underpinned by in vitro studies demonstrating the inflammatory actions of oxidized LDL on intimal cells (35, 36, 39). A possible contribution from infectious agents or bacterial components such as LPS has been suggested by detection of *Chlamydia pneumoniae* (40) and increased expression of the LPS receptor Toll-like receptor-4 (3) in atherosclerotic specimens. These results are in agreement with the observation that atheroma formation is accelerated in atheroma-prone rabbits treated with LPS (4).

At the molecular level, endothelial cells demonstrate increased adhesion molecule and chemokine expression during plaque development (7, 41), and macrophages are the predominant cell of the mononuclear cell infiltrate. Murine models of atheroma have exemplified the importance of chemokine expression in atherogenesis. Indeed, atherosclerosis-susceptible, LDL receptor-deficient mice that were irradiated and repopulated with marrow cells lacking the neutrophil chemokine receptor CXCR-2 had reduced atheroma (42). This array of data prompted us to examine endothelial cell chemokine production in response to oxidized LDL, TNF-α, and LPS. We demonstrate here that all three stimuli increased production of the neutrophil chemokine IL-8 (Table I and Fig. 2a) in endothelial cells. We also show for the first time that brief exposure to the neutrophil enzyme HNE increases endothelial cell IL-8 production (see *Results*) in a similar fashion to its previously published effects on lung epithelial cells (43, 44) and that HNE pretreatment potentiated the IL-8 response to subsequent stimulation by LPS and oxidized LDL (Table I). In accordance with previously published work (9), we found that a more prolonged incubation of HNE with endothelial cells was cytotoxic (Fig. 1a). Although neutrophils are not present in large quantities within atherosclerotic plaques, myeloperoxidase, a major neutrophil protein, has been identified as a key mediator of plaque development (45, 46). The observation that α defensin, a further neutrophil granule-derived protein, is present within the coronary artery intima (47) and may
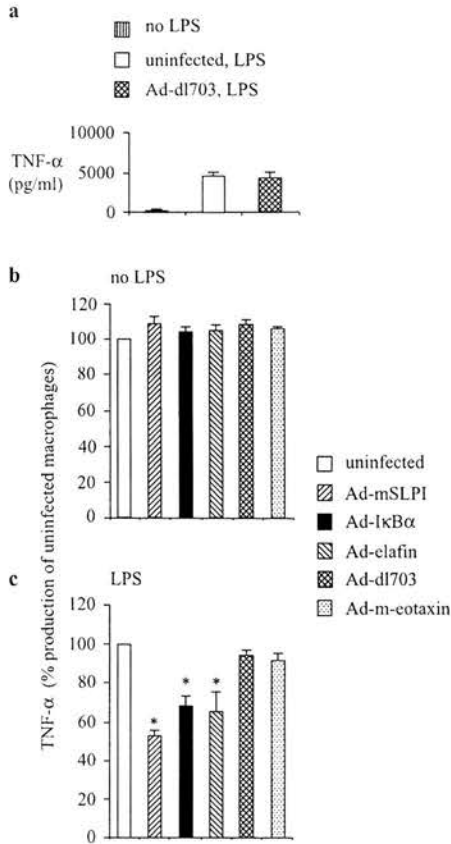
FIGURE 3. Ad-elafin and Ad-mSLPI reduced macrophage TNF-α production in response to LPS stimulation. Adenoviral infections were performed (100 PFU/cell) as described in *Materials and Methods*, and LPS was added on day 7 of culture. Conditioned medium was removed after 3 h for TNF-α ELISA. *a*, Representative experiment from one donor (mean and SD from triplicate wells) showing TNF-α production from untreated cells and the response after stimulation with LPS (1 ng/ml) in uninfected and Ad-dl703-infected macrophages. *b*, TNF-α production in infected, nonstimulated cells. *c*, TNF-α production in response to infected and LPS-stimulated macrophages (1 ng/ml). TNF-α production is expressed as a percentage of uninfected cells. Data in *b–c* are means and SDs from three donors performed in triplicate. *, $p < 0.01$, significantly less than Ad-m-eotaxin-infected cells.

FIGURE 4. Ad-elafin and Ad-mSLPI had no effect on IL-8 production by A549 epithelial cells in response to LPS stimulation. A549s were grown to confluence in 48-well Costar plates, infected with adenovirus vectors (100 PFU/cell), and stimulated with LPS using the HUVEC protocol described in Fig. 1. *a*, IL-8 production in response to LPS stimulation (100 ng/ml). Data represent the mean and SD from triplicate wells. *b*, Basal IL-8 release from infected nonstimulated A549s. *c*, IL-8 production from infected A549s in response to LPS (100 ng/ml). Data represent the means and SDs from three experiments performed in triplicate. IL-8 concentration is expressed as a percentage of uninfected cells. *, $p < 0.05$; **, $p < 0.001$; significantly lower than Ad-m-eotaxin-infected cells.

interact with LDLs (48), supports our hypothesis that neutrophil-derived HNE augments endothelial cell inflammatory responses to oxidized LDL and LPS.

We chose, therefore, to investigate whether Ad-mediated overexpression of HNE inhibitors would modulate the inflammatory responses of endothelial cells observed in the first part of our study. Elafin and mSLPI are cationic low-m.w. protease inhibitors with spectrums of antiprotease activity that include HNE, proteinase 3, and porcine pancreatic elastase for elafin and HNE, trypsin, and chymotrypsin for mSLPI (11). In humans, these protease inhibitors show 40% protein sequence homology and have been characterized from a variety of epithelial lining fluids (49). SLPI and elafin are present in monocytes, alveolar macrophages, and neutrophils, albeit to varying degrees (11, 50). The N-terminal of elafin provides a substrate for transglutamination and binding to interstitial molecules, potentially accounting for the colocalization of elafin with tissue transglutaminase in human coronary arteries (10).

Using a novel technique involving precomplexing of adenovirus with cationic liposomes, we were able to significantly augment Ad gene delivery in HUVECs. Other workers have also demonstrated
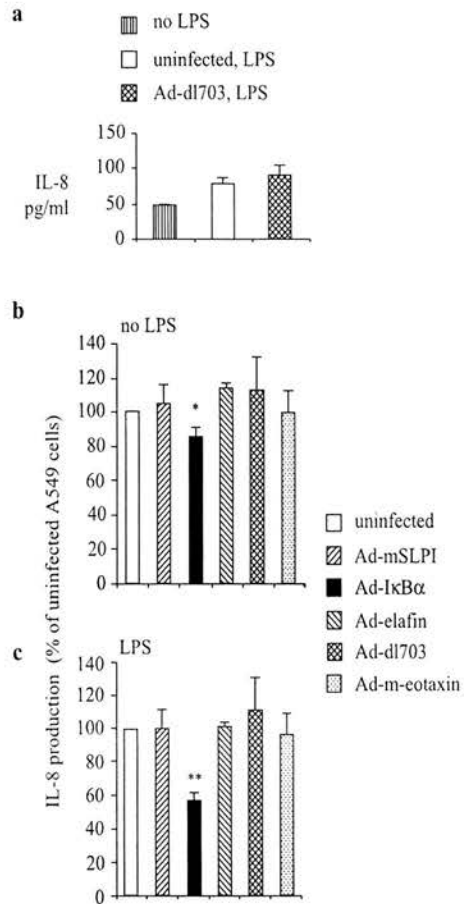
that precomplexing cationic compounds, including calcium phosphate precipitates and liposomes with Ad, augment gene delivery both in vivo and in vitro (31, 51–53). Using our methodology, Ad-mediated elafin overexpression in HUVECs prevented direct HNE damage (Fig. 1*a*) and inhibited HNE-induced IL-8 production (Fig. 1*b*). Remarkably, the elafin inhibitory effect was comparable to that of the NF-κB inhibitory subunit IκBα, suggesting that elafin and IκBα may share a common HNE inhibitory pathway. Walsh et al. (44) have recently shown that HNE signals through the MyD88-IL-1R-associated kinase-TNFR-associated factor-6-NF-κB pathway, and a recent report has demonstrated Toll-like receptor 4-mediated IL-8 induction by HNE (54). Our new findings extend in endothelial cells the above-mentioned observations in epithelial cells and support promoter mutation studies indicating that NF-κB is the predominant *cis*-acting element in IL-8 gene expression (55).

Importantly, Ad-elafin has modulatory effects even in the absence of HNE (Fig. 1*b*), suggesting that elafin may be exerting additional anti-inflammatory effects beyond neutralization of HNE. This possibility was tested further in a range of cell types by

FIGURE 5. Ad-elafin, Ad-mSLPI, and Ad-IκBα reduced NF-κB activation in HUVECs after stimulation with LPS. Cells were grown to confluence in 24-well Costar plates and infected with adenovirus vectors (100 PFU/cell) according to the protocols in Fig. 1, and nuclear proteins were prepared for EMSA 1 h after stimulation with LPS. Specificity of binding was demonstrated by disappearance of the NF-κB band with a mutated NF-κB oligo (Δ probe). Nuclear proteins from two separate experiments were run in pairs on the same gel. *a*, EMSAs of nuclear proteins (7 μg) from cells infected with Ad vectors and stimulated with LPS at 100 ng/ml, 1 μg/ml, and 5 μg/ml. *b*, The mean intensities of the corresponding NF-κB bands for uninfected and adenovirus-infected cells were determined using ImageQuant software and expressed as arbitrary densitometric units on the *y*-axis.

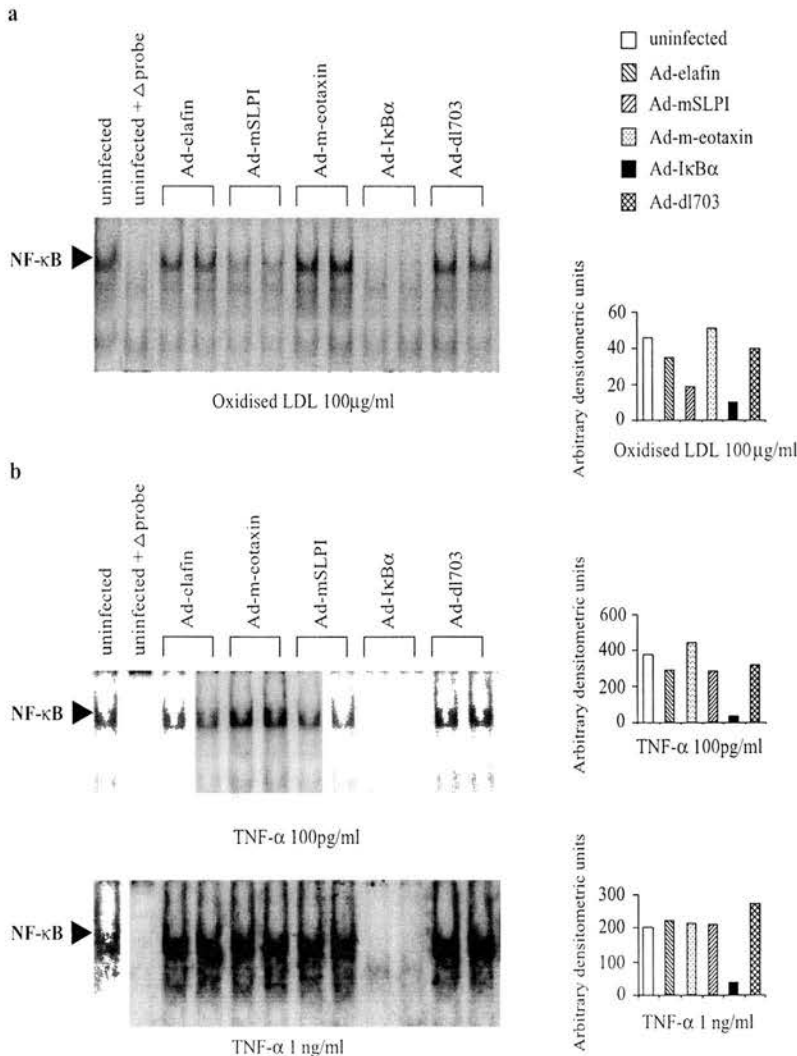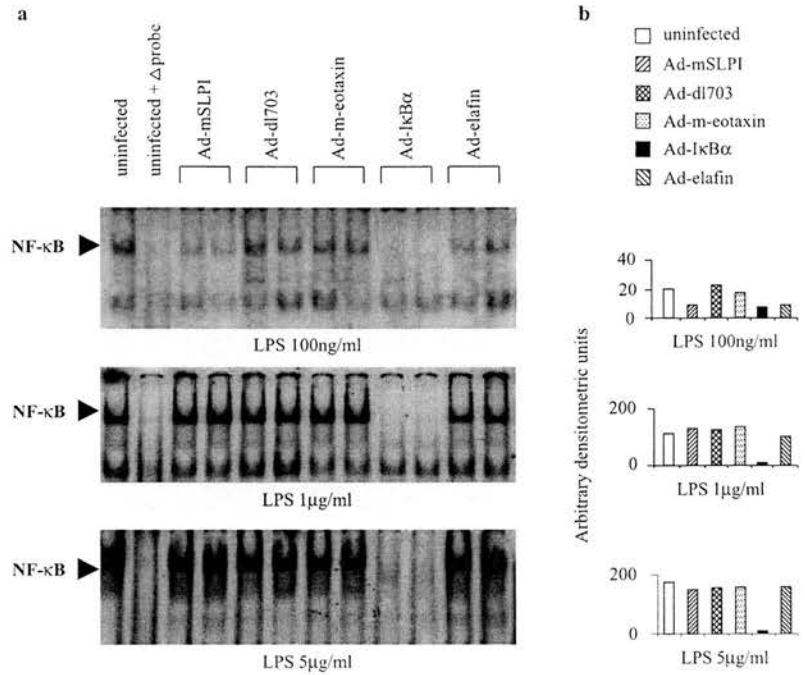**FIGURE 6.** Ad-elafin, Ad-mSLPI, and Ad-IκBα reduced NF-κB activation in HUVECs after stimulation with oxidized LDL and TNF-α. EMSAs were performed on nuclear proteins prepared according to the protocols in Fig. 5. *a*, Oxidized LDL-stimulated cells (100 ng/ml). *b*, TNF-α-stimulated cells. EMSAs are shown with corresponding densitometry.

FIGURE 7. Ad-elafin, Ad-mSLPI, and Ad-IκBα reduced NF-κB activation in macrophages after stimulation with LPS. Macrophages were cultured in 12-well Costar plates and infected with adenovirus vectors as in Fig. 3. Cells were stimulated with LPS (1 ng/ml) for 1 h on day 7, and EMSAs were performed on nuclear extracts (7 μg) as in Fig. 5 (representative gel from an experiment repeated on two separate donors). Corresponding densitometry of NF-κB bands is also shown.
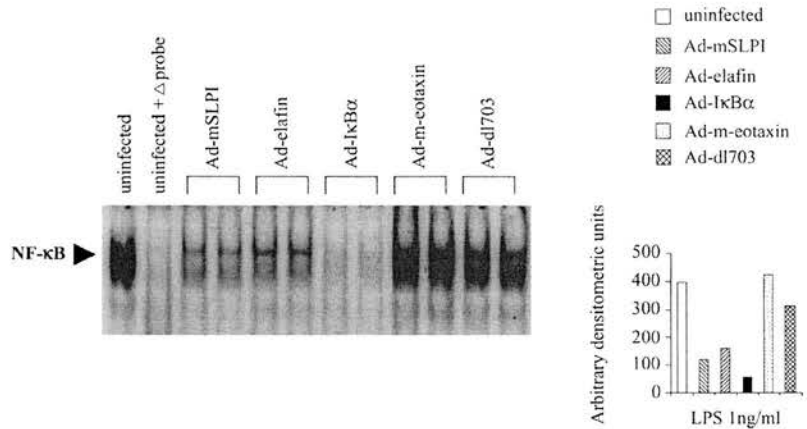
comparing the anti-inflammatory actions of elafin, its homologue mSLPI (previously shown to inhibit LPS) (12, 13), and IκBα. In HUVECs, Ad-elafin and Ad-mSLPI significantly reduced IL-8 production in basal conditions and in response to TNF-α, LPS, and oxidized LDL (Fig. 2, *a–d*). Because human macrophages are relatively refractory to Ad infection expressing low levels of adenoviral receptors (56), we used our Ad-lipofectamine technique on these cells and showed that elafin expression was increased vastly (see *Results*). Overexpression of elafin, mSLPI, and IκBα significantly reduced macrophage TNF-α production in response to LPS stimulation (Fig. 3c). These results confirm the previously known anti-LPS activity of mSLPI (12, 13) using a different approach and establish for the first time the broad-ranging antagonism of elafin and mSLPI against different stimuli, suggesting a general role in dampening inflammation.

Interestingly, Ad-elafin and Ad-mSLPI had no inhibitory effect on basal or LPS-induced IL-8 production by lung epithelial cells; however, Ad-IκBα was inhibitory (Fig. 4, *a* and *b*), possibly reflecting a cellular or organ-specific action for these antiproteases. Indeed, recent work from our own group suggests that overexpression of elafin is not anti-inflammatory and may prime murine lung innate immune responses after an LPS challenge (57, 58).

Because both IL-8 and TNF-α production are dependent on NF-κB-regulated transcription (59), we investigated whether elafin could also interfere with the NF-κB pathway. NF-κB activity is increased within the intimal cells of human plaques and is a possible therapeutic target regulating the expression of many proatherogenic genes (60). We performed EMSAs to examine the effects of the Ad vectors on NF-κB activation in HUVECs and macrophages. Oxidized LDL increases endothelial cell production of reactive oxygen species and activates NF-κB through interaction with the lectin-like oxidized LDL receptor 1 scavenger receptor (61), and oxidized LDL, LPS, and TNF-α stimulation were associated with increased activity of the proinflammatory transcription factor in HUVECs (Figs. 5 and 6) (62, 63). After Ad-elafin and Ad-mSLPI infection, NF-κB activity was reduced in LPS- (Fig. 5), oxidized LDL- (Fig. 6a), and TNF-α-stimulated HUVECs (Fig. 6b). This provides evidence for an inhibitory effect before or at the level of gene transcription for these stimuli. Ad-elafin and Ad-mSLPI also reduced LPS-induced macrophage NF-κB activation in accordance with their inhibitory action on production of the NF-κB-regulated proinflammatory cytokine TNF-α (Fig. 7). This was further studied by Western blot analysis, which showed that Ad-elafin and Ad-mSLPI inhibited NF-κB activity by reducing TNF-α- and LPS-induced IκBα degradation (Fig. 8). Interestingly, and as demonstrated by others (64), Ad-IκBα did not prevent endogenous IκBα degradation, confirming

that overexpression of IκBα can saturate the endogenous IκBα degrading cellular machinery. IκBα protein content was highest in the Ad-IκBα-infected cells (Fig. 8) mirroring the EMSA results, which showed that IκBα was most efficient at down-regulating NF-κB activity (Figs. 6 and 7). Consistent with its inhibitory activity on NF-κB in the present work, SLPI$^{-/-}$ murine macrophages demonstrate sustained increases in NF-κB activation after LPS stimulation (65). Accordingly, Lentsch et al. (14) demonstrated that inhibition of NF-κB activity in a rat immune complex lung injury model, after administration of human SLPI, was associated with increased levels of the IκBβ inhibitory subunit. In that model, mutated human SLPI sequences coding for proteins that lack trypsin inhibitory activity failed to inhibit NF-κB activation (66). Although SLPI has been shown to bind physically to LPS (67), Jin et al. (12) as well as J. McMichael (unpublished observations) in our group have reported that SLPI-containing medium was unable to transfer LPS-inhibiting activity to fresh cells, suggesting that extracellular SLPI may not be able to interfere with LPS signaling. Two reports have supported an intracellular mode of action for this secreted protein. Zhu et al. (13) showed that a SLPI construct lacking a leader sequence and hence coding for a nonsecreted protein was still able to exert its anti-LPS effect and subsequent NF-κB activity. More recently (68), SLPI's anti-inflammatory activity against LPS was shown to be inhibited by
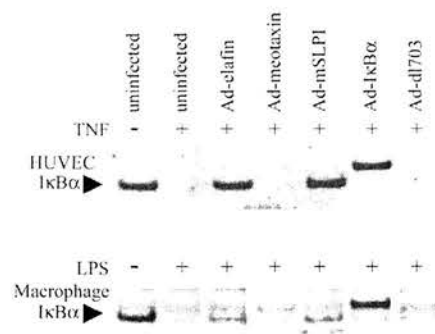
FIGURE 8. Ad-elafin, Ad-mSLPI, and Ad-IκBα protected HUVECs and macrophages from IκBα degradation. HUVECs and macrophages (uninfected or infected with Ad constructs) were stimulated with TNF-α (100 pg/ml, *upper panel*) or LPS (1 ng/ml, *lower panel*), respectively, for 10 min (preliminary experiments were performed to determine optimal timing; data not shown). Total cell extracts were obtained and Western blot analysis was performed for IκBα content as outlined in *Materials and Methods*. Ad-derived IκBα migrates slightly behind endogenous IκBα. Results are representative of experiments performed in duplicate.

4543

proteasome inhibitors. In addition to SLPI and elafin, other serine protease inhibitors have been shown to block NF-κB activation through inhibition of proteosomal proteases (69, 70).

Our results do not exclude elafin and mSLPI interference with parallel proinflammatory signaling pathways activated by TNF-α, LPS, and oxidized LDL because inhibition of cytokine production was more striking than was the sole suppression of NF-κB activation (particularly for TNF-α) supporting this possibility.

In conclusion, our experiments have shown for the first time that overexpression of HNE inhibitors is protective against HNE-mediated endothelial cell damage and proinflammatory signaling in both endothelial cells and macrophages and can, through NF-κB inhibition, attenuate inflammatory responses to LPS, TNF-α, and oxidized LDL. Overall, our data support the concept of endogenous defense molecules such as elafin and SLPI working as effectors of innate immunity to protect tissues against maladaptive inflammatory responses. We believe that the properties of these molecules make them attractive anti-inflammatory agents in a range of diseases, including arterial wall inflammation occurring during atherosclerosis.

Acknowledgments

References

1. Glass, C. K., and J. L. Witztum. 2001. Atherosclerosis: the road ahead. *Cell* 104:503.

2. Barath, P., M. C. Fishbein, J. Cao, J. Berenson, R. H. Helfant, and J. S. Forrester. 1990. Detection and localization of tumor necrosis factor in human atheroma. *Am. J. Cardiol.* 65:297.

3. Vink, A., A. H. Schoneveld, J. J. van der Meer, B. J. van Middelaar, J. P. Sluijter, M. B. Smeets, P. H. Quax, S. K. Lim, C. Borst, G. Pasterkamp, and D. P. de Kleijn. 2002. In vivo evidence for a role of Toll-like receptor 4 in the development of intimal lesions. *Circulation* 106:1985.

4. Lehr, H. A., T. A. Sagban, C. Ihling, U. Zahringer, K. D. Hungerer, M. Blumrich, K. Reifenberg, and S. Bhakdi. 2001. Immunopathogenesis of atherosclerosis: endotoxin accelerates atherosclerosis in rabbits on hypercholesterolemic diet. *Circulation* 104:914.

5. Libby, P., D. Egan, and S. Skarlatos. 1997. Roles of infectious agents in atherosclerosis and restenosis: an assessment of the evidence and need for future research. *Circulation* 96:4095.

6. Simonini, A., M. Moscucci, D. W. Muller, E. R. Bates, F. D. Pagani, M. D. Burdick, and R. M. Strieter. 2000. IL-8 is an angiogenic factor in human coronary atherectomy tissue. *Circulation* 101:1519.

7. Koch, A. E., S. L. Kunkel, W. H. Pearce, M. R. Shah, D. Parikh, H. L. Evanoff, G. K. Haines, M. D. Burdick, and R. M. Strieter. 1993. Enhanced production of the chemotactic cytokines interleukin-8 and monocyte chemoattractant protein-1 in human abdominal aortic aneurysms. *Am. J. Pathol.* 142:1423.

8. Buffon, A., L. M. Biasucci, G. Liuzzo, G. D'Onofrio, F. Crea, and A. Maseri. 2002. Widespread coronary inflammation in unstable angina. *N. Engl. J. Med.* 347:5.

9. Smedly, L. A., M. G. Tonnesen, R. A. Sandhaus, C. Haslett, L. A. Guthrie, R. B. Johnston, Jr., P. M. Henson, and G. S. Worthen. 1986. Neutrophil-mediated injury to endothelial cells: enhancement by endotoxin and essential role of neutrophil elastase. *J. Clin. Invest.* 77:1233.

10. Sumi, Y., N. Inoue, H. Azumi, T. Seno, M. Okuda, K. Hirata, S. Kawashima, Y. Hayashi, H. Itoh, and M. Yokoyama. 2002. Expression of tissue transglutaminase and elafin in human coronary artery: implication for plaque instability. *Atherosclerosis* 160:31.

11. Sallenave, J. M. 2000. The role of secretory leukocyte proteinase inhibitor and elafin (elastase-specific inhibitor/skin-derived antileukoprotease) as alarm antiproteinases in inflammatory lung disease. *Respir. Res.* 1:87.

12. Jin, F. Y., C. Nathan, D. Radzioch, and A. Ding. 1997. Secretory leukocyte protease inhibitor: a macrophage product induced by and antagonistic to bacterial lipopolysaccharide. *Cell* 88:417.

13. Zhu, J., C. Nathan, and A. Ding. 1999. Suppression of macrophage responses to bacterial lipopolysaccharide by a non-secretory form of secretory leukocyte protease inhibitor. *Biochim. Biophys. Acta* 1451:219.

14. Lentsch, A. B., J. A. Jordan, B. J. Czermak, K. M. Diehl, E. M. Younkin, V. Sarma, and P. A. Ward. 1999. Inhibition of NF-κB activation and augmentation of IκBβ by secretory leukocyte protease inhibitor during lung inflammation. *Am. J. Pathol.* 154:239.

15. Lentsch, A. B., H. Yoshidome, R. L. Warner, P. A. Ward, and M. J. Edwards. 1999. Secretory leukocyte protease inhibitor in mice regulates local and remote organ inflammatory injury induced by hepatic ischemia/reperfusion. *Gastroenterology* 117:953.

16. O'Blenes, S. B., S. H. Zaidi, A. Y. Cheah, B. McIntyre, Y. Kaneda, and M. Rabinovitch. 2000. Gene transfer of the serine elastase inhibitor elafin protects against vein graft degeneration. *Circulation* 102(Suppl. 3):III289.

17. Cowan, B., O. Baron, J. Crack, C. Coulber, G. J. Wilson, and M. Rabinovitch. 1996. Elafin, a serine elastase inhibitor, attenuates post-cardiac transplant coronary arteriopathy and reduces myocardial necrosis in rabbits after heterotopic cardiac transplantation. *J. Clin. Invest.* 97:2452.

18. Lewin, M. H., J. R. Arthur, R. A. Riemersma, F. Nicol, S. W. Walker, M. Millar, A. F. Howie, and G. J. Beckett. 2002. Selenium supplementation acting through the induction of thioredoxin reductase and glutathione peroxidase protects the human endothelial cell line Eahy926 from damage by lipid hydroperoxides. *Biochim. Biophys. Acta* 1593:85.

19. Fryer, H. J., G. E. Davis, M. Manthorpe, and S. Varon. 1986. Lowry protein assay using an automatic microtiter plate spectrophotometer. *Anal. Biochem.* 153:262.

20. Zitnik, R. J., J. Zhang, M. A. Kashem, T. Kohno, D. E. Lyons, C. D. Wright, E. Rosen, I. Goldberg, and A. C. Hayday. 1997. The cloning and characterization of a murine secretory leukocyte protease inhibitor cDNA. *Biochem. Biophys. Res. Commun.* 232:687.

21. Chomczynski, P. 1993. A reagent for the single-step simultaneous isolation of RNA, DNA and proteins from cell and tissue samples. *BioTechniques* 15:532.

22. Xing, Z., Y. Ohkawara, M. Jordana, F. Graham, and J. Gauldie. 1996. Transfer of granulocyte-macrophage colony-stimulating factor gene to rat lung induces eosinophilia, monocytosis, and fibrotic reactions. *J. Clin. Invest.* 97:1102.

23. Graham, F., and L. Prevec. 1991. Manipulation of adenovirus vectors. In *Methods in Molecular Biology: Gene Transfer and Expression Protocols 7*. E. J. Murray, ed. Humana Press, Clifton, NJ, p. 109.

24. Ng, P., R. J. Parks, D. T. Cummings, C. M. Evelegh, U. Sankar, and F. L. Graham. 1999. A high-efficiency Cre/loxP-based system for construction of adenoviral vectors. *Hum. Gene Ther.* 10:2667.

25. Jobin, C., S. Haskill, L. Mayer, A. Panja, and R. B. Sartor. 1997. Evidence for altered regulation of IκBα degradation in human colonic epithelial cells. *J. Immunol.* 158:226.

26. Sallenave, J. M., Z. Xing, A. J. Simpson, F. L. Graham, and J. Gauldie. 1998. Adenovirus-mediated expression of an elastase-specific inhibitor (elafin): a comparison of different promoters. *Gene Ther.* 5:352.

27. Bett, A. J., W. Haddara, L. Prevec, and F. L. Graham. 1994. An efficient and flexible system for construction of adenovirus vectors with insertions or deletions in early regions 1 and 3. *Proc. Natl. Acad. Sci. USA* 91:8802.

28. Gimbrone, M. A., Jr., R. S. Cotran, and J. Folkman. 1974. Human vascular endothelial cells in culture: growth and DNA synthesis. *J. Cell Biol.* 60:673.

29. McCutcheon, J. C., S. P. Hart, M. Canning, K. Ross, M. J. Humphries, and I. Dransfield. 1998. Regulation of macrophage phagocytosis of apoptotic neutrophils by adhesion to fibronectin. *J. Leukocyte Biol.* 64:600.

30. Lieber, M., B. Smith, A. Szakal, W. Nelson-Rees, and G. Todaro. 1976. A continuous tumor-cell line from a human lung carcinoma with properties of type II alveolar epithelial cells. *Int. J. Cancer* 17:62.

31. Fasbender, A., J. Zabner, M. Chillon, T. O. Moninger, A. P. Puga, B. L. Davidson, and M. J. Welsh. 1997. Complexes of adenovirus with polycationic polymers and cationic lipids increase the efficiency of gene transfer in vitro and in vivo. *J. Biol. Chem.* 272:6479.

32. Simoes, S., V. Slepushkin, E. Pretzer, P. Dazin, R. Gaspar, M. C. Pedroso de Lima, and N. Duzgunes. 1999. Transfection of human macrophages by lipoplexes via the combined use of transferrin and pH-sensitive peptides. *J. Leukocyte Biol.* 65:270.

33. Maizel, J. V., Jr., D. O. White, and M. D. Scharff. 1968. The polypeptides of adenovirus. I. Evidence for multiple protein components in the virion and a comparison of types 2, 7A, and 12. *Virology* 36:115.

34. Staal, F. J., M. Roederer, L. A. Herzenberg, and L. A. Herzenberg. 1990. Intracellular thiols regulate activation of nuclear factor κB and transcription of human immunodeficiency virus. *Proc. Natl. Acad. Sci. USA* 87:9943.

35. Claise, C., M. Edeas, J. Chalas, A. Cockx, A. Abella, L. Capel, and A. Lindenbaum. 1996. Oxidized low-density lipoprotein induces the production of interleukin-8 by endothelial cells. *FEBS Lett.* 398:223.

36. Yeh, M., N. Leitinger, R. de Martin, N. Onai, K. Matsushima, D. K. Vora, J. A. Berliner, and S. T. Reddy. 2001. Increased transcription of IL-8 in endothelial cells is differentially regulated by TNF-α and oxidized phospholipids. *Arterioscler. Thromb. Vasc. Biol.* 21:1585.

37. Reid, P. T., M. E. Marsden, G. A. Cunningham, C. Haslett, and J. M. Sallenave. 1999. Human neutrophil elastase regulates the expression and secretion of elafin (elastase-specific inhibitor) in type II alveolar epithelial cells. *FEBS Lett.* 457:33.

38. Rothenberg, M. E., A. D. Luster, and P. Leder. 1995. Murine eotaxin: an eosinophil chemoattractant inducible in endothelial cells and in interleukin 4-induced tumor suppression. *Proc. Natl. Acad. Sci. USA* 92:8960.

39. Lei, Z. B., Z. Zhang, Q. Jing, Y. W. Qin, G. Pei, B. Z. Cao, and X. Y. Li. 2002. OxLDL upregulates CXCR2 expression in monocytes via scavenger receptors and activation of p38 mitogen-activated protein kinase. *Cardiovasc. Res.* 53:524.

40. Kuo, C. C., A. Shor, L. A. Campbell, H. Fukushi, D. L. Patton, and J. T. Grayston. 1993. Demonstration of *Chlamydia pneumoniae* in atherosclerotic lesions of coronary arteries. *J. Infect. Dis.* 167:841.

41. Poston, R. N., D. O. Haskard, J. R. Coucher, N. P. Gall, and R. R. Johnson-Tidey. 1992. Expression of intercellular adhesion molecule-1 in atherosclerotic plaques. *Am. J. Pathol.* 140:665.

42. Boisvert, W. A., R. Santiago, L. K. Curtiss, and R. A. Terkeltaub. 1998. A leukocyte homologue of the IL-8 receptor CXCR-2 mediates the accumulation of macrophages in atherosclerotic lesions of LDL receptor-deficient mice. *J. Clin. Invest.* 101:353.

43. Sallenave, J. M., J. Shulmann, J. Crossley, M. Jordana, and J. Gauldie. 1994. Regulation of secretory leukocyte proteinase inhibitor (SLPI) and elastase-specific inhibitor (ESI/elafin) in human airway epithelial cells by cytokines and neutrophilic enzymes. *Am. J. Respir. Cell Mol. Biol.* 11:733.

44. Walsh, D. E., C. M. Greene, T. P. Carroll, C. C. Taggart, P. M. Gallagher, S. J. O'Neill, and N. G. McElvaney. 2001. Interleukin-8 up-regulation by neutrophil elastase is mediated by MyD88/IRAK/TRAF-6 in human bronchial epithelium. *J. Biol. Chem.* 276:35494.

45. Daugherty, A., J. L. Dunn, D. L. Rateri, and J. W. Heinecke. 1994. Myeloperoxidase, a catalyst for lipoprotein oxidation, is expressed in human atherosclerotic lesions. *J. Clin. Invest.* 94:437.

46. Hazen, S. L., and J. W. Heinecke. 1997. 3-Chlorotyrosine, a specific marker of myeloperoxidase-catalyzed oxidation, is markedly elevated in low density lipoprotein isolated from human atherosclerotic intima. *J. Clin. Invest.* 99:2075.

47. Barnathan, E. S., P. N. Raghunath, J. E. Tomaszewski, T. Ganz, D. B. Cines, and A. al-R. Higazi. 1997. Immunohistochemical localization of defensin in human coronary vessels. *Am. J. Pathol.* 150:1009.

48. Higazi, A. A., T. Nassar, T. Ganz, D. J. Rader, R. Udassin, K. Bdeir, E. Hiss, B. S. Sachais, K. J. Williams, E. Leitersdorf, and D. B. Cines. 2000. The α-defensins stimulate proteoglycan-dependent catabolism of low-density lipoprotein by vascular cells: a new class of inflammatory apolipoprotein and a possible contributor to atherogenesis. *Blood* 96:1393.

49. Schalkwijk, J., O. Wiedow, and S. Hirose. 1999. The trappin gene family: proteins defined by an N-terminal transglutaminase substrate domain and a C-terminal four-disulphide core. *Biochem. J.* 340:569.

50. Sallenave, J. M., M. Si-Tahar, G. Cox, M. Chignard, and J. Gauldie. 1997. Secretory leukocyte proteinase inhibitor is a major leukocyte elastase inhibitor in human neutrophils. *J. Leukocyte Biol.* 61:695.

51. Pecher, G., G. Spahn, T. Schirrmann, H. Kulbe, M. Ziegner, J. A. Schenk, and V. Sandig. 2001. Mucin gene (MUC1) transfer into human dendritic cells by cationic liposomes and recombinant adenovirus. *Anticancer Res.* 21:2591.

52. Erbacher, P., M. T. Bousser, J. Raimond, M. Monsigny, P. Midoux, and A. C. Roche. 1996. Gene transfer by DNA/glycosylated polylysine complexes into human blood monocyte-derived macrophages. *Hum. Gene Ther.* 7:721.

53. Fasbender, A., J. H. Lee, R. W. Walters, T. O. Moninger, J. Zabner, and M. J. Welsh. 1998. Incorporation of adenovirus in calcium phosphate precipitates enhances gene transfer to airway epithelia in vitro and in vivo. *J. Clin. Invest.* 102:184.

54. Devaney J. M., C. M. Greene, C. C. Taggart, T. P. Carroll, S. T. O'Neill, and N. G. McElvaney. 2003. Neutrophil elastase up-regulates interleukin-8 via Toll-like receptor 4. *FEBS Lett.* 544:129.

55. Roebuck, K. A. 1999. Regulation of interleukin-8 gene expression. *J. Interferon Cytokine Res.* 19:429.

56. Huang, S., R. I. Endo, and G. R. Nemerow. 1995. Upregulation of integrins $\alpha_v\beta_3$ and $\alpha_v\beta_5$ on human monocytes and T lymphocytes facilitates adenovirus-mediated gene delivery. *J. Virol.* 69:2257.

57. Simpson, A. J., G. A. Cunningham, D. J. Porteous, C. Haslett, and J. M. Sallenave. 2001. Regulation of adenovirus-mediated elafin transgene expression by bacterial lipopolysaccharide. *Hum. Gene Ther.* 12:1395.

58. Sallenave, J. M., G. A. Cunningham, R. M. James, G. McLachlan, and C. Haslett. 2003. Regulation of pulmonary and systemic bacterial lipopolysaccharide responses in transgenic mice expressing human elafin. *Infect. Immun.* 71:3766.

59. Foxwell, B., K. Browne, J. Bondeson, C. Clarke, R. de Martin, F. Brennan, and M. Feldmann. 1998. Efficient adenoviral infection with IκBα reveals that macrophage tumor necrosis factor α production in rheumatoid arthritis is NF-κB dependent. *Proc. Natl. Acad. Sci. USA* 95:8211.

60. Brand, K., S. Page, A. K. Walli, D. Neumeier, and P. A. Baeuerle. 1997. Role of nuclear factor-κB in atherogenesis. *Exp. Physiol.* 82:297.

61. Cominacini, L., A. F. Pasini, U. Garbin, A. Davoli, M. L. Tosetti, M. Campagnola, A. Rigoni, A. M. Pastorino, V. Lo Cascio, and T. Sawamura. 2000. Oxidized low density lipoprotein (ox-LDL) binding to ox-LDL receptor-1 in endothelial cells induces the activation of NF-κB through an increased production of intracellular reactive oxygen species. *J. Biol. Chem.* 275:12633.

62. Hawiger, J., R. A. Veach, X. Y. Liu, S. Timmons, and D. W. Ballard. 1999. IκB kinase complex is an intracellular target for endotoxic lipopolysaccharide in human monocytic cells. *Blood* 94:1711.

63. Zen, K., A. Karsan, T. Eunson, E. Yee, and J. M. Harlan. 1998. Lipopolysaccharide-induced NF-κB activation in human endothelial cells involves degradation of IκBα but not IκBβ. *Exp. Cell Res.* 243:425.

64. Heimberg, H., Y. Heremans, C. Jobin, R. Leemans, A. K. Cardozo, M. Darville, and D. L. Eizirik. 2001. Inhibition of cytokine-induced NF-κB activation by adenovirus-mediated expression of a NF-κB super-repressor prevents β-cell apoptosis. *Diabetes* 50:2219.

65. Ashcroft, G. S., K. Lei, W. Jin, G. Longenecker, A. B. Kulkarni, T. Greenwell-Wild, H. Hale-Donze, G. McGrady, X. Y. Song, and S. M. Wahl. 2000. Secretory leukocyte protease inhibitor mediates non-redundant functions necessary for normal wound healing. *Nat. Med.* 6:1147.

66. Mulligan, M. S., A. B. Lentsch, M. Huber-Lang, R. F. Guo, V. Sarma, C. D. Wright, T. R. Ulich, and P. A. Ward. 2000. Anti-inflammatory effects of mutant forms of secretory leukocyte protease inhibitor. *Am. J. Pathol.* 156:1033.

67. Ding, A., N. Thieblemont, J. Zhu, F. Jin, J. Zhang, and S. Wright. 1999. Secretory leukocyte protease inhibitor interferes with uptake of lipopolysaccharide by macrophages. *Infect. Immun.* 67:4485.

68. Taggart, C. C., C. M. Greene, N. G. McElvaney, and S. O'Neill. 2002. Secretory leucoprotease inhibitor prevents lipopolysaccharide-induced IκBα degradation without affecting phosphorylation or ubiquitination. *J. Biol. Chem.* 277:33648.

69. Jobin, C., C. A. Bradham, M. P. Russo, B. Juma, A. S. Narula, D. A. Brenner, and R. B. Sartor. 1999. Curcumin blocks cytokine-mediated NF-κB activation and proinflammatory gene expression by inhibiting inhibitory factor I-κB kinase activity. *J. Immunol.* 163:3474.

70. Mansell, A., A. Reinicke, D. M. Worrall, and L. A. O'Neill. 2001. The serine protease inhibitor antithrombin III inhibits LPS-mediated NF-κB activation by TLR-4. *FEBS Lett.* 508:313.

Gene delivery of the elastase inhibitor elafin protects macrophages from neutrophil elastase-mediated impairment of apoptotic cell recognition

Peter A. Henriksen[a,b], Andrew Devitt[c], Yuri Kotelevtsev[b], Jean-Michel Sallenave[a,*]

[a]Rayne Laboratory, MRC Centre for Inflammation Research, Edinburgh University Medical School, Teviot Place, Edinburgh EH8 9AG, UK
[b]Centre for Cardiovascular Science, Edinburgh University Medical School, Edinburgh, UK
[c]Innate Immunity Group, MRC Centre for Inflammation Research, Edinburgh University Medical School, Edinburgh, UK

Abstract The resolution of inflammation is dependent on recognition and phagocytic removal of apoptotic cells by macrophages. Receptors for apoptotic cells are sensitive to degradation by human neutrophil elastase (HNE). We show in the present study that HNE cleaves macrophage cell surface CD14 and in so doing, reduces phagocytic recognition of apoptotic lymphocytic cells (Mutu 1). Using an improved method of adenovirus-mediated transfection of macrophages with the HNE inhibitor elafin, we demonstrate that elafin overexpression prevents CD14 cleavage and restores apoptotic cell recognition by macrophages. This approach of genetic modification of macrophages could be used to restore apoptotic cell recognition in inflammatory conditions.
© 2004 Federation of European Biochemical Societies. Published by Elsevier B.V. All rights reserved.

Keywords: Neutrophil elastase; Elafin; Macrophage; Apoptosis; Adenovirus; Gene therapy

1. Introduction

The removal of cells undergoing apoptosis or programmed cell death is an essential step in the resolution phase of the inflammatory response. Macrophages are particularly important in the processes of recognition and engulfment of apoptotic cells [1,2] and inflammatory mediators may impair these processes prolonging inflammation and tissue injury. Human neutrophil elastase (HNE) is a potent protease released by neutrophils during acute inflammation and mediates both direct tissue damage and the upregulation of pro-inflammatory cytokines such as interleukin (IL-8) [3–5]. HNE has also recently been demonstrated to impair apoptotic cell recognition by cleaving the phosphatidylserine receptor (PSR) on the surface of macrophages [6]. A variety of macrophage receptors have been implicated in apoptotic cell recognition, such as the

PSR and CD14 [6,7] and from these the former has been shown to be inactivated by HNE in patients with pulmonary inflammation [6]. Similarly, HNE has been shown to degrade CD14 on the surface of human peripheral blood monocytes and fibroblasts [8,9].

We have chosen to focus the present study on CD14 and reasoned that a strategy aiming at protecting CD14 from cleavage by HNE would be beneficial, favouring apoptotic cell removal in an inflammatory environment. For that purpose, we used an adenovirus (Ad) gene-transfer methodology involving complexing a recombinant Ad with the cationic liposome lipofectamine. Using this technique, we show that the HNE-mediated cleavage of CD14 and ensuing impairment of apoptotic cell recognition are inhibited by Ad-mediated overexpression of human elafin, a potent HNE inhibitor. Inhibitors of HNE are thought to comprise part of the human innate immune system. Elafin [10,11] is a potent inhibitor of HNE and proteinase 3 produced in the skin and airways, which is upregulated in response to early inflammatory cytokines such as tumour necrosis factor (TNF) and IL-1 [4]. Our group has recently demonstrated elafin as a multi-faceted molecule exhibiting direct antimicrobial activity [12] and an inhibitory effect on NF-κB mediated inflammatory cytokine production [13].

We demonstrate here for the first time that human macrophages can be genetically reprogrammed to overexpress elafin, from an HNE-mediated inflammatory phenotype, associated with apoptotic cell recognition deficiency, to a phagocytic competent phenotype. These findings have implications for the use of adenovirus in ex vivo applications of macrophages in inflammatory disorders.

2. Materials and methods

2.1. Reagents

HNE was obtained from Elastin Products (Owensville, MO). Recombinant elafin was a gift from Dr. J. Fitton, Astra-Zeneca (Macclesfield, UK). The monoclonal blocking antibody against CD14 (mAb 61D3) hybridoma (IgGl mouse anti-human) was originally obtained as a gift from J.D. Capra [14]. Penicillin G, streptomycin sulfate, and Iscove's modified DMEM were obtained from Life Technologies (Paisley, UK). X-Vivo 10 serum free culture medium was obtained from Cambrex Bio Science (Wokingham, UK). Falcon tissue culture material was from A.&J. Beveridge (Edinburgh, UK). 6-well, 48-well and 96-well tissue culture plates were obtained from Corning Costar

*Corresponding author. Fax: +44-1-31-650-4384.
E-mail address: jsallena@staffmail.ed.ac.uk (J.-M. Sallenave).

Abbreviations: HNE, human neutrophil elastase; 61D3, monoclonal blocking antibody against CD14; IL, interleukin; Ad, adenovirus; Ad-dl703, control (empty) adenoviral vector; PBS, phosphate-buffered saline; PSR, phosphatidylserine receptor; TNFα, tumour necrosis factor-α; GFP, green fluorescent protein

(High Wycombe, UK). All other chemicals were purchased from Sigma Chemicals (Poole, UK).

2.2. Adenovirus (Ad) constructs

The generation of El, E3 deleted Ad constructs Ad-elafin and Ad-dl703 ("empty" Ad control) has been described previously [15,16].

2.3. Macrophage isolation and FACS analysis

Mononuclear cells were isolated from peripheral blood as follows: freshly citrated blood was centrifuged at $400 \times g$ for 20 min and the platelet-rich plasma supernatant was used to prepare autologous serum by addition of $CaCl_2$ (10 mM final concentration). Leukocytes were isolated after removal of erythrocytes by sedimentation using 6% (w/v) dextran T500 in saline by fractionation on a discontinuous gradient of isotonic Percoll solutions made in Ca^{2+}/Mg^{2+}-free phosphate-buffered saline (PBS) (CMF-PBS). Percoll concentrations of 55%, 68% and 79% were used and the leukocytes were centrifuged at $700 \times g$ for 20 min. Mononuclear cells were aspirated from the 55%/68% interface and washed three times in CMF-PBS prior to culture. Monocytes were enriched from the mononuclear fraction by selectively attaching them to 6-well plates for 40 min at 37 °C. Non-adherent lymphocytes were removed and adherent monocytes were washed twice in PBS. Monocytes were then cultured in Iscove's modified DMEM containing 10% autologous serum, penicillin G (final concentration 100 U/ml) and streptomycin sulfate (final concentration 100 µg/ml) at 37 °C in a 5% CO_2 atmosphere. Maturation into macrophages with this culture protocol has previously been demonstrated using myeloid-specific markers, including CD16 and CD51/CD61 [17]. On culture day 4, macrophages were removed with cold CMF-PBS and plated at 70 000 cells/well on 48-well plates in X-Vivo 10 serum free culture medium. On culture day 6, Ad vectors were preincubated for 15 min at room temperature in X-vivo 10 medium with lipofectamine (Invitrogen, Paisley, UK) at a ratio of 5×10^4 lipofectamine molecules to each Ad particle (Ad particle concentration was determined from absorbance at 260 nm for each Ad construct according to established protocols) and added to day 6 macrophages at a multiplicity of infection (MOI) of 100. Macrophages were incubated in the virus-containing medium for 2 h before replenishment with X-vivo 10 growth medium.

Where indicated, HNE (1 µM) was added directly the following day and incubated for 1 h prior to removal. Following HNE treatments, cells were washed with ice cold CMF-PBS and suspended in 2% goat serum (Serotec Ltd, Oxford, UK). Cells were incubated with 61D3, a CD14 blocking monoclonal antibody [7], for 30 min, washed twice and then incubated with phycoerythrin-conjugated goat anti-mouse IgG secondary antibody for 15 min. Washed macrophages were then analysed on a FACScan cytometer (Becton Dickinson and Co.).

2.4. HNE inhibition assay

The HNE activity of macrophage supernatants, following incubation with HNE, was examined to determine any inhibitory effect conferred by infection with Ad-elafin or incubation with r-elafin. The HNE activity assay has been described in detail elsewhere [18]. Briefly, all dilutions were performed in assay buffer (50 mM Tris, 0.5 M NaCl and 0.1% Triton X-100, pH 8.0). Cell culture supernatant (90 µl) was incubated in a 96-well microtitre plate for 30 min at 37 °C before addition of the chromogeneic substrate N-methoxysuccinyl–Ala–Ala–Pro–Val–p-nitroanilide. The change in absorbance measured spectrophotometrically at 405 nm (MR5000 Plate Reader, Dynatech, Dynex, Billinghurst, UK) was expressed as a function of time. In a separate experiment to measure HNE activity within apoptotic Mutu cells, two independent batches of apoptotic Mutu cells (3 million cells) were pelleted and washed with PBS and lysed in 0.4 ml of HNE buffer assay. Cell lysate (50 µl) was added to a microtitre plate and HNE activity recorded according to the protocol described above.

2.5. Apoptotic cells recognition assays

Macrophages were prepared and Ad infections performed in X-vivo 10 serum free medium as above in 48-well plates. Where indicated, HNE (1 µM) and r-elafin (15 µg/ml = 2.5 µM) were added directly for 1 h prior to the interaction assay with apoptotic cells. The group I Burkitt lymphoma cell line Mutu I, induced into apoptosis by 16 h incubation with 1 µg/ml of the calcium ionophore ionomycin (Calbiochem, Nottingham, UK), was used as a source of apoptotic cells. Typically, around 70% of cells were apoptotic following this treatment

as determined by FACS analysis of annexin V staining. For some experiments, the 61D3 CD14-blocking monoclonal antibody was mixed with the apoptotic Mutu cells. The culture medium was removed and 750 000 apoptotic Mutu cells were added to each 48-well for 1 h at 37 °C before being washed extensively with ice cold CMF-PBS to remove unbound apoptotic cells. Cells were then fixed in 1% paraformaldehyde and stained with Diff-quick for counting. Cultures were scored by light microscopy according to the proportion of macrophages that had internalised or bound apoptotic Mutu cells by established criteria [7,19]. At least 300 macrophages were assessed per sample.

2.6. Statistics

Results are presented as means ± S.D. and differences between treatments were tested using the Student's t test.

3. Results and discussion

Macrophages are important phagocytic cells involved in the recognition and removal of apoptotic cells, integral processes in the resolution of the inflammatory response [1,2]. Recent data have suggested that HNE, a pro-inflammatory enzyme released during uncontrolled inflammation [3], may be responsible for the impairment of apoptotic cell recognition by macrophages, by cleaving key receptors on these cells [6]. The
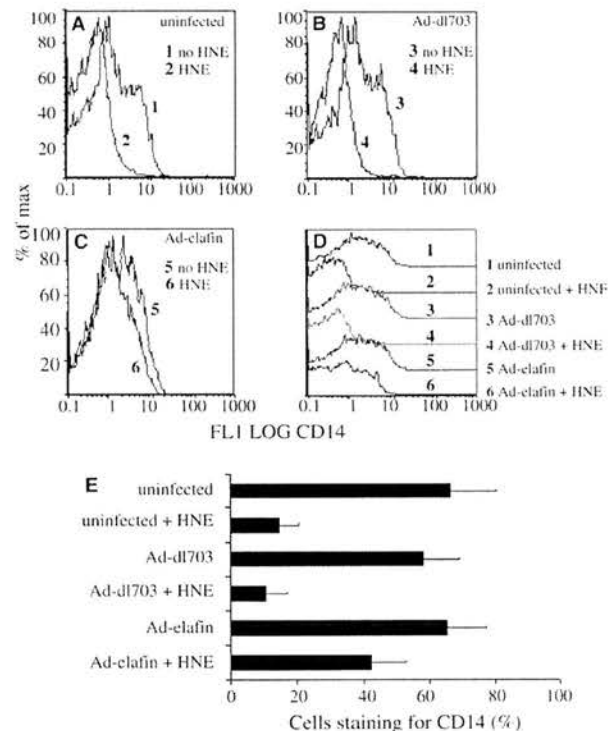

Fig. 1. The effect of HNE on surface expression of CD14 on human macrophages. Where indicated, macrophages were incubated with HNE (1 µM) for 1 h prior to removal. Binding of the 61D3 (anti-CD14) antibody was then analysed by flow cytometry. Adenovirus infections were performed at an MOI of 100 using the protocol with lipofectamine described in Section 2. (A) Uninfected cells. (B) Ad-dl703-infected cells (MOI 100). (C) Ad-elafin infected cells (MOI 100). (D) Composite figure illustrating 61D3 binding in the different conditions from a separate donor. (E) Mean percent of macrophages staining for CD14 ± S.D. Data are from experiments performed on two separate donors.

PSR was susceptible to HNE cleavage although the expression of other apoptotic cell recognition receptors, CD36 and CD32, was relatively preserved. We have demonstrated that CD14, a receptor with susceptibility to HNE, participates in the resolution phase of the inflammatory response as a cell surface receptor for apoptotic cells [7] in addition to acting as a receptor for bacterial lipopolysaccharide [20]. To test whether HNE could cleave macrophage CD14, we treated this cell type with purified HNE and analysed CD14 cell surface expression by FACS analysis. Compared to untreated cells, HNE-treatment drastically reduced the level of cell surface CD14 (Fig. 1A).

We decided to target HNE because of its deleterious action in inflammatory conditions and its central role in cleaving a variety of apoptotic cell receptors (CD14 and phosphatidyl-serine [6] being two out of a list likely to grow). We designed a gene therapy strategy to protect macrophages from the HNE-mediated cleavage of surface receptors. Traditional gene transfer vectors have proven disappointing for the transfection of macrophages [21] and we have previously developed a hybrid method, involving pre-complexing of adenovirus with cationic liposomes (lipofectamine) [13]. This method greatly enhances transfection in other cell types both in vitro and in vivo [22,23]. We have adapted this method for peripheral blood monocyte-derived macrophages and show here an impressive increase in transfection levels using green fluorescent protein (GFP) as a gene reporter (Fig. 2). Using this technique, 92% of macrophages exhibited GFP expression 24 h after infection with Ad-GFP (counting in a low power field). Similarly, when macrophages were infected with Ad-elafin/lipofectamine, elafin supernatant levels were increased from 10.4 ($\pm$4.11) ng/ml with Ad-elafin alone to 232 ($\pm$13.1) ng/ml (values are means and S.D. derived from a representative experiment performed in triplicate). Elafin was not detected in the supernatant from uninfected cells. Having established the disruptive activity of HNE on macrophage CD14 in our System (see above, Fig. 1A), we demonstrated that Ad-elafin inhibited HNE-mediated shedding of CD14 compared to macrophages infected with Ad-dl70/3, an Ad vector with no

transgene cassette (Fig. 1B and C). When serum-free supernatants were tested for HNE activity, most HNE was inhibited when a saturating concentration of r-elafin was added extracellularly (Fig. 3). Although Ad-elafin was efficient in preserving CD14 expression, it conferred by contrast a relatively modest, albeit significant, inhibition of HNE when compared to Ad-dl70/3 (Fig. 3). This result was predicted from the elafin concentrations in Ad-elafin infected cell supernatants that were theoretically not high enough to neutralise the quantity of HNE added.

Finally, we investigated the effect of HNE on macrophage apoptotic cell recognition and whether Ad-elafin had a protective role. A variety of cells, such as lymphocytes and neutrophils, are routinely used in experimental systems as apoptotic target cells. We chose Group 1 Burkitt lymphoma cells (Mutu I) over neutrophils because of the absence of endogenous HNE in the former (HNE levels were below the levels of detection from apoptotic mutu cell lysates, see Section 2), which could have interfered with our assays. Previous work has demonstrated that binding of viable Mutu cells is negligible in this system and any interaction that does occur is with spontaneously apoptotic Mutu cells [19]. Macrophages were either untreated/uninfected (control) or infected with Ad-elafin (Ad-dl70/3 as a control) and incubated where indicated with HNE. In a variation of these experiments, the CD14 blocking antibody 61D3 [7] was used in order to provide a positive control of CD14 blockade. Fig. 4 shows that HNE treatment of untransfected cells inhibited Mutu cell recognition by 54%, compared to untransfected cells alone. This level of inhibition was comparable to that of 61D3 treatment. The prominent role of CD14 (the 61D3 antigen) for interaction and initial tethering of apoptotic Mutu cells with human macrophages has previously been characterised. Blocking antibodies and
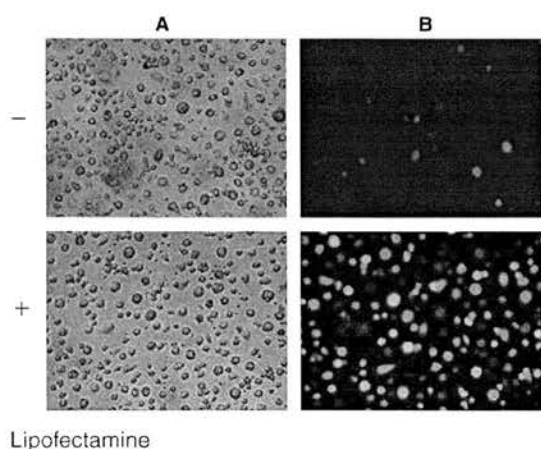

Fig. 2. Lipofectamine facilitates Ad-GFP infection of macrophages. Peripheral blood monocyte-derived macrophages were infected on culture day 6 with Ad-GFP (100 PFU/cell). Where indicated, virus was precomplexed with lipofectamine (+) according to protocols in Section 2. Photomicrographs were taken 24 h after Ad infection and GFP fluorescence was observed. (A) No filter and (B) green filter.
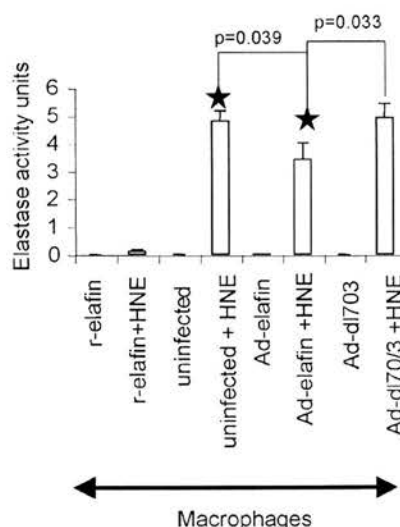

Fig. 3. Comparison of HNE inhibitory activity of macrophage culture supernatants. Macrophages were prepared and infected with Ad-vectors using the protocols described in Fig. 1. Following incubation with HNE, culture supernatants were removed for determination of residual HNE activity. Supernatants were transferred to a microtitre plate and cleavage of a chromogenic HNE substrate was measured spectrophotometrically over time. *P* values are given for the comparisons of Ad-dl703 (control adenovirus) and uninfected cells to Ad-elafin. Data are means $\pm$ S.D. from experiments performed in triplicate on three separate donors ($n = 3$).
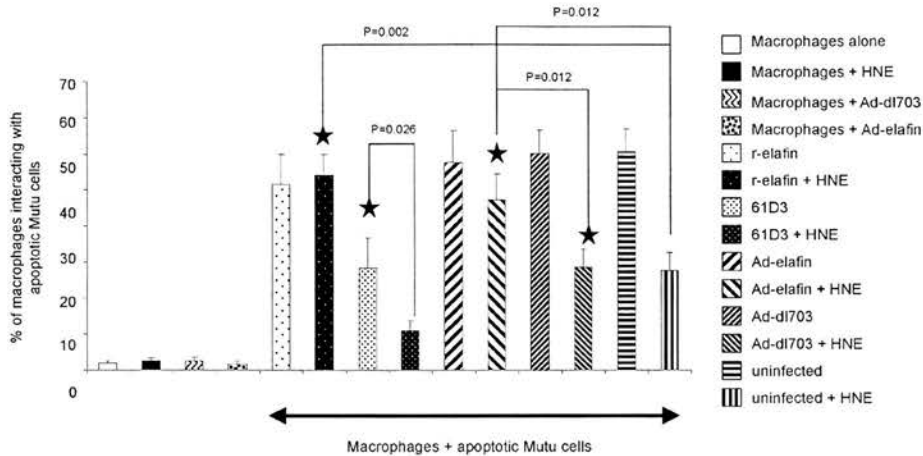
Fig. 4. Elafin protects macrophages from HNE-mediated impairment of Mutu cell recognition. Macrophages were cultured and infected with Ad vectors using the same protocol from Fig. 1. Where indicated, HNE (1 μM) and r-elafin (2.5 μM) were added in serum free X-vivo 10 medium for 1 h prior to adding the apoptotic Mutu target cells with or without 61D3 (CD14 blocking monoclonal antibody). After fixing and staining, the percentage of macrophages interacting with apoptotic Mutu cells was calculated. Interaction counts performed on macrophages that had not been exposed to Mutu cells are also shown to exclude any significant contribution from apoptotic cells originating from within the culture. P values are given for each comparison. Data are means ± S.D. from experiments performed in quadruplicate on three separate donors ($n = 3$).

peptides against the $\alpha_v\beta_3$, integrin (Vitronectin receptor) and CD36 produced little if any reduction of apoptotic Mutu cell interaction in this system [19]. Interestingly, when 61D3 and HNE were used in combination, a further decrease in recognition occurred, suggesting that the sites of action of 61D-3 and HNE are not identical. It is likely that in addition to cleaving CD14 (Fig. 1), HNE is interfering with additional (unidentified) surface receptors in our system and notably the degree of inhibition never approached 100% even with 61D3 and HNE together. HNE cleavage of the PSR was associated with reduced ingestion of apoptotic Jurkat cells by human macrophages [6] and the role of PSR cleavage in reducing interaction in our system is unknown.

When r-elafin was added extracellularly with HNE, macrophage recognition was restored to normal values. Similarly, when macrophages were transfected with Ad-elafin, prior to HNE challenge, a very significant increase in macrophage recognition of apoptotic cells was obtained, compared to untransfected cells and cells transfected with Ad-dl70/3, demonstrating the elafin transgene specific effect (Fig. 4). In addition, Ad-transfection on its own (Ad-dl70/3 and Ad-elafin) did not influence apoptotic cell recognition. HNE, Ad-elafin and Ad-dl703 had no effect alone on the background rate of apoptotic cell recognition in the absence of apoptotic Mutu cells (Fig. 4; 2nd, 3rd and 4th bars from the left).

These results illustrate the potential of elafin gene therapy to rescue the capacity of macrophages to recognise apoptotic cells in the presence of HNE. Although expression of CD14 was relatively preserved in Ad-elafin infected macrophages (Fig. 1C), the effect on residual supernatant HNE activity was less marked (Fig. 3) indicating the possibility that elafin may facilitate apoptotic cell recognition through additional mechanisms. Indeed, we have shown that elafin has broad ranging anti-inflammatory properties, inhibiting the action of the transcription factor NF-κB and the release of pro-inflammatory cytokines such as TNF and IL-8 [13]. Since HNE has been shown to have pro-inflammatory signalling effects [4,5], it is likely that the Ad-elafin transfection of macrophages provides a further anti-inflammatory signal beneficial to apoptotic cell

recognition. This signal would reinforce the endogenous anti-inflammatory phenotype conferred by binding of apoptotic cells to macrophages [24] that may otherwise be diminished by HNE. Interestingly, the endogenous synthesis of another neutrophil elastase inhibitor, secretory leukocyte protease inhibitor (SLPI), has recently been shown to be up-regulated following macrophage recognition of apoptotic cells [25]. However, as pointed out by Odaka et al. [25], the slow kinetics of production of SLPI after the apoptotic cell recognition event suggests that SLPI is unlikely to act in vivo at an autocrine level during the onset of the interaction but rather in a paracrine fashion, during phagocytosis of incoming cells.

In summary, we show here that using adenovirus as a gene transfer vector in a hybrid method with lipofectamine as a facilitating agent, it is possible to very efficiently transfect monocyte-derived macrophages ex vivo with elafin, a potent elastase inhibitor. This rescues these cells from an HNE-induced pro-inflammatory to an anti-inflammatory phenotype favouring apoptotic cell recognition and clearance. The potential for systemic delivery of macrophages transfected ex vivo with antinflammatory genes has been demonstrated in murine glomerulonephritis [26,27] and this methodology may prove useful in inflammatory conditions where direct use of adenovirus gene vectors is precluded, because of their intrinsic immunogenicity. Cystic fibrosis, characterised by an excessive load of unchecked HNE and a recognised "paralysis" of innate immune mechanisms [28], provides a fascinating model in which to test this paradigm.

References

[1] Savill, J., Dransfield, I., Gregory, C. and Haslett, C. (2002) A blast from the past: Clearance of apoptotic cells regulates immune responses. Nat. Rev. Immunol. 2, 965–975.

[2] Savill, J. and Fadok, V. (2000) Corpse clearance defines the meaning of cell death. Nature 407, 784–788.

[3] Lee, W.L. and Downey, G.P. (2001) Leukocyte elastase – physiological functions and role in acute lung injury. Am. J. Respir. Crit. Care Med. 164, 896–904.

[4] Sallenave, J.-M., Shulmann, J., Crossley, J., Jordana, M. and Gauldie, J. (1994) Regulation of secretory leukocyte proteinase inhibitor (SLPI) and elastase-specific inhibitor (ESI/elafin) in human airway epithelial cells by cytokines and neutrophilic enzymes. Am. J. Respir. Cell. Mol. Biol. 11, 733–741.

[5] Walsh, D.E., Greene, C.M., Carroll, T.P., Taggart, C.P., Gallagher, M., O'Neill, S.J. and McElvaney, N.G. (2001) Interleukin-8 up-regulation by neutrophil elastase is mediated by MyD88/IRAK/TRAF-6 in human bronchial epithelium. J. Biol. Chem. 276, 35494–35499.

[6] Vandivier, R.W., Fadok, V.A., Hoffmann, P.R., Bratton, D.L., Penvari, C., Brown, K.K., Brain, J.D., Accurso, F.J. and Henson, P.M. (2002) Elastase-mediated phosphatidylserine receptor cleavage impairs apoptotic cell clearance in cystic fibrosis and bronchiectasis. J. Clin. Invest. 109, 661–670.

[7] Devitt, A., Moffatt, O.D., Raykundalia, C., Capra, J.D., Simmons, D.L. and Gregory, C.D. (1998) Human CD14 mediates recognition and phagocytosis of apoptotic cells. Nature 392, 505–509.

[8] Le Barillec, K., Si-Tahar, M., Balloy, V. and Chignard, M. (1999) Proteolysis of monocyte CD14 by human leukocyte elastase inhibits lipopolysaccharide-mediated cell activation. J. Clin. Invest. 103, 1039–1046.

[9] Nemoto, E., Sugawara, S., Tada, H., Takada, H., Shimauchi, H. and Horiuchi, H. (2000) Cleavage of CD14 on human gingival fibroblasts cocultured with activated neutrophils is mediated by human leukocyte elastase resulting in down-regulation of lipopolysaccharide-induced IL-8 production. J. Immunol. 165, 5807–5813.

[10] Saheki, T., Ito, F., Hagiwara, H., Saito, Y., Kuroki, J., Tachibana, S. and Hirose, S. (1992) Primary structure of human elafin precursor preproelafin deduced from the nucleotide sequence of its gene and the presence of unique repetitive sequences in the prosegment. Biochem. Biophys. Res. Commun. 185, 240–246.

[11] Sallenave, J.-M. and Silva, A. (1993) Characterization and gene sequence of the precursor of elafin, an elastase-specific inhibitor in bronchial secretions. Am. J. Respir. Cell Mol. Biol. 8, 439–446.

[12] Simpson, A.J., Maxwell, A.I., Govan, J.R.W., Haslett, C. and Sallenave, J-M. (1999) Elafin (elastase-specific inhibitor) has antimicrobial activity against Gram-positive and Gram-negative respiratory pathogens. FEBS Lett. 452, 309–315.

[13] Henriksen, P.A., Hirt, M., Xing, Z., Wang, J., Webb, D.J., Haslett, C., Riemersma, R.A., Kotelevtsev, Y. and Sallenave, J.-M. (2004) Adenoviral gene delivery of elafin and secretory leucocyte protease inhibitor attenuates inflammatory responses of human endothelial cells and macrophages to atherogenic stimuli. J. Immunol 172, 4535–4544.

[14] Ugolini, V., Nunex, G., Smith, R.G., Statny, P. and Capra, J.D. (1980) Initial characterisation of monoclonal antibodies against human monocytes. Proc. Natl. Acad. Sci. USA 77, 6764–6768.

[15] Sallenave, J.-M. (2000) The role of secretory leukocyte proteinase inhibitor and elafin (elastase-specific inhibitor/skin-derived antileukoprotease) as alarm antiproteinases in inflammatory lung disease. Respir. Res. 1, 87–92.

[16] Bett, A.J., Haddara, W., Prevec, L. and Graham, F.L. (1994) An efficient and flexible system for construction of adenovirus vectors with insertions or deletions in early regions 1 and 3. Proc. Natl. Acad. Sci. USA 91, 8802–8806.

[17] McCutcheon, J.C., Hart, S.P., Canning, M., Ross, K., Humphries, M.J. and Dransfield, I. (1998) Regulation of macrophage phagocytosis of apoptotic neutrophils by adhesion to fibronectin. J. Leukoc. Biol. 64, 600–607.

[18] Sallenave, J.-M., Xing, Z., Simpson, A.J., Graham, F.L. and Gauldie, J. (1998) Adenovirus-mediated expression of an elastase-specific inhibitor (elafin): a comparison of different promoters. Gene Ther. 5, 352–360.

[19] Flora, P.K. and Gregory, C.D. (1994) Recognition of apoptotic cells by human macrophages: inhibition by a monocyte/macrophage-speciftc monoclonal antibody. Eur. J. Immunol. 24, 2625–2632.

[20] Ulevitch, R.J. and Tobias, P.S. (1995) Receptor-Dependent Mechanisms of Cell Stimulation by Bacterial-Endotoxin. Annu. Rev. Immunol. 13, 437–457.

[21] Huang, S., Endo, R.I. and Nemerow, G.R. (1995) Upregulation of integrins alpha v beta 3 and alpha v beta 5 on human monocytes and T lymphocytes facilitates adenovirus-mediated gene delivery. J. Virol. 69, 2257–2263.

[22] Fasbender, A., Zabner, J., Chillon, M., Moninger, T.O., Puga, A.P., Davidson, B.L. and Welsh, M.J. (1997) Complexes of adenovirus with polycationic polymers and cationic lipids increase the efficiency of gene transfer in vitro and in vivo. J. Biol. Chem. 272, 6479–6489.

[23] Toyoda, K., Ooboshi, H., Chu, Y., Fasbender, A., Davidson, B.L., Welsh, M.J. and Heistad, D.D. (1998) Cationic polymer and lipids enhance adenovirus-mediated gene transfer to rabbit carotid artery. Stroke 29, 2181–2188.

[24] Fadok, V.A., Bratton, D.L., Guthrie, L. and Henson, P.M. (2001) Differential effects of apoptotic versus lysed cells on macrophage production of cytokines: Role of proteases. J. Immunol. 166, 6847–6854.

[25] Odaka, C., Mizuochi, T., Yang, J. and Ding, A. (2003) Murine macrophages produce secretory leukocyte protease inhibitor during clearance of apoptotic cells: implications for resolution of the inflammatory response. J. Immunol. 171, 1507–1514.

[26] Zernecke, A., Weber, K.S.C., Erwig, L.P., Kluth, D.C., Schroppel, B., Rees, A.J. and Weber, C. (2001) Combinatorial model of chemokine involvement in glomerular monocyte recruitment: Role of CXC chemokine receptor 2 in infiltration during nephrotoxic nephritis. J. Immunol. 166, 5755–5762.

[27] Kluth, D.C., Ainslie, C.V., Pearce, W.P., Finlay, S., Clarke, D., Anegon, I. and Rees, A.J. (2001) Macrophages transfected with adenovirus to express IL-4 reduce inflammation in experimental glomerulonephritis. J. Immunol. 166, 4728–4736.

[28] Chmiel, J.F., Berger, M. and Konstan, M.W. (2002) The role of inflammation in the pathophysiology of CF lung disease. Clin. Rev. Allergy Immunol. 2.3, 5–27.